

1995

Mechanisms of poly(vinyl chloride) fire retardance and smoke suppression induced by copper additives

Jong Paul Jeng
College of William & Mary - Arts & Sciences

Follow this and additional works at: <https://scholarworks.wm.edu/etd>



Part of the [Materials Science and Engineering Commons](#), and the [Polymer Chemistry Commons](#)

Recommended Citation

Jeng, Jong Paul, "Mechanisms of poly(vinyl chloride) fire retardance and smoke suppression induced by copper additives" (1995). *Dissertations, Theses, and Masters Projects*. Paper 1539623866.
<https://dx.doi.org/doi:10.21220/s2-jdys-gf35>

This Dissertation is brought to you for free and open access by the Theses, Dissertations, & Master Projects at W&M ScholarWorks. It has been accepted for inclusion in Dissertations, Theses, and Masters Projects by an authorized administrator of W&M ScholarWorks. For more information, please contact scholarworks@wm.edu.

INFORMATION TO USERS

This manuscript has been reproduced from the microfilm master. UMI films the text directly from the original or copy submitted. Thus, some thesis and dissertation copies are in typewriter face, while others may be from any type of computer printer.

The quality of this reproduction is dependent upon the quality of the copy submitted. Broken or indistinct print, colored or poor quality illustrations and photographs, print bleedthrough, substandard margins, and improper alignment can adversely affect reproduction.

In the unlikely event that the author did not send UMI a complete manuscript and there are missing pages, these will be noted. Also, if unauthorized copyright material had to be removed, a note will indicate the deletion.

Oversize materials (e.g., maps, drawings, charts) are reproduced by sectioning the original, beginning at the upper left-hand corner and continuing from left to right in equal sections with small overlaps. Each original is also photographed in one exposure and is included in reduced form at the back of the book.

Photographs included in the original manuscript have been reproduced xerographically in this copy. Higher quality 6" x 9" black and white photographic prints are available for any photographs or illustrations appearing in this copy for an additional charge. Contact UMI directly to order.

UMI

A Bell & Howell Information Company
300 North Zeeb Road, Ann Arbor, MI 48106-1346 USA
313/761-4700 800/521-0600



**MECHANISMS OF POLY(VINYL CHLORIDE) FIRE RETARDANCE
AND SMOKE SUPPRESSION INDUCED BY COPPER ADDITIVES**

A Dissertation

Presented to

The Faculty of the Applied Science Program
The College of William and Mary in Virginia

In Partial Fulfillment

Of the Requirements for the Degree of
Doctor of Philosophy

by

Jong Paul Jeng

1995

UMI Number: 9537550

UMI Microform 9537550
Copyright 1995, by UMI Company. All rights reserved.

**This microform edition is protected against unauthorized
copying under Title 17, United States Code.**

UMI

**300 North Zeeb Road
Ann Arbor, MI 48103**

APPROVAL SHEET

This dissertation is submitted in partial fulfillment of
the requirements for the degree of

Doctor of Philosophy

Jong Paul Jeng
Author

Approved, March 1995

W. H. Starnes, Jr.
William H. Starnes, Jr.

Robert D. Pike
Robert D. Pike

Dennis M. Manos
Dennis M. Manos

Robert A. Orwoll
Robert A. Orwoll

Robert L. Vold
Robert Vold

TABLE OF CONTENTS

	Page
ACKNOWLEDGEMENTS -----	viii
LIST OF TABLES -----	ix
LIST OF SCHEMES -----	xi
LIST OF FIGURES -----	xiii
ABSTRACT -----	xviii
INTRODUCTION -----	2
1. Poly(vinyl chloride) and the Fire Hazard -----	2
2. Thermal Degradation of PVC -----	5
3. Mechanism of Benzene Formation -----	15
4. Smoke Suppression of PVC -----	17
5. Copper Compounds as Smoke Suppressants for PVC -----	27
6. Activated Copper and the Reductive Coupling Mechanism -----	30
EXPERIMENTAL -----	36
1. Synthesis of 7-Chlorotridecane -----	36
2. Synthesis of <u>trans</u> -4-Chloro-2-pentene -----	41
3. Synthesis of $\text{CuI}\cdot\text{P}(\underline{n}\text{-Bu})_3$ -----	45
4. Preparation of Lithium Naphthalenide -----	46

5. Preparation of Activated Copper Slurry -----	47
6. Production of Activated Copper Film -----	49
7. Reactions of Model Organic Halides with Activated Copper Slurry -----	50
8. Reactions of Model Organic Halides with Activated Copper Film -----	51
9. Reactions of Activated Copper with PVC in Solution -----	52
10. Thermal Degradation of PVC with Copper Additives -----	55
10-1. Measurements of the Rate of Dehydrochlorination -----	55
10-2. Determination of the Gel Content of Degraded PVC -----	57
11. PVC Model-Compound Pyrolysis Experiments -----	58
11-1. General Information -----	58
11-2. Reactions of Simple Secondary Chlorides with Copper Additives -----	59
11-3. Reactions of a Secondary Allylic Chloride with Copper Additives -----	59
11-4. Reactions of Conjugated Alkenes with Copper Additives -----	60
11-5. Reactions of a Mixture of Two Secondary Allylic Chlorides with Copper Metal -----	60

11-6.	Reactions of a Mixture of a Secondary Allylic Chloride and a Conjugated Alkene with Copper Additives -----	61
11-7.	Reactions of a Mixture of a Simple Secondary Chloride and a Secondary Allylic Chloride with Copper Additives ---	61
11-8.	Reactions of a Mixture of a Simple Secondary Chloride and a Conjugated Alkene with Copper Additives -----	62
11-9.	Reactions of a Secondary Chloride and Benzene with Copper Additives -----	62
11-10.	Reactions of Iodopentafluorobenzene with Copper Additives, Zinc Metal, or Molybdenum Trioxide -----	63
12.	Instrumental Analysis -----	64
12-1.	(Gas Chromatography)-(Mass Spectroscopy) (GC/MS) -----	64
12-2.	Thermogravimetric Analysis (TGA) -----	64
12-3.	Infrared (IR) Spectroscopy -----	65
12-4.	Nuclear Magnetic Resonance (NMR) Spectroscopy -----	65
12-5.	Acid-Base Titrimetry -----	65
12-6.	Ultracentrifugation -----	65
13.	Chemicals -----	66

RESULTS AND DISCUSSION -----	70
I. Study of Reductive Coupling via Activated	
Copper -----	70
1-1. Reactions of Model Organic Halides with	
Activated Copper -----	70
1-2. Reaction of Activated Copper with PVC in	
Solution -----	104
1-3. Reaction of PVC with Copper Additives	
in the Solid State -----	107
II. Model-Compound Pyrolysis Experiments -----	116
2-1. Pyrolysis of Simple Secondary	
Chlorides with Copper Additives -----	116
2-2. Pyrolysis of <u>trans</u> -4-Chloro-2-Pentene	
in the Presence of Copper Additives -----	129
2-3. Pyrolysis of Conjugated Alkenes in	
the Presence of Copper Additives -----	158
2-4. Pyrolysis of a Mixture of a Secondary	
Chloride and a Conjugated Diene in the	
Presence of Copper Additives -----	196
2-5. Reaction of a Mixture of 4-Chloro-2-	
pentene and 1,3,5-Hexatriene with	
Copper Metal -----	225
2-6. Pyrolysis of a Mixture of 3-Chloro-1-	
butene and 4-Chloro-2-pentene in the	
presence of Cu -----	237

2-7. Pyrolysis of Iodopentafluorobenzene in the Presence of Various Copper Additives -----	239
2-8. Reactions of a Simple Secondary Chloride or a Secondary Allylic Chloride with Benzene or Toluene -----	245
2-9. Reactions of a Mixture of a Simple Secondary Chloride and a Secondary Allylic Chloride in the Presence of Copper Additives -----	247
2-10. Reactions of 2-Chlorobutane and a Conjugated Diene or Triene in the Presence of Copper Additives -----	248
CONCLUSIONS -----	249
REFERENCES -----	252
VITA -----	262

ACKNOWLEDGEMENTS

The writer wishes to express his appreciation to Professor William H. Starnes, Jr., under whose direction this investigation was conducted, for his patient guidance and criticism throughout the investigation. The author is also indebted to Professors Dennis M. Manos, Robert D. Pike, Robert A. Orwoll, and Robert L. Vold for their careful reading and criticism of the manuscript. Appreciation is also expressed to Dr. Timothy Ho of the NASA Langley Research Center for his assistance in the thermogravimetric analysis. Finally, the support of this project by the International Copper Association is gratefully acknowledged.

LIST OF TABLES

Table	page
1. Homocoupling of Organohalides with Activated Copper Slurry at 0 °C in Ethyl Ether -----	72
2. Cross-coupling of Organohalides with Activated Copper Slurry at 0 °C in Ethyl Ether -----	73
3. Homocoupling and Cross-coupling of Organohalides with Activated Copper Slurry at 0 °C in THF -----	75
4. Homocoupling and Cross-coupling of Organohalides with Activated Copper Film at 25 °C -----	76
5. Gel Content of PVC Treated with Cu ⁰ Slurry in Solution -----	105
6. Yields for Dehydrochlorination of 2-Chlorobutane with Copper Additives at 200 °C for 1 h -----	118
7. Yields for Dehydrochlorination of 7-Chlorotridecane with Copper Additives at 200 °C for 1 h -----	119
8. Distributions of Heavy Products for 4-Chloro-2-pentene Pyrolyses -----	130
9. Representative Tentative Chemical Structures of the Heavy Products for the 4-Chloro-2-pentene Pyrolyses -----	132
10. Distributions of Degradation Products Obtained from Reaction of 2,4-Hexadiene with CuCl ₂ at 200 °C for 1 h -----	160
11. Representative Tentative Chemical Structures of the Heavy Products Listed in Table 10 -----	161

12.	Distribution of Degradation Products Obtained from Reaction of 1,3,5-Hexatriene with CuCl_2 at 200 °C for 1 h -----	181
13.	Distributions of Heavy Products from Pyrolyses of a Mixture of 4-Chloro-2-pentene and 2,4-Hexadiene -----	198
14.	Representative Tentative Chemical Structures of the Heavy Products from Pyrolyses of a Mixture of 4-Chloro-2-pentene and 2,4-Hexadiene -----	200
15.	Distribution of Heavy Products from Pyrolyses of a Mixture of 4-Chloro-2-pentene and 1,3,5-Hexatriene -----	226
16.	Representative Tentative Chemical Structures of the Heavy Products from Pyrolyses of a Mixture of 4-Chloro-2-pentene and 1,3,5-Hexatriene -----	227

LIST OF SCHEMES

Scheme	Page
1. Combustion of PVC -----	4
2. Thermal degradation of PVC -----	5
3. Dehydrochlorination from unsaturated repeating units and subsequent zip- elimination -----	7
4. Ionic-pair mechanism of HCl elimination -----	9
5. Radical mechanism of dehydrochlorination -----	10
6. Molecular mechanism of dehydrochlorination ---	11
7. Reaction pathways for pyrolysis of PVC -----	12
8. Formation of benzene by hexatriene mechanism -----	16
9. Benzene formation by octatetraene mechanism -----	16
10. PVC pyrolysis scheme -----	19
11. Model-compound reactions with MoO_3 and MoO_2Cl_2 -----	21
12. Mo(VI)-catalyzed olefin dimerization and chloroalkylation -----	23
13. Possible mechanism for Mo(VI)-catalyzed crosslinking in pyrolyzing PVC -----	24
14. Metal-catalyzed reductive coupling mechanism -----	25
15. Model-compound reactions with copper additives -----	29
16. Model-compound reactions with cuprous oxide -----	31

17.	Reaction scheme of 3-chloro-1-butene with Cu^{O} involving a radical intermediate ----	95
18.	Possible mechanism for the reaction of allylic chlorides with metal -----	97
19.	Possible mechanistic pathway for copper- induced organic halide reductive coupling reactions -----	102
20.	Lewis-acid-catalyzed dehydrochlorination and crosslinking reactions -----	121
21.	Ionic mechanism for dehydrochlorination of PVC in the presence of metal oxide -----	122
22.	Mechanism for dehydrochlorination of PVC in the presence of copper metal -----	123
23.	Mechanistic scheme for alkene formation in alkyl halide-Pd-atom reaction -----	125
24.	Formation of saturated carbon-carbon bonds from the polyene chains in PVC via Friedel-Crafts catalysis -----	126
25.	Formation of cyclohexene structure from the polyene chains in PVC via Diels-Alder cyclization -----	127
26.	Possible mechanistic pathways for the formation of $\text{C}_6\text{H}_{11}\text{Cl}$ and $\text{C}_6\text{H}_9\text{Cl}$ in the reaction of $^6_{2,4}$ -hexadiene with CuCl_2 -----	176
27.	Possible mechanistic pathway for the formation of $\text{C}_6\text{H}_9\text{Cl}$ in the reaction of $^6_{1,3,5}$ -hexatriene with CuCl_2 -----	180

LIST OF FIGURES

Figure	Page
1. Thermogravimetric curve of PVC recorded at 10 °C/min under nitrogen flow -----	14
2. IR spectrum of 7-chlorotridecane -----	38
3. ¹ H NMR spectrum of 7-chlorotridecane -----	39
4. GC/MS data for 7-chlorotridecane -----	40
5. IR spectrum of <u>trans</u> -4-chloro-2-pentene -----	42
6. ¹ H NMR spectrum of <u>trans</u> -4-chloro-2-pentene ---	43
7. GC/MS data for <u>trans</u> -4-chloro-2-pentene -----	44
8. GC/MS data for C ₈ H ₁₄ -----	77
9. GC/MS data for C ₈ H ₁₄ -----	78
10. GC/MS data for C ₈ H ₁₄ -----	79
11. GC/MS data for C ₈ H ₁₄ -----	80
12. GC/MS data for C ₈ H ₁₄ -----	81
13. GC/MS data for C ₈ H ₁₄ -----	82
14. GC/MS data for C ₈ H ₁₄ -----	83
15. GC/MS data for C ₁₀ H ₁₈ -----	84
16. GC/MS data for C ₁₀ H ₁₈ -----	85
17. GC/MS data for C ₁₀ H ₁₈ -----	86
18. GC/MS data for C ₉ H ₁₆ -----	87
19. GC/MS data for C ₆ H ₅ CH ₂ CH ₂ C ₆ H ₅ -----	89

20.	^1H NMR spectrum for $\text{C}_6\text{H}_5\text{CH}_2\text{CH}_2\text{C}_6\text{H}_5$ -----	90
21.	^{13}C NMR spectrum for $\text{C}_6\text{H}_5\text{CH}_2\text{CH}_2\text{C}_6\text{H}_5$ -----	91
22.	GC/MS data for $\text{CH}_3\text{C}_6\text{H}_4\text{CH}_2\text{CH}_2\text{C}_6\text{H}_4\text{CH}_3$ -----	92
23.	^1H NMR spectrum for $\text{CH}_3\text{C}_6\text{H}_4\text{CH}_2\text{CH}_2\text{C}_6\text{H}_4\text{CH}_3$ -----	93
24.	^{13}C NMR spectrum for $\text{CH}_3\text{C}_6\text{H}_4\text{CH}_2\text{CH}_2\text{C}_6\text{H}_4\text{CH}_3$ -----	94
25.	Gel content of solid PVC degraded under argon at 200 ± 2 °C -----	108
26.	Acid evolved from solid PVC at 200 ± 2 °C under argon -----	108
27.	Thermogravimetric curve of (1) PVC+Cu (2) PVC+Cu(HCOO) $_2$ (3) PVC control -----	111
28.	IR spectra for (1) PVC without heating (2) PVC+CuCl $_2$ (3) PVC+CuCl (4) PVC+Cu $_2$ O (5) PVC+Cu (6) PVC control -----	113
29.	GC/MS data for $\text{C}_{10}\text{H}_{14}$ -----	134
30.	GC/MS data for $\text{C}_{10}\text{H}_{16}$ -----	135
31.	GC/MS data for $\text{C}_{10}\text{H}_{16}$ -----	136
32.	GC/MS data for $\text{C}_{10}\text{H}_{16}$ -----	137
33.	GC/MS data for $\text{C}_{10}\text{H}_{17}$ -----	138
34.	GC/MS data for $\text{C}_{10}\text{H}_{18}$ -----	139
35.	GC/MS data for $\text{C}_{10}\text{H}_{17}\text{Cl}$ -----	140
36.	GC/MS data for $\text{C}_{10}\text{H}_{17}\text{Cl}$ -----	141
37.	GC/MS data for $\text{C}_{15}\text{H}_{24}$ -----	142
38.	GC/MS data for $\text{C}_{15}\text{H}_{24}$ -----	143
39.	GC/MS data for $\text{C}_{15}\text{H}_{24}$ -----	144
40.	GC/MS data for $\text{C}_{15}\text{H}_{25}\text{Cl}$ -----	145
41.	GC/MS data for $\text{C}_{20}\text{H}_{32}$ -----	146
42.	GC/MS data for $\text{C}_{25}\text{H}_{40}$ -----	147

43.	GC chromatogram of products obtained from 4-chloro-2-pentene and Cu after 1 h at 200 °C -----	148
44.	GC chromatogram of products obtained from 4-chloro-2-pentene and Cu ₂ O after 1 h at 200 °C -----	149
45.	GC/MS data for C ₆ H ₉ Cl -----	162
46.	GC/MS data for C ₆ H ₁₁ Cl -----	163
47.	GC/MS data for C ₁₂ H ₁₆ -----	164
48.	GC/MS data for C ₁₂ H ₁₈ -----	165
49.	GC/MS data for C ₁₂ H ₁₈ -----	166
50.	GC/MS data for C ₁₂ H ₁₈ -----	167
51.	GC/MS data for C ₁₂ H ₂₀ -----	168
52.	GC/MS data for C ₁₂ H ₂₀ -----	169
53.	GC/MS data for C ₁₂ H ₂₀ -----	170
54.	GC/MS data for C ₁₈ H ₂₆ -----	171
55.	GC/MS data for C ₁₈ H ₂₈ -----	172
56.	GC/MS data for C ₁₈ H ₃₀ -----	173
57.	GC/MS data for C ₆ H ₁₁ -----	174
58.	GC/MS data for C ₇ H ₁₄ -----	175
59.	GC/MS data for C ₆ H ₉ Cl -----	182
60.	GC/MS data for C ₁₂ H ₁₆ -----	183
61.	GC/MS data for C ₁₂ H ₁₆ -----	184
62.	GC/MS data for C ₁₂ H ₁₆ -----	185
63.	GC/MS data for C ₁₂ H ₁₆ -----	186
64.	GC/MS data for C ₁₂ H ₁₆ -----	187
65.	GC/MS data for C ₁₂ H ₁₆ -----	188

66.	GC/MS data for $C_{12}H_{16}$	-----	189
67.	GC/MS data for $C_{18}H_{27}$	-----	190
68.	GC/MS data for $C_{19}H_{20}$	-----	191
69.	GC/MS data for $C_6H_{11}Cl$	-----	203
70.	GC/MS data for $C_{10}H_{16}$	-----	204
71.	GC/MS data for $C_{10}H_{16}$	-----	205
72.	GC/MS data for $C_{10}H_{18}$	-----	206
73.	GC/MS data for $C_{11}H_{16}$	-----	207
74.	GC/MS data for $C_{11}H_{18}$	-----	208
75.	GC/MS data for $C_{11}H_{18}$	-----	209
76.	GC/MS data for $C_{12}H_{20}$	-----	210
77.	GC/MS data for $C_{10}H_{17}Cl$	-----	211
78.	GC/MS data for $C_{10}H_{17}Cl$	-----	212
79.	GC/MS data for $C_{11}H_{19}Cl$	-----	213
80.	GC/MS data for $C_{16}H_{26}$	-----	214
81.	GC/MS data for $C_{17}H_{28}$	-----	215
82.	GC/MS data for $C_{15}H_{25}Cl$	-----	216
83.	GC/MS data for $C_{16}H_{27}Cl$	-----	217
84.	GC/MS data for $C_{21}H_{34}$	-----	218
85.	GC chromatogram of a mixture of 4-chloro-2-pentene and 2,4-hexadiene pyrolyzed in the presence of Cu at 200 °C for 1 h	-----	219
86.	GC chromatogram of a mixture of 4-chloro-2-pentene and 2,4-hexadiene pyrolyzed in the presence of Cu_2O at 200 °C for 1 h	-----	220
87.	GC/MS data for C_6H_9Cl	-----	228
88.	GC/MS data for $C_{10}H_{18}$	-----	229

89.	GC/MS data for $C_{11}H_{16}$ -----	230
90.	GC/MS data for $C_{11}H_{16}$ -----	231
91.	GC/MS data for $C_{12}H_{16}$ -----	232
92.	GC/MS data for $C_{12}H_{17}Cl$ -----	233
93.	GC/MS data for $C_{17}H_{24}$ -----	234
94.	GC chromatogram of a mixture of 4-chloro- 2-pentene and 1,3,5-hexatriene pyrolyzed in the presence of Cu at 200 °C for 1 h -----	235
95.	GC/MS data for $C_6F_5-C_6F_5$ -----	240
96.	GC/MS data for C_6F_5D -----	242
97.	GC/MS data for C_6F_5H -----	243

ABSTRACT

Copper compounds are well-known to be effective smoke suppressants and fire retardants for poly(vinyl chloride) (PVC). The purpose of this study has been to elucidate the mechanisms of PVC fire retardance and smoke suppression induced by copper additives.

The experimental approaches have involved: (1) the use of activated copper to study PVC model-compound reactions and the crosslinking of PVC and (2) the pyrolysis of PVC model compounds in the presence of several copper additives in order to examine the chemical reactions involved in the formation of heavy products.

The results have shown that activated copper promotes the reductive coupling of PVC model compounds. The activated copper was either: (a) a slurry resulting from the reduction of $\text{CuI}\cdot\text{P}(\text{n-Bu})_3$ with lithium naphthalenide or (b) a film created by the pyrolysis of copper(II) formate. Both the slurry and the film were also capable of promoting the extensive crosslinking of PVC itself.

In small-scale sealed-ampule model-compound pyrolysis experiments, several chemical reactions were revealed that may account for the crosslinking chemistry that occurs in copper-containing PVC. These reactions include Lewis-acid-catalyzed oligomerization and chloroalkylation, reductive-coupling dimerization, alkene monochlorination, and aromatization.

For copper compounds, Lewis-acid catalysis is the major (if not the only) reaction pathway toward crosslinking; while in the case of high-purity copper metal, the reductive coupling mechanism apparently plays a major role in the crosslinking process.

Since the crosslinking of PVC is known to suppress the formation of the volatile aromatics whose combustion generates smoke, the results of this study indicate that copper-promoted Lewis-acid catalysis and reductive-coupling dimerization will tend to prevent the evolution of smoke from the burning polymer.

**MECHANISMS OF POLY(VINYL CHLORIDE) FIRE RETARDANCE
AND SMOKE SUPPRESSION INDUCED BY COPPER ADDITIVES**

INTRODUCTION

1. Poly(vinyl chloride) and the Fire Hazard

Poly(vinyl chloride) (PVC), $(-\text{CH}_2-\text{CHCl}-)_n$, is one of the oldest and most important bulk polymers in the plastics industry today.¹ Its production volume is second only to that of polyethylene in terms of tonnage.² The total consumption of PVC for construction markets in the U.S. alone exceeded 5.6 billion pounds in 1992 and is expected to continue to grow at a rate of more than 4% annually through 1997.³

The early manufacturing of PVC was done in order to provide a replacement for the very flammable celluloid (cellulose nitrate).⁴ Rigid PVC is inherently flame retardant due to its high chlorine content (56.7 weight percent), and this property has permitted the extensive use of plasticized PVC in applications such as insulation for electrical and communications cables where the possibility of flame spread by burning plastics must be minimized. The polymer also has found widespread use in toys, water pipelines, automotive trims, home interior furnishings, and many construction applications.^{3,4}

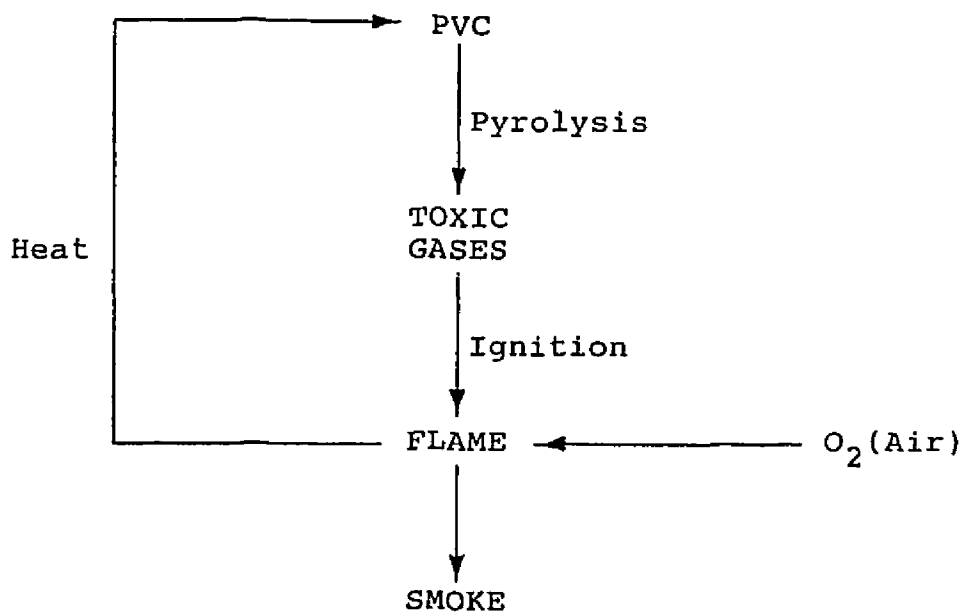
However, despite its low flammability, when PVC is forced to burn, it behaves like most organic materials and evolves a large amount of smoke and toxic gases, as is shown in Scheme 1.⁵ The combustibility of the polymer is enhanced further by the presence of certain additives such as plasticizers, lubricants, heat stabilizers, and fillers, which must be incorporated into commercial PVC formulations in order to achieve the mechanical and other properties desired.

The generation of smoke and toxic gases during the burning of PVC constitutes a major problem in a fire accident. Study has shown that when synthetic polymers are involved in a fire accident, the number of deaths is often very large even in quite small fires.⁶ This result is due to the additional hazards of suffocation by the smoke and poisoning by the fumes which are produced in large quantities from the burning polymers. Another harmful effect of smoke is that it severely limits visibility, making escape more difficult, which can lead to panic, and therefore significantly contributes to mortality rates.⁷ Thus experience has clearly shown that obscuration by smoke and its toxicity are of paramount importance in the sequence of events that lead to deaths in fires.⁸⁻¹⁰ In fact, the fire hazard associated with PVC has raised widespread concern from both the general public and the federal government, since the use of PVC has increased

gradually over the years and now it represents a large proportion of the materials of construction and furnishing of homes, as well as commercial and public buildings.³

Numerous efforts, therefore, have been made to overcome the problem of fire hazard associated with PVC by the use of smoke-suppressant and flame-retardant additives.

Meanwhile, the search for such additives for PVC also has been stimulated by the growing number of federal regulations for flame and smoke reduction in PVC that is used in home furnishings and public buildings. The search for more effective additives has led, in turn, to the extensive study of the thermal degradation of PVC and the mechanism of smoke suppression of PVC induced by additives of this type.

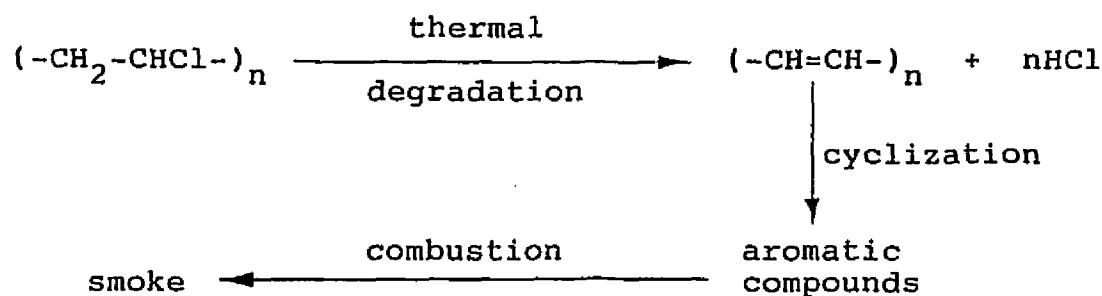


Scheme 1. Combustion of PVC.⁵

2. Thermal Degradation of PVC

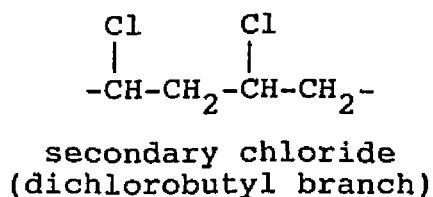
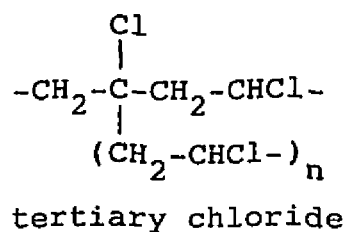
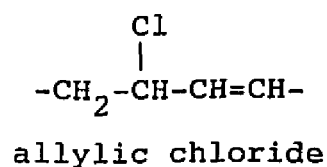
Rigid and plasticized PVC are thermally unstable, and the degradation process can occur at temperatures as low as 100-120 °C.^{11,12} The thermal degradation begins with the release of hydrogen chloride (HCl) and the formation of conjugated polyene sequences.¹²⁻¹⁵ The latter then rearrange and decompose to generate volatile aromatic compounds which are the source of smoke during the combustion of PVC (Scheme 2).^{16,17}

The initiation of the dehydrochlorination reaction of PVC can occur at normal unactivated monomer repeating units or at the labile defect sites in the polymer.^{11,12} The thermal instability of PVC is caused mainly by the presence of labile defect sites that are formed in the polymer during the polymerization process.^{11,12,19} Various labile sites have been proposed: (1) unsaturated chain ends, (2) chain ends substituted by initiator residues,

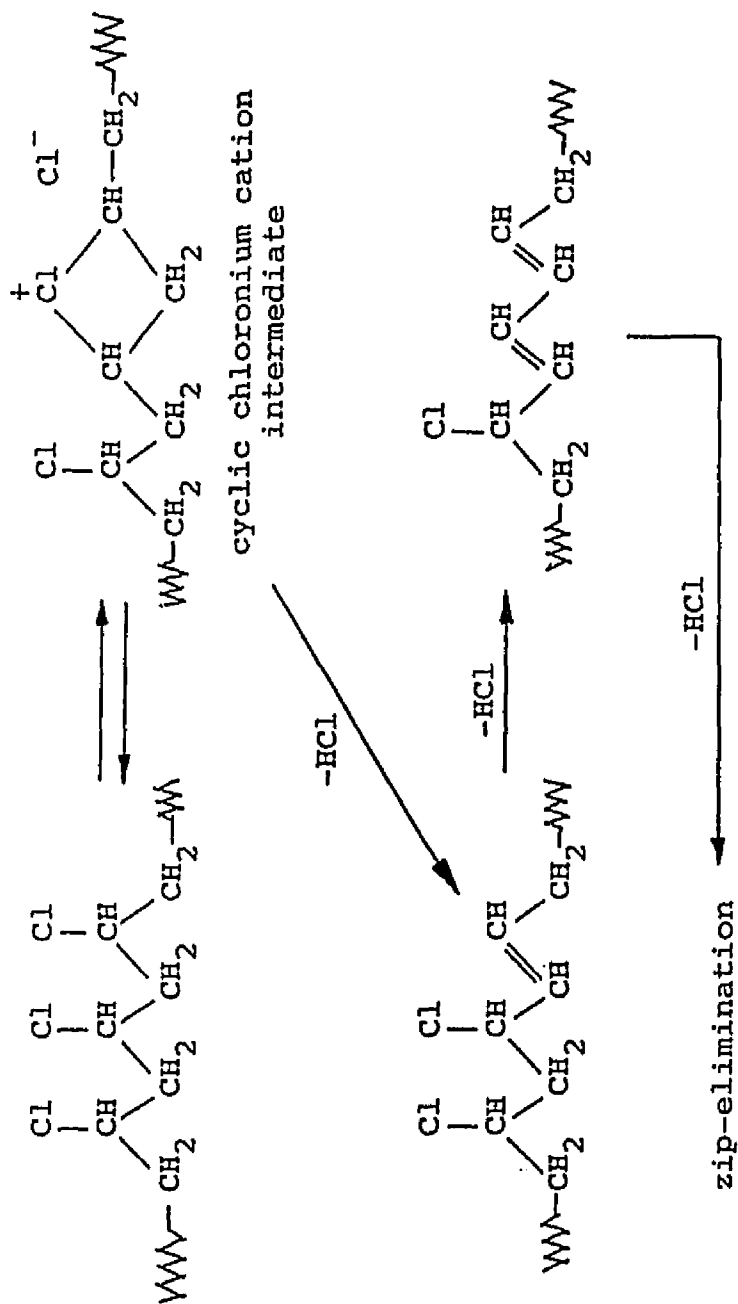


Scheme 2. Thermal degradation of PVC.¹⁸

(3) random unsaturation with allylic chlorine, (4) branch points with tertiary chlorine, (5) head-to-head units, and (6) oxygen present as a peroxide or carbonyl group.^{11,12,19,20} The most thermally unstable structures in PVC are the internal chloroallyl group and branch structures which contain secondary or tertiary chlorine as shown below.^{11,19-21} Defect structures containing

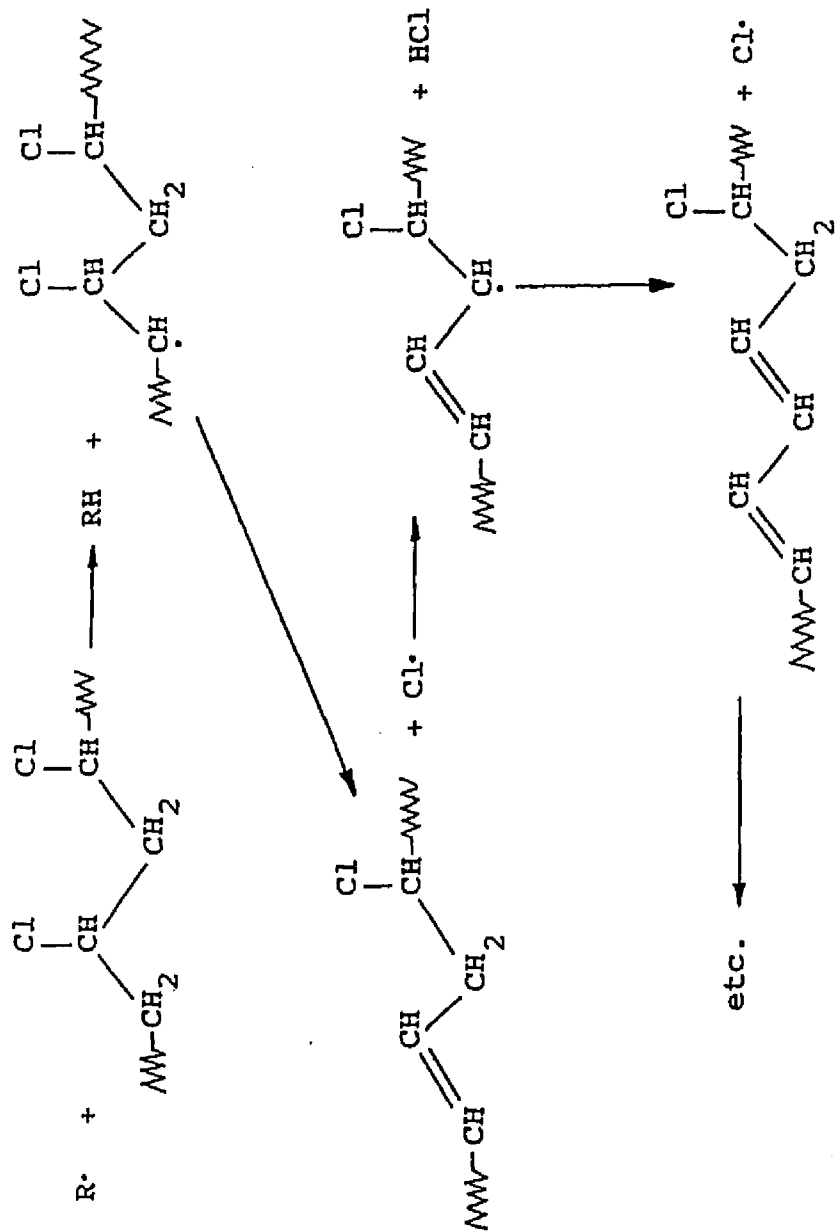


allylic chlorides are predicted by some workers²¹⁻²³ to have a more pronounced effect on dehydrochlorination than secondary and tertiary chlorides. However, other researchers^{24,25} consider tertiary chloride to be of prime importance. Experimental evidence¹¹ indicates that the loss of HCl can occur from regular repeating units via a cyclic chloronium cation intermediate, a process that results in the formation of allylic chloride which can then trigger zip-elimination of HCl to form polyene sequences, as is shown in Scheme 3.



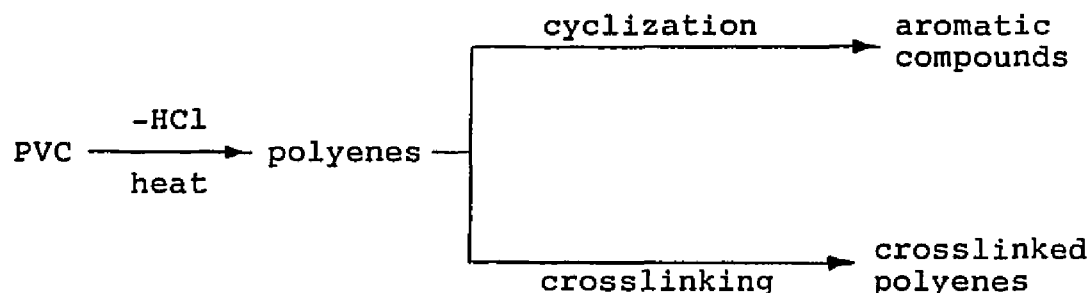
Scheme 3. Dehydrochlorination from unactivated repeating units and subsequent zip-elimination.¹¹

At least three other principal mechanisms have been proposed as explanations for the initiation of the dehydrochlorination reaction and the rapid growth of polyene sequences. First, there is the ionic-pair mechanism (Scheme 4),¹² which involves the initial loss of chloride ion and formation of a secondary, secondary allylic, or tertiary cation in the polymer, followed by elimination of hydrogen ion. A new allylic chloride group formed in the polymer backbone could then trigger zip-elimination. Second, there is the radical mechanism (Scheme 5),^{11,12} which begins via abstraction of a hydrogen atom from PVC by a free radical, $R\cdot$, in the system. The free chlorine radical formed next can abstract a hydrogen atom from the polymer to produce HCl and an allylic radical in the chain; subsequent loss of another chlorine radical can then give two conjugated double bonds. The repetition of these processes can therefore lead to the formation of polyene sequences. Third, there is the molecular mechanism (Scheme 6),¹² which invokes a four-membered cyclic transition state whereby HCl is lost as a molecule, leading to formation of an internal allylic chloride group which can initiate the zip-elimination reaction. Recent experimental evidence²⁶ supports the proposition that allylic and tertiary chloride structures cause thermal dehydrochlorination of PVC in the condensed phase by a mechanism involving ions or polar concerted transition states.



Scheme 5. Radical mechanism of dehydrochlorination.^{11,12}

The generation of polyene sequences during thermal degradation of PVC can affect physical appearance of the polymer and cause the polymer to turn yellow, red brown, and eventually black. The mechanical and electrical properties of the polymer also deteriorate rapidly.¹ In addition, polyene formation provides a starting point for two important chemical reaction pathways that eventually determine the flame-resistance ability of PVC during pyrolysis and combustion (Scheme 7).²⁷ First, the polyenes can start a cyclization process through which benzene and other aromatic compounds are formed.¹⁶ As noted above, these aromatic compounds are sources of smoke during burning of PVC.²⁸ Second, polyenes can also form crosslinks during pyrolysis, a process that competes with the formation of benzene and gives a thermally stable char residue which tends to cool the substrate, exclude the oxygen necessary for combustion, and reduce the quantity of toxic gases and smoke.⁴ Many metal compounds are well-known to be



Scheme 7. Reaction pathways for pyrolysis of PVC.²⁷

smoke suppressants that function in the condensed phase. These additives can divert the reaction of polyene sequences away from benzene formation and favor the pathway which causes crosslinking and charring of PVC.²⁸

A wide variety of aromatic compounds is released during the thermal degradation of PVC.²⁷ The main components include benzene, toluene, xylenes, styrene, indene, naphthalene, biphenyl and even anthracene. According to the studies conducted by Ballistreri and co-workers,²⁹ there are two temperature maxima for formation of organic aromatic compounds during pyrolysis of PVC: one at about 287 °C, and the other at about 347 °C. In the first maximum of emission, benzene is formed very efficiently along with HCl. With temperature increases, the amount of benzene released from PVC decreases, and other aromatics such as toluene, naphthalene, and methylnaphthalenes are produced more efficiently around the second maximum. More recently Montaudo and Puglisi²⁷ conducted thermal gravimetric analysis (TGA) which confirmed that two steps are involved in the thermal degradation of PVC (Figure 1). Based on the TGA curve shown in Figure 1, the first weight loss occurs at about 320 °C due to the evolution of HCl and unsubstituted aromatic compounds (benzene, naphthalene, anthracene, etc.). The second weight loss occurs at about 450 °C and gives mainly substituted aromatic compounds (toluene, methylnaphthalenes, etc.).

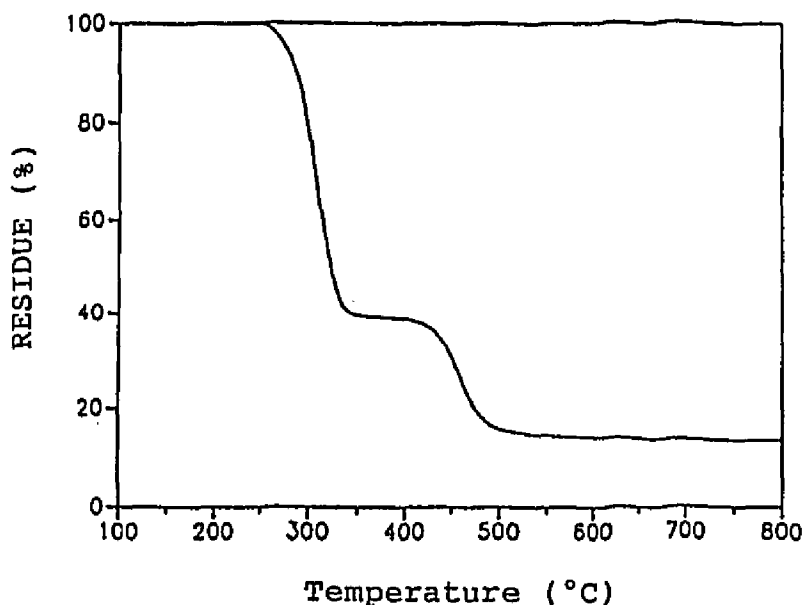


Figure 1. Thermogravimetric curve of PVC recorded at 10 °C/min under nitrogen flow.²⁷

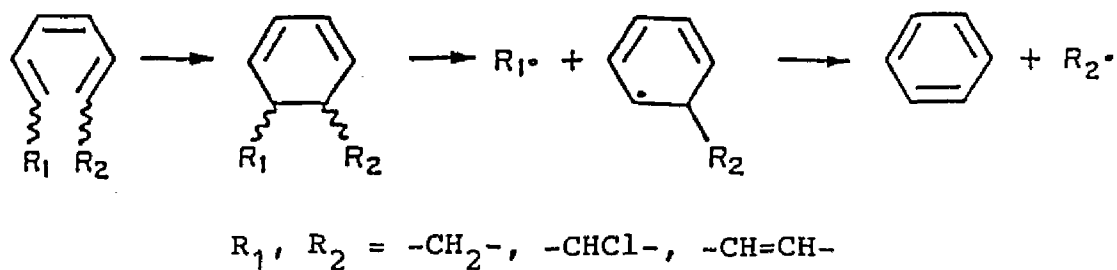
Aliphatic hydrocarbons also are generated in very small quantities in the second step and were considered to be only secondary thermal degradation products, formed from the alkyaromatics initially evolved from PVC.²⁷

Many studies point out that benzene is the most abundant aromatic compound formed at the early stage of PVC pyrolysis^{28,30,31}, and the combustion of benzene is considered to be a principal source of smoke under flaming conditions.²⁸ Therefore, a better understanding of the mechanism(s) by which benzene is formed would provide insight into the mechanism by which smoke suppressants and char-forming additives function in PVC, and hence

facilitate the design and development of more effective smoke suppressants for this polymer.

3. Mechanism of Benzene Formation

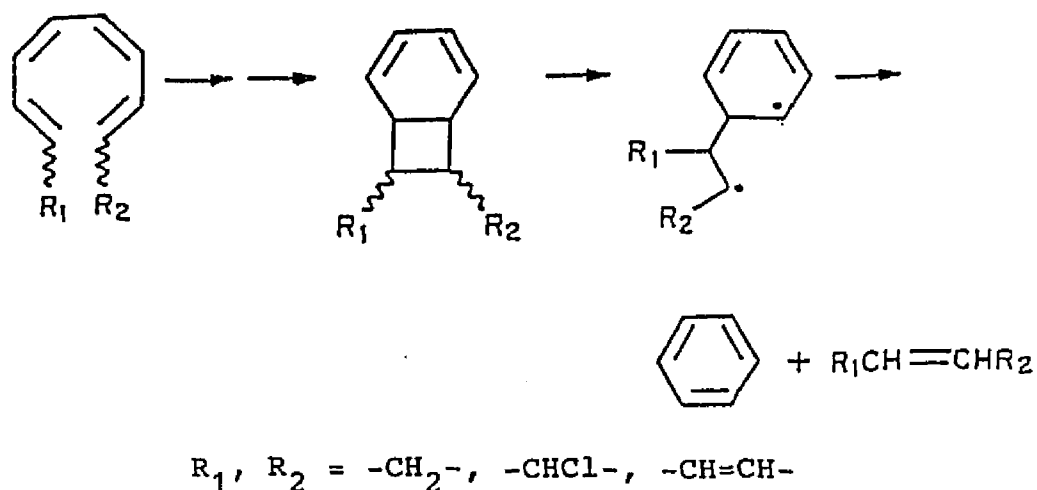
The chemical mechanism of benzene formation during the pyrolysis of PVC has been studied extensively.²⁷⁻⁴¹ The generation of polyene sequences precedes the cyclization process through which benzene and other aromatics are formed.^{17,28} All mechanistic proposals related to intermolecular routes to benzene formation appear to be excluded by the isotopic labeling experiments of O'Mara¹⁷ and Starnes et al.^{38,42} In the experiments of O'Mara, mixtures of protio PVC and completely perdeuterio PVC were pyrolyzed and yielded mainly mixtures of completely protio or completely deuterio benzene with only trace amounts of isotopic cross-over benzenes.¹⁷ Other researchers have also studied and verified the intramolecular cyclization mechanism.⁴²⁻⁴⁴ Starnes and Edelson²⁸ in their studies of the effects of the steric configuration of the polymer upon the extent of benzene formation pointed out that only cis-polyene structures are capable of cyclization and subsequent benzene elimination. They also proposed an intramolecular hexatriene mechanism²⁸ (Scheme 8) for benzene formation which is supported by a large body of data.



Scheme 8. Formation of benzene by hexatriene mechanism.²⁸

The hexatriene mechanism involves the intramolecular Diels-Alder cyclization of a triene moiety into a cyclohexadiene structure which is converted into benzene by two successive C-C homolyses.

In addition to the hexatriene mechanism for benzene formation, there is also a possible octatetraene mechanism²⁸ (Scheme 9) that was discussed by Starnes and Edelson.



Scheme 9. Benzene formation by octatetraene mechanism.²⁸

Additional evidence for benzene production from polyene intermediates is provided by several experimental observations. First, the rate of benzene evolution is enhanced in the presence of HCl,^{45,46} and it remains rapid after excess HCl has been removed.⁴⁶ Since HCl can catalyze the dehydrochlorination reaction of PVC during pyrolysis to produce polyene sequences,²⁸ these results indicate that polyene intermediates are involved in benzene formation. Second, benzene formation from polyene precursors is supported by the observation of auto-accelerating evolution of benzene under conditions that should lead to a constant concentration of HCl in the polymer.⁴⁶⁻⁴⁸ Finally, studies showed that a preliminary thermal dehydrochlorination of PVC will increase the amount of benzene evolved upon subsequent pyrolysis at higher temperatures.³¹ This result suggests that mild thermolysis gives relatively high yields of intermediate structures that can be converted into benzene by further heating.

4. Smoke Suppression of PVC

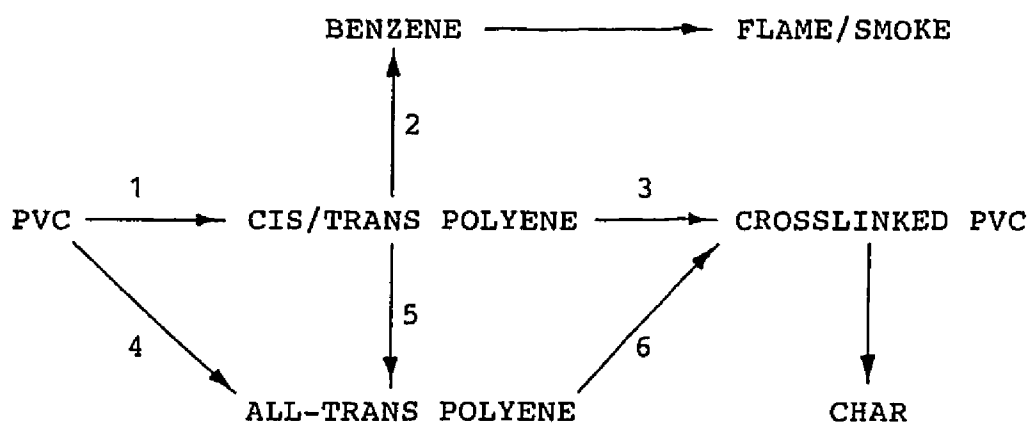
The search for more effective smoke suppressants for PVC has led to the examination of a large number of chemical compounds. Transition metal compounds, particularly oxides and chlorides, have been reported to

be the most effective smoke suppressants for this polymer.^{30,49,50}

The mechanisms of action of smoke-suppressing metal additives, which seem to alter the pyrolysis chemistry of the polymer, is a subject still under study. Different additives may function as smoke suppressants by different mechanisms. Some additives such as hydrated alumina function in a purely physical way by providing a heat sink which retards the pyrolysis of the polymer.^{51,52} Other compounds such as antimony trioxide act to yield radical scavengers in the gas phase which inhibit the flame propagation reactions.⁵² Many transition metal compounds are also known to function as smoke suppressants in the condensed phase. The addition of these additives to rigid PVC has been reported⁵³ to have three general effects: (1) smoke formation is reduced; (2) char formation is enhanced; (3) evolution of volatile aromatic compounds is reduced. These effects have been observed for numerous metal additives, including compounds of molybdenum, copper, iron, nickel, and bismuth.⁵³

The most important mechanistic theory was developed by researchers at Bell Laboratories during 1979-82 to account for the smoke-suppressing effect of MoO_3 on the combustion of PVC.^{28,37,38,54} Starnes and Edelson²⁸ proposed a Lewis-acid theory to explain these effects (Scheme 10). According to this theory, PVC initially

undergoes dehydrochlorination upon pyrolysis to generate linear polyene sequences having a low proportion of cis alkene segments (step 1), and benzene is then formed only through the intramolecular cyclization of these segments (step 2). When a Lewis acid (e.g., MoO_3) is added into the polymer matrix, benzene formation is suppressed by the following competing reactions that are acid-catalyzed: (1) the crosslinking of polyenes having cis double-bond segments (step 3; cyclohexadienes derived from these segments could experience crosslinking, as well), (2) the formation of all-trans polyene segments (step 4), and (3) the isomerization of cis-alkene moieties into the more thermodynamically stable trans arrangement (step 5).

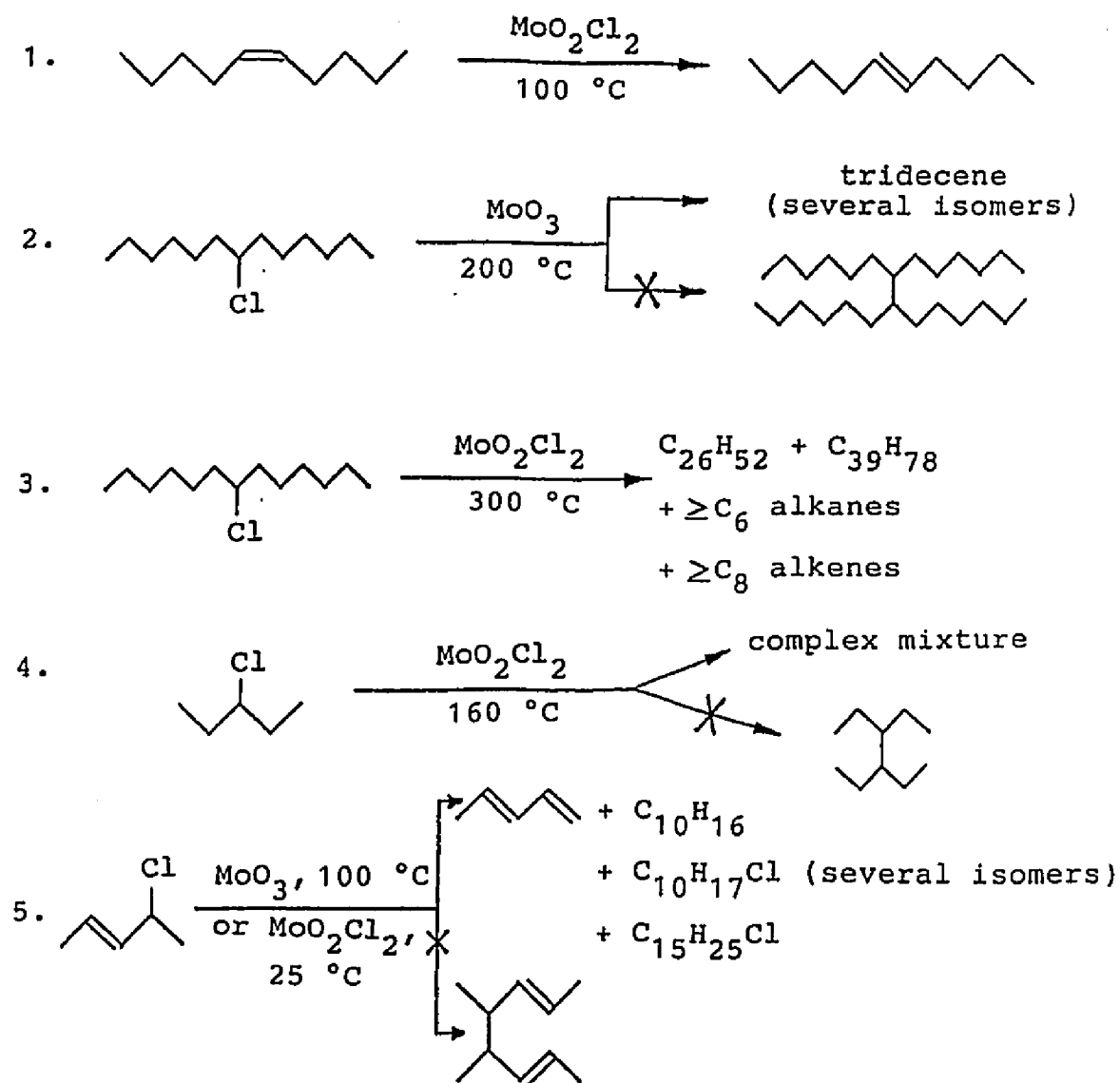


Scheme 10. PVC pyrolysis scheme.²⁸

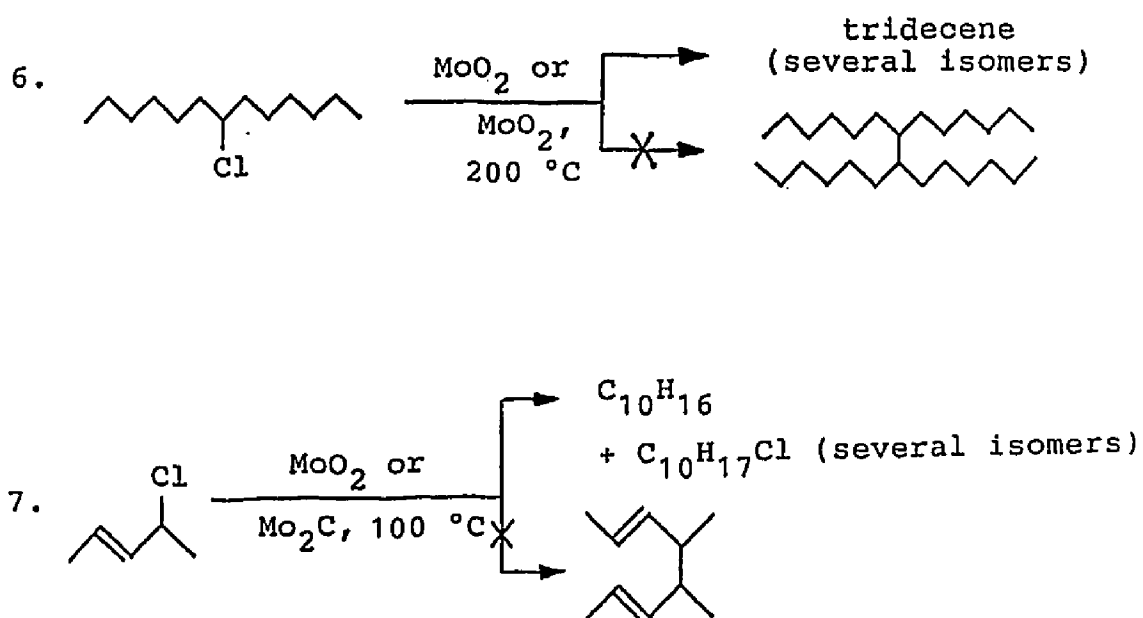
A further series of experiments with several low-molecular-weight model compounds in the presence of MoO_3

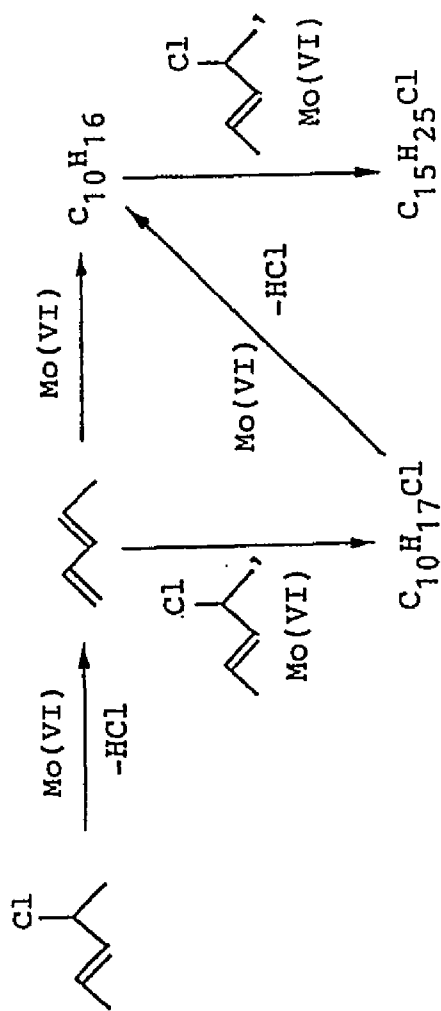
or MoO_2Cl_2 (which would be formed in PVC from MoO_3 and HCl) gave products which would be expected according to the Lewis-acid theory.³⁸ In summary, the principal mechanism of smoke suppression induced by MoO_3 involves the following Lewis-acid-catalyzed reactions: dehydrochlorination, alkene oligomerization, alkene isomerization, and chloroalkylation. Some of the model-compound reactions are summarized in Scheme 11. In these reactions, MoO_2Cl_2 was found to be able to convert cis-5-decene into trans-5-decene (reaction 1), a result which supports the cis-trans isomerization in the Lewis-acid theory. The model-compound reactions where 7-chlorotridecane, 3-chloropentane, and trans-4-chloro-2-pentene were treated with MoO_3 , MoO_2 , Mo_2C , or MoO_2Cl_2 (reactions 2-7) all gave degradation products that are consistent with the occurrence of Lewis-acid-catalyzed reactions. The reactions of Lewis-acid-catalyzed olefin dimerization and chloroalkylation (Friedel-Crafts reaction) for 4-chloro-2-pentene may occur via the routes illustrated in Scheme 12. Analogous reactions occurring in pyrolyzing PVC would lead to a crosslinked polymer (Scheme 13) and, ultimately, to char.³⁹

In addition to the Lewis-acid theory, Lattimer and Kroenke³⁰ have suggested a reductive coupling mechanism to account for the smoke-suppressing action of MoO_3 in the combustion of PVC. This mechanism can be represented by the catalytic redox cycle comprised of equations 1 and

Scheme 11. Model-compound reactions with MoO_3 and MoO_2Cl_2 .³⁸

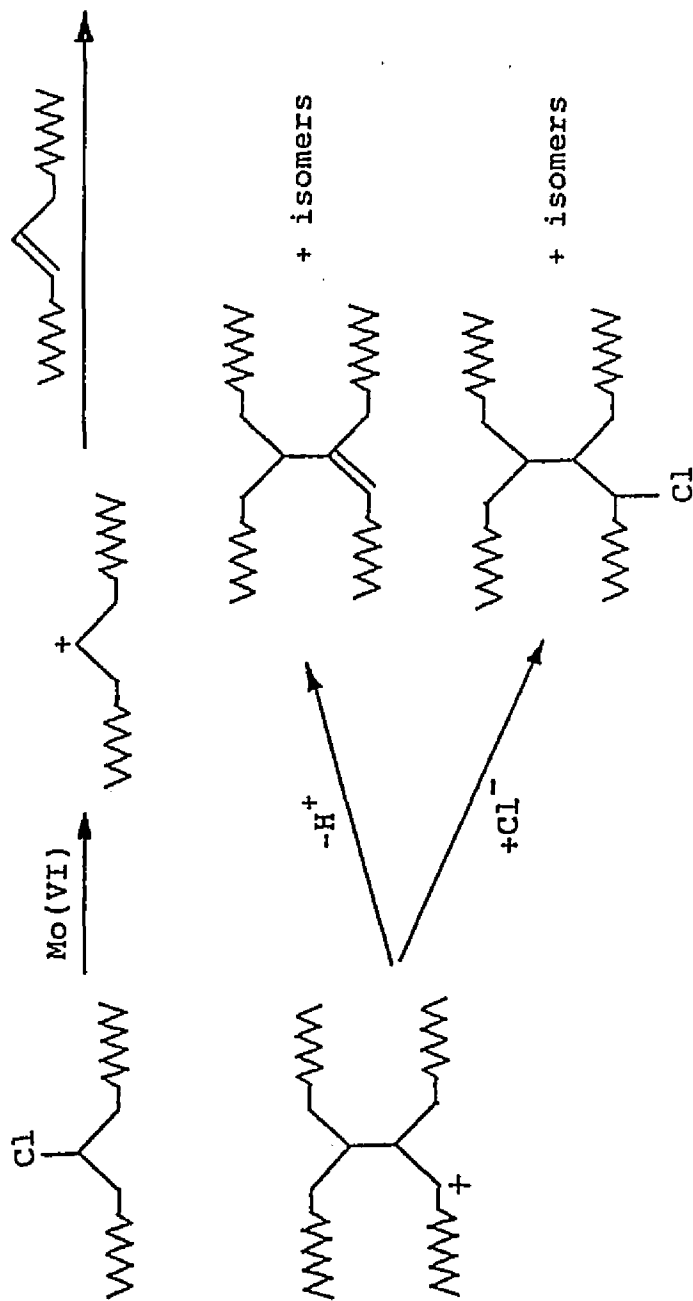
Scheme 11. Continued

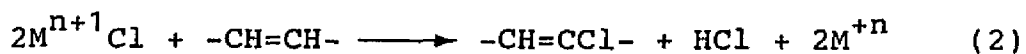
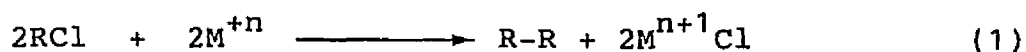




Scheme 12. Mo(VI)-catalyzed olefin dimerization and chloroalkylation. 39

Scheme 13. Possible mechanism for Mo(VI)-catalyzed crosslinking
in pyrolyzing PVC.³⁹



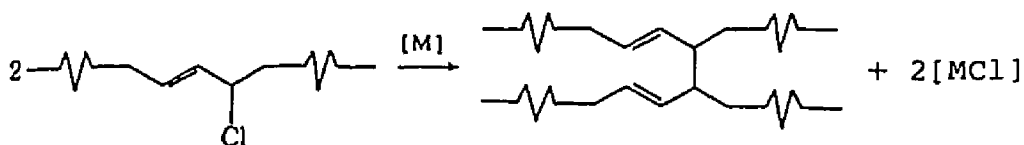


[RCl = PVC; M = a metal]

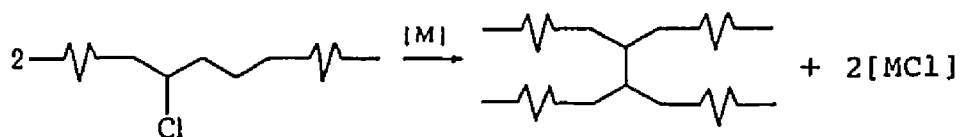
Scheme 14. Metal-catalyzed reductive coupling mechanism.³⁰

2 in Scheme 14, where the metal ligands are not specified. In effect, the MoO_3 acts as a coupling agent to join together allylic or alkyl chain segments during thermal degradation of the polymer:

(a) Allylic Site Coupling



(b) Alkyl Site Coupling



This mechanism, as proposed by Lattimer and Kroenke,³⁰ would lead to "early crosslinking" and was based on results obtained from studying the effects of MoO_3 (and other metal-based additives) in ordinary, perdeuterated, and highly syndiotactic PVC. Lattimer and Kroenke³⁰ believed

that reductive coupling best explained the following effects of MoO_3 on PVC: (1) reduction of smoke formation, (2) reduction of aromatic pyrolysate formation, and (3) effective promotion of char formation.

The reductive coupling mechanism has several features which make it attractive as a smoke-suppressant mechanism:³⁰ (1) it predicts early chlorine removal from PVC chains, which, according to Lattimer and Kroenke,³⁰ could help to explain the catalyzed dehydrochlorination at lower temperatures and the increased dehydrochlorination rate for MoO_3 -PVC;³⁵ (2) it would promote the extensive crosslinking of PVC chains, which would lead to volatile pyrolysate (and smoke) reduction and to enhanced char formation; (3) since the coupling reaction can occur very early in the degradation process, an isolated allylic chlorine dehydrochlorination site can be attacked directly. The removal of an allylic chlorine provides a shortstop for further polyene chain propagation.

However, despite these attractive features, many model-compound studies^{38,44,49,55} have shown that the reductive coupling mechanism either does not operate or only plays a minor role in the formation of crosslinks during the pyrolysis of molybdenum-containing PVC. At the present time, there is an overwhelming amount of evidence to support the proposition that the Lewis-acid mechanism is the most reasonable explanation for the action

of molybdenum trioxide as a smoke suppressant and fire retardant for PVC.

5. Copper Compounds as Smoke Suppressants for PVC

Copper additives for PVC have attracted much attention in recent years, and their mechanism of smoke suppression has been extensively studied at the molecular level by several workers.^{39,49,56} In 1981, Kroenke examined a wide variety of metal compounds as potential smoke suppressants for PVC and found that copper compounds comprised the single most effective class of suppressants.⁵⁰ Copper additives such as copper metal (Cu), copper(I) oxide (Cu_2O), copper(II) oxide (CuO), copper(I) chloride (CuCl), and copper(II) chloride (CuCl_2) have been investigated mechanistically for this purpose.^{39,49,56}

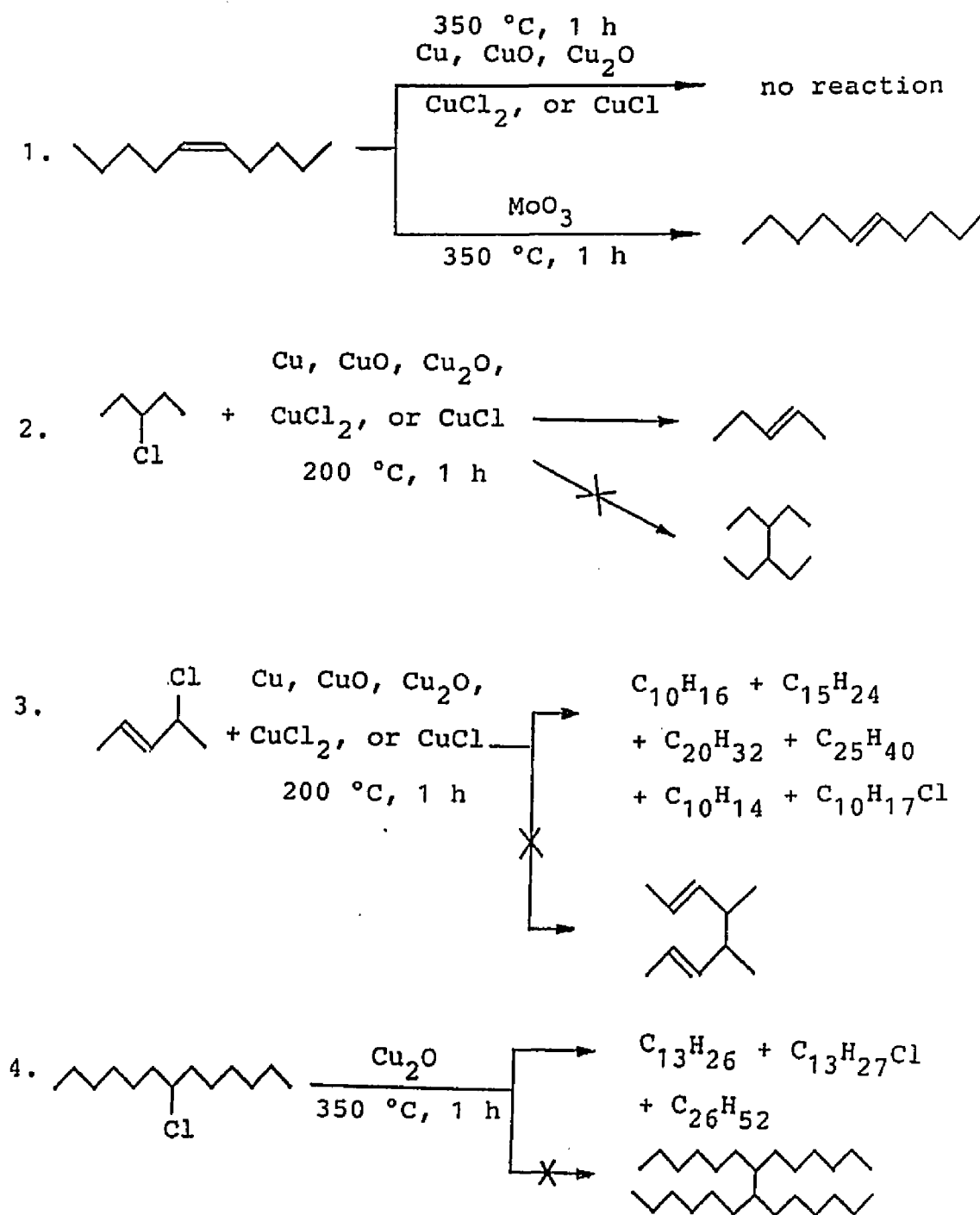
Copper compounds are, in general, only mild Lewis acids. Previous studies^{39,49,56} have revealed significant differences between their behavior and that of MoO_3 (a precursor of the strong Lewis acid, MoO_2Cl_2) in reactions with organic halides that are models for PVC. Very importantly, in contrast to MoO_3 , copper compounds do not promote cationic cracking reactions⁵⁶ which will cause the spread of fire by accelerating the production of volatile fuels from the char.^{38,55,57} Catalysis of char

cracking is, in fact, a major difficulty with the use of Lewis-acid chemistry for smoke suppression.

Recent model-compound studies conducted by Starnes and Huang^{56,58} suggest that copper additives (Cu, Cu₂O, CuO, CuCl₂, and CuCl) can function as mild Lewis-acid catalysts to accelerate dehydrochlorination and thus promote the extensive early crosslinking of PVC (by Friedel-Crafts type oligomerization and chloroalkylation), a process which reduces the amounts of volatile aromatic pyrolysates generated from the burning polymer. These researchers also demonstrated that copper compounds do not catalyze the cis-trans isomerization of cis-5-decene, a result indicating that the generation of all-trans conjugated polyene sequences, induced by copper additives, is not a major mechanism for smoke suppression in the copper-containing PVC.^{56,58} Similar to the MoO₃ model-compound studies,^{38,44,55} there was no trace of reductive-coupling products that could be detected by GC/MS in the work of Starnes and Huang.^{56,58} Some of the most important results of their model-compound reactions with copper additives are summarized in Scheme 15.

In an extension of the earlier work reported by Starnes and co-workers,³⁸ Lattimer and Kroenke⁴⁹ conducted similar closed-tube pyrolysis experiments to examine the reactions of cuprous oxide with the model compounds, 3-chloropentane, 2,4-dichloropentane and 2,4,6-trichloro-

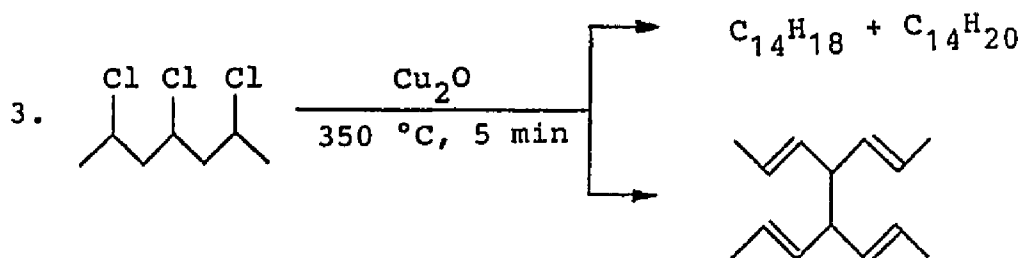
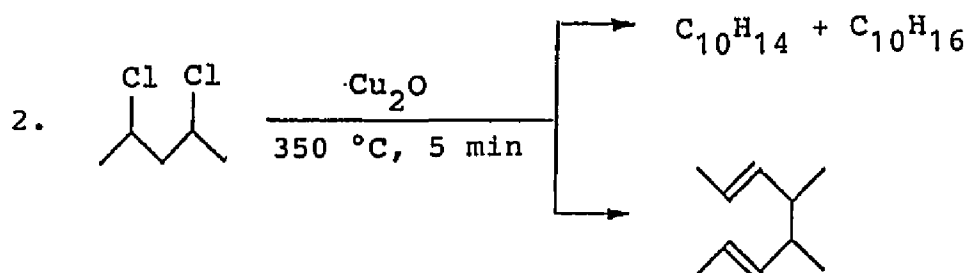
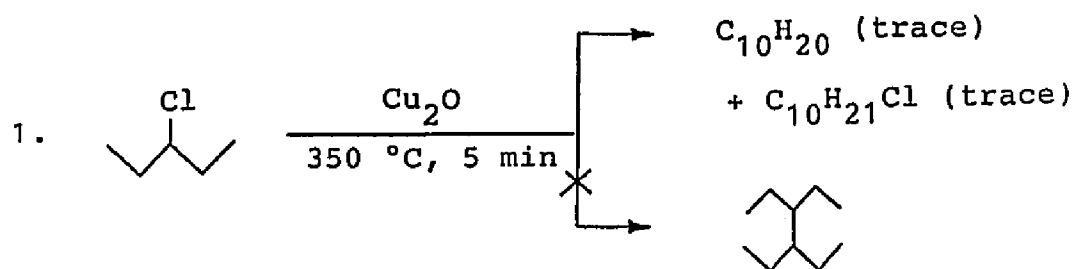
Scheme 15. Model-compound reactions with copper additives.^{56,58}



heptane. The results of these reactions are summarized in Scheme 16.⁴⁹ They led the authors⁴⁹ to conclude that Lewis-acid effects play a key role in copper-catalyzed PVC smoke retardation and that cuprous oxide serves as a smoke suppressant mainly by promoting dehydrochlorination, oligomerization and chloroalkylation reactions in burning PVC. In contrast to the results reported by Starnes and Huang,^{56,58} Lattimer and Kroenke⁴⁹ have demonstrated the presence of dimers ($C_{10}H_{18}$ and $C_{14}H_{22}$) with the molecular weights expected for reductive-coupling products in the pyrolysis experiments involving the reactions of 2,4-dichloropentane or 2,4,6-trichloroheptane with cuprous oxide. However, dimers that could only have resulted from Lewis-acid catalysis were found to be more abundant in each case. Thus the reductive coupling reactions were considered to be relatively minor contributors to the overall PVC crosslinking process.

6. Activated Copper and the Reductive Coupling Mechanism

Despite all the mechanistic studies of the role of copper compounds as smoke suppressants for PVC, relatively little has been conclusively established about the operation of the reductive coupling mechanism with these additives. However, possible occurrence of such a mechanism during

Scheme 16. Model-compound reactions with cuprous oxide.⁴⁹

the pyrolysis of copper-containing PVC is supported by the well-known ability of the Group IB metals, Cu, Ag, and Au, to promote reductive coupling reactions of organohalides under certain conditions.⁵⁹⁻⁶¹ Furthermore, it has been known for some time that, in burning PVC, higher-valent copper is readily reduced to the zero-valent metal,^{30,53} which should be produced in a highly active state and thus should be especially effective in promoting reductive coupling reactions such as equation 1 in Scheme 14. In the pyrolysis of PVC with copper(II) sulfide, for example, significant quantities of copper metal and copper(I) oxide have been detected in the char residues.³⁰ Lattimer and Kroenke⁵³ have also demonstrated that all the metal-containing smoke suppressants tested in their experiments yield predominantly low-valent metal products in the chars.

A recent trend in research in this area has been the pyrolysis of model compounds to help distinguish among the various proposed smoke suppression mechanisms. Many researchers^{39,49,56,58} have conducted model-compound studies involving the thermal degradation of PVC model compounds with copper additives at temperatures between 200 °C and 350 °C under anaerobic conditions. Copper metal, in the form of powder, was also studied in these experiments.^{39,56,58} However, in all cases, the reductive-coupling products expected to be induced by copper metal

were not detected. Huang⁶² has suggested that the copper powder may have been surface-oxidized initially and consequently may have been prohibited from catalyzing the reductive coupling of model compounds. Although the closed-tube pyrolysis reactions conducted by Huang⁶² were performed under high vacuum, and the copper metal powder was of very high purity (99.995%), its surface oxidation could not be entirely ruled out. Therefore, to conduct experimental studies of the reductive coupling mechanism, a highly reactive form of zero-valent copper, made in situ, needed to be used first in order to clarify the situation. Direct study of the effects of this type of copper on PVC model compounds and on PVC itself provided us with a starting point in this area of research.⁶³

The overall research objective of the work described in this dissertation was to elucidate, in more detail than had previously been reported, the functional role of copper additives as smoke suppressants in rigid PVC and, in particular, to obtain more insight into the possible operation of the reductive coupling mechanism. The results reported here represent part of an extensive and continuing investigation concerning the mechanism of fire retardance and smoke suppression in the copper-containing polymer. Our experimental approaches have involved: (1) the use of activated copper (Cu^0) to study PVC model-compound reactions and the crosslinking of PVC and (2) the pyrolysis

of PVC model compounds with different copper additives in sealed ampules in order to examine all of the possible chemical reactions involved in the formation of heavy products. The results obtained from studies of this type have been shown to be able to provide remarkable amounts of information about the possible mechanisms of smoke-suppressant action.^{39,49,56,58}

Our results obtained from experiments with activated copper and allylic chloride model compounds suggest that the reductive coupling mechanism is indeed a viable process in PVC. The Cu^0 that caused coupling of these models was either (a) a slurry resulting from the reduction of $\text{CuI}\cdot\text{P}(\underline{n}\text{-Bu})_3$ with lithium naphthalenide^{64,65} or (b) a film created by the pyrolysis of copper(II) formate.⁶⁶ Significantly, both the slurry and the film were also demonstrated to be capable of promoting the extensive crosslinking of PVC itself.

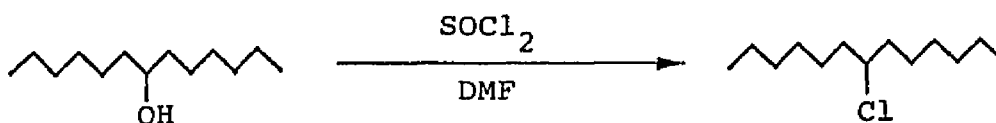
In addition to the results of the activated-copper studies, on the basis of small-scale sealed-ampule model-compound pyrolysis experiments, several chemical reactions were revealed to account (at least potentially) for the crosslinking chemistry that occurs in copper-containing PVC. These reactions include Lewis-acid-catalyzed oligomerization and chloroalkylation, reductive-coupling dimerization, Diels-Alder cyclization, alkene mono-halogenation (rechlorination), and aromatization. For

copper compounds, Lewis-acid catalysis is the major (if not the only) reaction pathway toward crosslinking; while in the case of high-purity copper metal, the reductive coupling mechanism apparently plays a major role in the crosslinking process.

Since the crosslinking of PVC is known to suppress the formation of the volatile aromatics whose combustion generates smoke, the results of the model-compound studies also indicate that copper-promoted Lewis-acid catalysis and reductive-coupling dimerization will tend to prevent the evolution of smoke from the burning polymer. Reductive coupling of PVC now appears to be worthy of further study with other additives within the context of smoke suppression and fire retardance.

EXPERIMENTAL

1. Synthesis of 7-Chlorotridecane



The 7-chlorotridecane was synthesized according to the procedure described by Hudson and de Spinoza.⁶⁷ Into a 250-mL three-necked round-bottom flask equipped with a reflux condenser (height, 200 mm), thionyl chloride (8.2 g, 69 mmol) was added dropwise by addition funnel to 25 mL of *N,N*-dimethylformamide (DMF) with stirring under a nitrogen atmosphere. The temperature of the reaction flask was kept at 0 °C in an ice-water bath to prevent possible violent exothermic decomposition of the complex.⁶⁸ 7-Tridecanol powder (12.5 g, 63 mmol) was first dissolved in 10 mL of thionyl chloride and then introduced slowly by addition funnel into the reaction flask, which was kept at 0 °C. At the end of the addition, the resultant mixture was brought to gentle reflux at approximately 150 °C by

use of a heating mantle for 1 h. The mixture was allowed to cool to room temperature and combined with 100 mL of deionized (DI) water. It then was transferred to a 250-mL separatory funnel and extracted with five 50-mL portions of ethyl ether. The combined extracts were transferred to a 250-mL separatory funnel and washed in succession with 50 mL of DI water and 50 mL of saturated aqueous sodium chloride solution. The organic layer was collected and dried over molecular sieves (effective pore size 4×10^{-8} cm) or MgSO_4 for 24 h. After the drying agent had been removed by filtration, the volatile ether was removed on a rotary evaporator, and the mixture then was subjected to vacuum distillation (at 25 °C, 4 torr). The highly concentrated dark brown residue finally was subjected to silica gel chromatography (using hexanes followed by gradient mixtures of hexanes/ethyl acetate) to afford 2.00 g of 7-chlorotridecane with 99.5% purity, based on GC analysis: IR (neat) (Figure 2) 2928, 2857, 1466, 1378, 726, and 665 cm^{-1} (medium, C-Cl stretch); ^1H NMR (300 MHz, CDCl_3) (Figure 3) δ 3.85 (m, $J = 6.10$ Hz, 1H, CHCl), 1.0-2.0 (m, 20H, CH_2), and 0.90 ppm (t, $J = 3.75$ Hz, 6H, CH_3); GC (Figure 4) 99.5% GC area purity, the side product is 6-tridecene; MS (EI) (Figure 4) m/e 182 ($\text{M}^+ - \text{HCl}$), 154, 139, 126, 111, 97, 83, 69, 55, 41 (base peak), and 28; the molecular ion peak (M^+ , m/e 218) was not observed.

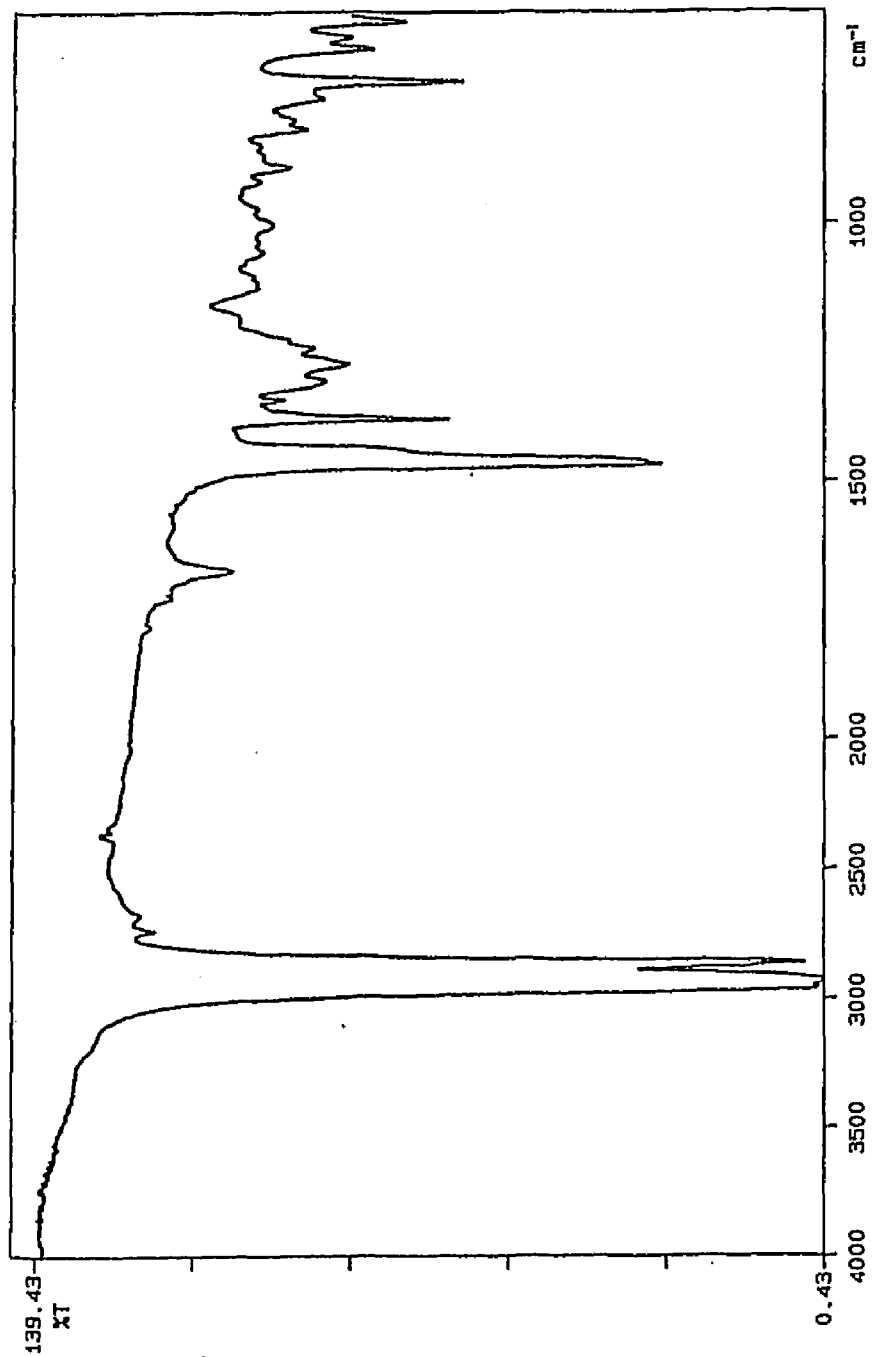


Figure 2. IR spectrum of 7-chlorotridecane.

Figure 3. ^1H NMR spectrum of 7-chlorotridecane.

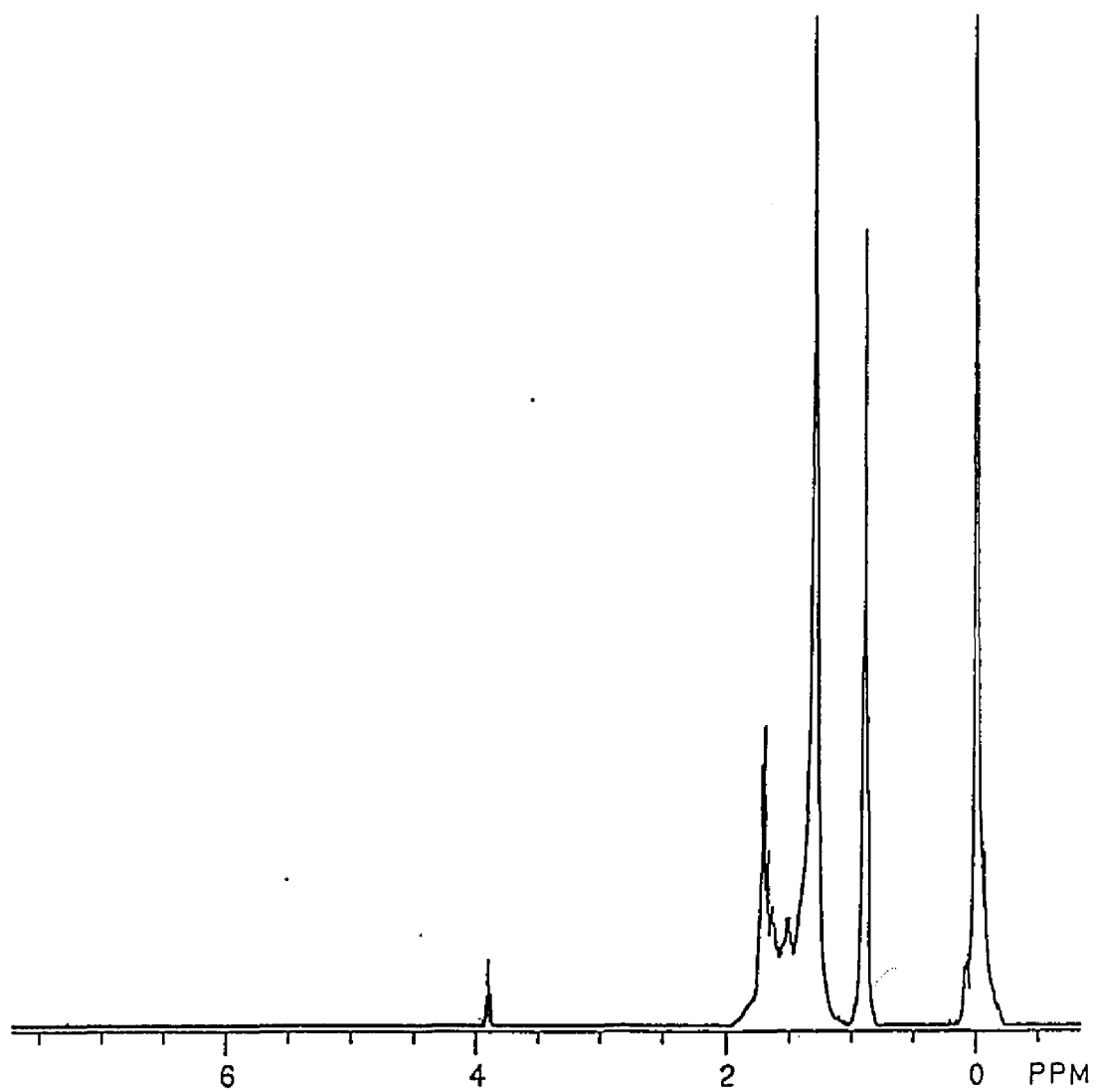
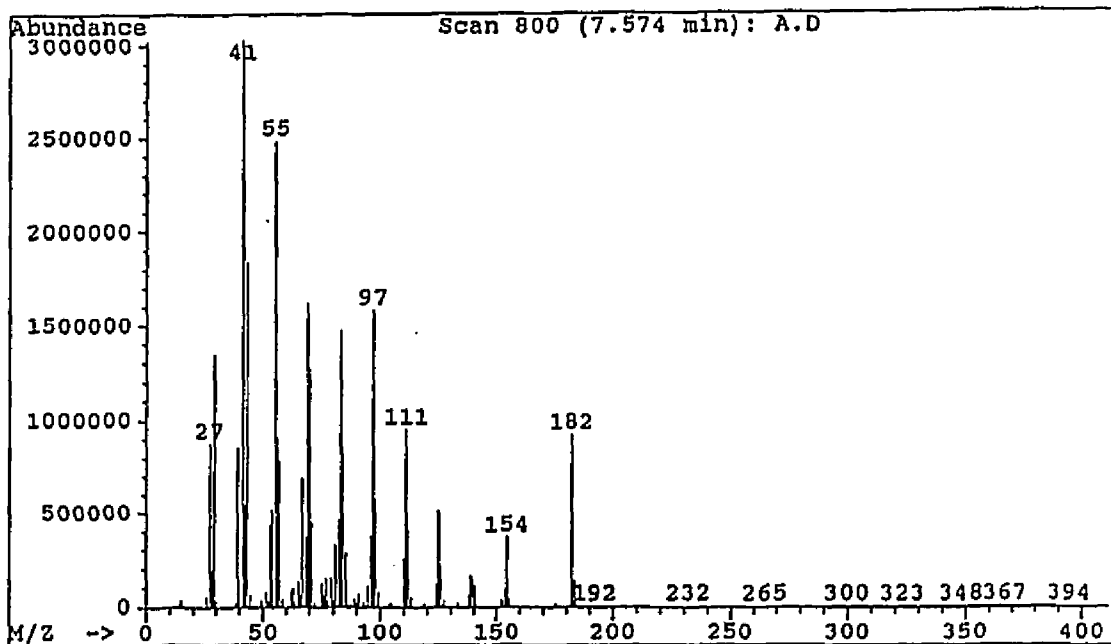
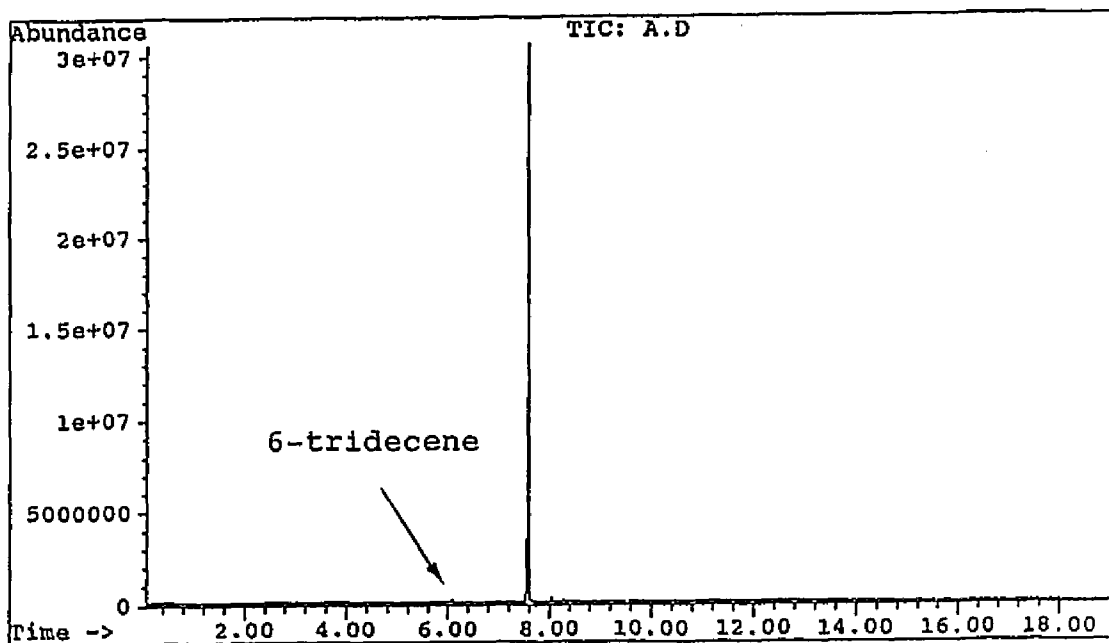
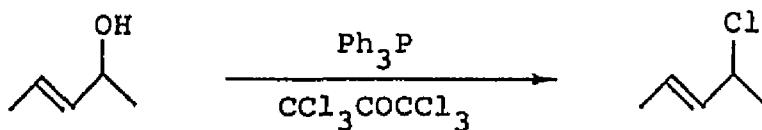


Figure 4. GC/MS data for 7-chlorotridecane.



2. Synthesis of trans-4-Chloro-2-pentene



The trans-4-chloro-2-pentene was synthesized according to the method published by Magid and co-workers.^{69,70} In a 100-mL round-bottom flask, trans-3-penten-2-ol (4.78 g, 54 mmol) was dissolved in 20 mL of hexachloroacetone. The solution was cooled to 0 °C in an ice-water bath, and Ph₃P powder (14.00 g, 53 mmol) was added slowly over a period of 20 min with vigorous stirring. The solution was then allowed to warm to room temperature and stirred until a thick slurry was formed (30 min). Immediate vacuum distillation of the thick slurry (without filtering off the solid) at 25 °C (4 torr) into a liquid-nitrogen-cooled receiver afforded a colorless liquid which was identified as trans-4-chloro-2-pentene (3.20 g, 57%) with 99% purity by GC: IR (neat) (Figure 5) 2987, 2921, 1670, 1450, 1377, 1216, 1163, 1016, 962 (strong, trans alkene), 888, 789, 762, 741, and 646 cm⁻¹; ¹H NMR (300 MHz, CDCl₃) (Figure 6) δ 1.44 (d, J = 6.10 Hz, 3H, CHClCH₃), 1.67 (d, J = 5.40 Hz, 3H, =CHCH₃), 4.45-4.57 (m, J = 6.96 Hz, 1H, CHCl), and 5.55-5.72 ppm (m, J = 6.42 Hz, 2H, CH=CH); GC (Figure 7) 99% purity; MS (EI) (Figure 7) m/e 104 and 106 (M⁺), 89, 69 (base peak), and 53. The peak at m/e 106 (M) (due

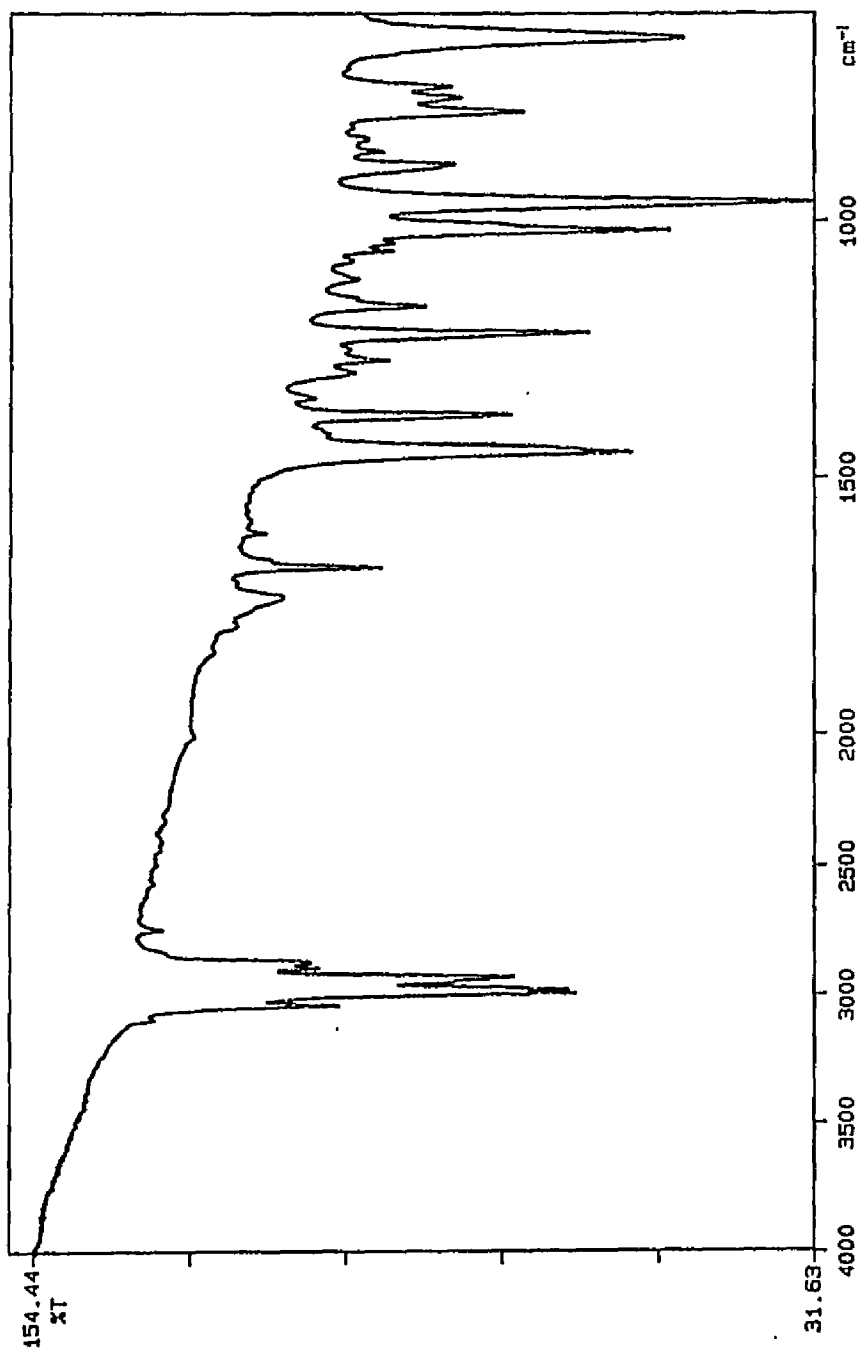


Figure 5. IR spectrum of trans-4-chloro-2-pentene.

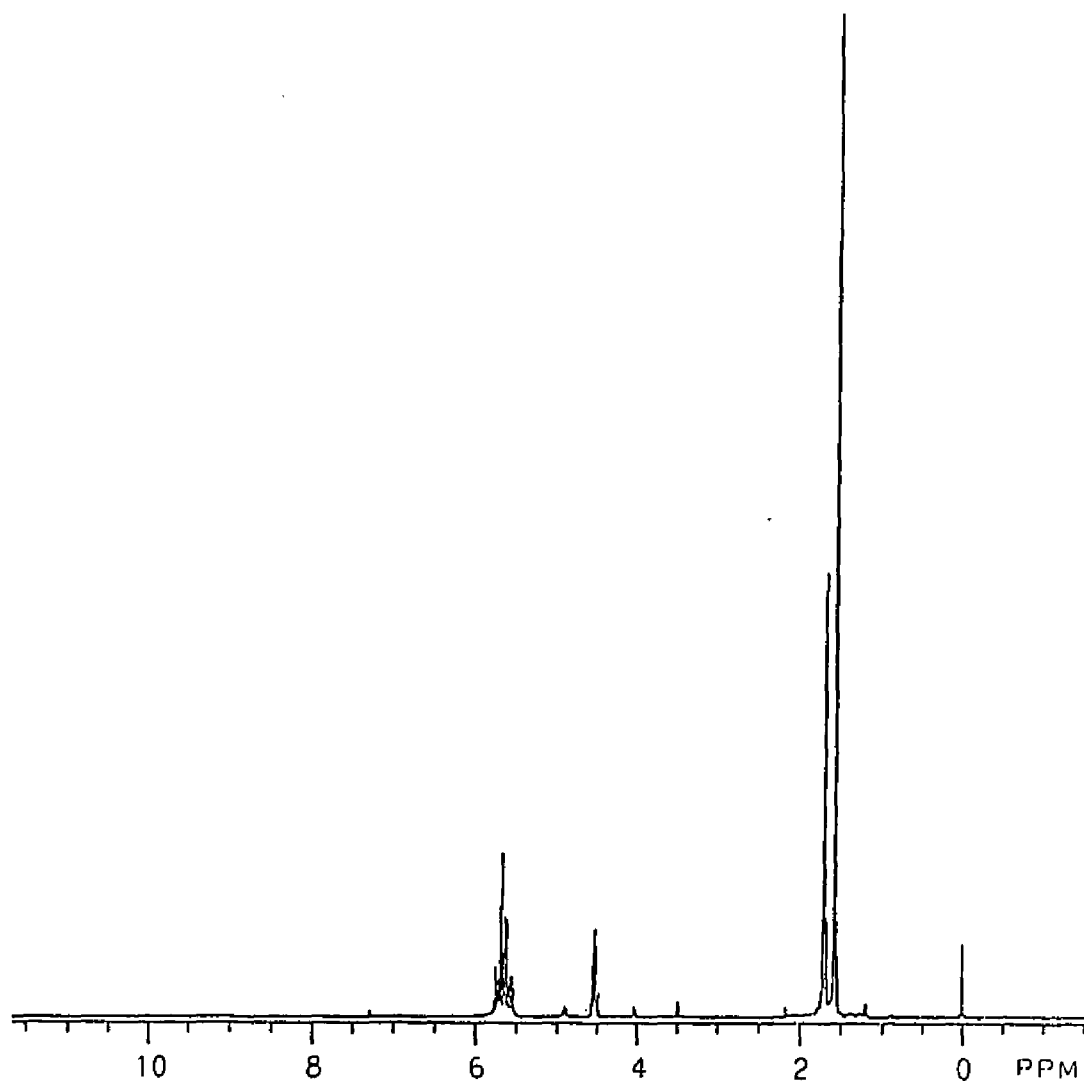
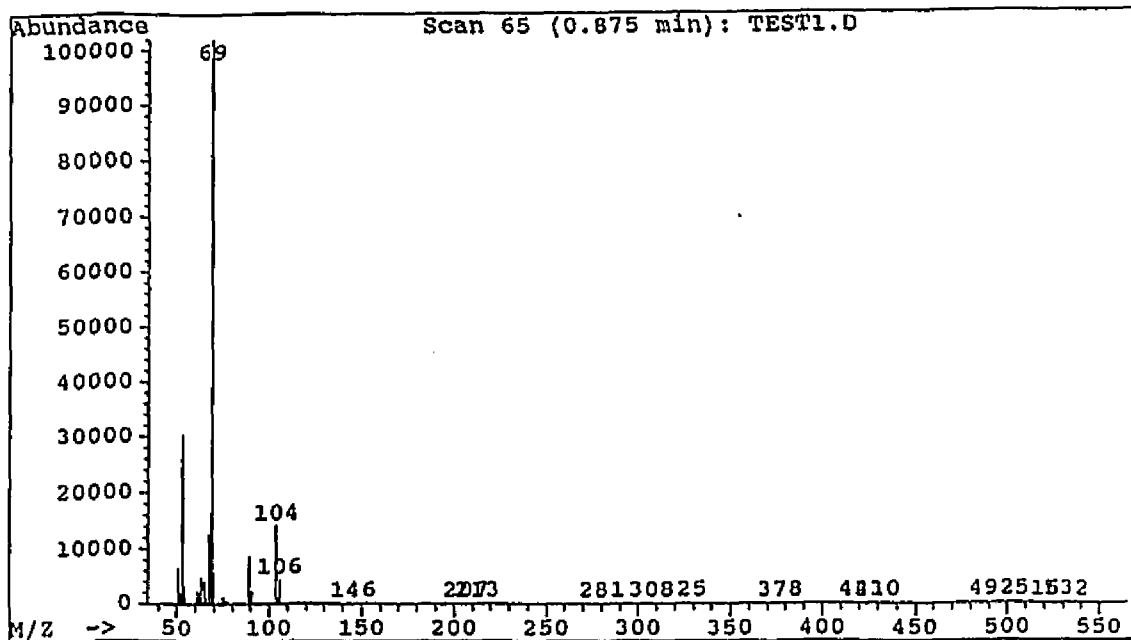
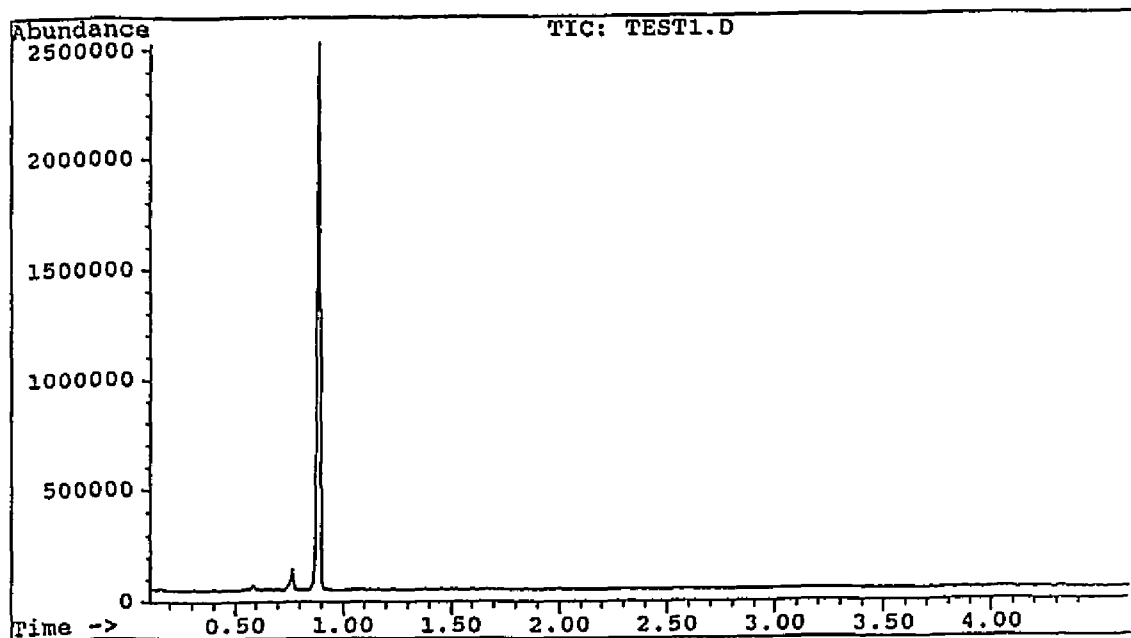


Figure 6. ^1H NMR spectrum of trans-4-chloro-2-pentene.

Figure 7. GC/MS data for trans-4-chloro-2-pentene.

to ^{37}Cl) with one-third the intensity of the peak at m/e 104 establishes the presence of one chlorine atom in the compound.

3. Synthesis of $\text{CuI}\cdot\text{P}(\underline{n}\text{-Bu})_3$

The copper complex was prepared by the method of Kauffman and Teter⁷¹ from tri-n-butylphosphine and copper(I) iodide. In a 500-mL Erlenmeyer flask, CuI (13.15 g, 69 mmol) was dissolved in a solution prepared from 130 g of KI and 100 mL of H_2O . The solution was shaken with a small amount of activated carbon (about 1 g) to remove the light yellow color, then filtered with suction, and transferred into a 250-mL Erlenmeyer flask. Next, $\text{P}(\underline{n}\text{-Bu})_3$ (12.5 mL, 50 mmol) was added via syringe into the clear solution with vigorous stirring, and the formation of a greasy yellow material was noted when the addition was complete. The solution was brought to gentle boiling by a heating plate for 1 min, allowed to cool to room temperature, and filtered with suction to collect the light yellow crystals, which were washed with three 50-mL portions of saturated potassium iodide solution in order to remove any remaining copper(I) iodide. They then were washed in succession with two 100-mL portions of DI water and one 50-mL portion of 95% ethanol. After air-drying, the crude crystals were obtained in a

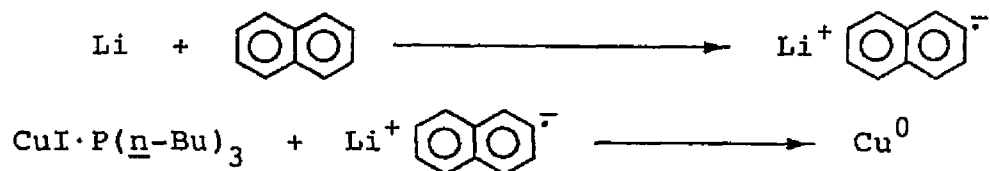
yield of 19.00 g (96%). They were purified by recrystallization from a boiling mixture of 115 mL of ethanol and 75 mL of isopropyl alcohol, first cooling slowly to room temperature without shaking and then cooling in an ice-water bath. The resultant rod-shaped white crystals were recovered by suction filtration and washed with three 50-mL portions of fresh solvent (95% ethanol) before being subjected to two further recrystallizations according to the same procedure. After air-drying in vacuo (25 °C, 4 torr) overnight, they weighed 9.30 g and had a melting point of 75±1 °C.⁷¹ The crystals were refrigerated in a dry, air-tight brown bottle until needed and were used as soon as possible.

4. Preparation of Lithium Naphthalenide

The lithium naphthalenide was prepared according to a procedure described by Ginah and coworkers.⁷² In an argon drybox lithium metal wire (0.08 g, 11 mg-atom) was first washed several times with hexanes to remove mineral oil, then cut into several small pieces and put into a flame-dried 50-mL two-necked round-bottom flask along with a slight excess of naphthalene (1.54 g, 12 mmol). One neck of the flask was capped with a silicone rubber septum, and another was attached to a condenser that was fitted with a two-way connector which led to an argon source

and a gas bubbler. The system was purged with dry argon for 5 min; then 10 mL of THF, freshly distilled from Na/benzophenone, was syringed into the flask, and stirring was commenced. Stirring was continued at 25 °C for at least two hours until the lithium metal had completely dissolved. The resultant dark green solution of lithium naphthalenide was kept in a dry argon atmosphere and used as soon as possible.

5. Preparation of Activated Copper Slurry



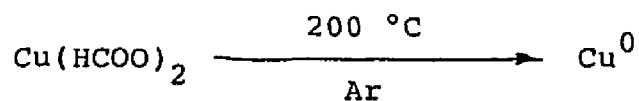
The highly reactive copper metal slurry (high-surface-area copper) was prepared according to the procedure described by Rieke and Hudnall.⁷² Under a flow of dry argon, $\text{CuI} \cdot \text{P}(\underline{n}\text{-Bu})_3$ (3.93 g, 10 mmol) was placed into a flame-dried 50-mL two-necked round-bottom flask equipped with a condenser, a silicone rubber septum, and a small Teflon-clad stirring bar. The condenser was fitted with a two-way connector which led to an argon source and a gas bubbler. The $\text{CuI} \cdot \text{P}(\underline{n}\text{-Bu})_3$ was dissolved by syringing into the flask freshly distilled anhydrous THF (10 mL)

or anhydrous ethyl ether (10 mL). The preformed dark green lithium naphthalenide solution (11 mmol) was then drawn up into a syringe and quickly injected into the stirred solution of $\text{CuI}\cdot\text{P}(\underline{n}\text{-Bu})_3$, which was kept at 0 °C by an ice-water bath. After approximately one minute, a dark brown activated copper slurry was formed and was ready for use in subsequent reactions. The activated copper could be kept for at least 30 min and used with only a slight loss of reactivity, but for best results, it should be used as soon as possible.

To remove any unchanged lithium naphthalenide from the activated copper slurry, an ultracentrifugation technique was employed. Under an argon atmosphere a freshly prepared slurry (5 mL, 2.50 mmol) was transferred via a flame-dried syringe (flushed with argon before use) into a flame-dried 10-mL test tube (filled with argon) and equipped with a rubber stopper. The slurry was diluted with 5 mL of anhydrous ethyl ether that was added via a flame-dried syringe. The mixture was then shaken for 10 s and subjected to ultracentrifugation at 3200 rpm for 3-5 min. After careful removal of 5 mL of ether from the solution by syringe, a fresh 5-mL portion of anhydrous ether was added, and the ultracentrifugation was repeated as before. This washing procedure was repeated several times. Its success depended upon the careful protection of the solution from external air and moisture, and it

was performed within the shortest possible period of time. It was judged to be complete when GC/MS analysis showed that no trace of naphthalene was present. The test tube then contained a thick black slurry of reductant-free activated copper, which was used immediately for subsequent reactions.

6. Production of Activated Copper Film



The production of activated copper film in a solid-state reaction was based on the early studies of the pyrolysis of metal formates conducted by Körösy.⁶⁶ Copper(II) formate (1.50 g, 9.80 mmol) was first finely ground with the aid of an agate mortar and pestle and then placed into a 50-mL two-necked round-bottom flask. The flask had one neck attached directly to an argon source. The other neck was attached to a two-necked glass joint having one outlet connected to a gas bubbler and the other capped with a rubber septum. The glass joint was packed with glass wool and Drierite to absorb the water produced during the pyrolysis of the copper(II) formate. Under a

constant flow of dry argon (9 psi, 120 mL/min), the flask was heated with a Bunsen burner to approximately 200 °C until a red smoke was evolved. At this point the heating was continued for another 10 s while a brilliant mirror of metallic copper was deposited on the bottom surface of the flask. The copper film was allowed to cool to room temperature and then was used immediately for subsequent reactions.

7. Reactions of Model Organic Halides with Activated Copper Slurry

A model organic halide (10 mmol) or a mixture of two such halides (5 mmol of each) was injected quickly via a glass syringe into an activated copper slurry (10 mmol) with vigorous stirring under an argon atmosphere. The resultant mixture was allowed to react for 5 min, then subjected to workup procedures and analyzed by GC/MS.

In the case of the activated copper slurry from which any unchanged lithium naphthalenide had been removed by repetitive washing, a model organic halide (2.5 mmol) or a mixture of two such halides (1.25 mmol of each) was injected via syringe into the 10-mL test tube containing the slurry (2.5 mmol). The resultant mixture was analyzed immediately (within 5 min) by GC/MS. No workup procedures

were performed in this experiment.

Workup: At the end of the reaction period, HCl (0.01 M, 25 mL) was added into the resultant mixture. The mixture was stirred for 1 min and transferred to a separatory funnel. The organic layer was then collected immediately and subjected to GC/MS analysis. Identities of the products were established by comparing them to authentic commercial samples or to products prepared from coupling reactions between organolithium reagents and the corresponding organic halides.

8. Reactions of Model Organic Halides with Activated Copper Film

A brilliant copper mirror generated by pyrolysis of copper(II) formate (1.50 g, 9.8 mmol) was allowed to cool to room temperature, and a model organic halide (9.8 mmol) or a mixture of two such halides (4.9 mmol of each) was injected quickly onto the mirror under a constant flow of argon (9 psi, 120 mL/min). The reactants were swirled for about one minute to ensure maximum surface contact between the copper film and the model compound(s); then the reaction products were immediately (within 5 min) subjected to GC/MS analysis without workup procedures. Identities of the coupled products were established

according to the methods described above in Section 7.

9. Reactions of Activated Copper with PVC in Solution

All of the requisite glassware was dried overnight in an oven and allowed to cool under argon. A 250-mL three-necked round-bottom flask was charged with 2.00 g of PVC and a Teflon stirring bar. This flask was equipped with a silicone rubber septum (for injections), a high-temperature thermometer, and a Liebig condenser (height, 400 mm) that was attached to a two-way connector leading to a gas bubbler and an argon source. The desired solvent (50 mL) was added by syringe to the reaction vessel under argon, and stirring was commenced.

For control experiments without activated copper, the stirred PVC solution was brought to gentle reflux for the desired length of time (depending upon the solvent used) by using a heating mantle. After cooling to room temperature, the solution was subjected to workup procedures.

For reactions involving activated copper slurry, the PVC solution was brought to gentle reflux first, and the freshly formed dark brown slurry (20 mmol) then was injected by syringe immediately into the reaction flask. Low-boiling solvent from the slurry distilled off rapidly,

and the reaction was subsequently allowed to proceed for different lengths of time that depended upon the solvent used for each experiment. At the end of the heating time, the mixture was allowed to cool to room temperature and subjected to workup procedures.

In the case of reactions involving activated copper film, a different procedure was used. A high-boiling-point solvent (phenyl ether, 50 mL, bp 257-259 °C) was introduced into a 250-mL three-necked round-bottom flask along with 2.00 g of PVC powder and 1.00 g of copper(II) formate. The mixture was stirred vigorously under argon and brought to gentle reflux (between 250 and 259 °C) by a heating mantle. A brilliant mirror was generated around the bottom of the flask after two to three minutes of heating, and some gel was formed at once. The reaction was then allowed to proceed for an additional 10 min before the mixture was subjected to workup procedures.

Workup: To collect any crosslinked PVC (gel), the mixture was first poured into a 500-mL beaker containing a Teflon stirring bar and 400 mL of THF. The gel which stayed on the walls of the reaction flask was scraped off and added to the beaker. Then the contents of the beaker were stirred overnight and filtered with suction on a Büchner funnel. Next, the collected gel was subjected to Soxhlet extraction with THF for 24 h. In the case of experiments with activated copper slurry or film, prior

to Soxhlet extraction the gel was washed three times with 250-mL portions of concentrated ammonium hydroxide to eliminate any remaining copper(II) species. [The formation of the blue ammonia copper(II) complex, $\text{Cu}(\text{NH}_3)_6^{+2}$, served as an indication of Cu(II) residues left in the gel.] Finally, the gel was dried in a vacuum oven at 60 °C and 4 torr for 24 h, then weighed for gel content calculations. [In the case of reactions involving activated copper film, corrections were made by subtracting 0.10 g from the final gel weight for any possible Cu^0 and Cu(I) residues left in the gel in order to determine the actual weight of PVC gel.]

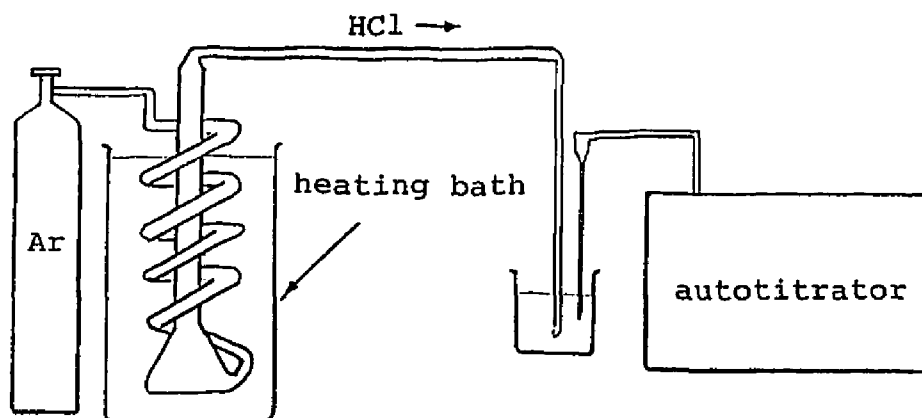
The gel content was calculated according to the following equation:

$$\text{Gel Content} = \frac{\text{corrected weight of PVC gel (g)}}{\text{initial weight of PVC (g)}} \times 100\%$$

10. Thermal Degradation of PVC with Copper Additives

10-1. Measurements of the Rate of PVC Dehydrochlorination

To determine the rate of dehydrochlorination during thermal degradation of PVC, a technique involving an intermittent titration by alkali of hydrogen chloride absorbed in water was used.⁷³⁻⁷⁷ In our experiments, a Pyrex glass apparatus with a coiled tube for preheating the inlet argon gas was used as shown below. The inlet



of the coiled tube was located at the bottom of the degradation flask (25 mL), and the evolved HCl was swept by argon to the top of the flask and then into a capillary tube, from which it was bubbled into a 150-mL beaker containing 100 mL of DI water. The pH of the water was

adjusted to 7.00 with aqueous sodium hydroxide (0.0101-0.0099 N) before the degradation experiment was started, and it was kept at that value throughout the entire degradation process by intermittent titration with the automatic titrator containing the aqueous sodium hydroxide solution (0.0101-0.0099 N). The dehydrochlorination rates were determined from tangents, drawn at a chosen reaction extent, of plots of the amount of evolved hydrogen chloride vs. reaction time.

The thermal degradation of PVC with a copper additive was carried out by placing the PVC sample (1.00 g) with the additive (0.10 g) into the apparatus described above. The PVC and the additive had previously been pulverized and mixed thoroughly with the aid of an agate mortar and pestle. The degradation vessel was first purged with argon for 30 min at a rate of 80 mL/min and then immersed into a thermostated silicone oil bath which had been previously adjusted to the degradation temperature (200 ± 2 °C) by a thermal controller. The amount of HCl gas evolved was followed closely for 3 h by intermittent titration with standard alkali, using the Brinkmann autotitrator (see above), while the rate of the purging argon was kept at 80 mL/min (9 psi) throughout the degradation process.

The rate of dehydrochlorination was calculated according to the following equations:

$$\text{Loss of HCl} = \frac{[0.01(N) \times V(\text{mL}) \times 10^{-3} \times 36.5(\text{g/mol})]}{1.00 \text{ (g)}} \times 100$$

$$= (0.0365V)\%$$

(V = total volume of NaOH used for titration)

$$\text{or } d[\text{HCl}]/dt = \frac{0.01(N) \times V(\text{mL}) \times 10^{-3}}{1.00 \text{ (g)} \times t \text{ (min)}} \quad (\text{mol/g-min})$$

10-2. Determination of the Gel Content of Degraded PVC

At the end of the degradation, the reaction flask was allowed to cool to room temperature under argon, and the degraded PVC was removed by scraping with a copper wire. Gel remaining in the flask was rinsed out with THF. All of the degraded PVC (gel) was combined, placed in a Whatman cellulose thimble (internal diameter x length = 33 x 118 mm) and subjected to Soxhlet extraction with THF for 24 h under nitrogen. Finally, the gel was oven-dried at 60 °C under 4 torr for 24 h and weighed. The weight of PVC gel was corrected by subtracting the net weight of thimble and the copper additive, and the gel content was calculated according to the following equation:

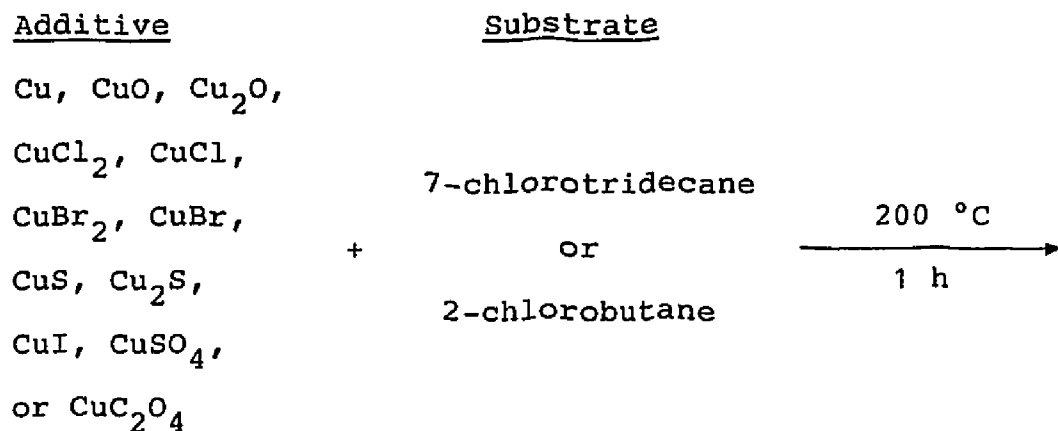
$$\text{Gel Content} = \frac{\text{corrected weight of insoluble gel (g)}}{\text{initial weight of PVC (1.00 g)}} \times 100\%$$

11. PVC Model-Compound Pyrolysis Experiments

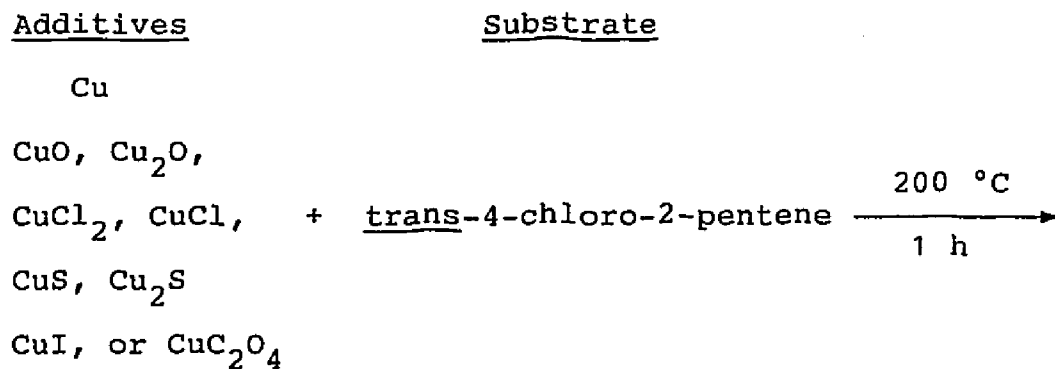
11-1. General Information

All of these reactions were conducted on a small scale. Typically, a PVC model compound (0.10 mL) or a mixture of two PVC model compounds (0.05 mL of each) was mixed with a copper additive (0.01 g) and placed into a borosilicate glass ampule (volume, 5 mL; diameter, 16.5 mm; height, 84 mm). The ampule was then degassed by the freeze-pump-thaw technique and sealed under high vacuum (1×10^{-4} torr, two cycles). The pyrolysis experiment was carried out by immersing the entire ampule in a silicone oil bath at 200 ± 2 C° for 1 h. At the end of the pyrolysis, the ampule was allowed to cool to room temperature, then immersed in liquid nitrogen and opened with a score file. Immediately after the ampule had returned to room temperature, the resultant mixtures were analyzed by GC/MS. In some cases where the mixtures were too viscous for direct analysis or contained very little liquid, a small amount of THF (about 0.5 mL) was added as an extraction solvent.

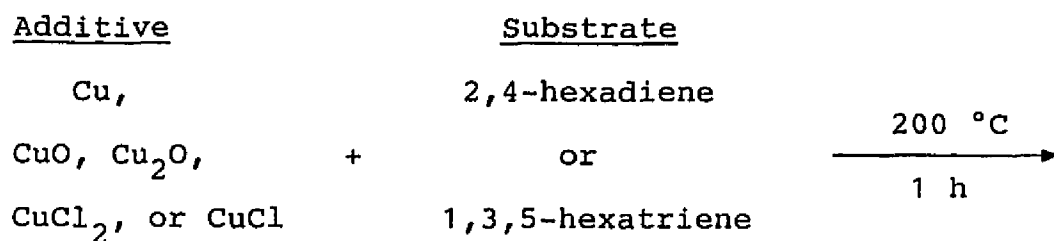
11-2. Reactions of Simple Secondary Chlorides with Copper
Additives



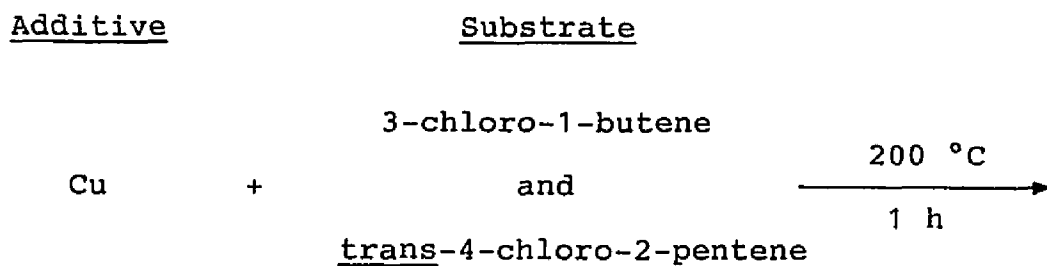
11-3. Reactions of a Secondary Allylic Chloride with Copper
Additives



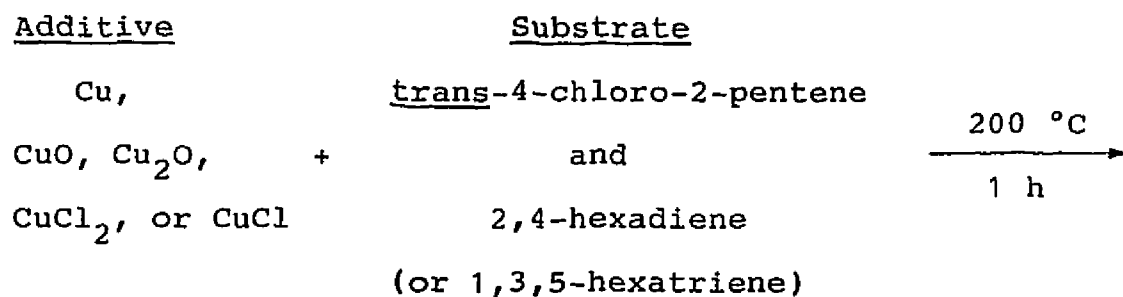
11-4. Reactions of Conjugated Alkenes with Copper
Additives



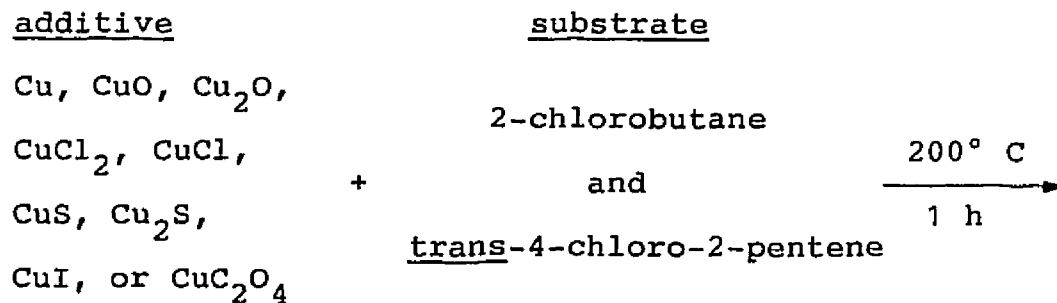
11-5. Reaction of a Mixture of Two Secondary Allylic
Chlorides with Copper Metal



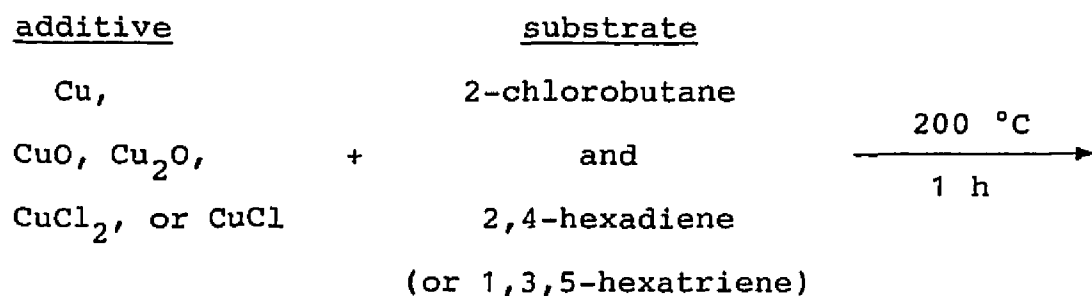
11-6. Reactions of a Mixture of a Secondary Allylic Chloride and a Conjugated Alkene with Copper Additives



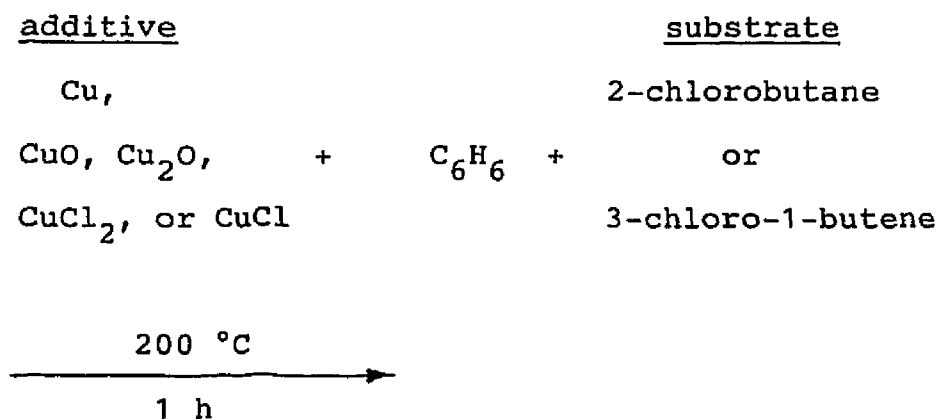
11-7. Reactions of a Mixture of a Simple Secondary Chloride and a Secondary Allylic Chloride with Copper Additives



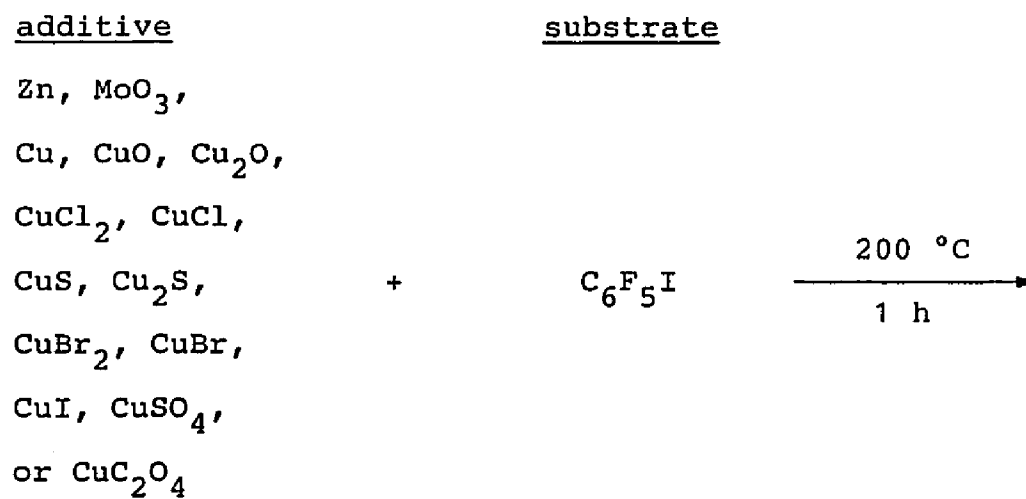
11-8. Reactions of a Mixture of a Simple Secondary Chloride
and a Conjugated Alkene with Copper Additives



11-9. Reactions of a Secondary Chloride and Benzene with
Copper Additives



11-10. Reactions of Iodopentafluorobenzene with Copper
Additives, Zinc Metal, or Molybdenum Trioxide



12. Instrumental Analysis

12-1. (Gas Chromatography)-(Mass Spectroscopy) (GC/MS)

The GC/MS analyses were performed on either a Hewlett-Packard HP 5980A/5988A apparatus or an HP 5890/5971A apparatus. Both GC instruments were temperature programmable and were equipped with thermal conductivity detectors. Two fused-silica capillary GC columns were used: column I (HP-5) consisted of diphenyl- (5%) and dimethylpolysiloxane (95%); column II (HP-1) consisted entirely of dimethylpolysiloxane. Both mass spectrometers were equipped with a mass selective detector, a 70-eV electron-impact ion source, a hyperbolic quadrupole mass filter consisting of four hyperbolic molybdenum rods, and a continuous dynode electron multiplier. The carrier gas was He, and the GC injection port temperature was set in the range of 200-250 °C, depending upon the sample injected, in order to minimize dehydrochlorination during the analyses. The temperature program was set at a heating rate of 5-20 °C/min.

12-2. Thermogravimetric Analysis (TGA)

Thermogravimetric analysis was performed on a Seiko TG/DTA 220 instrument at a heating rate of 50 °C/min in air.

12-3. Infrared (IR) Spectroscopy

The IR spectra were recorded on a Perkin-Elmer 1600 Series FTIR spectrometer, using neat samples in NaCl cells or pressed into KBr pellets.

12-4. Nuclear Magnetic Resonance (NMR) Spectroscopy

Both ^1H and ^{13}C NMR spectra were recorded on a General Electric QE-300 (300 MHz for ^1H and 75 MHz for ^{13}C) FTNMR spectrometer that was interfaced with a Nicolet 1280 data processor. Chemical shifts were reported in ppm (δ) with Me_4Si as an internal reference ($\delta = 0.00$).

12-5. Acid-Base Titrimetry

Automatic titration of HCl was performed with a Brinkmann 702 SM Titrino titrator and aqueous NaOH solution (0.0101-0.0099 N).

12-6. Ultracentrifugation

Ultracentrifugation was performed with a centrifuge (Wilkins-Anderson Co.) at a speed of 3000 rpm for 3-5 min.

13. Chemicals

1. Copper, Cu, powder, 99.999%, d 8.920, Aldrich Chemical Company, Inc.
2. Copper(II) Oxide, CuO, 99.999+%, d 6.315, Aldrich Chemical Company, Inc.
3. Copper(I) Oxide, Cu₂O, 99.5%, 60 mesh, Alfa/Johnson Matthey Company.
4. Copper(II) Chloride, CuCl₂, 99.999%, mp 620 °C, d 3.386, Aldrich Chemical Company, Inc.
5. Copper(I) Chloride, CuCl, 99.995%, mp 430 °C, d 4.140, Aldrich Chemical Company, Inc.
6. Copper(II) Bromide, CuBr₂, 99%, mp 498 °C, d 4.770, Aldrich Chemical Company, Inc.
7. Copper(I) Bromide, CuBr, 98%, mp 504 °C, d 4.710, Aldrich Chemical Company, Inc.
8. Copper(II) Sulfide, CuS, 99+%, 100 mesh, Aldrich Chemical Company, Inc.
9. Copper(I) Sulfide, Cu₂S, d 5.600, Aldrich Chemical Company, Inc.
10. Copper(I) Iodide, CuI, 98%, mp 605 °C, d 5.620, Aldrich Chemical Company, Inc.
11. Copper(II) Formate, Cu(HCOO)₂, Pfaltz & Bauer, Inc.
12. Copper(II) Oxalate, CuC₂O₄·1/2 H₂O, Pfaltz & Bauer, Inc.
13. Copper(II) Sulfate, CuSO₄, 99.7%, Fisher Scientific.

14. Molybdenum Trioxide, MoO_3 , ACS Reagent Grade, ICN Biochemicals.
15. Molybdenum Carbonyl, $\text{Mo}(\text{CO})_6$, Pfaltz & Bauer, Inc.
16. Zinc, Zn, powder, 99.998%, 100 mesh, Aldrich Chemical Company, Inc.
17. Poly(vinyl chloride), powder, inherent viscosity 1.02, relative viscosity 2.40, Aldrich Chemical Company, Inc.
18. Magnesium Sulfate, MgSO_4 , anhydrous, Fisher Scientific.
19. Lithium, Li, wire, 99.9% in mineral oil, Aldrich Chemical Company, Inc.
20. Naphthalene, C_{10}H_8 , 99%, mp 80-82 °C, Aldrich Chemical Company, Inc.
21. Tri-n-butylphosphine, $\text{P}(\text{n-C}_4\text{H}_9)_3$, 99%, bp 150 °C/50 mm, d 0.812, Aldrich Chemical Company, Inc.
22. Hexanes, C_6H_{14} , bp 68-72 °C, Aldrich Chemical Company, Inc.
23. Tetrahydrofuran, $\text{C}_4\text{H}_8\text{O}$, bp 65.9-66.1 °C, Fisher Scientific.
24. Ethyl Ether, $\text{C}_4\text{H}_{10}\text{O}$, anhydrous, 99+%, bp 34.6 °C, Aldrich Chemical Company, Inc.
25. 2-Propanol, $\text{C}_3\text{H}_8\text{O}$, bp 82 °C, Fisher Scientific.
26. Ethyl Alcohol, $\text{C}_2\text{H}_6\text{O}$, 95%, bp 78 °C, denatured, Fisher Scientific.
27. Activated Carbon, 100 mesh, Aldrich Chemical Company, Inc.

28. Potassium Iodide, KI, 99%, mp 681 °C, d 3.130, Aldrich Chemical Company, Inc.
29. 3-Chloro-1-butene, C₄H₇Cl, 98%, bp 62-65 °C, d 0.900, Aldrich Chemical Company, Inc.
30. trans-3-Penten-2-ol, C₅H₁₀O, 96%, bp 119-121 °C, d 0.843, Aldrich Chemical Company, Inc.
31. Hexachloroacetone, C₃OCl₆, 99%, bp 66-70 °C/6 mm, d 1.743, Aldrich Chemical Company, Inc.
32. Triphenylphosphine, P(C₆H₅)₃, 99%, bp 377 °C, mp 79-81 °C, Aldrich Chemical Company, Inc.
33. N,N-Dimethylformamide, HCON(CH₃)₂, 99.8%, bp 153 °C, mp -61 °C, d 0.944, Aldrich Chemical Company, Inc.
34. 7-Tridecanol, C₁₃H₂₈O, 98%, Wiley Organics.
35. Thionyl Chloride, SOCl₂, 99+%, bp 79 °C, mp 105 °C, d 1.631, Aldrich Chemical Company, Inc.
36. Iodopentafluorobenzene, C₆F₅I, 99%, bp 161 °C, d 2.204, Aldrich Chemical Company, Inc.
37. Deuterium Oxide, D₂O, 99.9 atom % D, d 1.107, Aldrich Chemical Company, Inc.
38. α-Chloro-p-xylene, C₈H₉Cl, 99%, bp 200 °C, d 1.062, Pfaltz & Bauer, Inc.
39. 2,4-Hexadiene, C₆H₁₀, 99%, bp 82 °C, d 0.729, Aldrich Chemical Company.
40. 2-Methoxyethyl Ether, C₆H₁₄O₃, 99+%, bp 162 °C, mp -64 °C, d 0.937, Aldrich Chemical Company, Inc.

41. Benzyl Bromide, C_7H_7Br , 98%, bp 198-199 °C, mp -3 to -1 °C, d 1.438, Aldrich Chemical Company, Inc.
42. Phenyl Ether, $C_{12}H_{10}O$, 99+%, bp 259 °C, mp 26-30 °C, d 1.073, Aldrich Chemical Company, Inc.
43. Anisole, C_7H_8O , anhydrous, 99+%, bp 154 °C, d 0.995, Aldrich Chemical Company, Inc.
44. 1,2-Dichlorobenzene, $C_6H_4Cl_2$, 99%, bp 178 °C/763 mm, mp -18 to -17 °C, d 1.305, Aldrich Chemical Company, Inc.

RESULTS AND DISCUSSION

I. Study of Reductive Coupling via Activated Copper

1-1. Reactions of Model Organic Halides with Activated Copper

Early mechanistic studies conducted by Lattimer and Kroenke³⁰ suggested that zero-valent copper metal can promote reductive coupling reactions during thermal degradation of copper-containing PVC; and since copper metal in its bulk state is relatively unreactive, it became apparent that to conduct direct studies of the reductive coupling mechanism, an activated form of copper metal would need to be studied first. To investigate the effects of the activated copper (Cu^0) on PVC model organic halides, two different methods were used to produce the activated metal. The first method⁷⁰ involved the reduction of the $\text{CuI}\cdot\text{P}(\underline{n}\text{-Bu})_3$ complex by lithium naphthalenide in an ethereal solvent in order to give a finely divided (high-surface area) black copper powder suspended in the solvent (Cu^0 slurry). The second method involved the pyrolysis of

copper(II) formate powder to generate a highly reactive copper film.⁶⁶ Based on the results of GC/MS analyses, these two different forms of activated copper were shown to be able to promote rapid reductive coupling of organic halides under very mild conditions.

The results of the reactions of these forms of copper with a variety of organic halides are summarized in Tables 1-4. The most significant feature of these data is that both types of activated copper metal caused very rapid reductive coupling of primary and secondary allylic chlorides. Since allylic moieties were known to occur in both virgin and thermally degraded PVC specimens,⁷⁸⁻⁸¹ this finding suggested that activated copper would promote reductive coupling reactions readily among the PVC polymer chains as well, and that these coupling reactions could ultimately lead to the extensive crosslinking of the polymer.

In the case of the PVC model allylic chlorides, the GC/MS data for the homocoupled and cross-coupled products are shown in Figures 8-18. Interestingly, both 1-chloro-2-butene and 3-chloro-1-butene yielded exactly the same coupled products when treated with either one of the two different forms of activated copper. In addition to the coupling of the allylic chloride model compounds, the activated copper slurry and film both demonstrated their ability to promote similar rapid coupling of the highly

Table 1
Homocoupling of Organohalides with Activated Copper Slurry
at 0 °C in Ethyl Ether

entry	organic halide	product	yield ^a (%)
1	3-chloro-1-butene	C ₈ H ₁₄ ^b	54±2 (16±2)
2	1-chloro-2-butene	C ₈ H ₁₄ ^b	48±2 (22±1)
3	2-chlorobutane	C ₈ H ₁₈	28±3 (5±2)
4	1-chlorobutane	C ₈ H ₁₈	5±2 (0)
5	4-bromooctane	C ₁₆ H ₃₄	40±3 (6±2)
6	1-bromohexane	C ₁₂ H ₂₆	8±2 (3±1)
7	2-iodobutane	C ₈ H ₁₈	61±3 (25±3)
8	1-iodobutane	C ₈ H ₁₈	36±2 (8±3)
9	p-methylbenzyl chloride	C ₁₆ H ₁₈	47±1 (20±3)
10	benzyl bromide	C ₁₄ H ₁₄	41±3 (12±3)

a. GC area percentages based on amount of starting material; values shown are averages derived from duplicate runs; yields shown in parentheses were obtained from Cu⁰ freed of lithium naphthalenide reductant.

b. Mixtures of several isomers.

Table 2
Cross-Coupling of Organohalides with Activated Copper Slurry
at 0 °C in Ethyl Ether

entry	organic halides ^a	products ^b	yield ^c (%)
1	3-chloro-1-butene and <u>trans</u> -4-chloro- 2-pentene	C ₈ H ₁₄	18±2 (4±2)
		C ₉ H ₁₆	26±3 (2±1)
		C ₁₀ H ₁₈	33±3 (4±1)
2	3-chloro-1-butene and 2-chlorobutane	C ₈ H ₁₄	8±3 (4±2)
		C ₈ H ₁₆	18±2 (4±2)
		C ₈ H ₁₈	2±1 (0)
3	3-chloro-1-butene and 1-chlorobutane	C ₈ H ₁₄	25±2 (6±3)
		C ₈ H ₁₆	15±3 (4±2)
		C ₈ H ₁₈	2±1 (0)
4	2-chlorobutane and 1-chlorooctane	C ₈ H ₁₈	4±2 (0)
		C ₁₂ H ₂₆	0 (0)
		C ₁₆ H ₃₄	6±3 (0)
5	4-bromooctane and 1-bromohexane	C ₁₆ H ₃₄	23±3 (4±1)
		C ₁₄ H ₃₀	8±2 (2±1)
		C ₁₂ H ₂₆	2±1 (0)
6	3-chloro-1-butene and 4-bromooctane	C ₈ H ₁₄	30±3 (9±1)
		C ₁₂ H ₂₄	8±3 (2±1)
		C ₁₆ H ₃₄	6±2 (0)

(continued)

Table 2. Continued

entry	organic halides ^a	products ^b	yield ^c (%)
7	3-chloro-1-butene and 1-bromohexane	C ₈ H ₁₄	34±2 (12±3)
		C ₁₀ H ₂₀	7±2 (3±1)
		C ₁₂ H ₂₆	2±1 (0)
8	2-iodobutane and 1-iodohexane	C ₈ H ₁₈	21±2 (12±3)
		C ₁₀ H ₂₂	7±3 (2±1)
		C ₁₂ H ₂₆	13±1 (5±2)
9	3-chloro-1-butene and 2-iodobutane	C ₈ H ₁₄	33±3 (9±2)
		C ₈ H ₁₆	13±1 (4±1)
		C ₈ H ₁₈	9±1 (2±1)
10	3-chloro-1-butene and 1-iodobutane	C ₈ H ₁₄	38±2 (11±2)
		C ₈ H ₁₆	11±3 (7±1)
		C ₈ H ₁₈	12±3 (5±2)

a. Equimolar amounts of reactants.

b. Several isomers for C₈H₁₄, C₈H₁₆, C₉H₁₆, C₁₀H₁₈, C₁₀H₂₀,
and C₁₂H₂₄.

c. GC area percentages based on amount of starting material;
values shown are averages derived from duplicate runs;
yields shown in parentheses were obtained from Cu⁰ freed
of lithium naphthalenide reductant.

Table 3
Homocoupling and Cross-Coupling of Organohalides with
Activated Copper Slurry at 67 °C in THF

entry	organic halide(s)	product(s) ^a	yield ^b (%)
1	3-chloro-1-butene	C ₈ H ₁₄	19±2
2	<u>trans</u> -4-chloro-2-pentene	C ₁₀ H ₁₈	36±3
3	3-chloro-1-butene and <u>trans</u> -4-chloro-2-pentene	C ₈ H ₁₄	24±2
		C ₉ H ₁₆	30±1
		C ₁₀ H ₁₈	23±2
4	4-chlorooctane	C ₁₆ H ₃₄	7±3
5	3-chloro-1-butene and 4-chlorooctane	C ₈ H ₁₄	20±2
		C ₁₂ H ₂₄	5±2
		C ₁₆ H ₃₄	0
6	7-chlorotridecane	C ₂₆ H ₅₄	9±2
7	3-chloro-1-butene and 7-chlorotridecane	C ₈ H ₁₄	28±2
		C ₁₇ H ₃₄	2±1
		C ₂₆ H ₅₄	0

a. Several isomers for C₈H₁₄, C₉H₁₆, C₁₀H₁₈.

b. GC area percentages based on amount of starting material; values shown are averages derived from duplicate runs.

Table 4
Homocoupling and Cross-Coupling of Organohalides with
Activated Copper Film at 25 °C

entry	organic halide(s)	products ^a	yield ^b (%)
1	3-chloro-1-butene	C ₈ H ₁₄	20±2
2	1-chloro-2-butene	C ₈ H ₁₄	30±3
3	<u>trans</u> -4-chloro-2-pentene	C ₁₀ H ₁₈	24±2
4	3-chloro-1-butene and <u>trans</u> -4-chloro-2-pentene	C ₈ H ₁₄	26±1
		C ₉ H ₁₆	12±3
		C ₁₀ H ₁₈	24±2
5	p-methylbenzyl chloride	C ₁₆ H ₁₈	21±2
6	benzyl bromide	C ₁₄ H ₁₄	14±3

a. Several isomers for C₈H₁₄, C₉H₁₆, and C₁₀H₁₈.

b. GC area percentages based on amount of starting material; values shown are averages derived from duplicate runs.

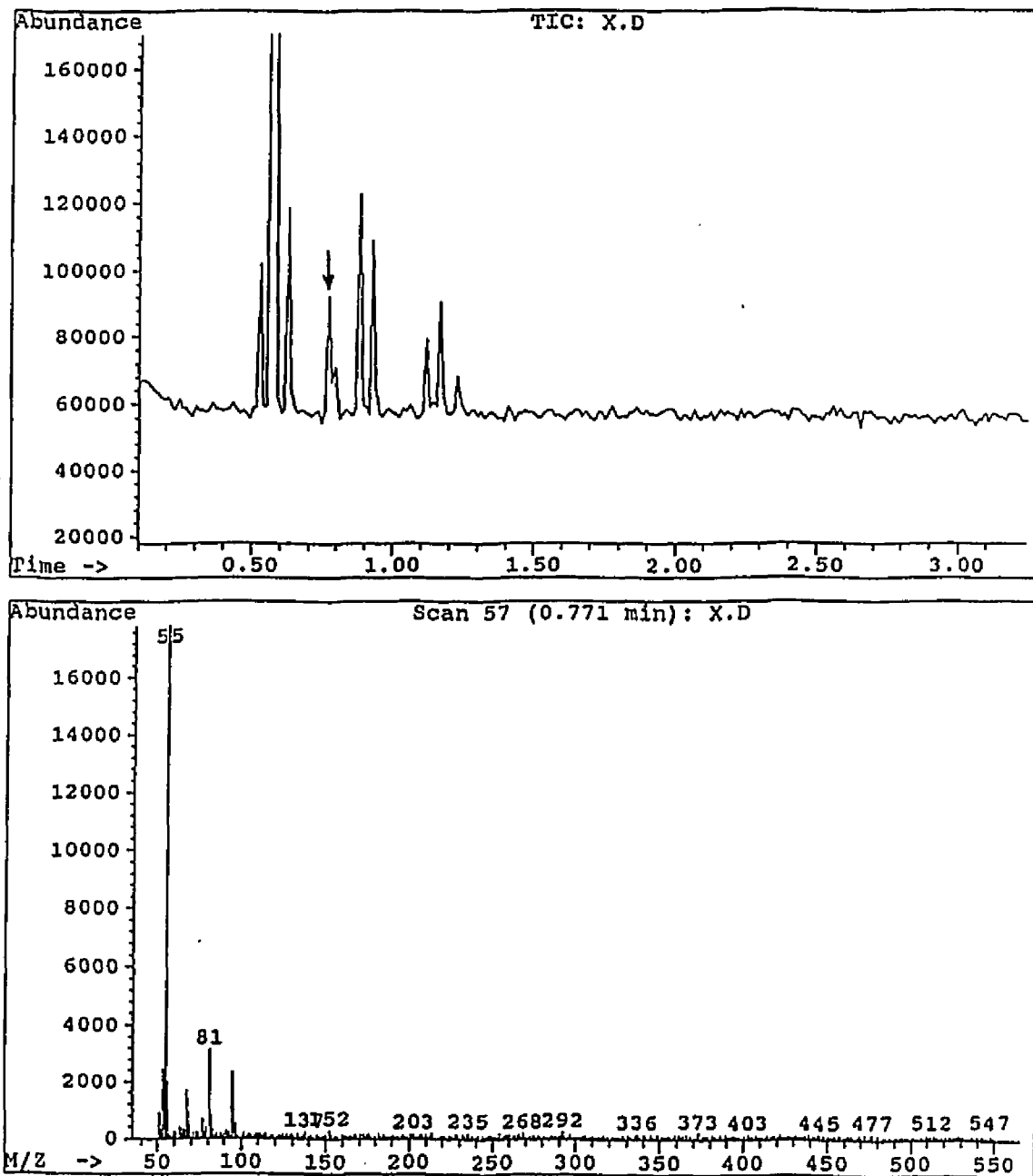
Figure 8. GC/MS data for C_8H_{14} 

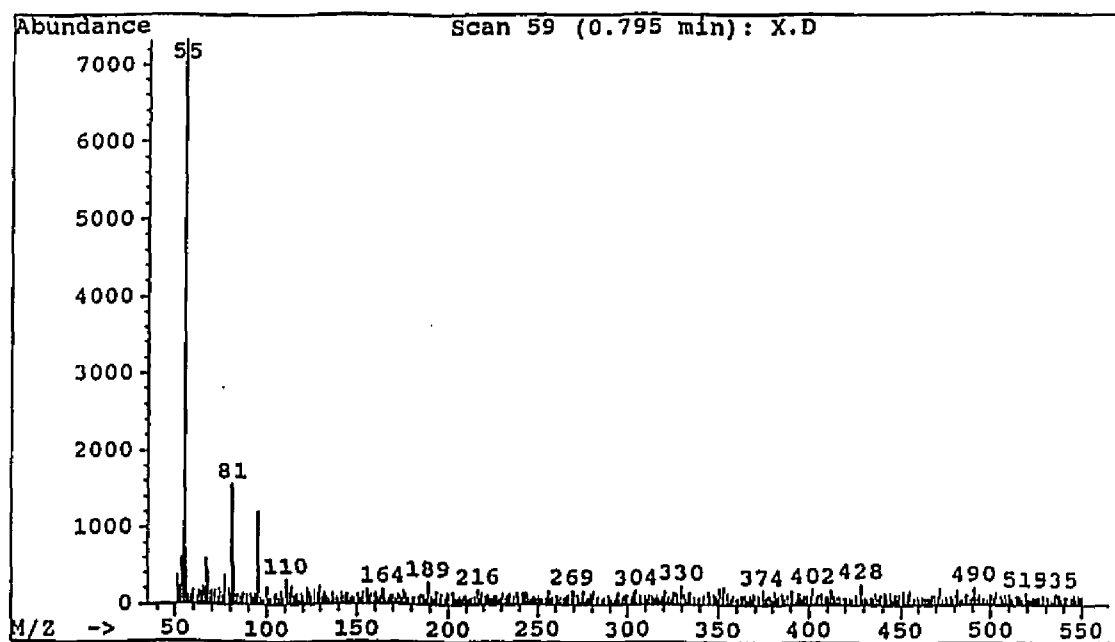
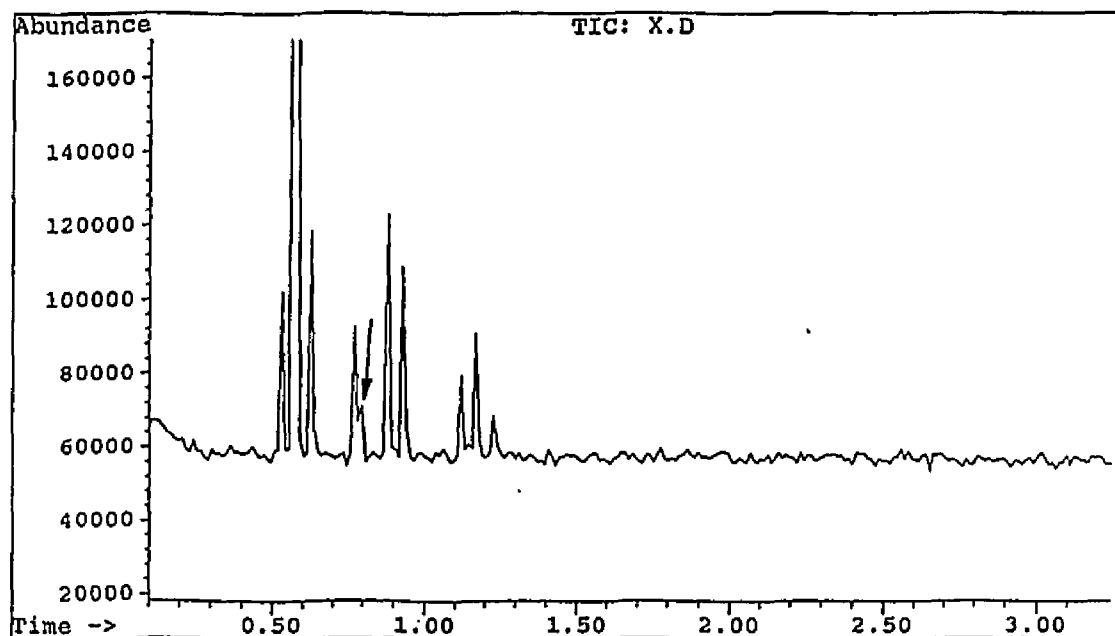
Figure 9. GC/MS data for C_8H_{14} 

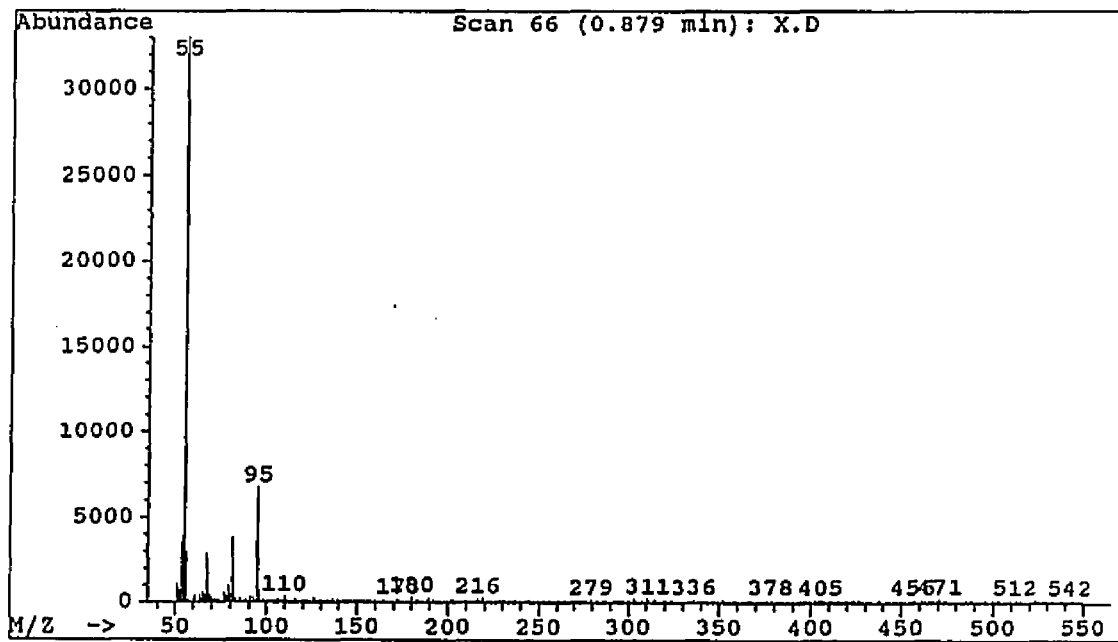
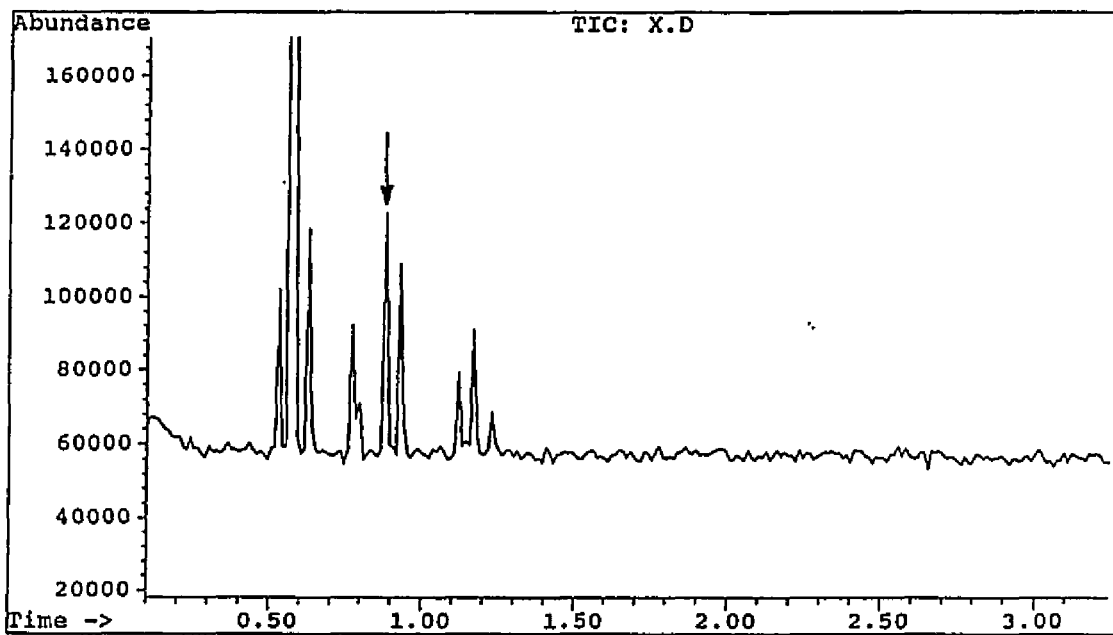
Figure 10. GC/MS data for C_8H_{14} 

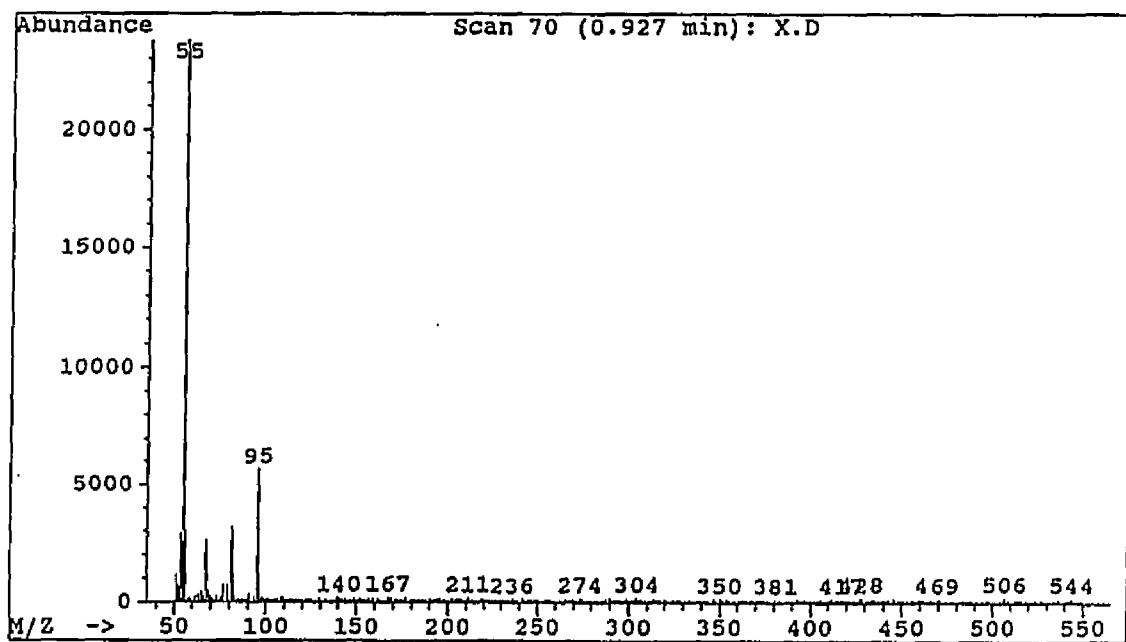
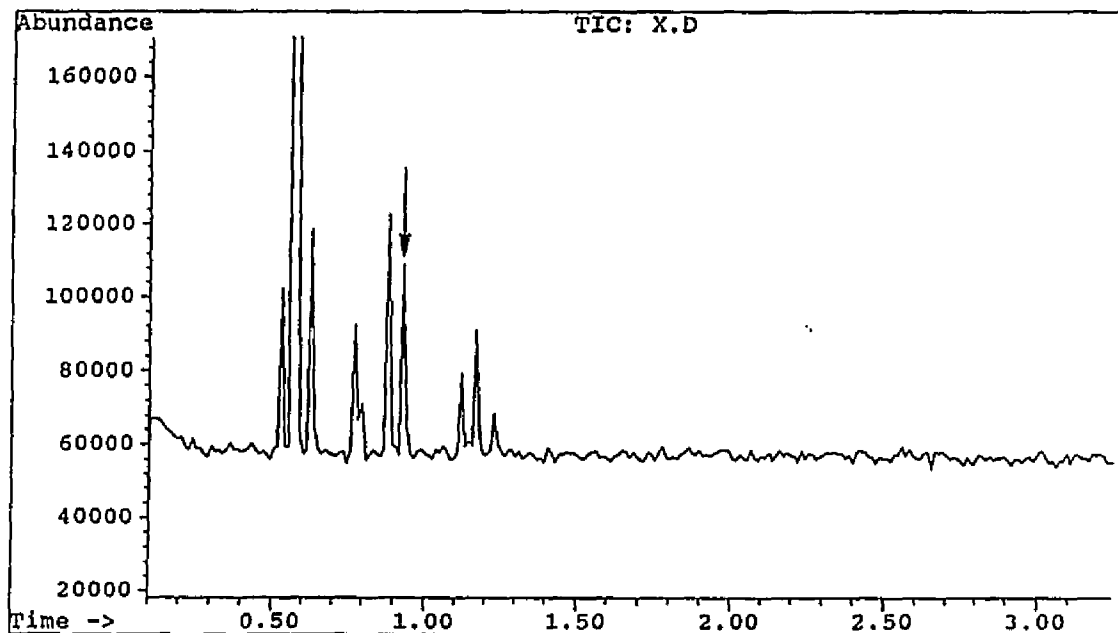
Figure 11. GC/MS data for C_8H_{14} 

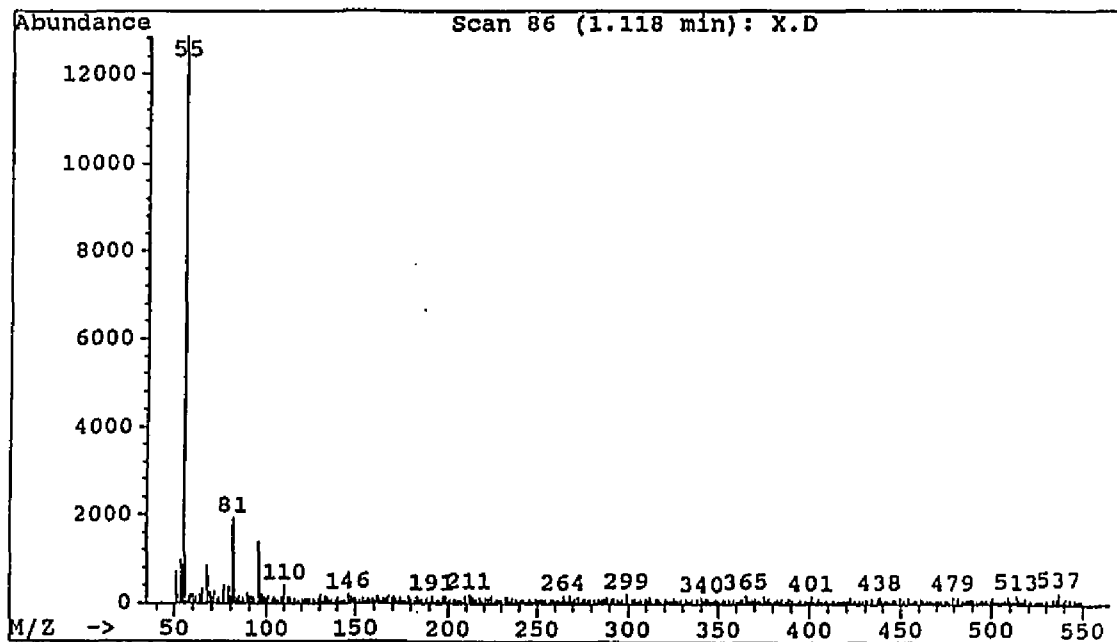
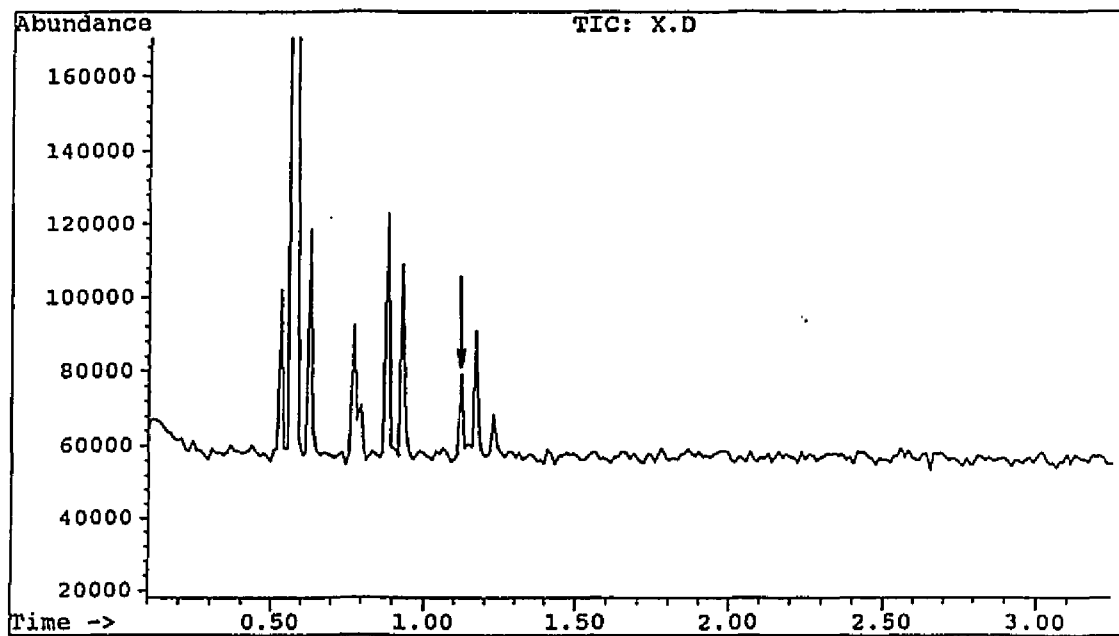
Figure 12. GC/MS data for C_8H_{14} 

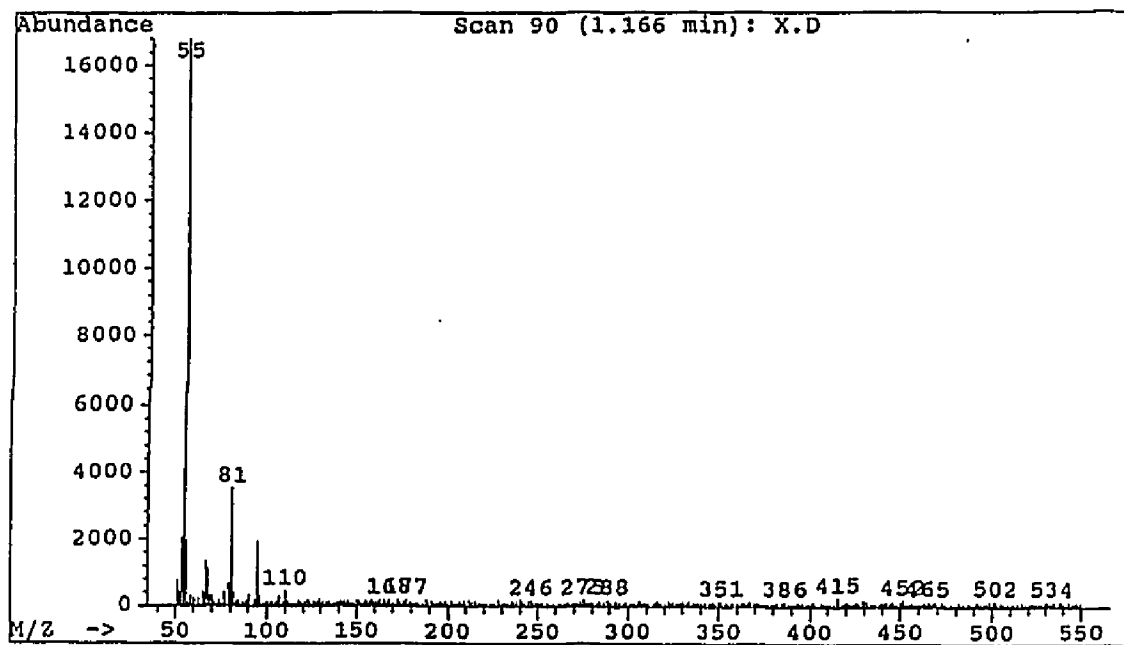
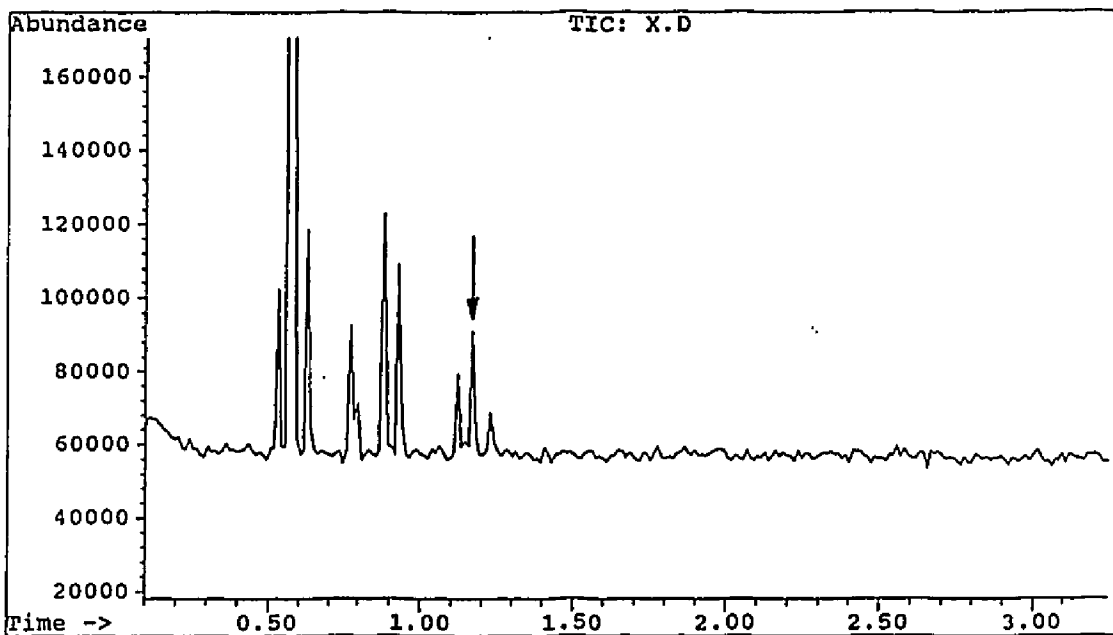
Figure 13. GC/MS data for C_8H_{14} 

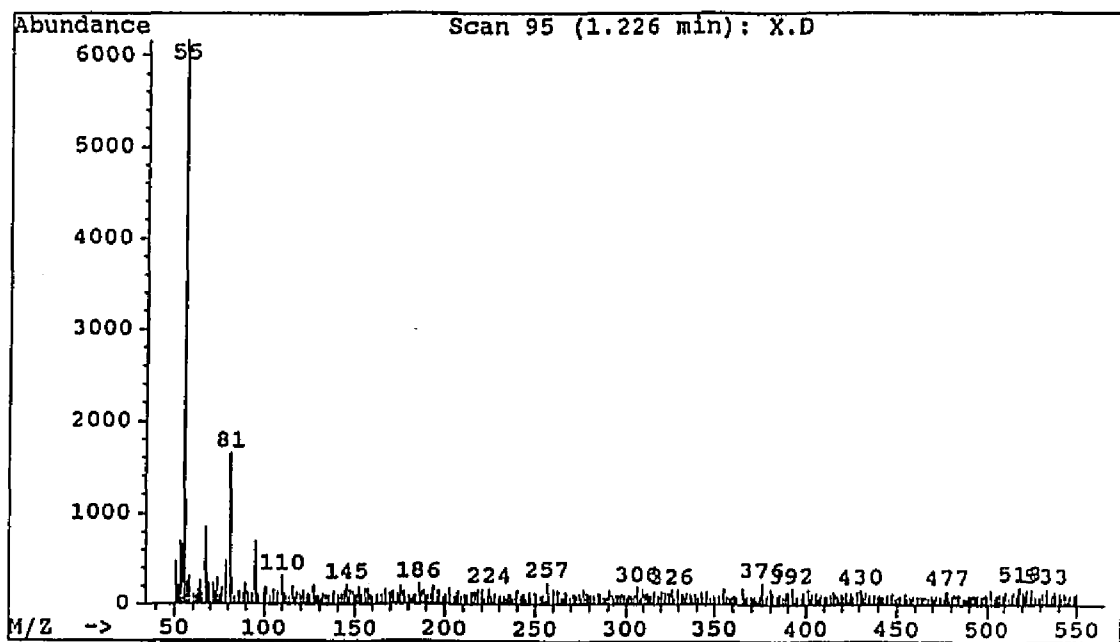
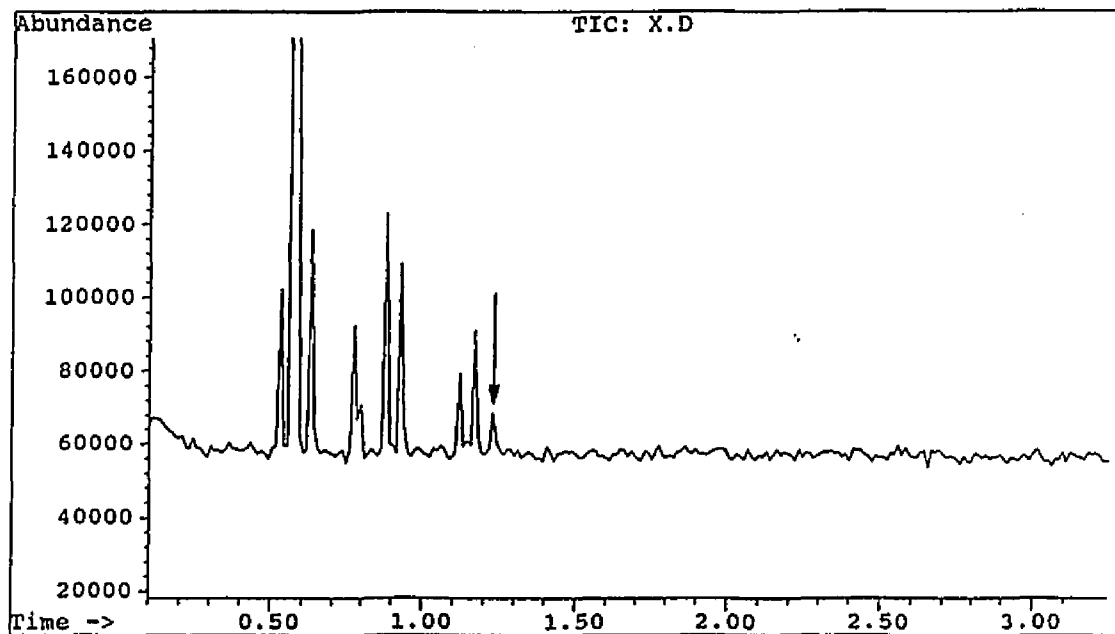
Figure 14. GC/MS data for C_8H_{14} 

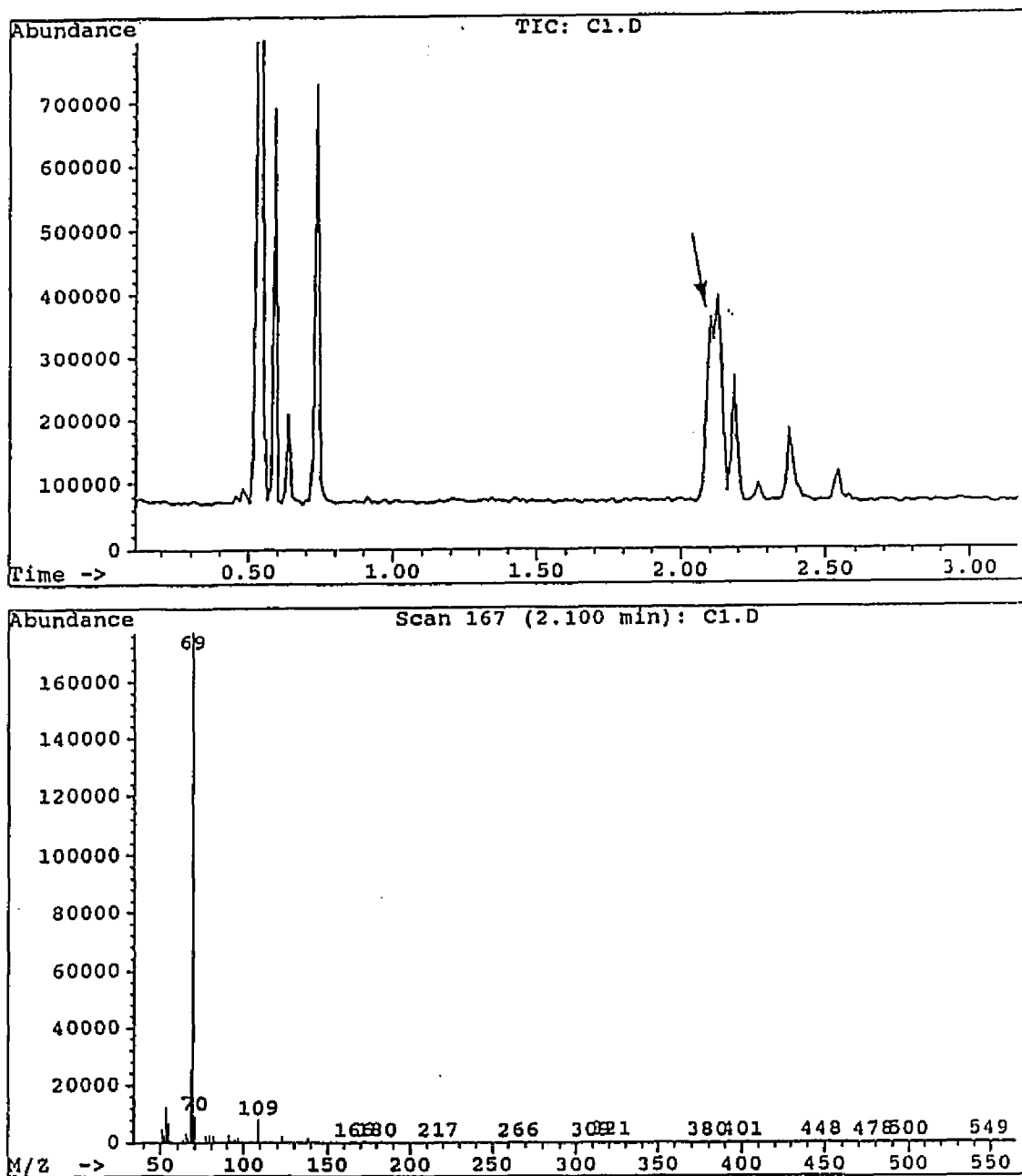
Figure 15. GC/MS data for $C_{10}H_{18}$ 

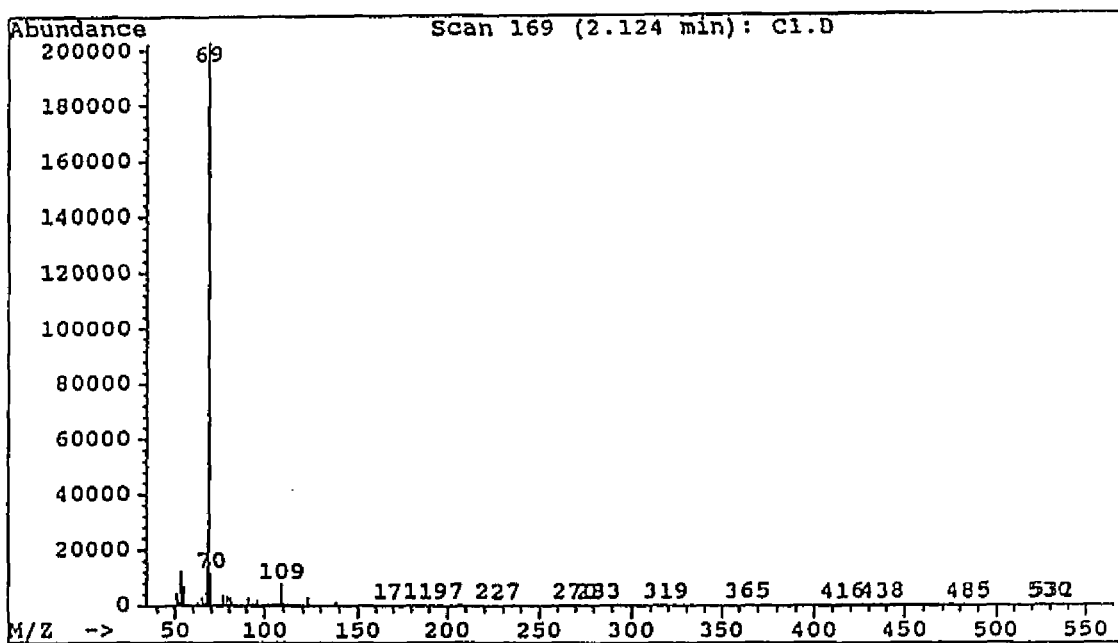
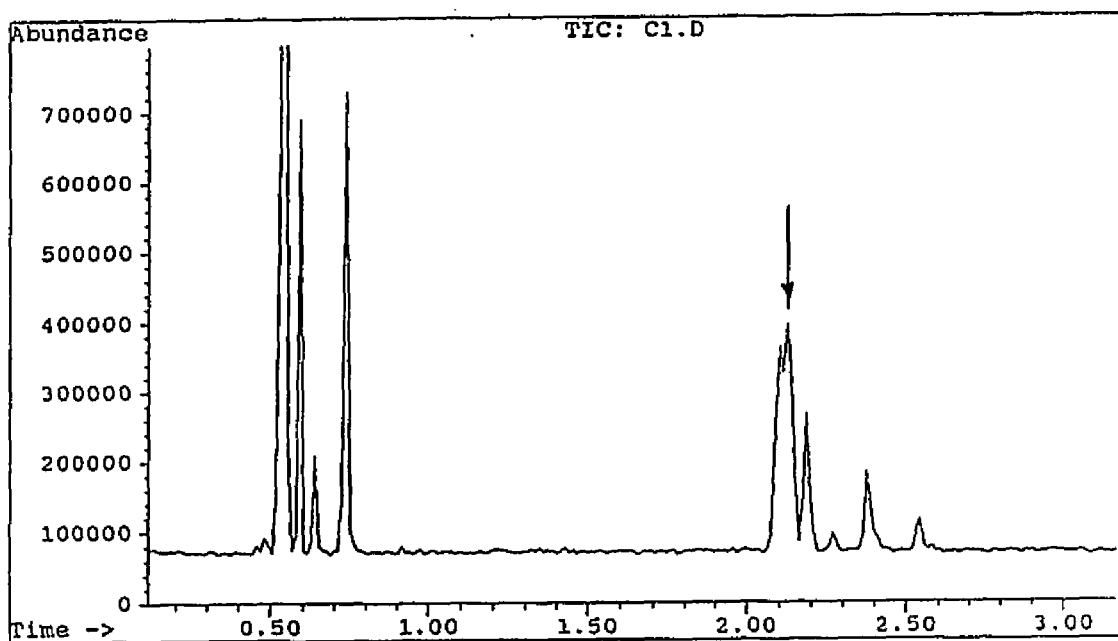
Figure 16. GC/MS data for $C_{10}H_{18}$ 

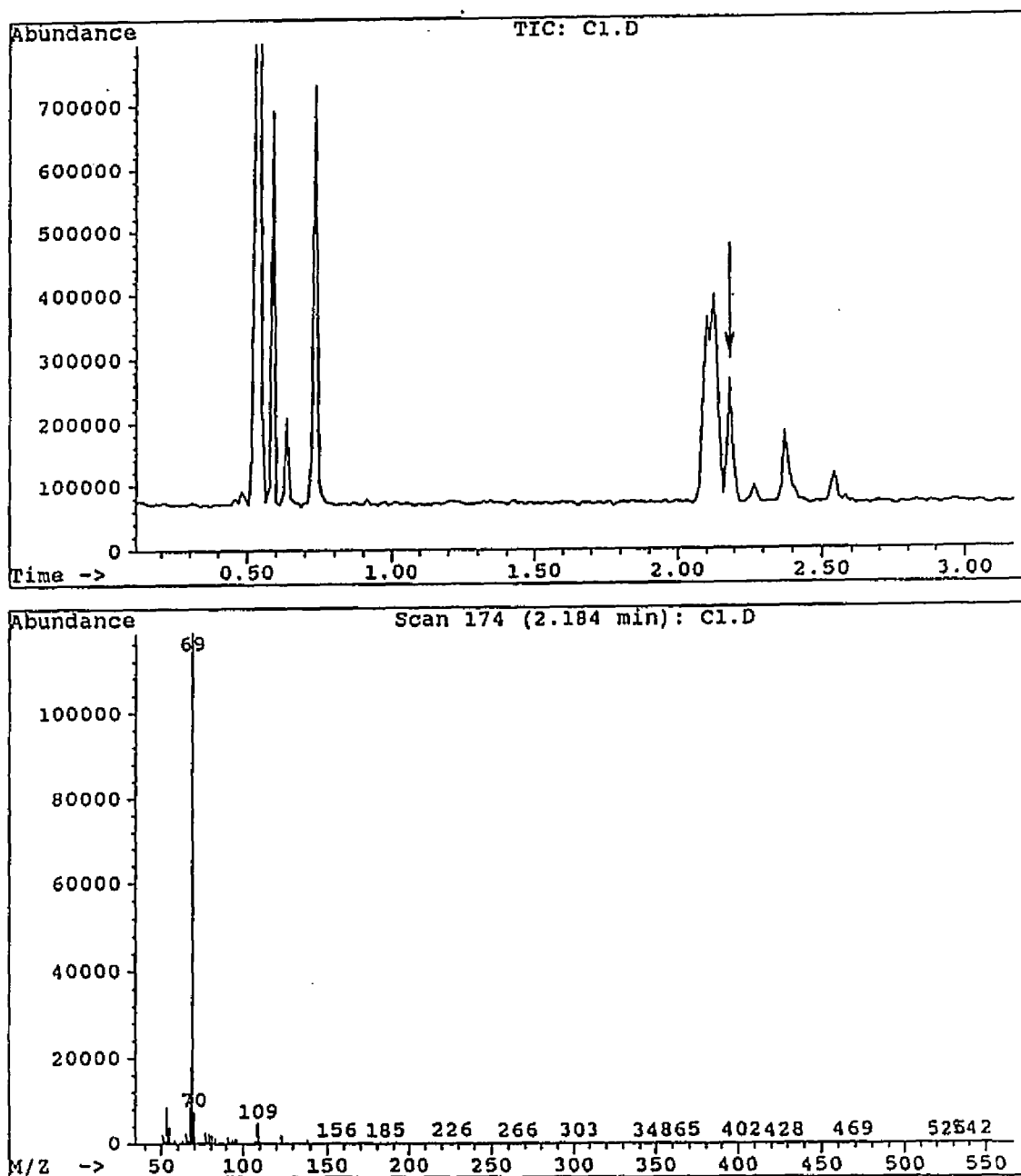
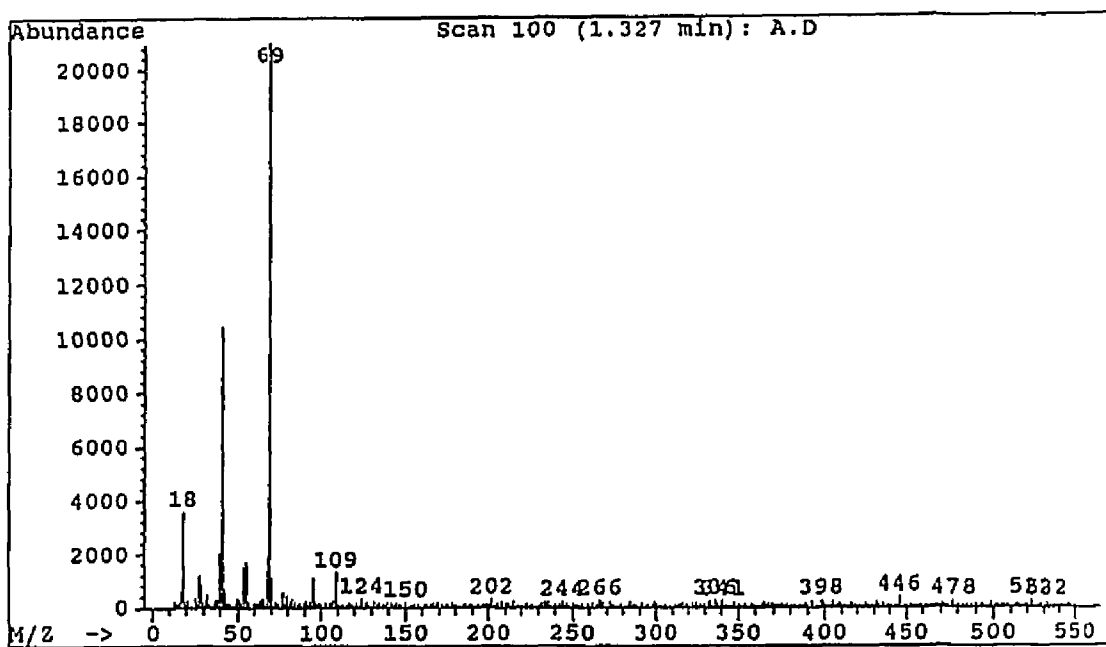
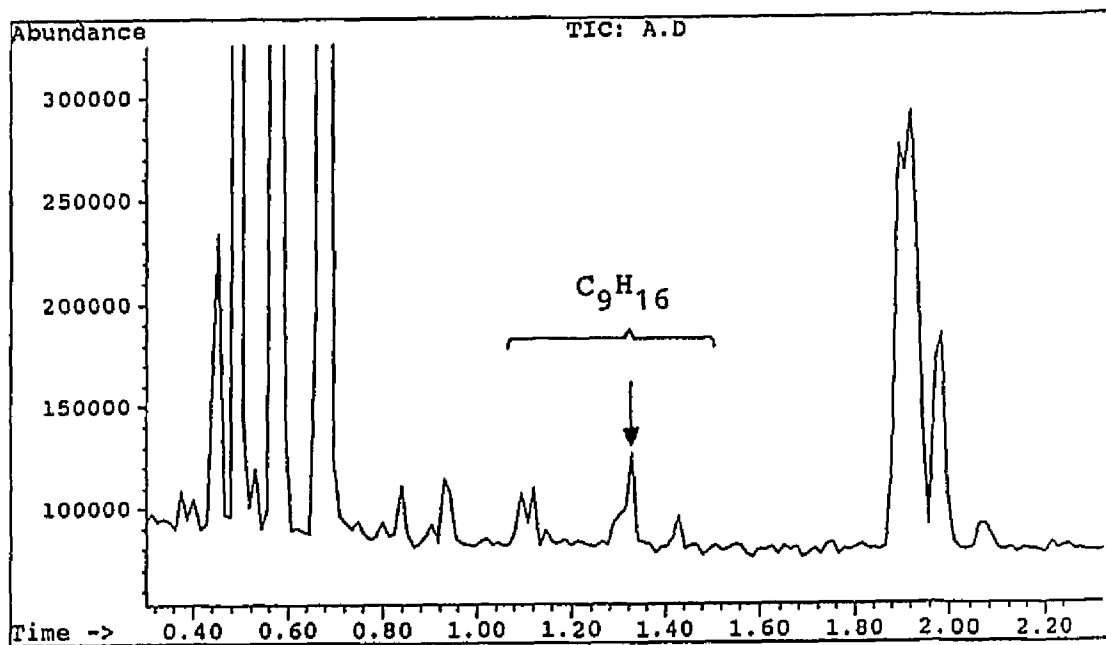
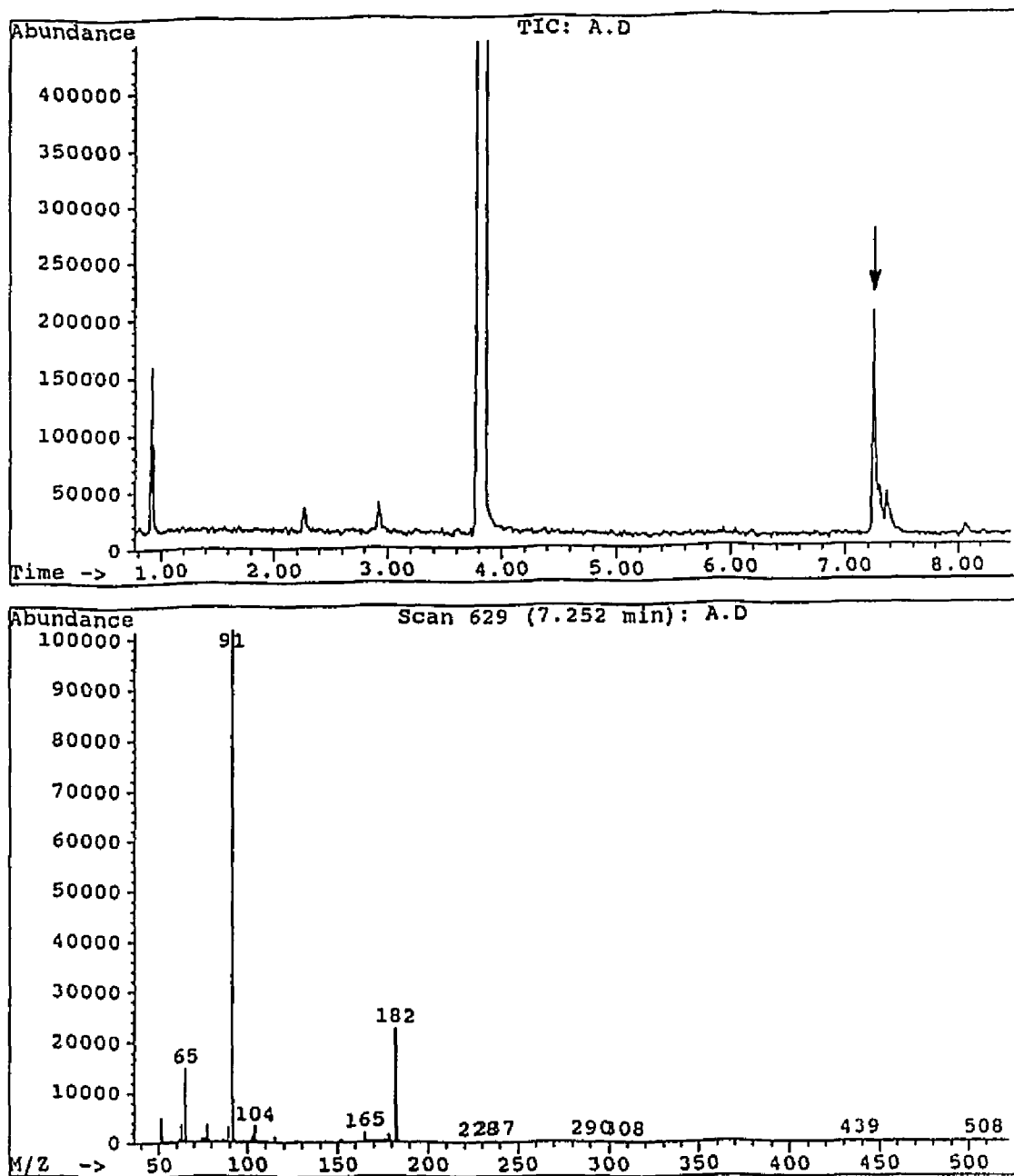
Figure 17. GC/MS data for $C_{10}H_{18}$ 

Figure 18. GC/MS data for C_9H_{16} 

reactive benzyl halides as well. The GC/MS data and both the ^1H and ^{13}C NMR spectra for the coupled products $(\text{C}_6\text{H}_5\text{CH}_2)_2$ and $(\text{CH}_3\text{C}_6\text{H}_4\text{CH}_2)_2$ are shown in Figures 19-24.

The activated copper metal slurry was shown to be able to promote the rapid (within less than 1 min) reductive coupling of a wide variety of organic monohalides (chlorides, bromides, or iodides), including simple secondary chlorides, at temperatures ranging from 0 to 67 °C in low to moderate yields (see Tables 1-3). These results were consistent, in general, with the earlier activated copper studies conducted by Rieke, Ebert, and other workers.^{64,65}

As shown by the GC/MS information in Figures 8-14, a total of seven isomeric coupled products was obtained in the reaction of activated copper slurry with 3-chloro-1-butene. Although complete spectroscopic characterizations were not available for all of these products, their GC retention times and the ion fragment patterns in the mass spectra clearly indicated that they were indeed formed by reductive coupling. Moreover, the production of seven isomers can be rationalized according to a reaction scheme involving a radical intermediate (Scheme 17). Based on this scheme, the assignment of all seven peaks in the GC chromatogram (see Figures 8-14) can be tentatively made. As the GC chromatogram shows, the seven peaks can be divided into three groups. The left side and the middle part of

Figure 19. GC/MS data for $C_6H_5CH_2CH_2C_6H_5$ 

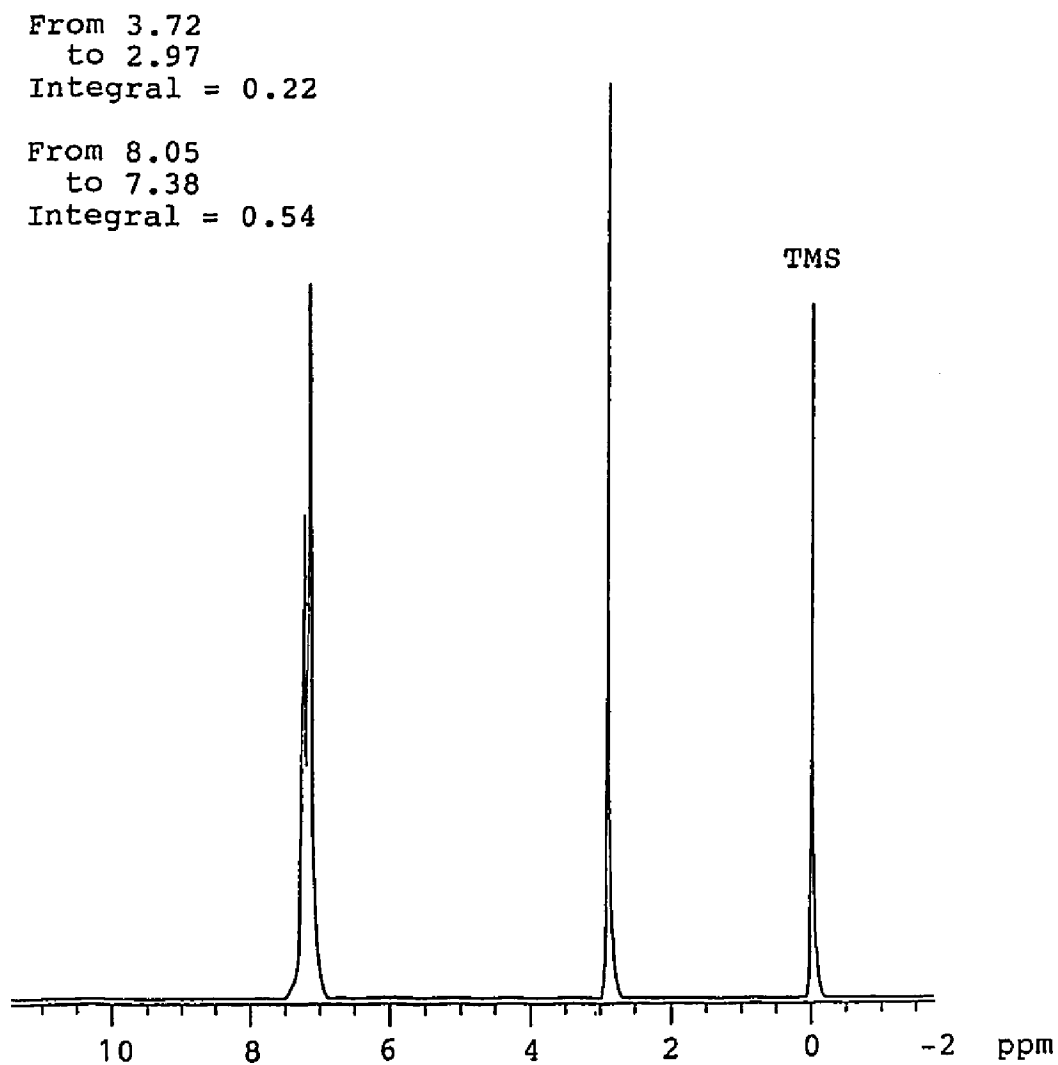


Figure 20. ^1H NMR spectrum for $\text{C}_6\text{H}_5\text{CH}_2\text{CH}_2\text{C}_6\text{H}_5$

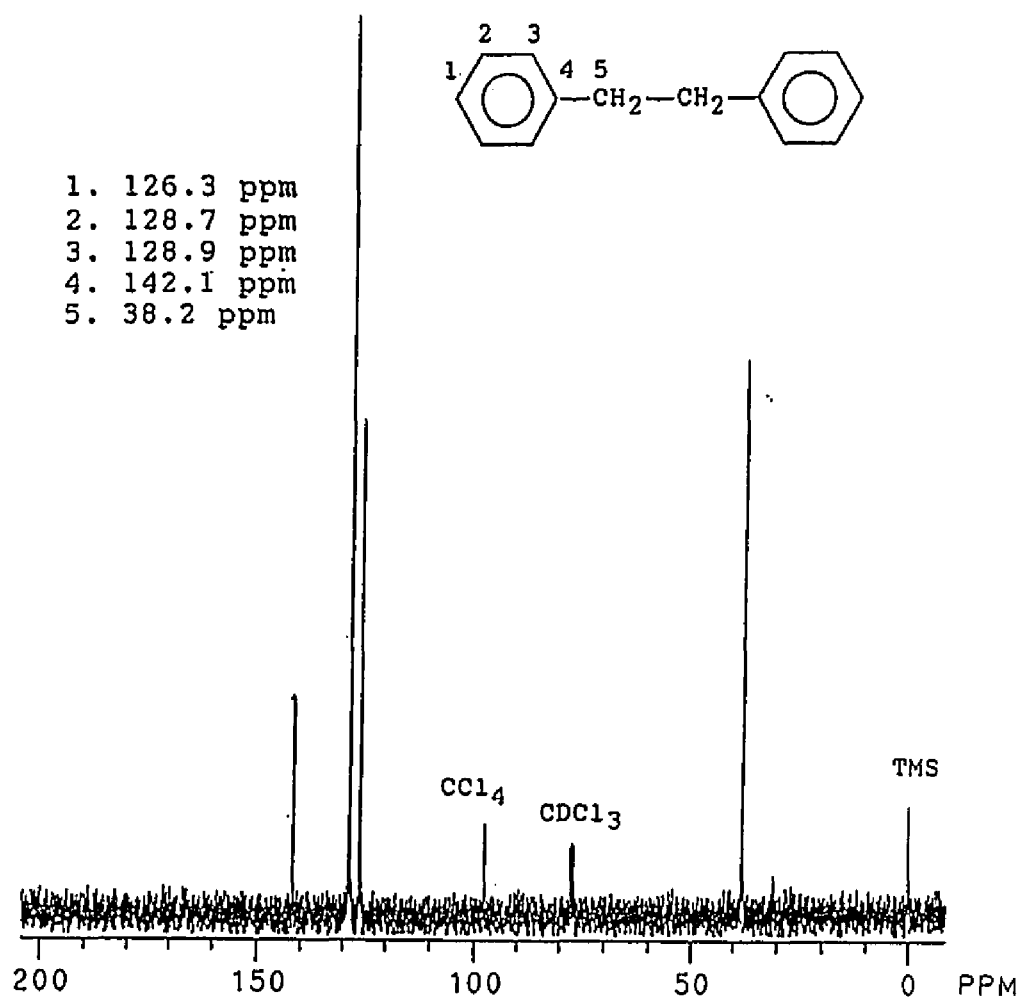
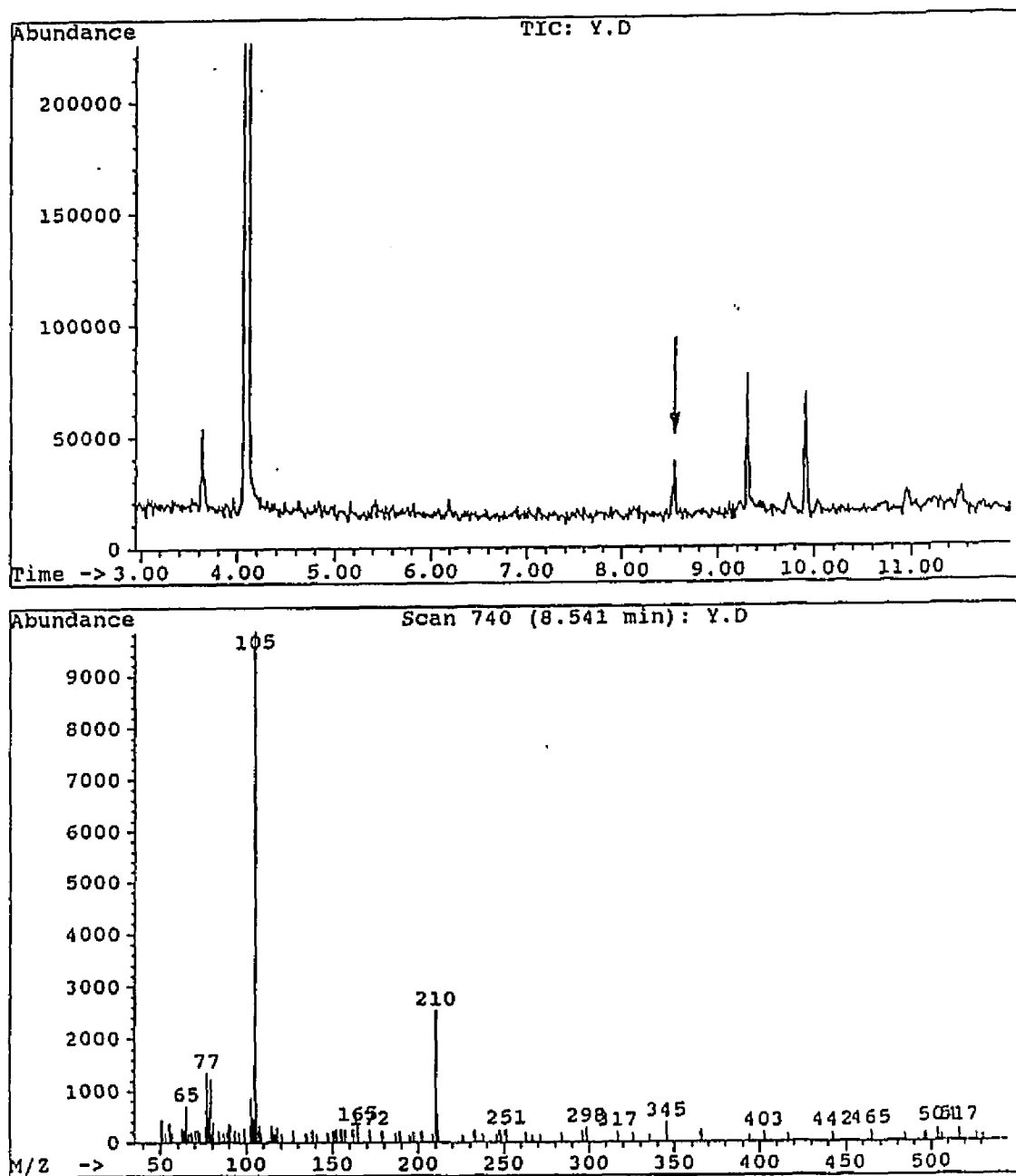


Figure 21. ^{13}C NMR spectrum for $\text{C}_6\text{H}_5\text{CH}_2\text{CH}_2\text{C}_6\text{H}_5$

Figure 22. GC/MS data for $\text{CH}_3\text{C}_6\text{H}_4\text{CH}_2\text{CH}_2\text{C}_6\text{H}_4\text{CH}_3$ 

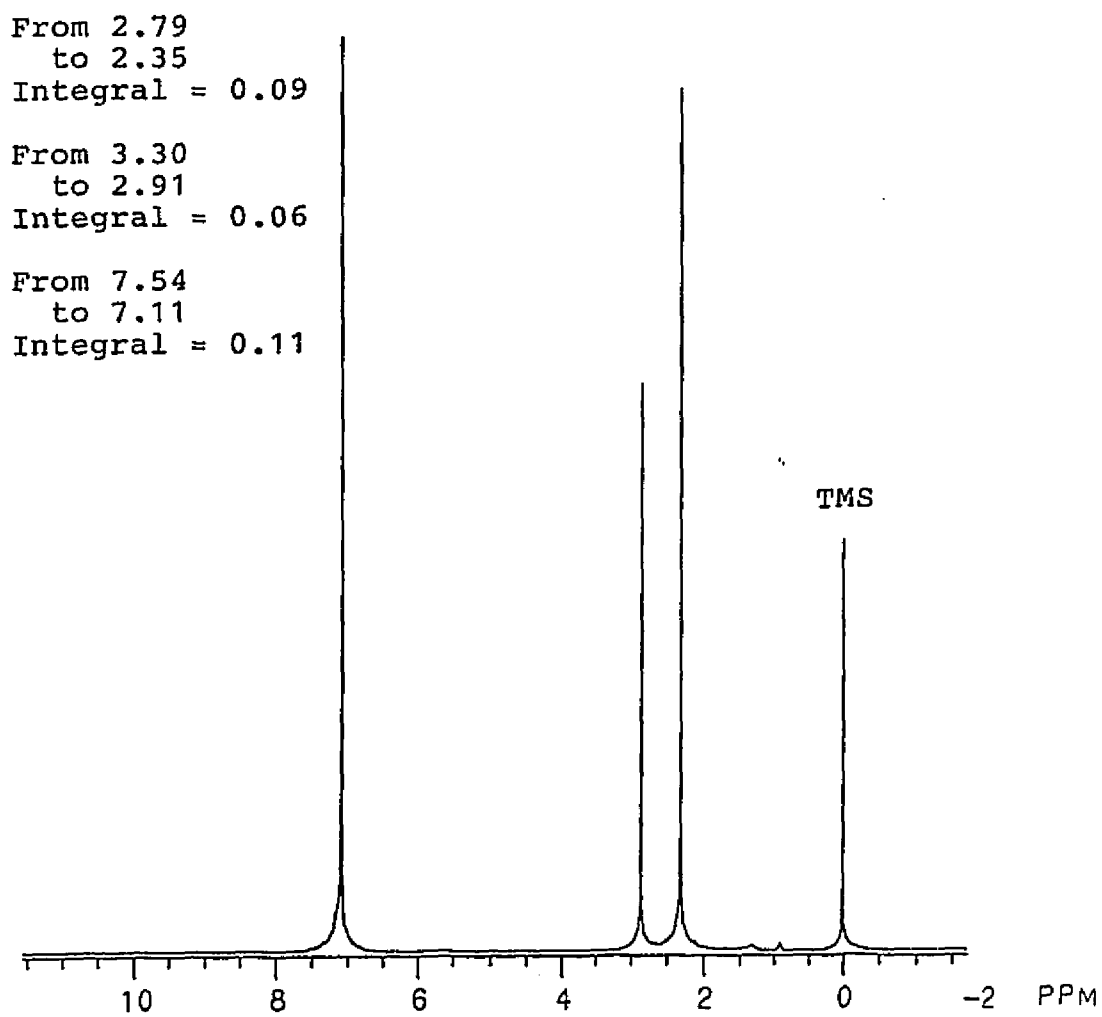


Figure 23. ^1H NMR spectrum for $\text{CH}_3\text{C}_6\text{H}_4\text{CH}_2\text{CH}_2\text{C}_6\text{H}_4\text{CH}_3$

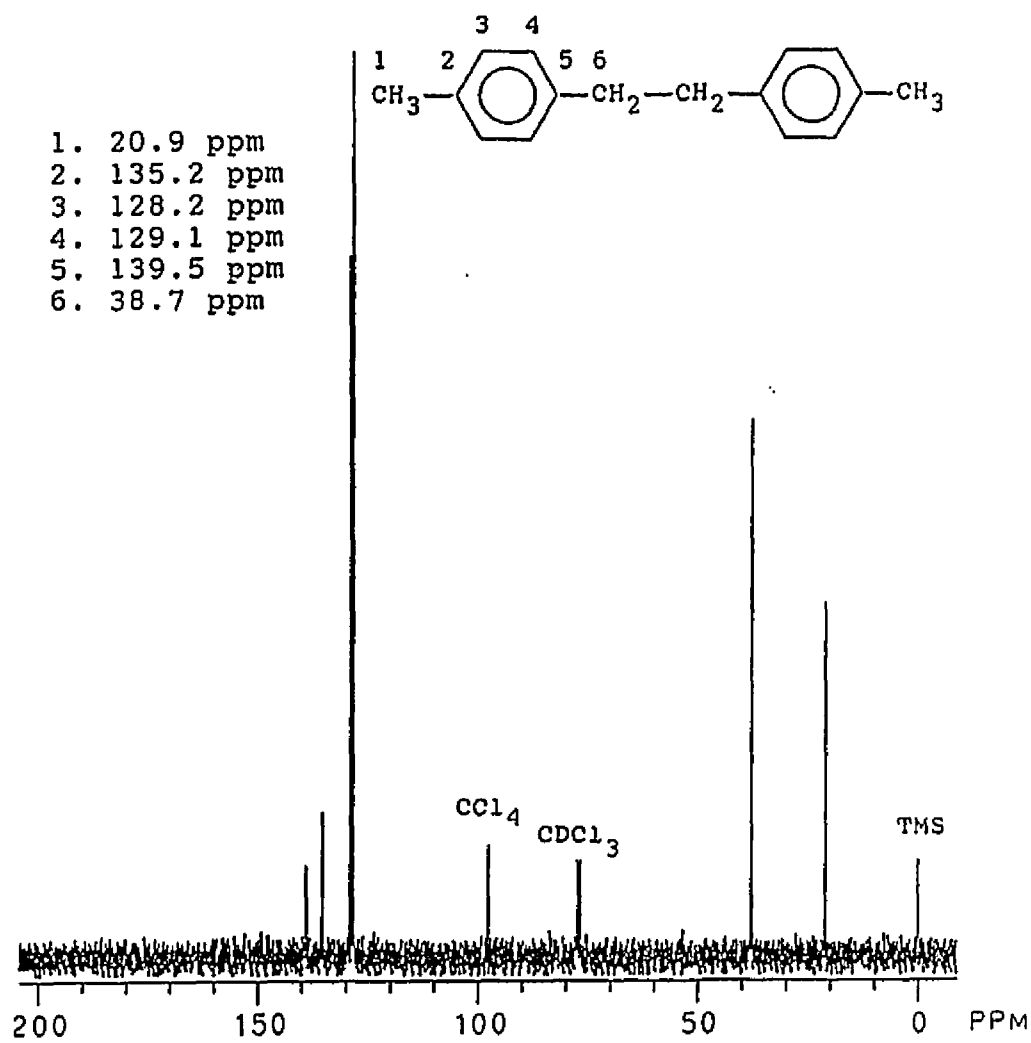
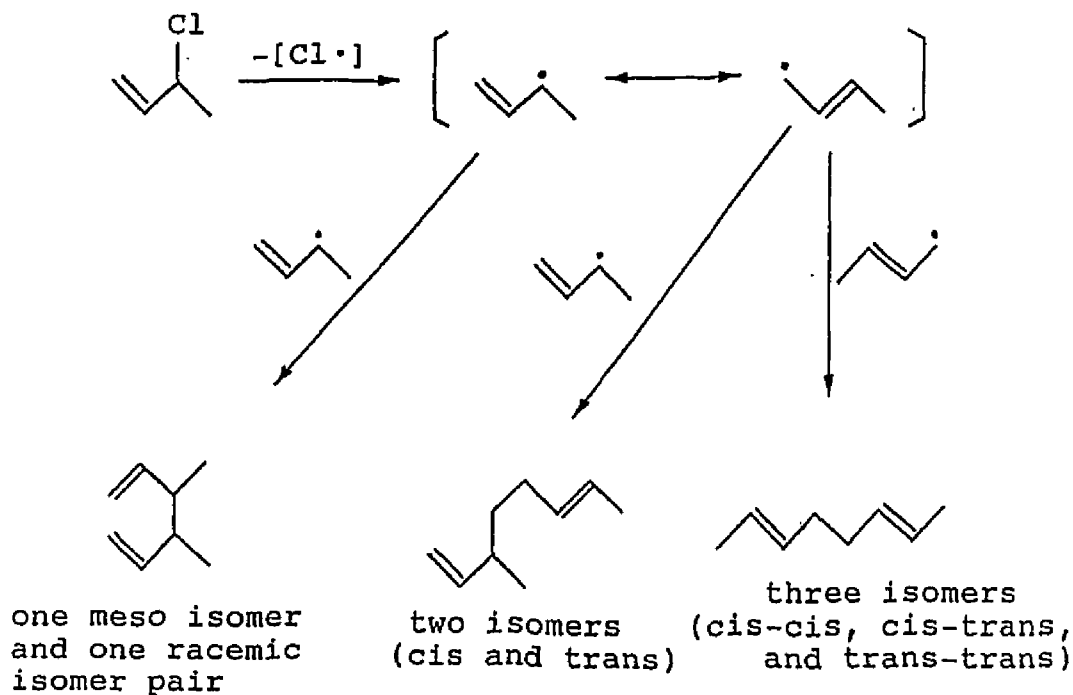


Figure 24. ^{13}C NMR spectrum for $\text{CH}_3\text{C}_6\text{H}_4\text{CH}_2\text{CH}_2\text{C}_6\text{H}_4\text{CH}_3$

Scheme 17



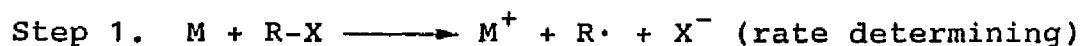
the chromatogram each contain two peaks, while the right side contains three peaks. Since the secondary allylic radical resonance structure has a greater stability than the primary one, the coupled products formed via the former structure might appear in the highest yields. Therefore, the meso and racemic diastereomers can be assigned tentatively to the middle part of the chromatogram, which consists of two strong peaks. On the other hand, the less stable primary resonance forms could produce the three straight-chain dimers which are shown on the right side of the chromatogram. Another supporting piece of evidence for the assignment of these peaks is that the straight-chain alkenes usually have a higher boiling point than their

branched isomers; and since a higher boiling point usually indicates a longer GC retention time, the three isomeric coupled products shown in the right side of the chromatogram can be identified as 2,6-hexadienes due to their straight-chain structures. Further identification of these three peaks can be achieved tentatively according to their steric configurations, in that a trans isomer usually has a higher boiling point (and a longer retention time) than a cis one. However, thermodynamic stabilities predict that the yields should be $t,t > t,c > c,c$.

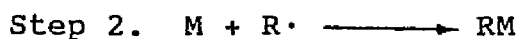
Based on the data shown in Tables 1 and 2, the observed reactivity of the organic halides towards the activated copper slurry decreased in the order $RI > RBr > RCl$, which is in agreement with the results reported by Ebert and co-workers.^{64,65} The reactivity sequence of these alkyl halides is compatible with carbon-halogen bond cleavage being the rate-determining step for the formation of organometallic species.⁸² It also suggests that radical intermediates may be involved in the formation of coupled products.⁸² Allylic halides, for example, are known to react with many different metals (such as Li, Na, K, and Mg) to form organometallic compounds which dissociate to give stable but reactive allyl radicals (Scheme 18).⁸²

Rieke and co-workers,^{64,72,83} in their extensive studies of activated copper metal, had demonstrated that

Scheme 18



or



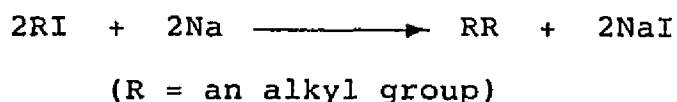
(M = metal; R = allyl radical; X = halide.)

the activated copper slurry prepared by reducing $\text{CuI}\cdot\text{P}(\underline{n}\text{-Bu})_3$ with lithium naphthalenide exhibits very high reactivity towards organic halides. However, we realized that this process suffers from the disadvantages of the need for a solvent that dissolves the metal salt and the fact that some metal salts are not cleanly reduced, in particular the salts of the transition metals. We suspected that some of the reductant (in this case, lithium naphthalenide) was not completely consumed in the reduction process and thus would contribute, in part at least, to the formation of the reductive-coupling products. Therefore, to clarify this situation, a series of control experiments was conducted with model organic halides in the sole presence of lithium naphthalenide (without copper iodide

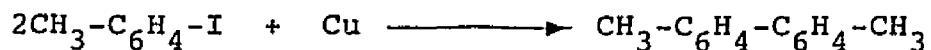
complex). The results showed that lithium naphthalenide, as suspected, could also cause the reductive coupling to occur. This finding led us to conduct another series of model-compound experiments wherein the lithium naphthalenide in the slurry was removed by repetitively washing with fresh solvent. The resulting reductant-free slurry was demonstrated to promote reductive coupling as well (see Tables 1 and 2); however, in this case the yields of coupled products were lower than those obtained from reactions with the original untreated slurry. The latter result could have been brought about primarily by decreases in slurry activity^{64,65} during the washing operations.

In comparison to the activated copper slurry, solid state copper film produced by pyrolytic decomposition of copper(II) formate powder⁶⁶ was found to promote the rapid homocoupling and cross-coupling of only highly reactive halides such as primary and secondary allylic chlorides at room temperature in moderate yields (see Table 4).

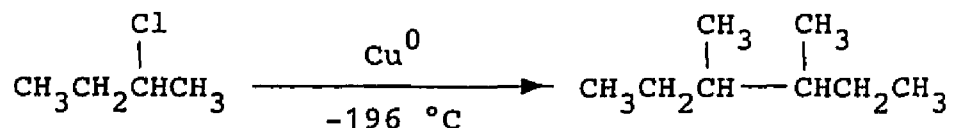
In general, the reductive coupling reactions of the PVC model organic chlorides induced by activated copper are very similar to two well-known organometallic reactions. One of these is the Wurtz coupling reaction, in which alkyl halides (e.g., iodides) are coupled by treatment with sodium



metal, as shown above. The other reaction is the Ullmann coupling process, in which an aryl iodide is heated with copper powder to produce the biaryl product, as shown below.



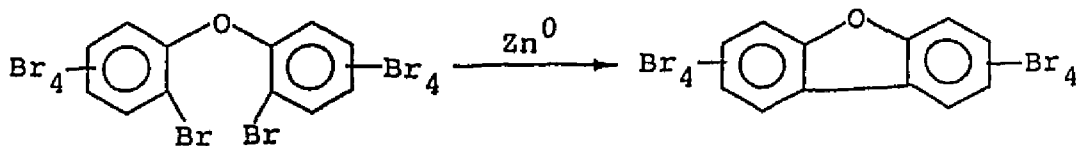
In contrast to the slurry, the activated film was unable to promote any reductive coupling reactions of simple secondary organic monohalides (chlorides, bromides, or iodides). The reasons for this lack of reactivity of the film have not been clarified thus far, but may be connected with the experimental conditions such as temperature or the reaction atmosphere. Activated copper metal can be very sensitive to temperature and moisture, and another researcher⁸⁴ has shown that much more carefully controlled experimental conditions may be required in order for the reductive coupling reaction to occur. Using macrocondensation techniques at -196°C , Timms⁸⁴ has studied the use of atomic Cu^0 in the dehalogenation of simple secondary alkyl halides and has found that the Cu^0 reacts with sec-butyl chloride to form the coupling product, 3,4-dimethyl hexane, in high yield (70%). Therefore, in view of this



result, it appears that temperature and other experimental

conditions are critical and can greatly affect the reactivity of activated copper toward simple secondary chlorides.

In addition to activated copper, many other highly reactive zero-valent metals have been demonstrated to promote reductive coupling reactions of organic halides under various experimental conditions. First of all, in a pyrolysis experiment similar to the copper(II) formate pyrolysis, we have demonstrated that molybdenum hexacarbonyl, $\text{Mo}(\text{CO})_6$, when heated at approximately 155°C under an argon atmosphere, gives a brilliant molybdenum mirror. This highly reactive form of Mo^0 metal has been shown to promote the reductive coupling of 3-chloro-1-butene under very mild conditions (GC yield, $11 \pm 3\%$). Secondly, Drews and co-workers⁸⁵ in their studies of the formation mechanisms of volatile antimony species during pyrolytic degradation and combustion, discovered that highly reactive metal species such as Sb^0 , Bi^0 , or Zn^0 , generated from reduction of their corresponding oxides, can promote the coupling reaction of an organic bromide, apparently due to the high surface areas of the metals:

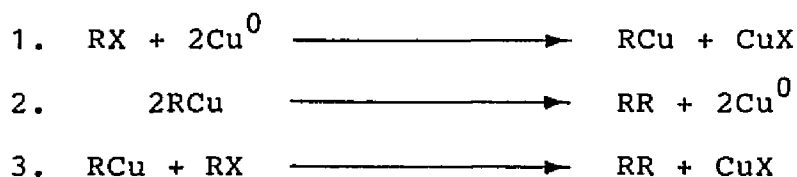


These researchers concluded that in the presence of such active metal species, direct attack on the organic bromide will readily occur.⁸⁵

In addition to the homocoupling reactions of organic halides induced by activated copper metal, two different secondary allylic chlorides also experienced rapid cross-coupling. As is shown by the data in Tables 2-4, when these chlorides were mixed in equimolar amounts and allowed to react with the activated copper (copper slurry or copper film), a mixture was formed that consisted of all three of the possible coupled products in approximately equal quantities (see entry 1 in Table 2, entry 3 in Table 3, and entry 4 in Table 4). These results are, in general, in agreement with the previous studies conducted by Ebert and Rieke.⁸³ These results also suggest that the activated copper can promote reductive coupling reactions between any two allylic chloride segments in the PVC polymer chains, and that this cross-coupling process can occur very early and promote the extensive crosslinking of PVC.

The chemistry of copper-induced organic halide reductive coupling reactions may be explained according to the mechanism proposed by Ginah and co-workers.⁶⁵ The mechanistic pathway involves an alkylcopper intermediate (Scheme 19). As is shown in this scheme, step 1 involves the oxidative addition of copper to the alkyl halide to produce the alkylcopper and copper(I) halide. In step

Scheme 19



2, the alkylcopper thermally decomposes at temperatures above 0 °C to give the homocoupled product along with elemental copper.⁸⁶ In step 3, the organocopper compound reacts quickly with the alkyl halide at lower temperatures to produce the corresponding coupled product.⁸⁷ In view of our experimental conditions, step 2 probably is the major step involved in the formation of the reductively coupled materials. It is worthy of note that a copper halide, CuX, is also produced along with the coupled product, and that since CuX (or its oxidation product, CuX₂) is a weak Lewis acid, it may contribute to the crosslinking of PVC (e.g., via Friedel-Crafts oligomerization) to some extent as well.⁵⁸

In summary, the results of the present model compound studies showed that reductive coupling of allylic chlorides could be brought about by activated forms of copper metal under very mild conditions. Experiments with the activated copper film and organic halides clearly demonstrated for the first time that the reductive coupling of organic chlorides can occur in the presence of a highly reactive

solid-state form of zero-valent copper metal. From a mechanistic perspective, one of the most important aspects of these results is the further confirmation of the existence of the reductive coupling mechanism. The results also suggest that the allylic chloride moieties which are well-known to occur in both virgin and thermally degraded PVC specimens should couple readily upon exposure to activated copper, and that the coupling reaction could ultimately lead to the extensive crosslinking of PVC. If chemical pathways could be designed to generate activated copper efficiently during the burning of PVC, then the copper additives used for this purpose could prove to be very effective smoke suppressants and fire retardants for the polymer.

1-2. Reaction of Activated Copper with PVC in Solution

The ability of activated copper to promote the reductive coupling of PVC model compounds led us to examine the reaction of activated copper with PVC itself. To study the reaction of activated copper slurry with PVC in solution, four different solvents with varying boiling points were employed. The slurry prepared from reduction of $\text{CuI}\cdot\text{P}(\underline{n}\text{-Bu})_3$ by lithium naphthalenide in THF was allowed to react with each PVC solution at reflux temperature. The results showed that the activated copper slurry was able to promote rapid and extensive crosslinking of PVC, and the crosslinking percentages (or gel contents) are summarized in Table 5. In each case a control experiment performed under the same experimental conditions, but without the activated copper slurry, gave no polymeric gel after refluxing for two hours (0.5 h for phenyl ether).

The data in Table 5 reveal the high reactivity of PVC toward the copper slurry. Even though rather low molar concentrations of Cu^0 (0.28 M) and PVC (0.64 M) were used, a large amount of gel was produced in every experiment, and the gel yield was relatively insensitive to temperature at the three lowest temperatures selected. The effect of temperature on the crosslinking of PVC is reminiscent of results reported by Ginah and co-workers,⁶⁵ who found that coupling yields obtained from organic halides and

Table 5
Gel Contents of PVC Treated with Cu^0 Slurry in Solution

solvent	temp, °C	time, h	gel ^a (%)
THF	66±2	2.0	79±2
anisole	155±2	2.0	92±2
<u>o</u> -dichlorobenzene	174±2	2.0	88±2
phenyl ether	257±2	0.5	90±2

a. Mean values obtained from duplicate runs.

induced by activated copper slurry were rather insensitive to several solvent and temperature combinations. To further ensure that the crosslinking was caused solely by the activated copper slurry, two additional control experiments were performed for each solvent. In the first control experiment, only $\text{CuI} \cdot \text{P}(\underline{n}\text{-Bu})_3$ complex was added to a PVC solution in an additive:polymer mole ratio of 1:4. In the second experiment, only lithium naphthalenide was added to a PVC solution at the same mole ratio of additive to polymer. Both solutions were then allowed to reflux for two hours (0.5 h for phenyl ether), and in each case no crosslinked PVC (gel) was found to be present. These

results clearly confirm that the activated copper slurry was the reagent that caused the extensive crosslinking of the polymer.

Experiments involving the generation of activated copper from copper(II) formate (1.00 g) in the presence of phenyl ether (100 mL) and PVC (2.00 g) were conducted under the same conditions. The PVC solution was brought to reflux at about 257 °C under argon for 10-15 min, and the results indicated that the activated copper film produced in this way also promoted rapid and extensive crosslinking of PVC, yielding a gel content of 69%. In view of the 0% gel content obtained from a control run performed in the absence of copper(II) formate under the same conditions, it could be concluded that activated copper (Cu^0), was indeed the crosslinking promoter.

Direct microstructure analysis of the degraded PVC is needed to account for the observed extensive crosslinking brought about by the activated copper slurry or the activated copper film. Nevertheless, in view of the results of our model-compound studies shown in Tables 1-4, it certainly seems reasonable to believe that a major role in the crosslinking process was played by reductive coupling.

1-3. Reaction of PVC with Copper Additives in the Solid State

Results obtained from the studies described above indicated that the reductive coupling of both PVC and PVC model allylic halides could be brought about by either an activated copper slurry or an activated copper film created by the pyrolysis of copper(II) formate. These observations led us to study the reaction of the activated copper film with PVC powder in the solid state. In addition to the copper film obtained from the Cu(II) formate, a highly purified copper powder (99.999%) obtained from a commercial source (Aldrich Chemical Co.) was used for comparative studies of gelation effectiveness. This metal powder already had been demonstrated (see below) to promote the reductive coupling of primary and secondary allylic chlorides at 200 °C.

The thermal degradation of PVC with a copper additive was carried out by mixing the PVC (10 parts) with the additive (1 part) using an agate mortar and pestle, and then heating the mixture in a Pyrex flask at 200±2 °C for 1-3 h under argon. The results of these experiments are shown in Figure 25, which reveals that both types of copper additive caused rapid gel formation which, in the case of copper(II) formate, seems very likely to have been effected by the activated Cu^0 that would have been formed

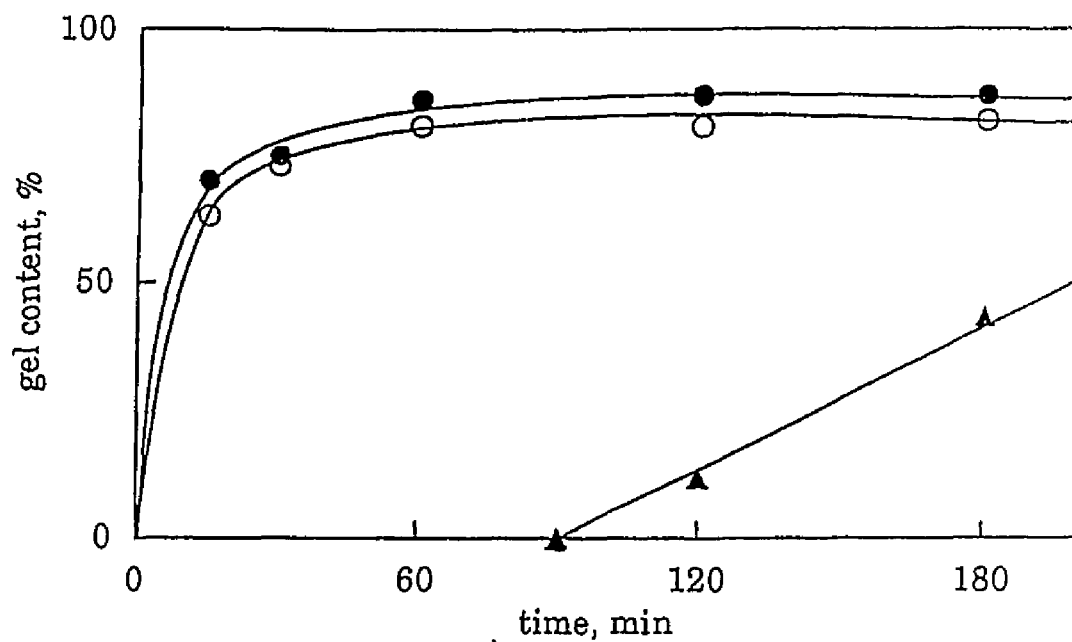


Figure 25. Gel content of solid PVC degraded under argon at 200 ± 2 °C. ▲, no additive; O, with Cu° powder (purity, 99.999%); ●, with Cu(II) formate.

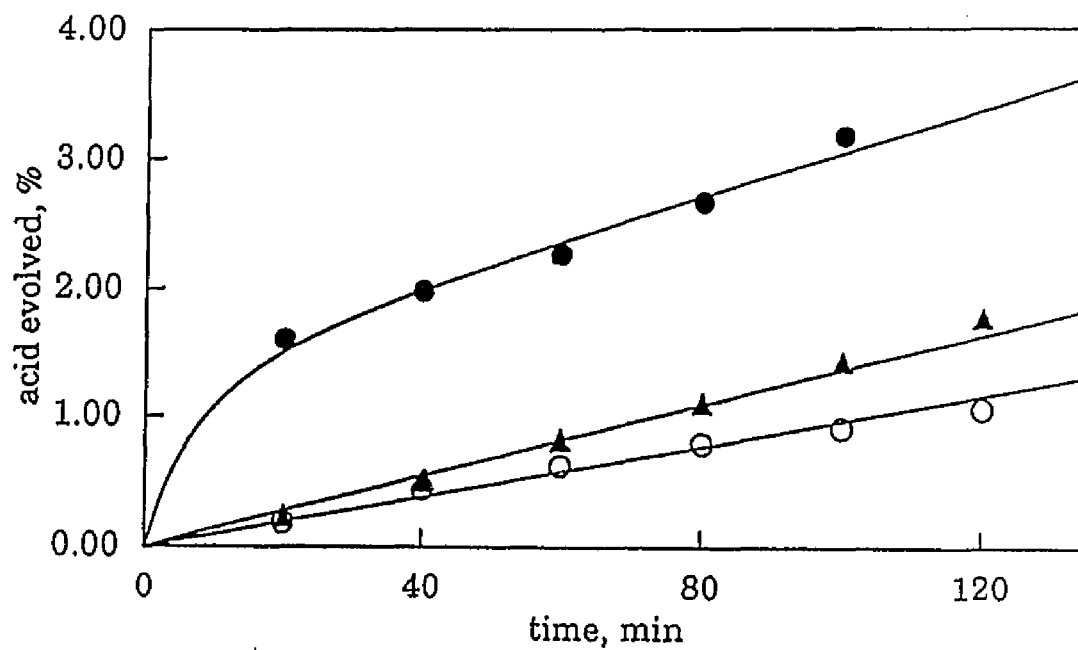
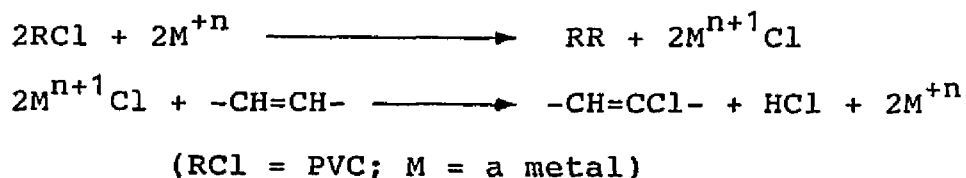


Figure 26. Acid evolved from solid PVC at 200 ± 2 °C under argon. ▲, no additive; O, with Cu° powder (purity, 99.999%); ●, with Cu(II) formate.

at the temperature of the experiment.

By means of acid-base titrimetry, dehydrochlorination rates were determined for solid PVC samples under conditions that were identical to those of the experiments of Figure 25. The rate curves are shown in Figure 26, where the initial rapid rate found with copper(II) formate is believed to have been caused by the evolution of formic acid and/or carbon dioxide. Separate rate measurements performed with copper(II) formate alone gave a rapid rate during the first 40 min which was identical to that obtained with PVC plus copper(II) formate. After 40 min, the rate enhancement by the copper(II) formate in PVC was insignificant, and the rate curve then leveled off to about the same slope as that for PVC alone. In contrast, the high-purity copper powder reduced the rate of dehydrochlorination slightly throughout the reaction period. Neither of these observations is consistent with Lewis-acid catalysis, which should have led to faster rates.^{39,55,58,62}

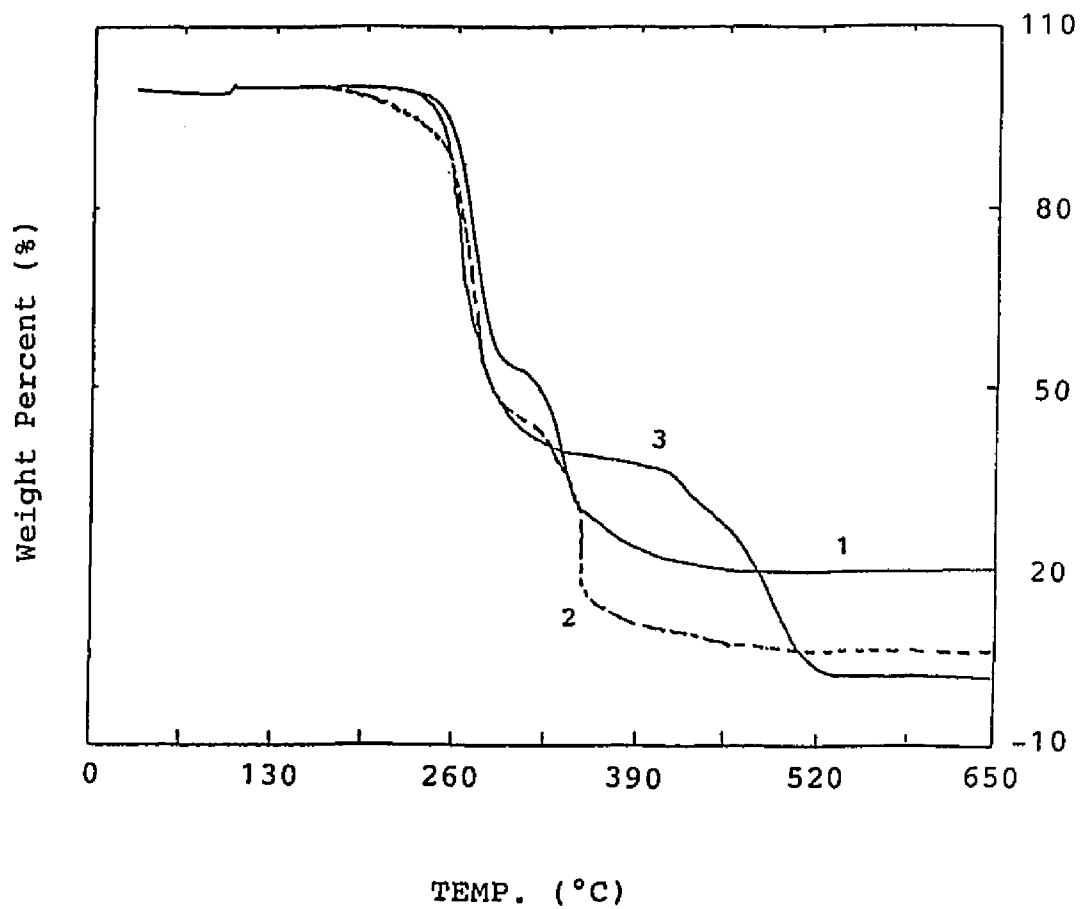
Based on the reductive coupling mechanism proposed by Lattimer and Kroenke³⁰, the following scheme may explain in part, if not completely, the observed decrease in rate of dehydrochlorination:



As shown here, the redox cycle involved in the reductive coupling mechanism produces only one mole of HCl for every two moles of RCl. Consequently, the copper additives which function according to this scheme should not, at least, accelerate the rate of dehydrochlorination of PVC to such an extent as in the case of Lewis-acid catalysis. The effects of the copper additives on the rate of dehydrochlorination, shown in Figure 26, suggest, therefore, that reductive coupling may be involved in the degradation process. It is pertinent to mention here, however, that some contradictory results with respect to the rate of dehydrochlorination of PVC in the presence of copper additives (and other metal additives such as FeCl_3) have been reported by many researchers,⁸⁸⁻⁹¹ and that the reasons for the contradictions have not been clarified so far. Interestingly, some authors⁹² have suggested recently that copper(II) formate may prove to be an effective thermal stabilizer for vinylidene chloride copolymers.

Thermogravimetric analyses (TGA's) of the PVC samples treated with copper(II) formate and copper powder further suggested that these additives may serve as potential fire retardants and smoke suppressants for PVC by promoting crosslinking via the reductive coupling mechanism. As is shown in Figure 27, when copper(II) formate or high-purity copper powder was incorporated into the PVC in a 1 to 10 weight ratio before degradation in air, the final

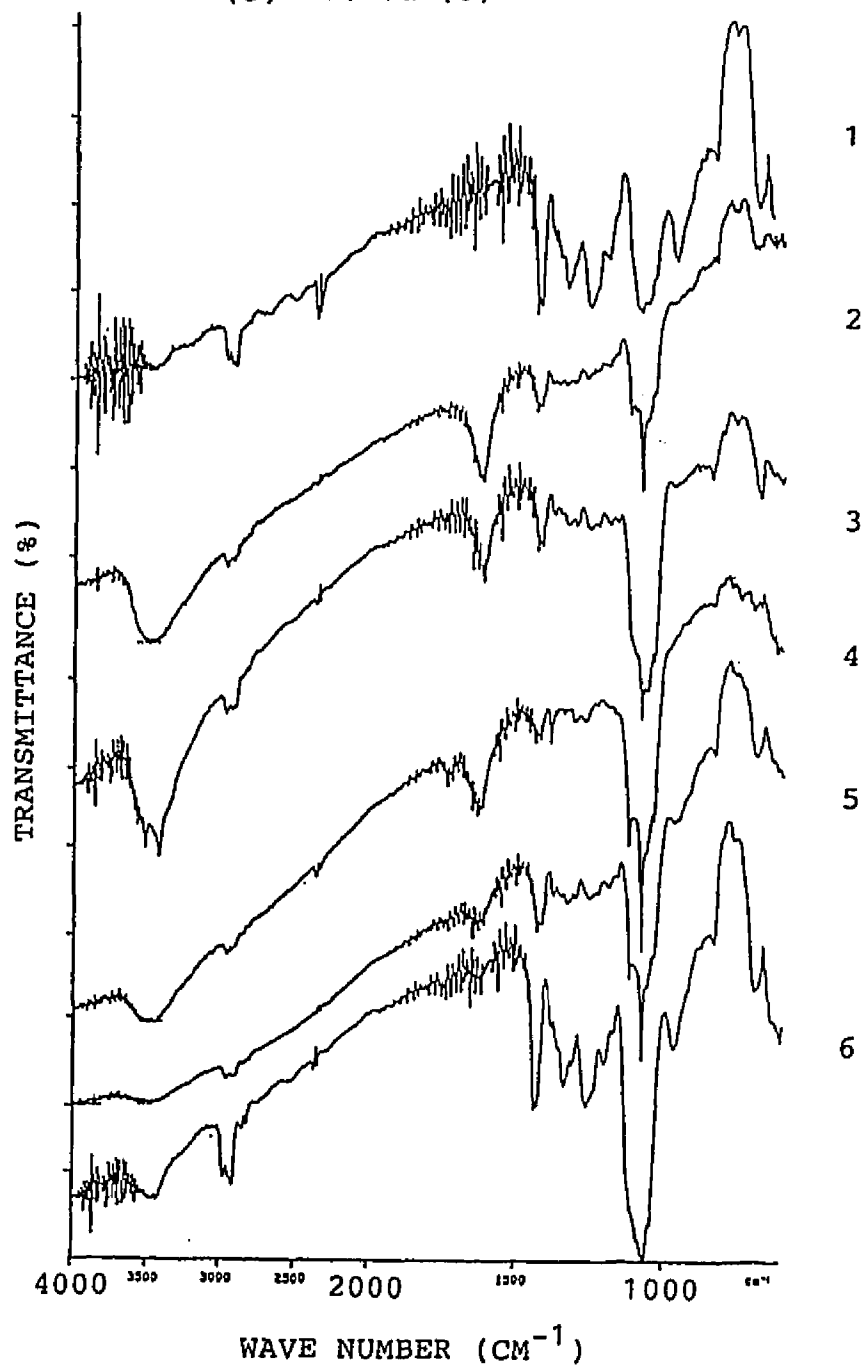
Figure 27. Thermogravimetric curve of (1) PVC+Cu
(2) PVC+Cu(HCOO)₂ (3) PVC control.



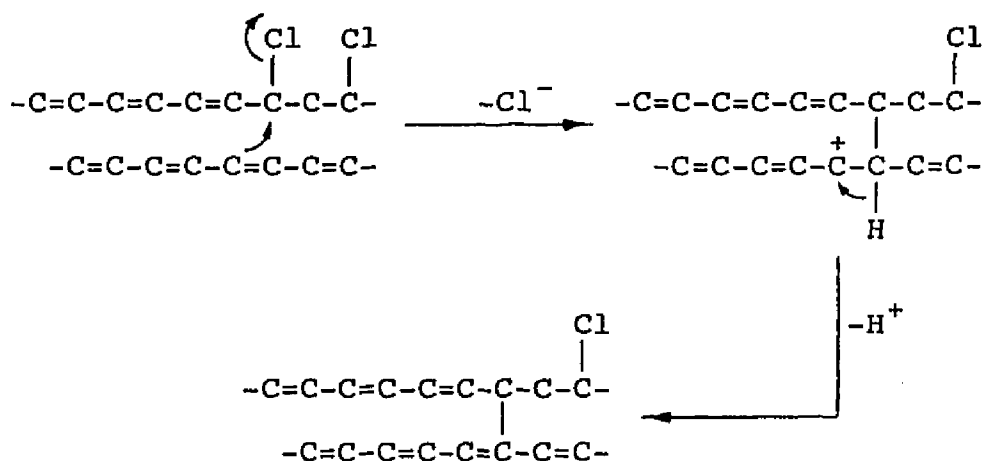
weight loss was less than for the untreated PVC control sample. In the copper(II) formate experiment, the weight loss due to the volatiles formed from the additive were not corrected for; thus the actual weight loss from the PVC should be less than is indicated by the TGA data.

Infrared spectra of PVC samples were taken after thermal degradation. Figure 28 shows the differences between a PVC control sample degraded without additives and those degraded with various copper additives (incorporated into the PVC in a 1 to 10 weight ratio) at 200 °C for 1 h under argon. The most significant difference between the control sample and those treated with the copper metal is the appearance of the absorption bands between 1640 and 1680 cm^{-1} which are indications of alkene C=C bonds. The IR spectrum of the untreated PVC does not show any distinct olefin bands, but olefin bands are clearly recognizable for PVC samples treated with Cu_2O , CuCl , and CuCl_2 . However, the PVC sample treated with the high-purity copper metal powder also does not show distinct olefin bands. The result of the IR analysis shows that the high-purity copper powder does not promote the thermal dehydrochlorination of PVC to the same degree as the Lewis-acid-type copper additives. This result also suggests that the reductive coupling mechanism may be responsible, at least in part, for the observed disappearance of the olefinic IR absorption. According to the mechanism for

Figure 28. IR spectra for (1) PVC without heating
(2) PVC+CuCl₂ (3) PVC+CuCl (4) PVC+Cu₂O
(5) PVC+Cu (6) PVC control.



Friedel-Crafts alkylation, an allylic chlorine atom in a PVC chain may be replaced, as shown below, during the



thermal degradation. This substitution can block the polyene propagation (zipper reaction) in one chain. On the other hand, on the basis of the reductive coupling mechanism, the formation of one C-C bond between two PVC chains would disrupt the polyene propagation in both chains, as indicated below. This process obviously would result



in less extensive dehydrochlorination of PVC. Considering that the propagation of polyene sequences may be disrupted

more extensively by the reductive coupling mechanism, the very weak olefinic IR absorption band provides additional evidence to support and rationalize the role of reductive coupling.

II. Model-Compound Pyrolysis Experiments

To investigate the likely effects of copper additives on the crosslinking of PVC, four different types of model compound (simple secondary chloride, secondary allylic chloride, conjugated diene, and conjugated triene) which are analogous to structural segments of normal or degraded PVC were pyrolyzed at 200 °C for 1 h under anaerobic conditions. The pyrolysis experiments were conducted on a very small scale using 0.05 mL of model compound (or a total volume of 0.10 mL when two models were used together) and 0.01 g of copper additive which were mixed in an ampule sealed under high vacuum. The resultant pyrolysates were identified by GC/MS methods, using authentic samples for comparison whenever possible, and these analyses were carried out under conditions where further dehydrochlorination of the models was eliminated. The analyses showed that the degradation products were, in general, very complex mixtures.

2-1. Pyrolysis of simple secondary chlorides with copper additives

Two model compounds, 7-chlorotridecane and 2-chlorobutane, were pyrolyzed with twelve different copper

additives at 200 °C for 1 h. Analyses of the degradation products by GC/MS showed that, in all cases, the copper additives catalyzed the dehydrochlorination of both models to produce 6-tridecene and 2-butene, respectively, in low to moderate yields. The yield data are summarized in Tables 6 and 7. The control samples of both model compounds degraded without copper additives strongly resisted dehydrochlorination. Also, in all cases, there was no GC evidence for the formation of heavy materials or cracking products. These results are in agreement with previous model-compound studies^{39,49,56,58,62} where similar simple secondary chlorides and a series of copper additives were degraded under anaerobic conditions.

The results in Tables 6 and 7 suggest that copper additives are capable of promoting the early dehydrochlorination of PVC in order to form polyene sequences. Lewis-acid-catalyzed PVC dehydrochlorination reactions induced by copper compounds have been studied and verified by many researchers.^{39,56,58} Three mechanisms: radical, ionic, and molecular (see Schemes 4-6),^{11,12} can be used to explain these results. The ionic mechanism has been widely accepted by many workers.^{18,93-97} Copper salts may be regarded as Lewis acids which can facilitate C-Cl heterolysis to form an ion pair during the thermal degradation of the polymer.^{18,28} Starnes and Edelson,²⁸ in their studies of MoO₃ as a smoke suppressant for PVC, have pointed out

**Table 6. Yields for Dehydrochlorination of 2-Chlorobutane
with Copper Additives at 200 °C for 1 h**

Copper Additive	Yield of 2-Butene(%) ^a
No Additive	< 1
Cu	19 ± 3
Cu ₂ O	28 ± 2
CuO	15 ± 2
CuI	22 ± 3
CuCl	5 ± 3
CuCl ₂	11 ± 2
CuBr	7 ± 2
CuBr ₂	7 ± 1
Cu ₂ S	11 ± 2
CuS	14 ± 2
CuC ₂ O ₄	10 ± 1
CuSO ₄	7 ± 3

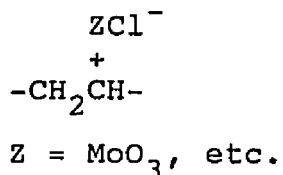
- a.
1. Three runs for each case.
 2. GC area percentages based on total starting amount of 2-chlorobutane.
 3. Deviations shown are the average deviations.

Table 7. Yields for Dehydrochlorination of 7-Chlorotridecane with Copper Additives at 200 °C for 1 h

Copper Additive	Yield of 6-Tridecene(%) ^a
No Additive	5 ± 1
Cu	29 ± 2
Cu ₂ O	33 ± 1
CuO	20 ± 2
CuI	19 ± 2
CuCl	25 ± 2
CuCl ₂	21 ± 3
CuBr	21 ± 1
CuBr ₂	22 ± 1
Cu ₂ S	23 ± 1
CuS	28 ± 2
CuC ₂ O ₄	33 ± 1
CuSO ₄	19 ± 2

- a. 1. Two runs for each case.
 2. GC area percentages based on total starting amount of 7-chlorotridecane.

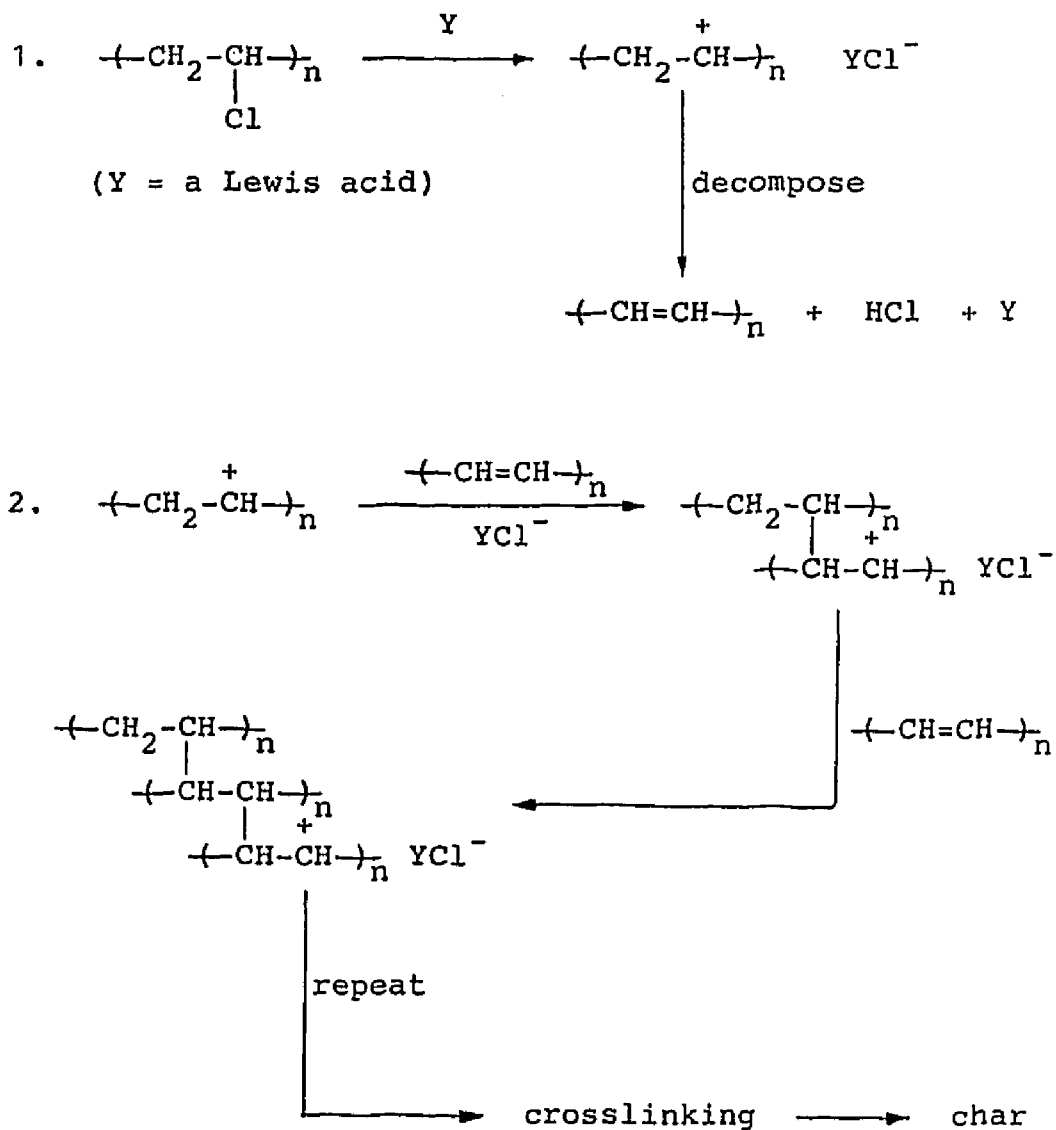
that a Lewis acid can accelerate this heterolysis by coordinating with the chlorine anion, as shown below.



According to this mechanism, the halogen may be attacked by MoO_3 either before ionization or after the formation of a carbenium chloride ion pair, and since the equilibrium constant for ionization can be increased by the coordination, due to the low acidity of the complex Mo(VI) anion, the HCl elimination is likely to be enhanced.

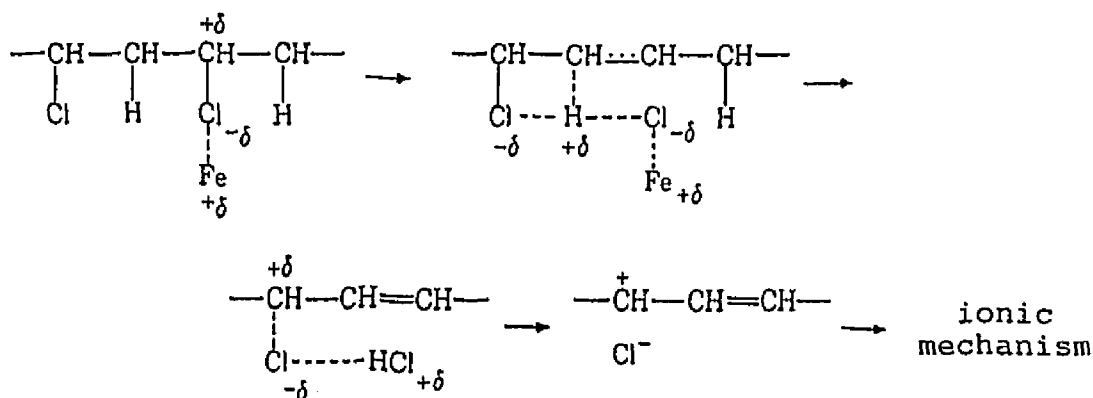
Carty and co-workers,¹⁸ in their study of iron(III) chloride (a strong Lewis acid) as a smoke suppressant for PVC, proposed a similar mechanism involving ion pairing and Lewis-acid catalysis (Scheme 20). This mechanism may be regarded as general for all the Lewis-acid-catalyzed PVC dehydrochlorination reactions which lead to the final extensive crosslinking of PVC. According to Scheme 20, the Lewis acid, Y (a metal additive), can react with PVC by accepting a chloride anion from the polymer to form an ion pair. The carbenium ion formed, being relatively unstable, decomposes into alkene, HCl , and metal compound Y. Then a reaction occurs wherein an intact portion of a PVC chain activated by Lewis acid Y alkylates a partially

Scheme 20. Lewis-acid-catalyzed dehydrochlorination and crosslinking reactions.¹⁸



degraded part of another chain. This step initiates a series of reactions which can ultimately lead to cross-linking of PVC and form a char. Abu-Isa⁹⁸ studied the degradation of PVC in the presence of many different metal oxides and proposed a similar ionic mechanism in which a metal atom in the oxide attacks a chlorine atom in PVC (Scheme 21). The dehydrochlorination of PVC in the presence of copper additives can be rationalized by an analogous process.

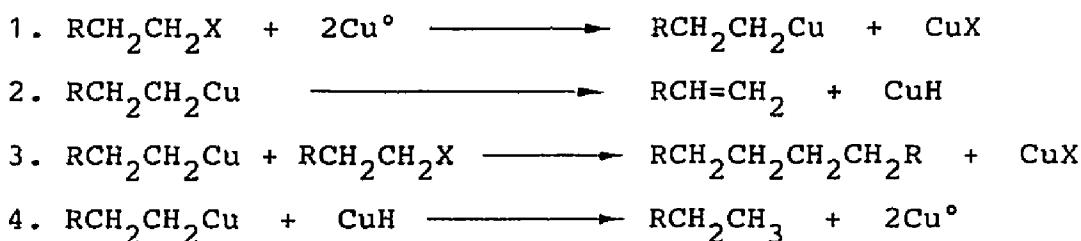
Scheme 21



In the case of high-purity copper metal (99.999%), two different chemical mechanisms may be involved in the dehydrochlorination of PVC. First of all, the copper metal could be partially oxidized prior to use, and therefore it might serve as a Lewis-acid catalyst in the form of cuprous or cupric oxide to catalyze the early dehydrochlorination of PVC via the ionic mechanism.^{18,93-97} Secondly,

the copper metal might promote extensive dehydrochlorination to form conjugated double bonds according to the mechanism proposed by Ginah and co-workers⁶⁵ (Scheme 22). According

Scheme 22



to this mechanism, the organocopper species is formed first in the reaction of alkyl halide with activated copper (step 1). Then the organocopper may produce an alkene by elimination of CuH (step 2). Some workers have, in fact, pointed out that Cu powder strongly catalyzes the thermal dehydrochlorination of PVC,^{39,91} and Cu₂O has been reported to be converted into Cu (activated Cu⁰) and CuO during the combustion of PVC.⁵³ According to Scheme 22, the copper metal can not only promote the formation of alkene, but also generate a reductive-coupling product (step 3) under certain favorable conditions.⁶⁵ The reductive coupling reaction can then promote early and extensive crosslinking of the polymer.³⁰ However, no trace amounts of homocoupling products (C₈H₁₈ and C₂₆H₅₄) were detected by our GC/MS analyses in the case of both 2-chlorobutane and 7-chlorotri-decane.

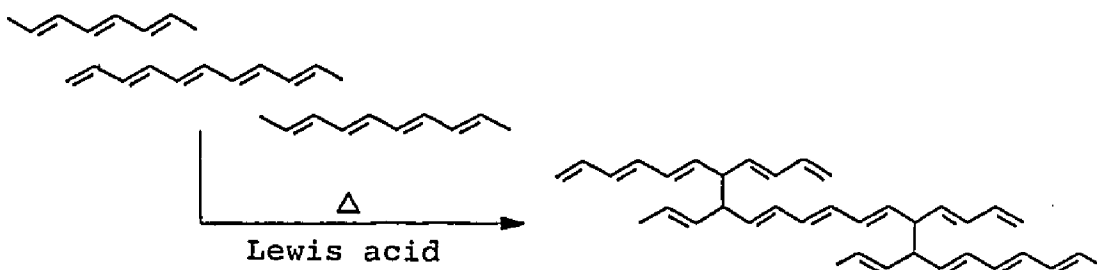
Another related mechanistic scheme was proposed by Klabunde and Roberts⁹⁹ in their studies of Pd atom reactions with organic halides (carried out by macroscale co-condensation techniques), in order to account for the formation of alkenes (Scheme 23). This mechanistic scheme bears close similarity to the one proposed by Ginah and co-workers,⁶⁵ and it may also be used to explain the dehydrochlorination of simple secondary chlorides in the presence of copper metal.

The mechanism of the Lewis-acid-catalyzed cross-linking of PVC, at this point, based on the model-compound studies, is considered to be closely related to the formation of polyene sequences. The formation of internal double bonds promoted by copper species may proceed by random elimination of HCl, and the subsequent formation of internal conjugated double bonds can be very rapid and extensive. Propagation of double bonds to form polyene sequences (zipper reaction) has, in fact, been suggested to be about four orders of magnitude faster than the uncatalyzed random elimination of HCl from regular monomeric units.¹⁰⁰ Polyene segments could undergo further reaction to form crosslinked structures in degraded PVC.²⁸ This process would compete with the parallel intramolecular cyclization of the polyene sequences to form benzene, which is a major source of smoke (see Schemes 7 and 10).²⁸ The number of crosslinked polyene chains produced may be

higher than that formed in the pyrolysis of pure PVC, leading to a significant increase in the residual char formed by pyrolysis.

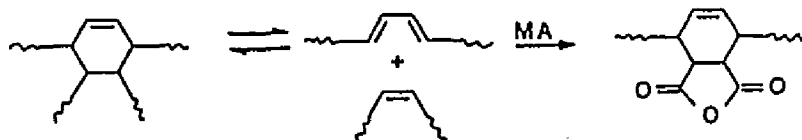
Several chemical reactions could take place to form different types of crosslinked PVC structures from the conjugated polyene sequences. In addition to the type of structure already shown in Scheme 20, there are other possibilities. First, crosslinks may be generated in the presence of copper additives (Lewis acids) by direct linking of the polyene chains with the formation of saturated carbon-carbon bonds via Friedel-Crafts catalysis, as shown in Scheme 24.²⁷

Scheme 24



Secondly, the Diels-Alder cyclization process could occur if segments with a diene and a dienophile structure were facing each other, and the cyclohexene structure thus formed could serve as a linkage between two polymer chains, as shown in Scheme 25.^{12,13} The formation of this type of

Scheme 25



structure is supported by the ability of maleic anhydride (MA, a strong dienophile) to destroy a major fraction of the crosslinks in a thermally degraded PVC sample.^{12,13} Kuzmany and co-workers¹⁰¹ have also shown that the crosslinking of polyacetylene can be attributed to the Diels-Alder reaction. Moreover, Světlý and co-workers¹⁰² have pointed out that intermolecular Diels-Alder additions of conjugated double bonds play an important role in the crosslinking process. In fact, in addition to the classical thermal 4+2 Diels-Alder cycloaddition, Lewis-acid-catalyzed Diels-Alder reactions have been reported by many workers.¹⁰³⁻¹⁰⁵ Lastly, according to the PVC pyrolysis scheme proposed by Starnes and Edelson²⁸ (see Scheme 10), PVC can undergo dehydrochlorination to generate linear polyene sequences having both trans and a low proportion of cis-substituted alkene units. These polyene sequences can then undergo the crosslinking reaction via Lewis-acid-catalyzed olefin oligomerization and chloroalkylation.^{28,56,58,62}

Although many details of the mechanism of crosslinking of PVC induced by copper additives have not been revealed at this point, based on the results of the current model-compound studies, copper additives have been demonstrated to catalyze the dehydrochlorination of PVC, and the formation of polyene sequences clearly constitutes the first step toward the final extensive crosslinking of the polymer.

Since the dehydrochlorination of simple secondary alkyl chlorides can lead to the formation of the highly reactive allylic chlorides and conjugated alkenes, the crosslinking chemistry involving these two types of structures in the presence of copper additives will be considered next.

2-2. Pyrolysis of 4-Chloro-2-pentene in the Presence of Copper Additives

To study the effects of copper additives on a secondary allylic chloride, 4-chloro-2-pentene was pyrolyzed in the presence of a variety of these additives at 200 °C for 1 h. In contrast to the simple secondary-chloride pyrolysis experiments, the GC/MS analyses of the pyrolysates showed that copper additives not only promoted the dehydrochlorination of 4-chloro-2-pentene, but also produced very complex mixtures which consisted of numerous heavy products whose molecular weights ranged from 134 to 340 (g/mol). The distributions of these heavy products are summarized in Table 8, and some tentative chemical structures for them are shown in Table 9. Among the nine different copper additives studied in these pyrolysis experiments, copper metal and cuprous oxide gave the most complex product mixtures, which included all of the heavy products that were produced by the other seven copper additives listed in Table 8. Representative GC/MS data for the heavy products with MW 134 to 340 are shown in Figures 29-42. The total GC chromatograms for the pyrolysates from the reactions of 4-chloro-2-pentene with Cu and Cu₂O are shown in Figures 43 and 44, respectively.

In general, the copper additives catalyzed two major types of chemical reaction to form a wide variety of heavy

Table 8

Distributions of Heavy Products for 4-Chloro-2-pentene Pyrolyses^a

MW	Formula	Control	Cu	Cu ₂ O	CuO	CuCl ₂	CuCl
134	C ₁₀ H ₁₄	0	3	3	16	trace	5
136	C ₁₀ H ₁₆	trace	9	18	34	53	25
137 ^b	C ₁₀ H ₁₇	trace	3	0	10	38	24
138	C ₁₀ H ₁₈	0	62	4	12	0	0
139 ^b	C ₁₀ H ₁₉	trace	1	0	0	0	0
172	C ₁₀ H ₁₇ ³⁵ Cl	trace	3	2	21	trace	40
204	C ₁₅ H ₂₄	0	16	23	2	3	2
240	C ₁₅ H ₂₅ ³⁵ Cl	0	trace	2	5	6	4
272	C ₂₀ H ₃₂	0	2	25	0	0	0
340	C ₂₅ H ₄₀	0	1	23	0	0	0

a. GC area percentages based on total peak area of groups of heavy products with specific molecular weight (MW).

b. Fragment from heavy product.

Table 8. Continued
 Distributions of Heavy Products for 4-Chloro-2-Pentene Pyrolyses

MW	Formula	Cu ₂ S	CuS	CuC ₂ O ₄	CuI
134	C ₁₀ H ₁₄	23	33	19	64
136	C ₁₀ H ₁₆	28	trace	34	10
137 ^b	C ₁₀ H ₁₇	0	0	0	0
138	C ₁₀ H ₁₈	0	0	0	0
139 ^b	C ₁₀ H ₁₉	0	0	0	0
172	C ₁₀ H ₁₇ ³⁵ Cl	33	trace	28	26
204	C ₁₅ H ₂₄	11	3	12	0
240	C ₁₅ H ₂₅ ³⁵ Cl	5	64	7	0
272	C ₂₀ H ₃₂	0	0	0	0
340	C ₂₅ H ₄₀	0	0	0	0

Table 9
Representative Tentative Chemical Structures of the Heavy
Products for the 4-Chloro-2-Pentene Pyrolyses

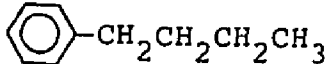
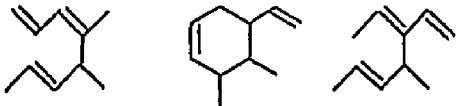
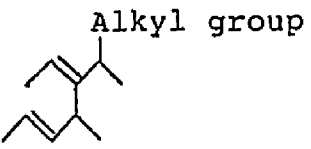
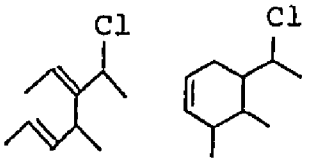
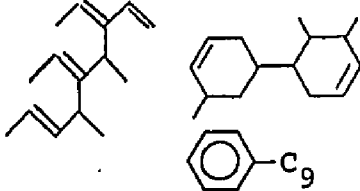
MW	Chemical Formula	Chemical Structure(s)
134	$C_{10}H_{14}$ (Fig. 29)	
136	$C_{10}H_{16}$ (Figs. 30-32)	
137	$C_{10}H_{17}$ (Fig. 33)	
138	$C_{10}H_{18}$ (Fig. 34)	
172	$C_{10}H_{17}^{35}Cl$ (Figs. 35 and 36)	
204	$C_{15}H_{24}$ (Figs. 37-39)	

Table 9. Continued

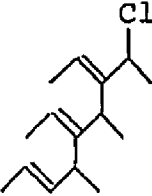
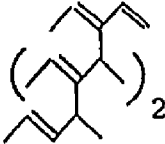
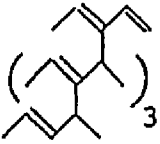
MW	Chemical Formula	Chemical Structure(s)
240	$C_{15}H_{25}^{35}Cl$ (Fig. 40)	 <p>The structure shows a seven-carbon chain with methyl groups at positions 2, 4, and 6, and a chlorine atom at position 1.</p>
272	$C_{20}H_{32}$ (Fig. 41)	 <p>The structure shows a cyclohexane ring with methyl groups at positions 1, 3, and 5, and a subscript 2 indicating two such molecules.</p>
340	$C_{25}H_{40}$ (Fig. 42)	 <p>The structure shows a cyclohexane ring with methyl groups at positions 1, 3, and 5, and a subscript 3 indicating three such molecules.</p>

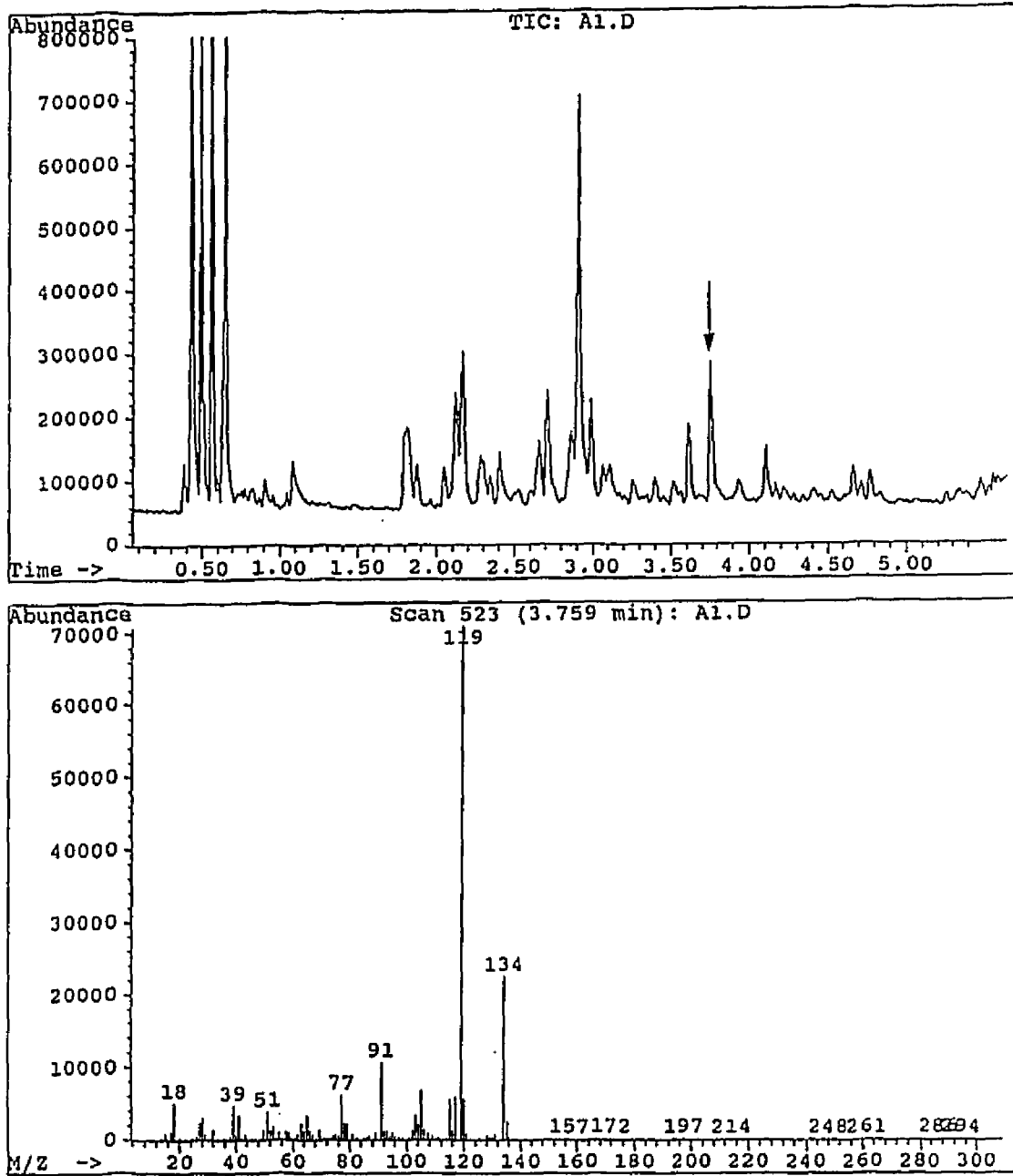
Figure 29. GC/MS data for $C_{10}H_{14}$ 

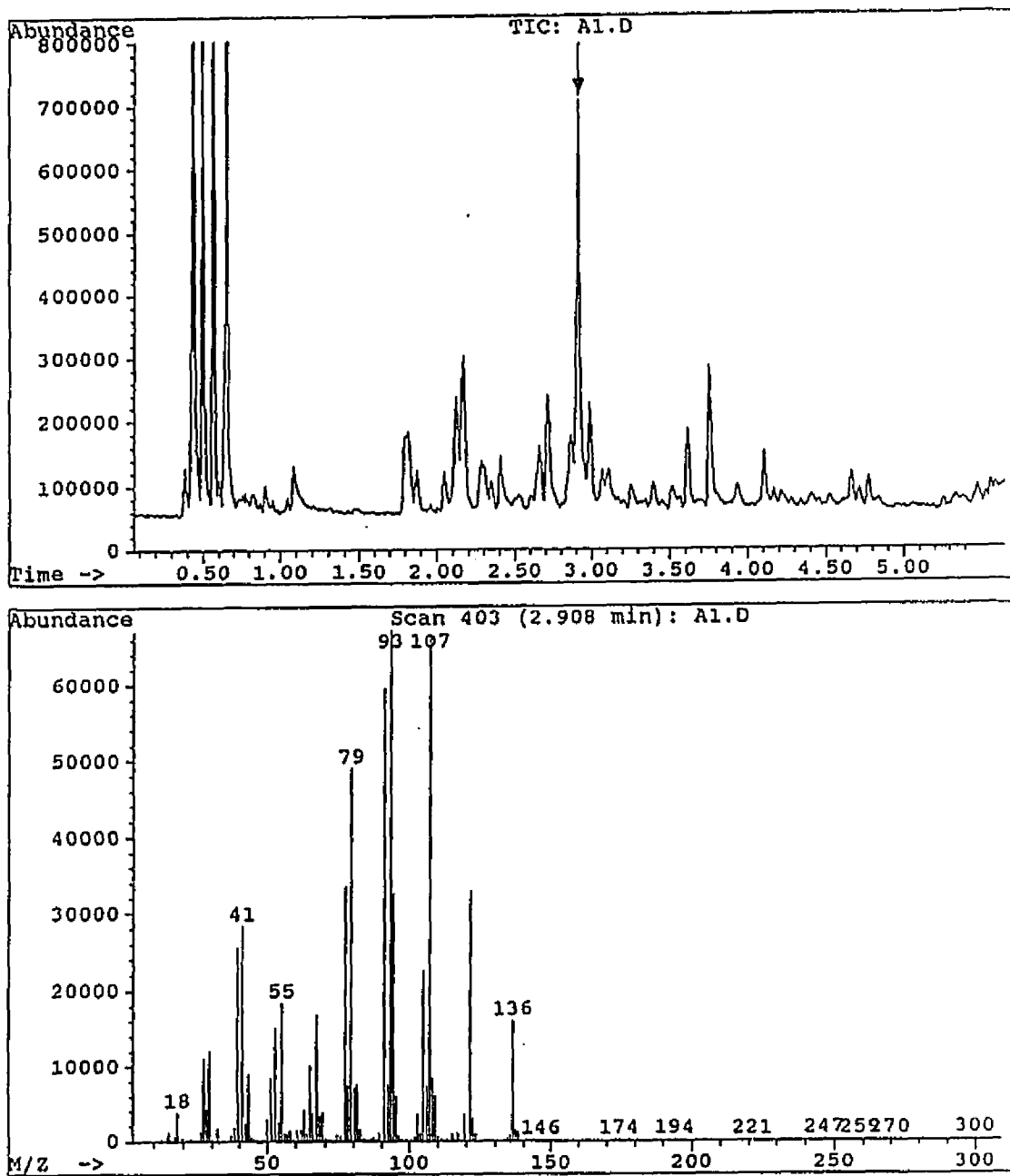
Figure 30. GC/MS data for $C_{10}H_{16}$ 

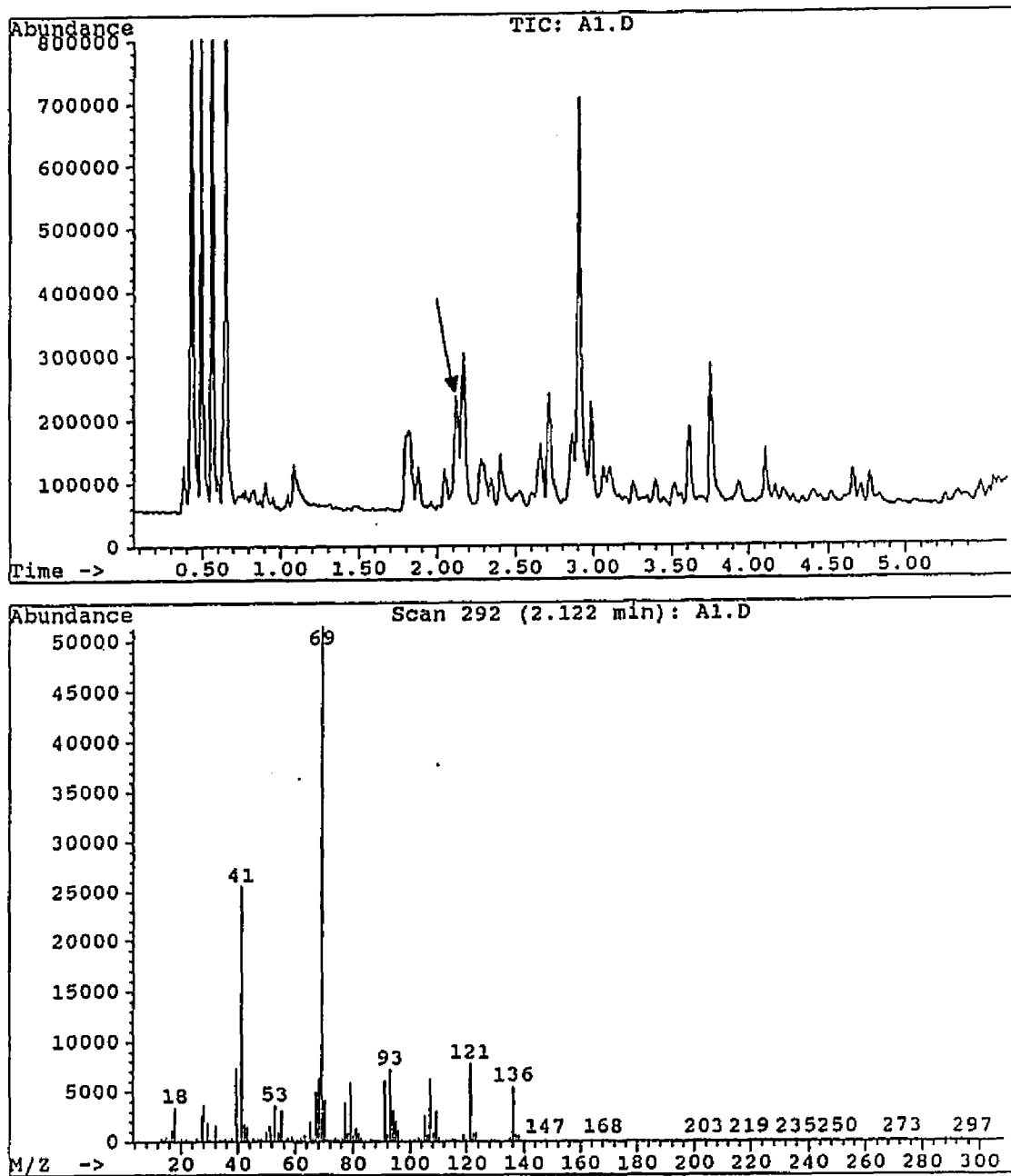
Figure 31. GC/MS data for $C_{10}H_{16}$ 

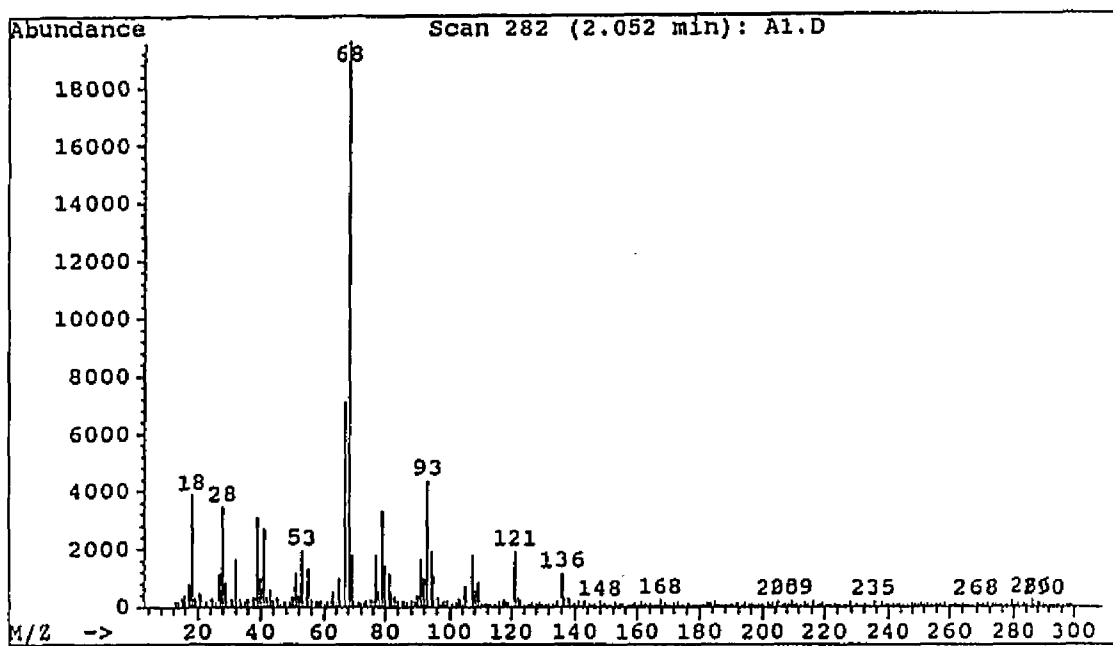
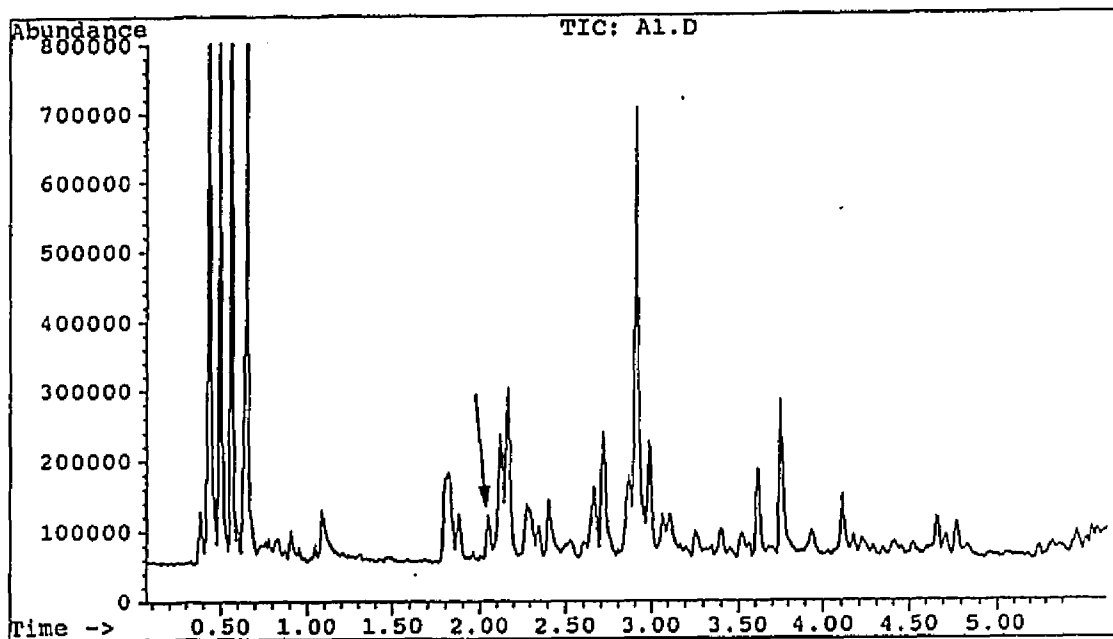
Figure 32. GC/MS data for $C_{10}H_{16}$ 

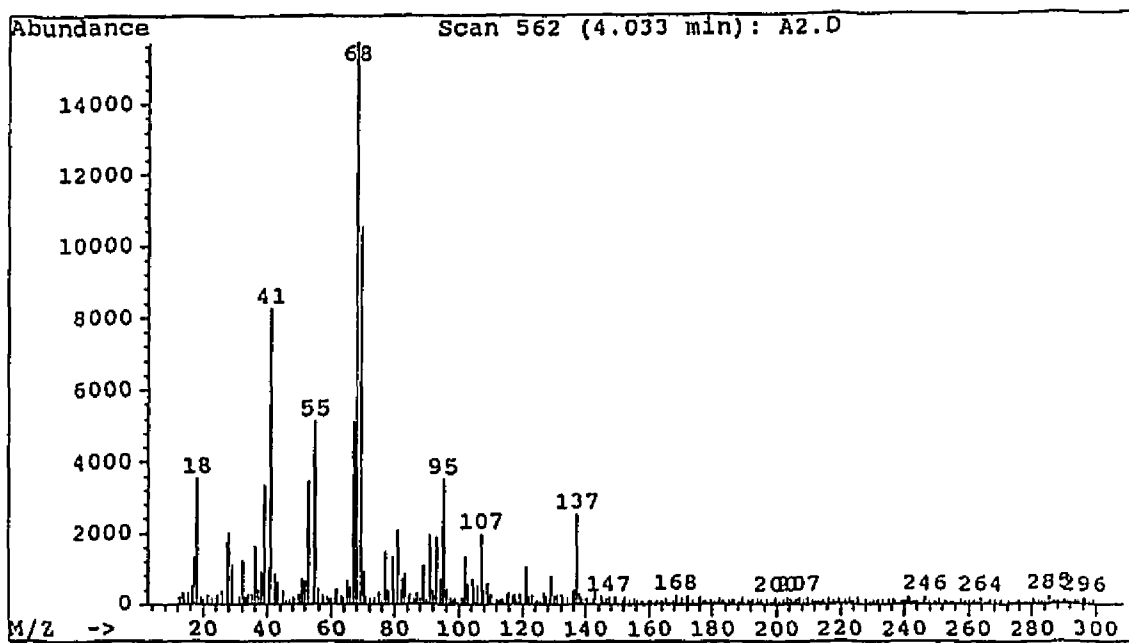
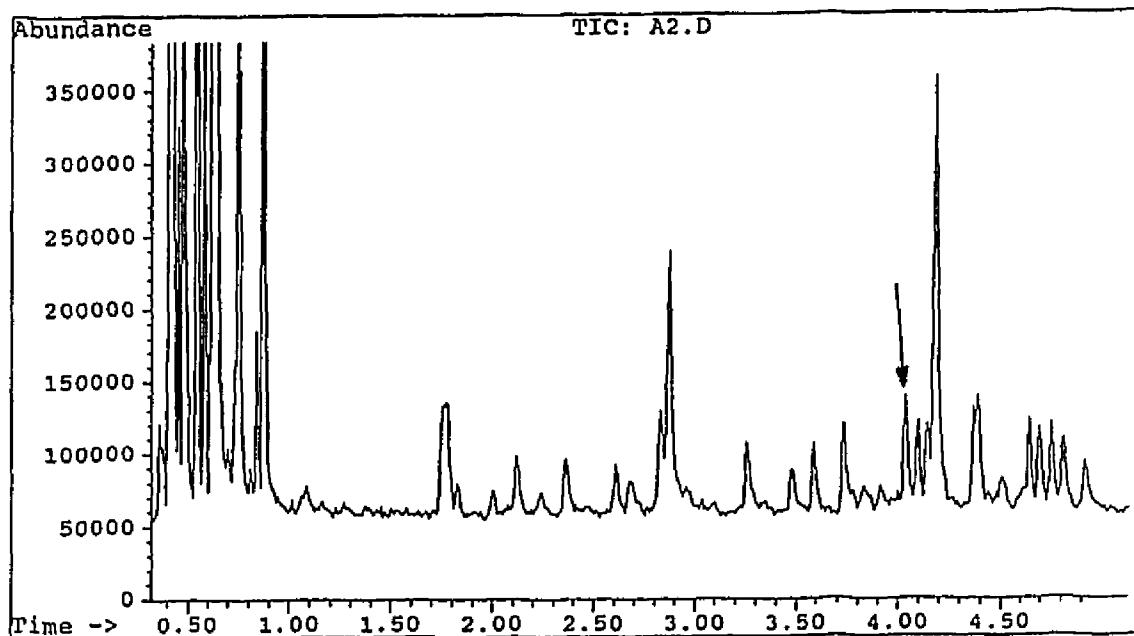
Figure 33. GC/MS data for $C_{10}H_{17}$ 

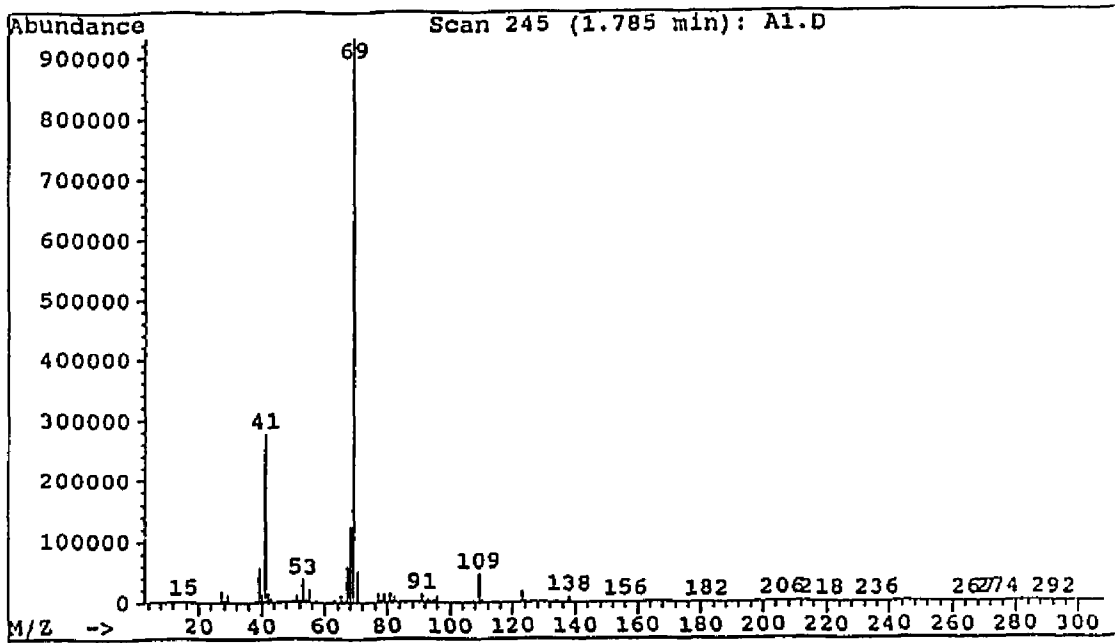
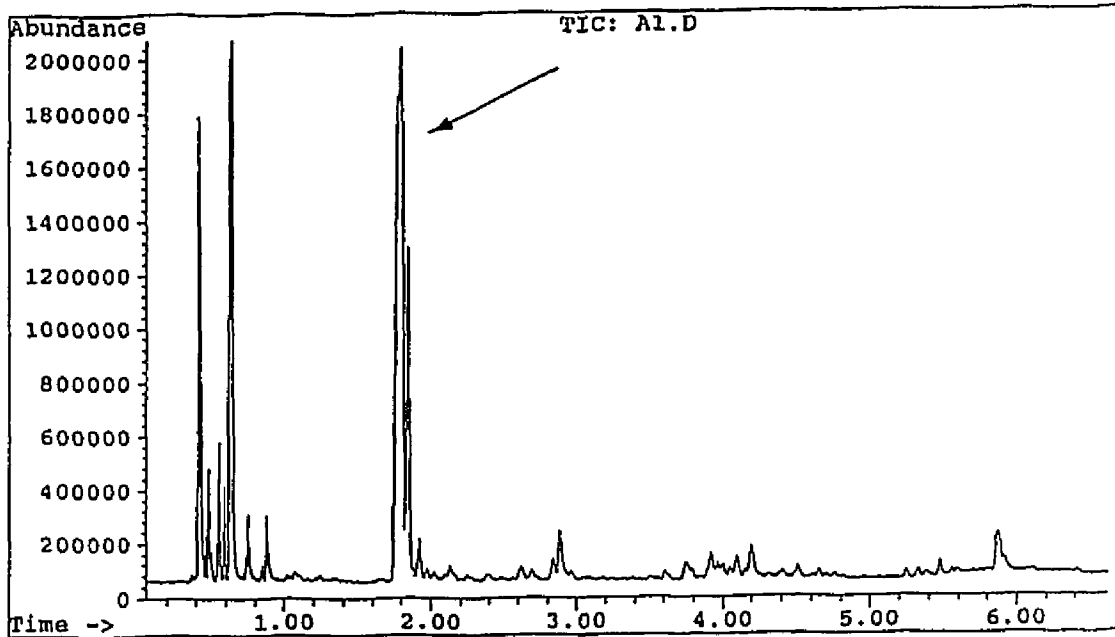
Figure 34. GC/MS data for $C_{10}H_{18}$ 

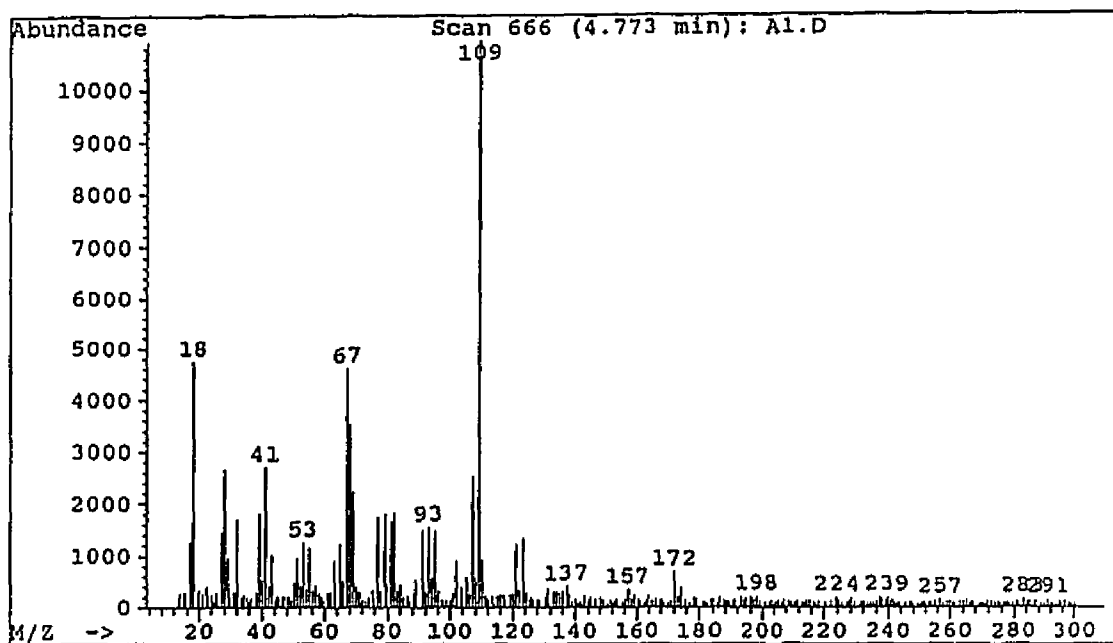
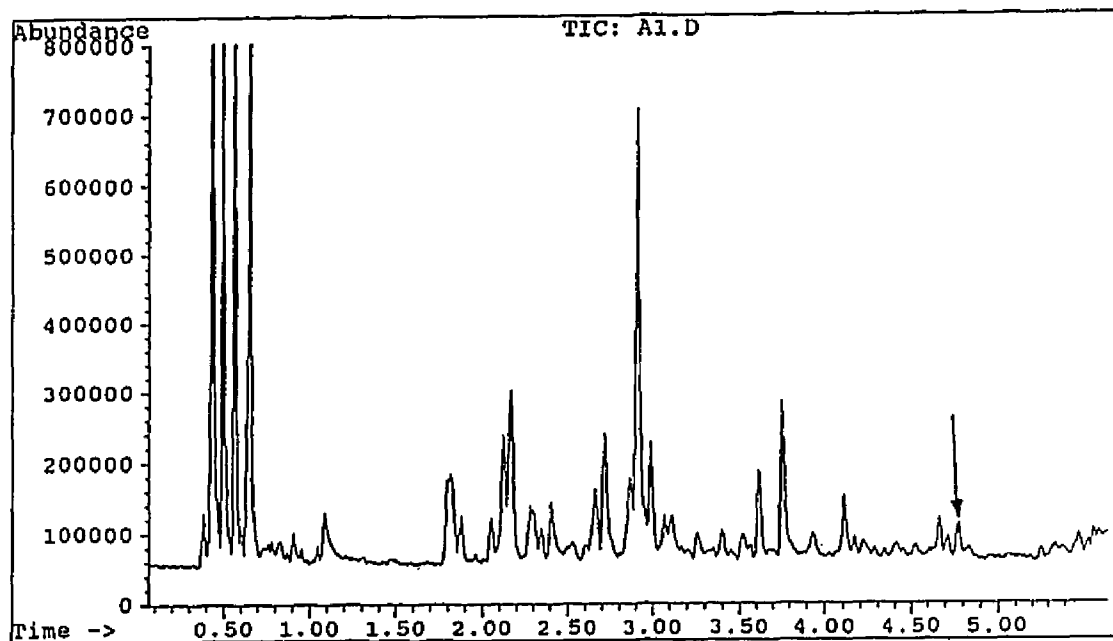
Figure 35. GC/MS data for $C_{10}H_{17}Cl$ 

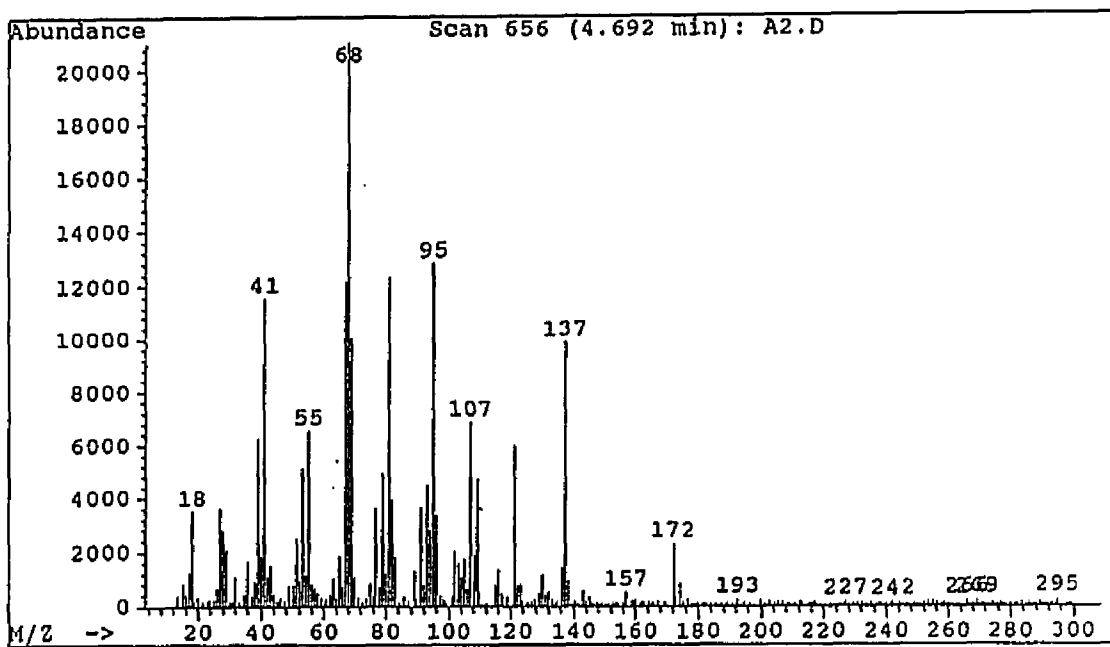
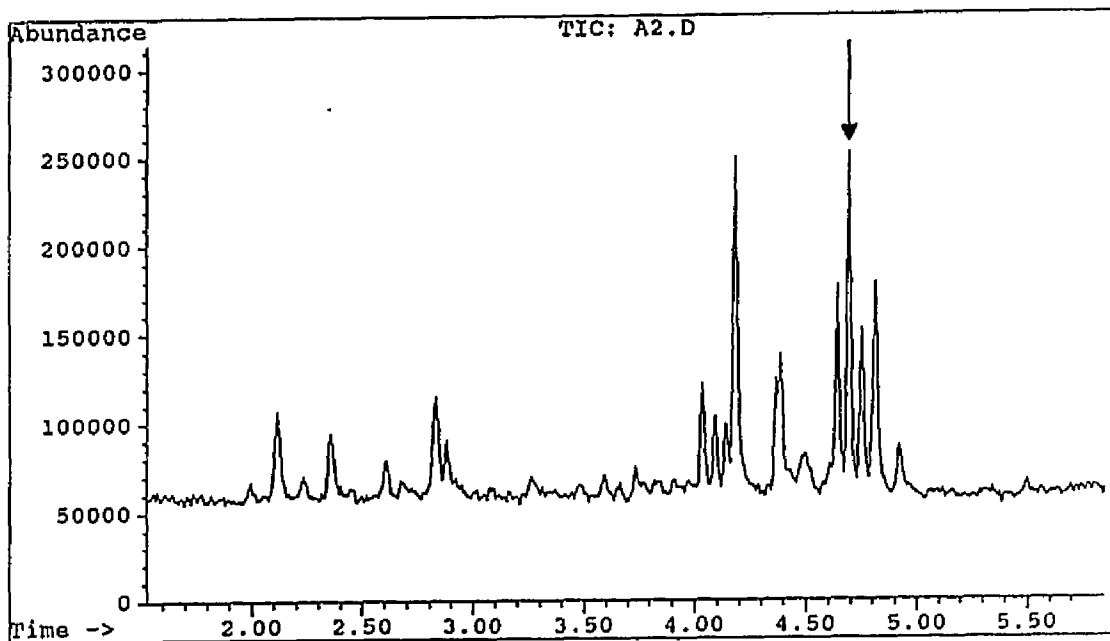
Figure 36. GC/MS data for $C_{10}H_{17}Cl$ 

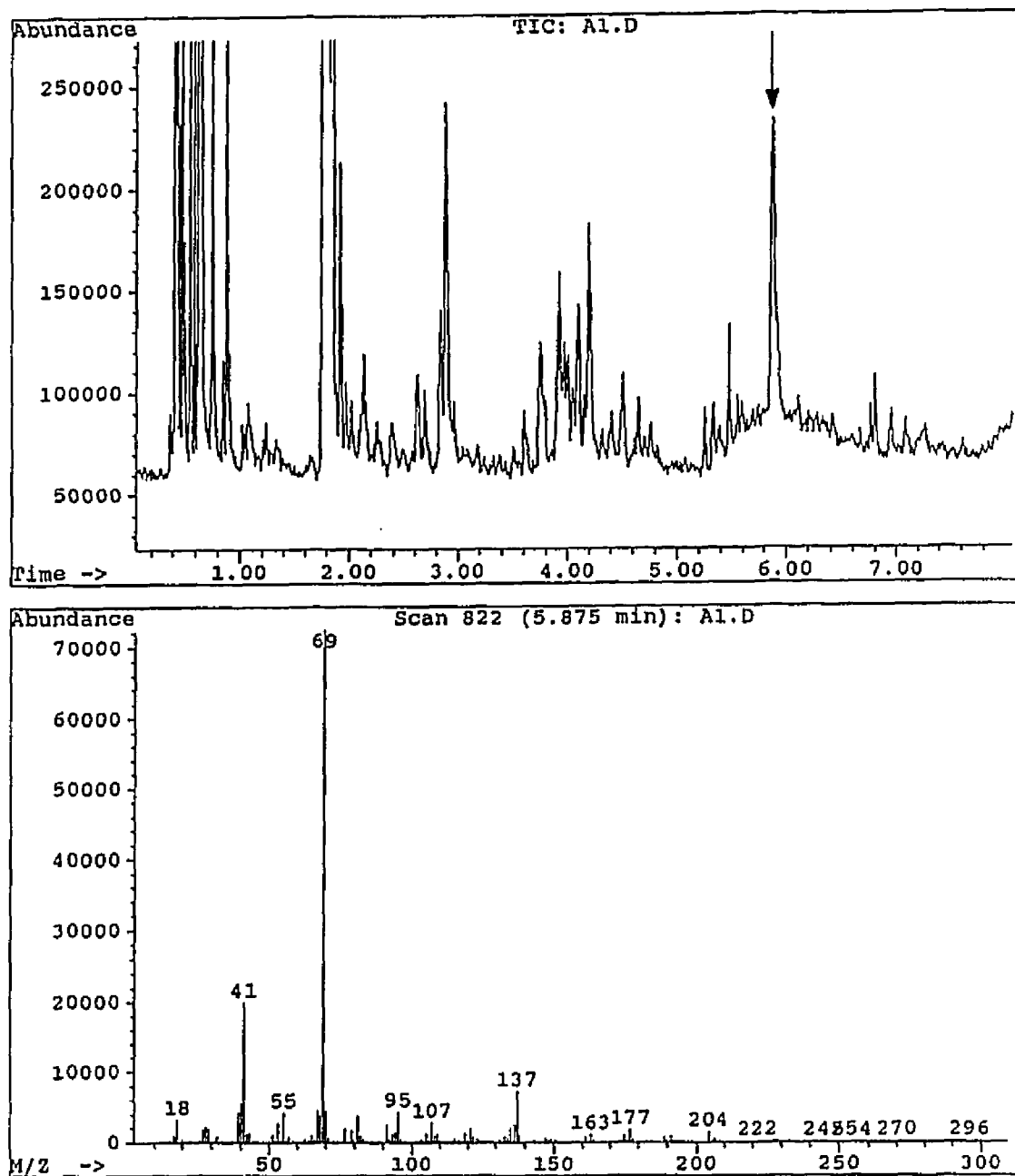
Figure 37. GC/MS data for $C_{15}H_{24}$ 

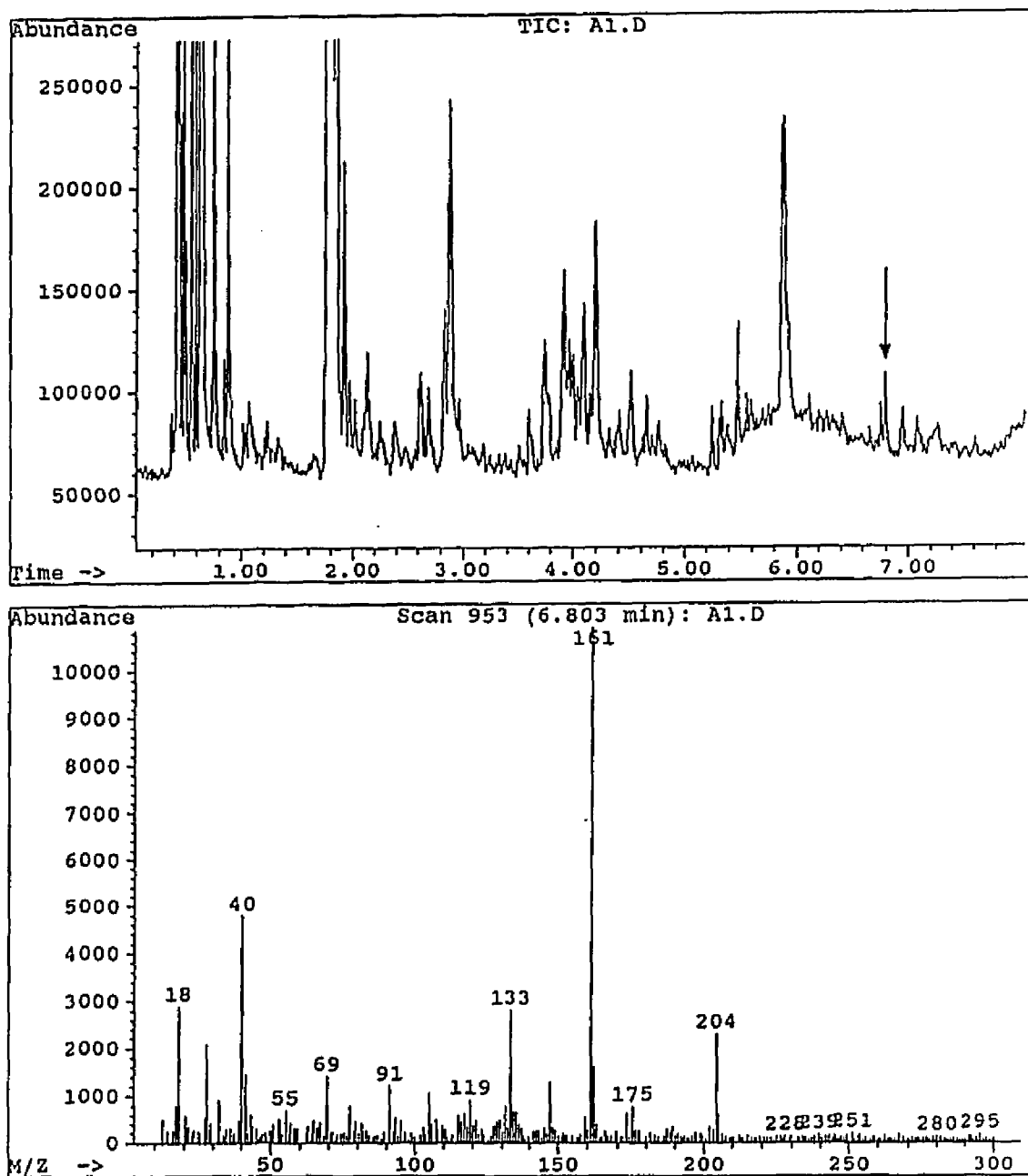
Figure 38. GC/MS data for $C_{15}H_{24}$ 

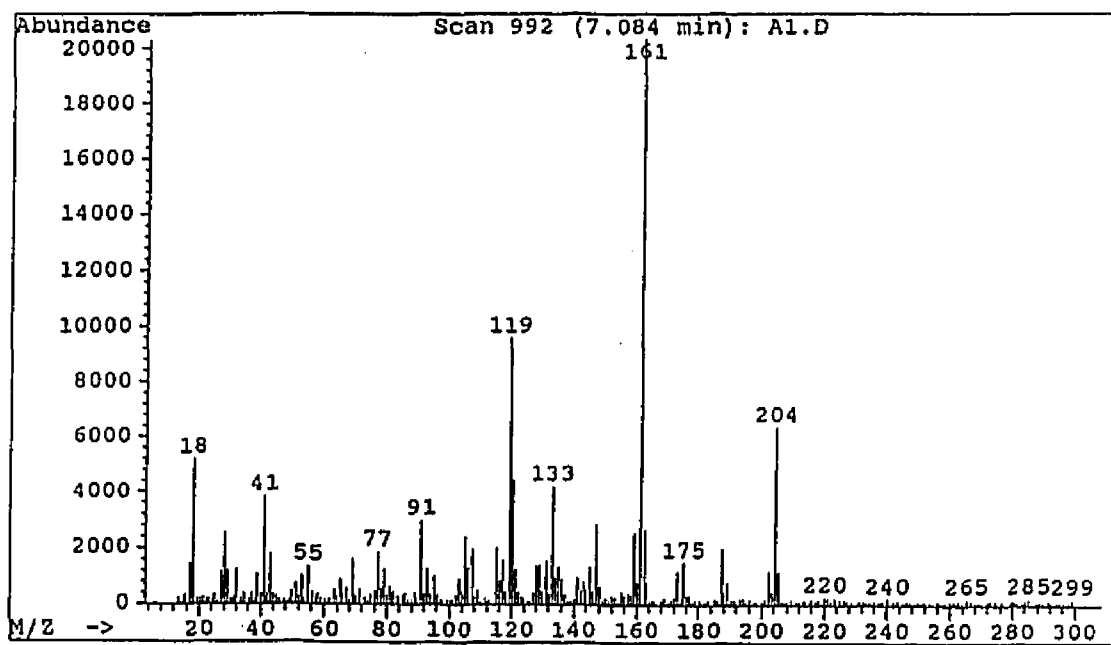
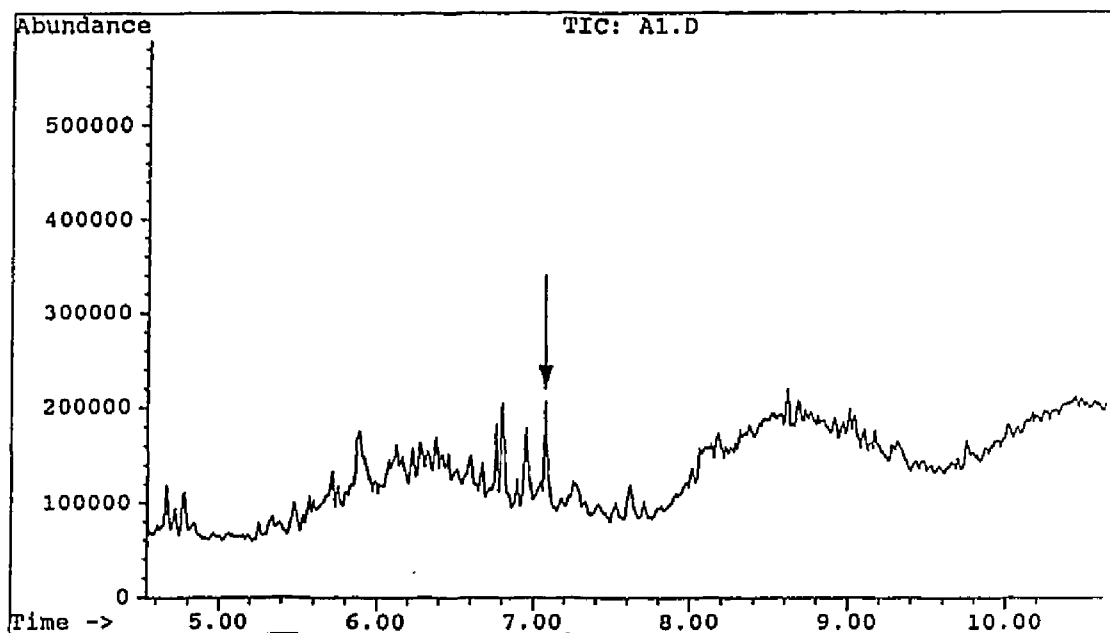
Figure 39. GC/MS data for $C_{15}H_{24}$ 

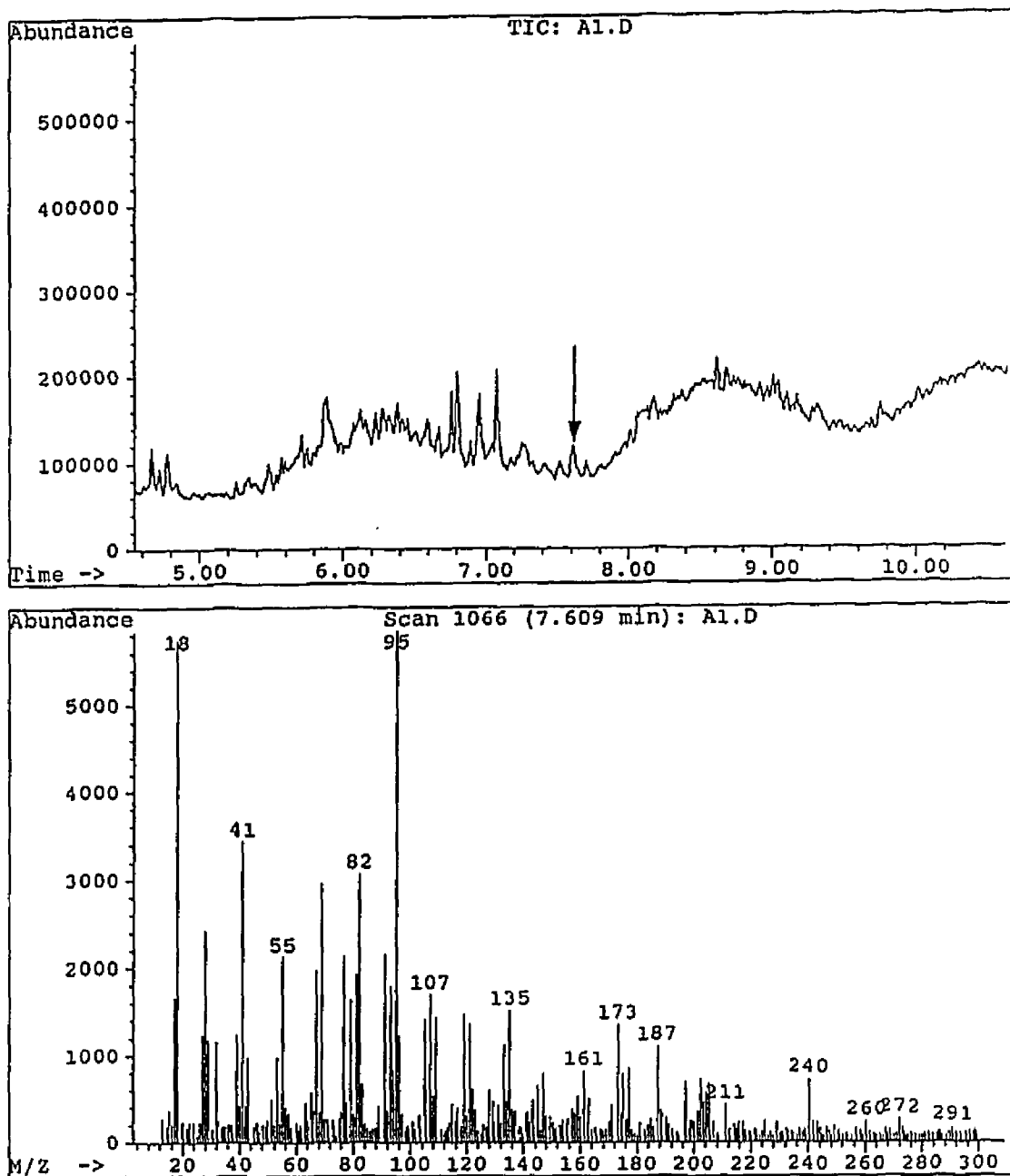
Figure 40. GC/MS data for $C_{15}H_{25}Cl$ 

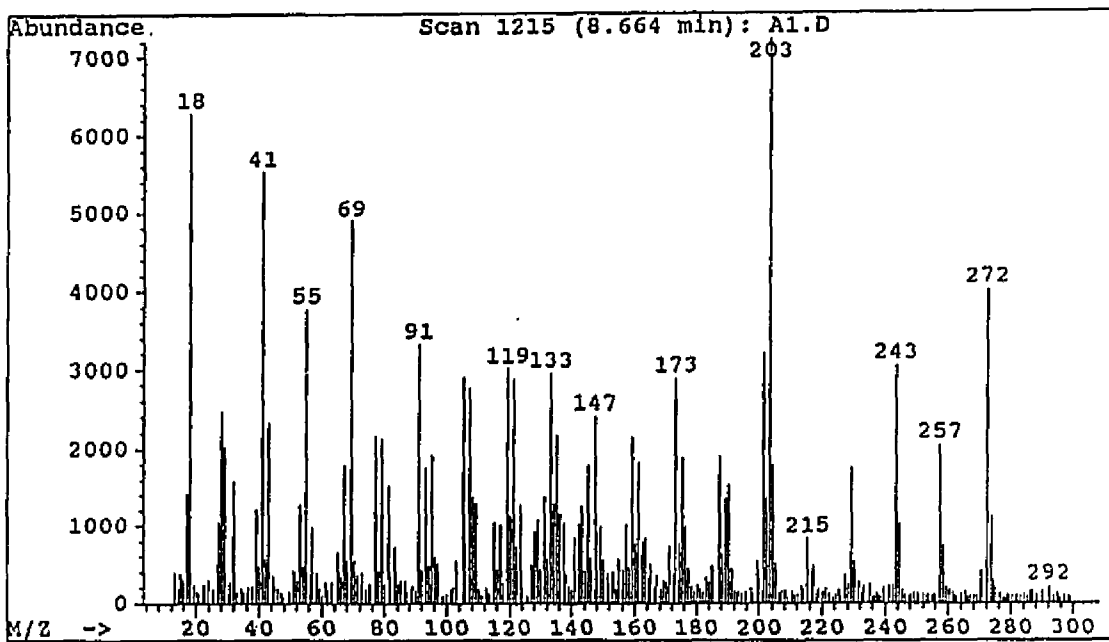
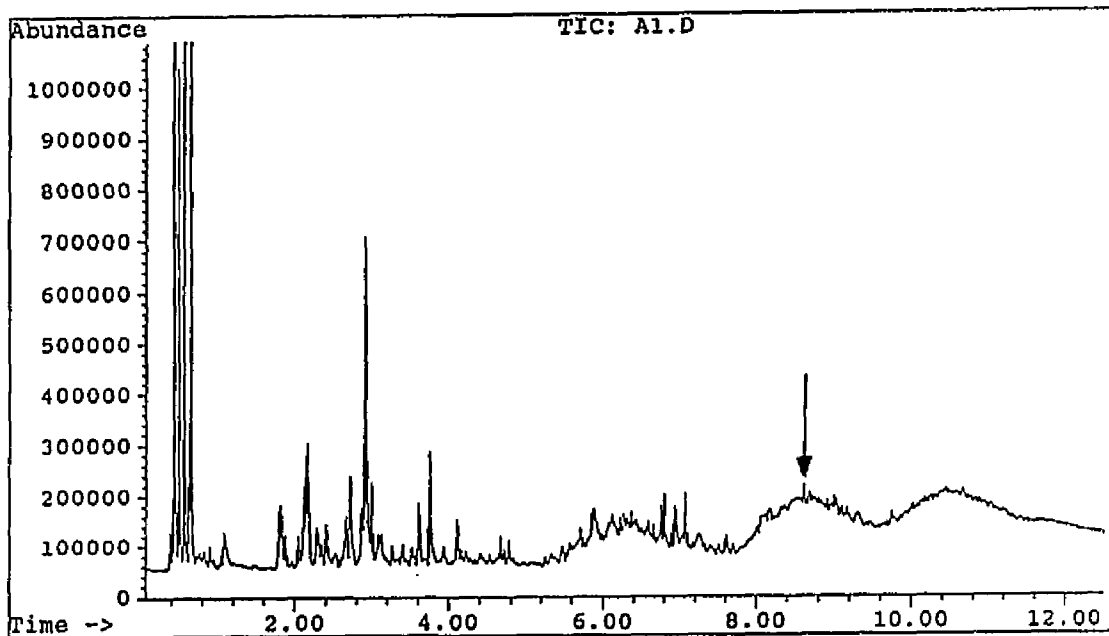
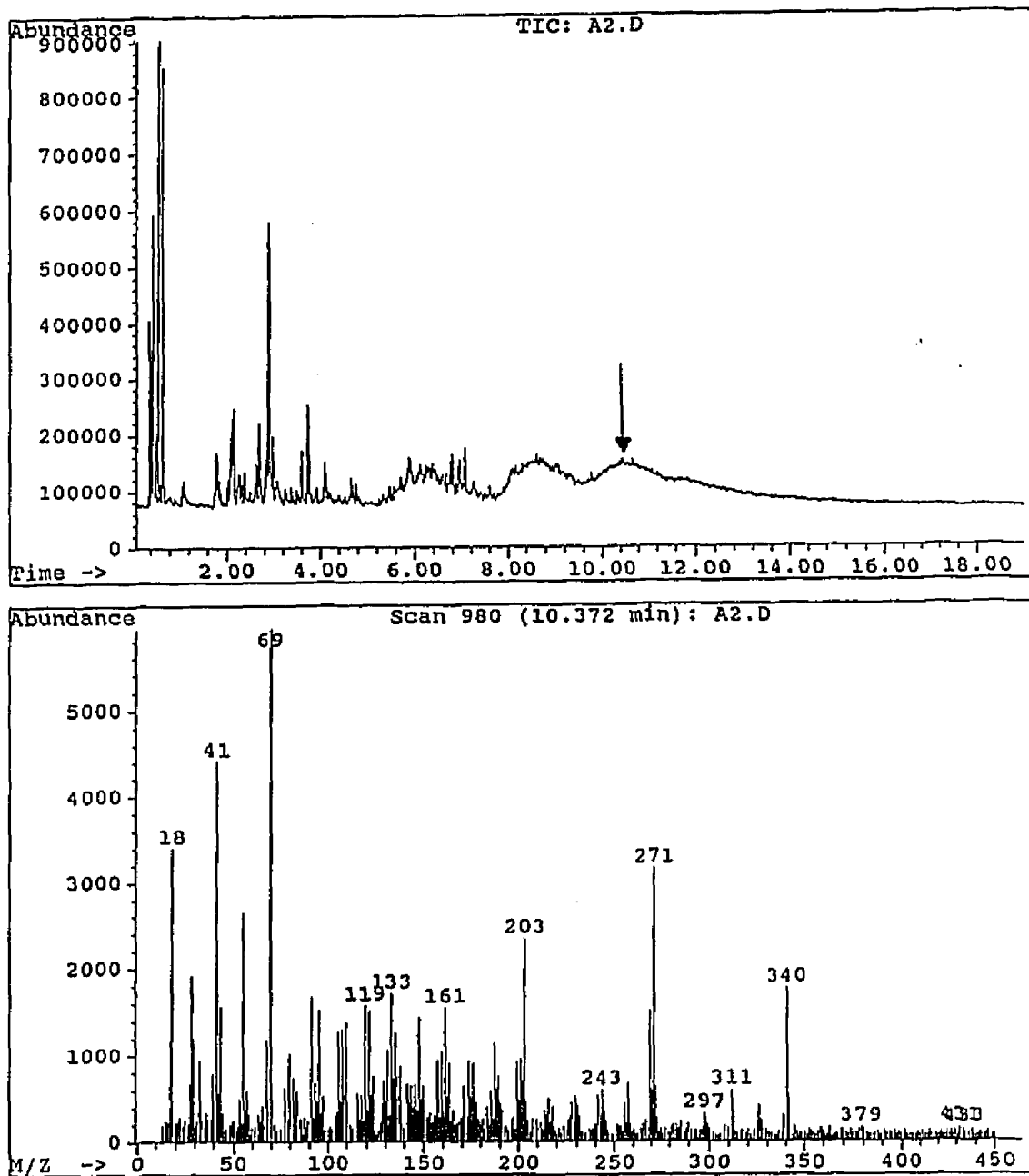
Figure 41. GC/MS data for $C_{20}H_{32}$ 

Figure 42. GC/MS data for $C_{25}H_{40}$ 

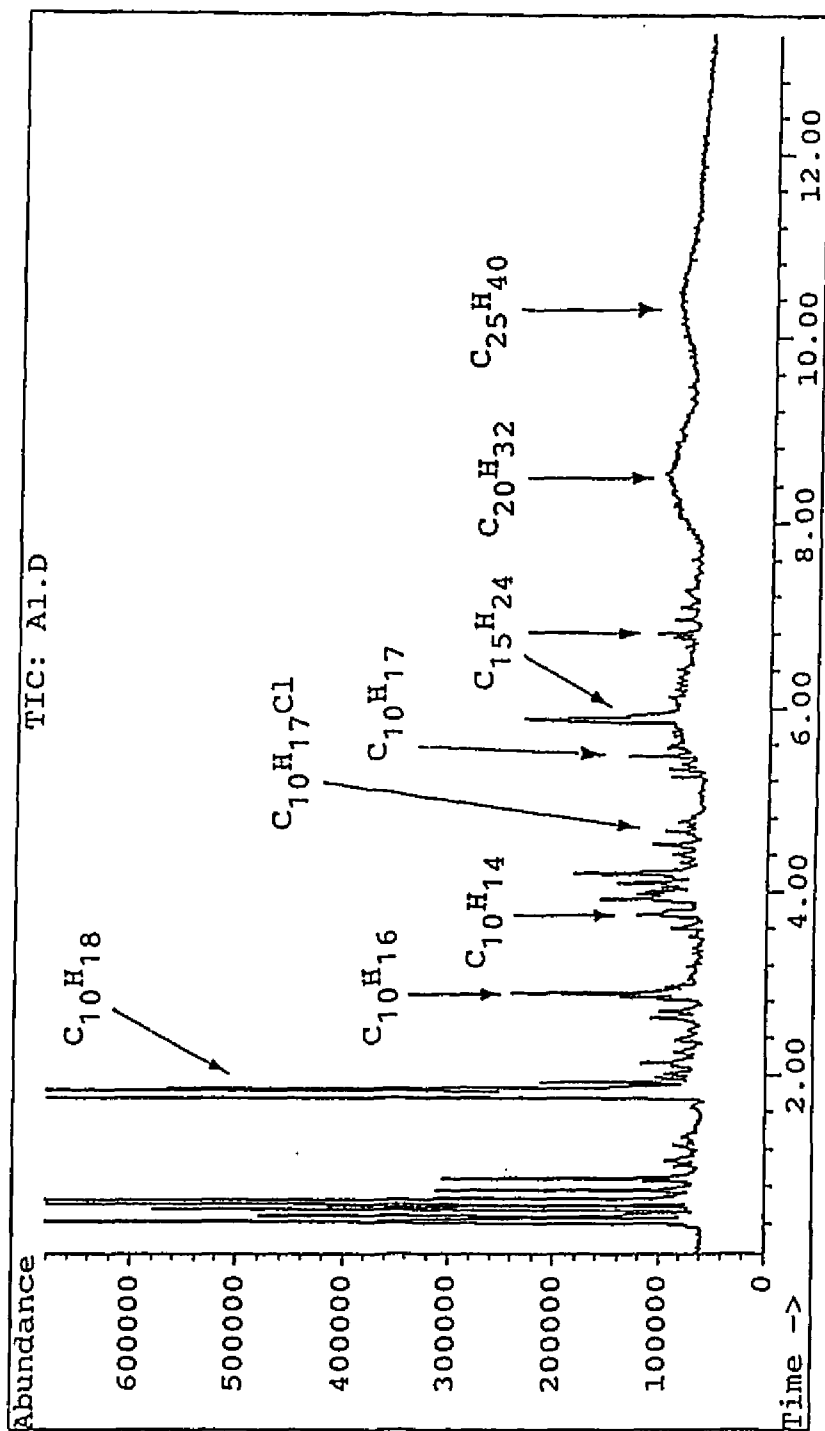


Figure 43. GC chromatogram of products obtained from

4-chloro-2-pentene and Cu after 1 h at 200 °C.

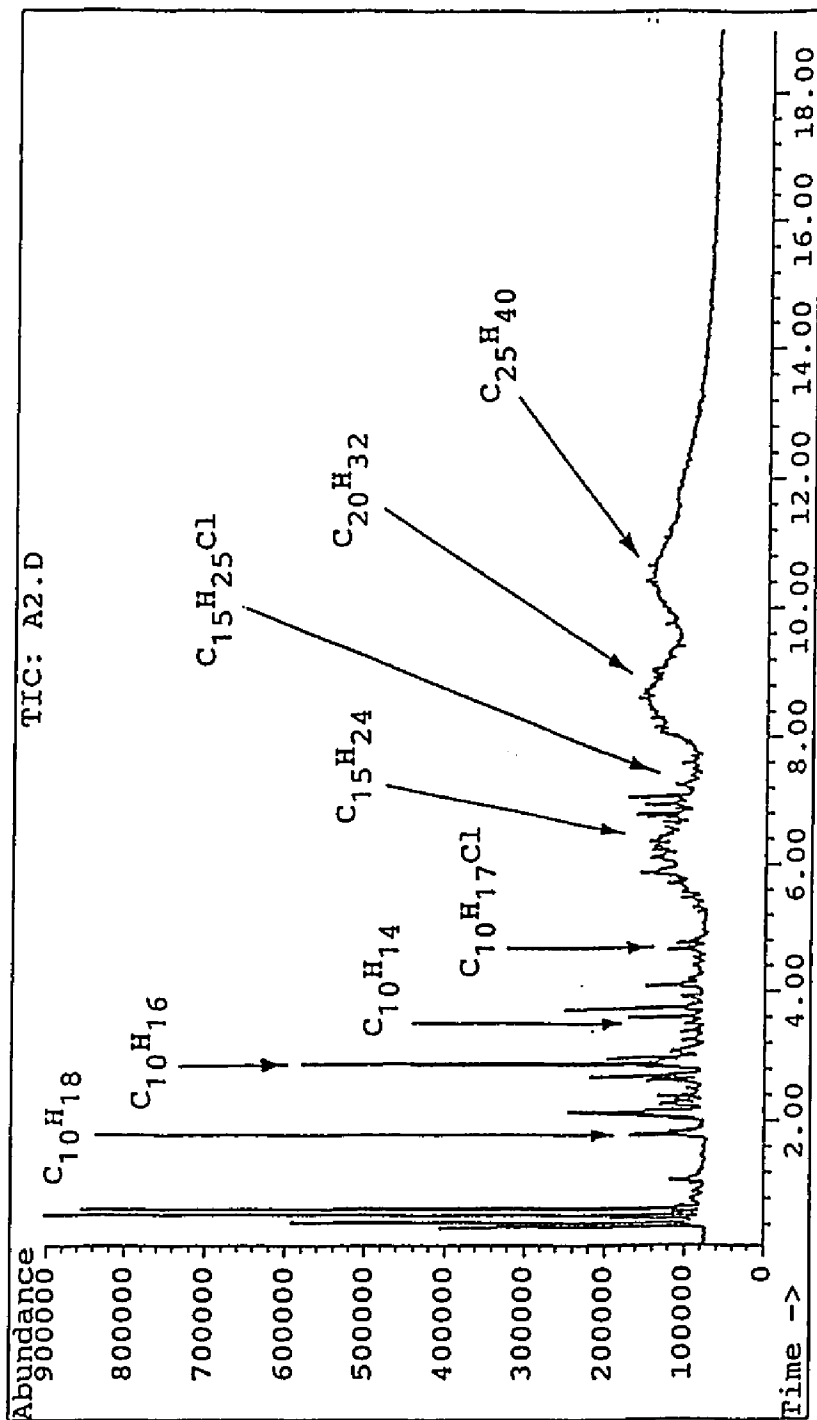


Figure 44. GC chromatogram of products obtained from

4-chloro-2-pentene and Cu_2O after 1 h at 200 °C.

products during the pyrolysis of 4-chloro-2-pentene: dehydrochlorination (to form 1,3-pentadiene) and oligomerization. There were no cracking products formed in any of the reactions, and the starting material was the largest component in the final mixture in each case. Control runs performed without copper additives at 200 °C for 1 h showed that 4-chloro-2-pentene gave 5 to 12% of 1,3-pentadiene (dehydrochlorination product) as the sole degradation product under these conditions.

In view of the results summarized in Table 8, the high-purity copper powder (99.999%) exhibits some unique catalytic properties, as compared to the other additives. Although all of the copper additives catalyzed the formation of numerous heavy products, the relative abundances and distributions of these products were quite different in each case, especially with the copper metal.

For the copper metal powder, the most abundant heavy products were the four isomeric $C_{10}H_{18}$ reductive-coupling dimers (MW 138), which accounted for 62% of the total amount of heavy products. The representative GC/MS traces for these products are shown in Figure 34, and these products were identified as the same dimers found in the previous model-compound studies, which involved the reactions of activated copper slurry or film with 4-chloro-2-pentene (see Tables 3 and 4 and Figures 15-17). The other heavy products (38%) were identified as oligomers formed by Lewis-

acid catalysis. Several $C_{10}H_{14}$ aromatic dimers were present, but they were very low in abundance.

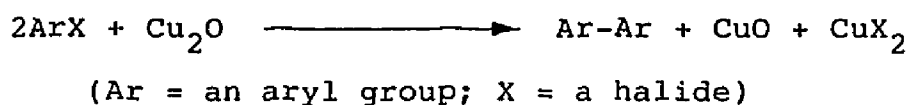
Cuprous oxide, on the other hand, promoted mainly the formation of Lewis-acid-catalyzed oligomers (dimers, trimers, tetramers, and pentamers), which accounted for nearly 96% of the total amount of heavy products in the reaction mixture. In this case, the reductive-coupling dimers amounted to only 4%. Very small amounts of aromatic dimers were also detected. In contrast to these results, Lattimer and Kroenke,⁴⁹ in their model-compound studies of 2,4-dichloropentane, conducted at 350 °C for 5 min, showed that Cu_2O promotes the formation of several $C_{10}H_{18}$ dimers (28%), along with Lewis-acid dimers, including $C_{10}H_{16}$ (31%) and $C_{10}H_{14}$ (saturated alkyl-substituted aromatic dimers, 41%). Starnes and Huang,⁵⁸ in their 4-chloro-2-pentene model-compound studies carried out at 200 °C for 1 h, reported that only Lewis-acid-catalyzed oligomers were formed in the presence of Cu_2O and that no trace of reductive-coupling products could be detected by GC/MS.

In the present investigation, similar results were also obtained from the pyrolysis of 4-chloro-2-pentene with CuO , in that the Lewis-acid-catalyzed oligomers (mainly dimers and trimers) were the most abundant heavy products, accounting for 88% of the total. In addition, with CuO , the yield of reductive-coupling dimers was only 12%. The other copper additives shown in Table 8 did not catalyze

the formation of reductive-coupling dimers, and in those cases the Lewis-acid-catalyzed oligomerization clearly played a major role in the formation of heavy products.

From a mechanistic perspective, one of the most important aspects of these experiments is their further confirmation of the occurrence of the reductive coupling reaction, which in the presence of high-purity copper metal is the principal route for the formation of heavy products. The high-purity copper metal used here may have contained some copper oxides as impurities. However, in view of our previous activated copper studies (see Section I), it is likely that the reductive coupling occurring in such reactions is brought about by the Cu^0 . Importantly, Lattimer and Kroenke⁴⁹ have reported that Cu_2O can be converted into Cu and CuO during the combustion of PVC. In addition, Cohen and co-workers¹⁰⁶ have observed catalytic effects of commercial copper powder on the Ullmann coupling of aryl halides such as *p*-iodotoluene. Similarly, the reductive-coupling products detected in our cuprous oxide and cupric oxide reaction mixtures suggest that Cu^0 may have been generated during the process of pyrolysis. Moreover, the low yields of these coupling products may have been due to the low efficiency of conversion of the oxides into highly reactive Cu^0 under the conditions of the present work. Catalytic effects in the coupling of aryl halides by cuprous oxide have been reported by Bacon

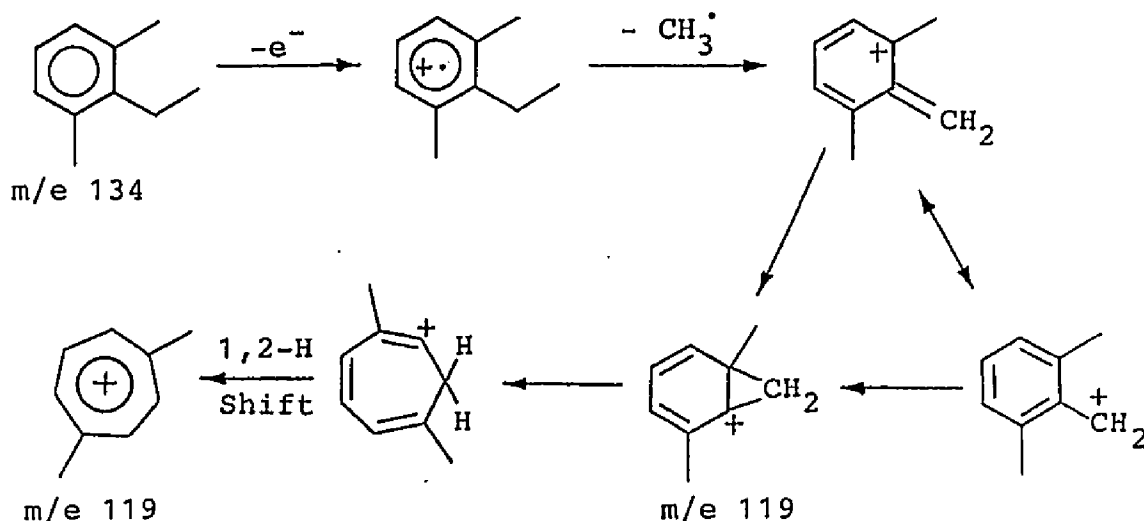
and co-workers.¹⁰⁷ They concluded that for particular halides, in particular solvents, cuprous oxide is capable of effecting a reasonable degree of coupling:



Further examination of the GC/MS data for the model-compound experiments revealed that several types of reactions probably were responsible for the formation of heavy products. In general, these reactions can be classified into five types: Diels-Alder cyclization, aromatization, Lewis-acid-catalyzed olefin oligomerization, chloroalkylation, and reductive-coupling dimerization.

Three isomeric aromatic $\text{C}_{10}\text{H}_{14}$ dimers (MW 134) were detected by GC/MS in all cases except for CuCl_2 , and they were relatively abundant in the case of CuO (16%), Cu_2S (23%), CuS (33%), CuC_2O_4 (19%), and CuI (64%), as shown in Table 8. These isomers (Figure 29) were tentatively identified as (saturated alkyl)-substituted C_4 -benzenes. Lattimer and Kroenke,⁴⁹ in their similar model-compound studies of 2,4-dichloropentane, observed that Cu_2O catalyzed the formation of several $\text{C}_{10}\text{H}_{14}$ isomers at 350 °C, and that they were relatively abundant (41%). Huang⁶² also detected these isomers in model-compound pyrolysis reactions involving 4-chloro-2-pentene and Cu_2O ,

and one of these isomers was assigned as 2,6-dimethylethylbenzene because a base peak having m/e 119 was detected in its mass spectrum and thought to be due to a resonance-stabilized benzyl ion or a substituted tropylium ion¹⁰⁸:



Numerous $C_{10}H_{16}$ isomers (MW 136, Figures 30-32) were detected in the reaction mixture for each copper additive, and they were the most abundant aliphatic heavy products found in the case of $CuCl_2$ (53%), $CuCl$ (25%), and CuC_2O_4 (53%). For Cu_2O a total of 14 isomers was detected. Two major reactions evidently were involved in the formation of these isomers: Diels-Alder cyclization (which leads to an intense base peak at m/e 68 that corresponds to the 1,3-pentadiene fragment from the retro-Diels-Alder reaction¹⁰⁹) and Friedel-Crafts dimerization. The Lewis-

acid dimers were more abundant than the Diels-Alder dimers in all cases except for CuCl, which gave nearly equal amounts of both types of dimers.

Chloroalkylation dimers, $C_{10}H_{17}Cl$ (MW 172, Figures 35 and 36), were found to be relatively abundant in the case of CuO (21%), CuCl (40%), Cu_2S (33%), CuC_2O_4 (28%), and CuI (26%).

Lewis-acid trimers, $C_{15}H_{24}$ (MW 204, Figures 37-39), were detected in the reaction mixtures for all copper additives except CuI, and they were relatively abundant in the case of Cu (16%), Cu_2O (23%), and Cu_2S (11%). Aliphatic trimers were more abundant than aromatic trimers (see Figures 37 and 38) except in the case of Cu_2O (see Figure 39), where both types of trimers were detected in nearly equal amounts.

Other high-molecular-weight heavy products such as $C_{15}H_{25}Cl$ trimers (MW 240, Figure 40), $C_{20}H_{32}$ tetramers (MW 272, Figure 41), and $C_{25}H_{40}$ pentamers (MW 340, Figure 42) showed numerous peaks in their chromatograms. Analyses by GC/MS indicated that these substances were all Lewis-acid-catalyzed (Friedel-Crafts) aliphatic oligomers, and no traces of aromatic (peak at m/e 77 which corresponds to the $C_6H_5^+$ fragment) or Diels-Alder products (intense peak at m/e 68 which corresponds to the 1,3-pentadiene fragment from the retro-Diels-Alder cyclization¹⁰⁹) were found among them. These oligomers were the most abundant

heavy products in the case of Cu_2O (50%) and CuS (64%).

As for the $\text{C}_{10}\text{H}_{17}$ isomers (MW 137, Figure 33), their odd molecular-ion peak must be a fragment rather than a parent ion. These aliphatic isomers may be derived from the heavy oligomers by the addition of extra hydrogens (from aromatization) to olefinic segments.

In summary: (1) all of the copper additives discussed in this section can promote the dehydrochlorination and oligomerization of 4-chloro-2-pentene; (2) in the case of copper metal, the reductive-coupling dimers are the most abundant heavy products found in the reaction mixtures; (3) copper additives, except copper metal, can serve as Lewis-acid catalysts that give oligomerization and chloro-alkylation products, and such products are the dominant components in the reaction mixtures; (4) reductive coupling products were not observed for any of the Lewis-acid-type copper additives except Cu_2O and CuO , and in the latter cases, these dimers were much less abundant than in the case of copper metal; (5) heavy products resulting from Diels-Alder cyclization were observed for all of the copper additives studied, but they were always relatively low in abundance; (6) aromatic dimers were fairly abundant in the case of CuO , Cu_2S , CuS , CuC_2O_4 , and CuI .

The results of the current model-compound studies have clearly shown that copper metal, when used in the form of high-purity powder, can promote the reductive

coupling of secondary allylic chlorides. Taken together with the results obtained from (a) the activated copper (slurry or film) model-compound experiments and (b) earlier PVC degradation studies,⁶³ these observations strongly suggest that in the presence of active copper metal (Cu^0), reductive coupling is the principal mechanism for the crosslinking of degraded PVC. Copper oxides, copper chlorides, and other Lewis-acid-type copper additives, on the other hand, showed the expected catalytic effects of Lewis acids on the formation of olefin oligomerization and chloroalkylation heavy products (Friedel-Crafts reaction). Thus it can be concluded that, in the presence of these copper compounds, Lewis-acid catalysis plays a major role in the formation of crosslinking structures in degraded PVC.

2-3. Pyrolysis of Conjugated Alkenes in the Presence of Copper Additives

In the previous section, copper additives were shown to be able to promote the dehydrochlorination of 4-chloro-2-pentene to form conjugated alkene, and since polyene sequences are well-known to participate in the crosslinking of PVC,²⁸ it was of interest to study the crosslinking chemistry of polyenes induced by copper additives. Two model compounds, 2,4-hexadiene and 1,3,5-hexatriene, were selected, therefore, for use in sealed-tube pyrolysis experiments. Five copper additives were allowed to react with these model compounds; they included high-purity copper metal powder (Cu, 99.999%), cuprous oxide (Cu₂O), cupric oxide (CuO), cuprous chloride (CuCl), and cupric chloride (CuCl₂).

A control experiment using 2,4-hexadiene without copper additives was performed at 200 °C for 1 h. Analysis by GC/MS showed that no reaction had occurred. Further experiments with 2,4-hexadiene and Cu, Cu₂O, CuO, or CuCl, performed at 200 °C for 1 h, all delivered the same result as the control run. However, results of particular significance were obtained from the reaction of 2,4-hexadiene with CuCl₂. When 2,4-hexadiene was treated with CuCl₂ at 200 °C for 1 h, a very complex mixture resulted. Analyses of the resultant degradation products

are summarized in Table 10, and representative GC/MS spectra for each component are shown in Figures 45-58. Based on the GC/MS analysis, the starting material was found to be the most abundant component. Although the mixture was much too complex for complete characterization, the chromatogram showed that it consisted of numerous heavy products with molecular weights ranging from 116 to 246 (Table 10). Their proposed representative chemical structures are shown in Table 11. The three $C_6H_{11}Cl$ isomers (MW 118, Figure 46) were found to be the principal degradation products. They were tentatively assigned as 4-chloro-2-hexene and its isomers. The evidence for the existence of one chlorine atom in the $C_6H_{11}^{35}Cl$ component is clearly provided by the M+2 mass spectral peak that is approximately one-third the intensity of the other molecular ion peak. In addition, the peak with m/e 83 indicates a possible 2-hexenyl fragment structure. The two C_6H_9Cl isomers (MW 116, Figure 45) were assigned as 3-chloro-2,4-hexadiene and its isomers. Their mass spectra show molecular fragment patterns similar to that of 4-chloro-2-hexene (except for the base peak with m/e 81 which was an indication of a possible 2,4-hexenyl fragment).

The formation of $C_6H_{11}Cl$ and C_6H_9Cl species may involve rechlorination as shown in Scheme 26; for the formation of 4-chloro-2-hexene, two extra hydrogens may become available to the system due to aromatization

Table 10. Distribution of Degradation Products Obtained
from Reaction of 2,4-Hexadiene with CuCl_2
at 200 °C for 1 h

MW	Chemical Formula	Yield (%) ^a
116 (Fig. 45)	$\text{C}_6\text{H}_9^{35}\text{Cl}$	10
118 (Fig. 46)	$\text{C}_6\text{H}_{11}^{35}\text{Cl}$	49
160 (Fig. 47)	$\text{C}_{12}\text{H}_{16}$	4
162 (Figs. 48-50)	$\text{C}_{12}\text{H}_{18}$	5
164 (Figs. 51-53)	$\text{C}_{12}\text{H}_{20}$	13
242 (Fig. 54)	$\text{C}_{18}\text{H}_{26}$	1
244 (Fig. 55)	$\text{C}_{18}\text{H}_{28}$	2
246 (Fig. 56)	$\text{C}_{18}\text{H}_{30}$	8
83 (Fig. 57)	C_6H_{11}	3
98 (Fig. 58)	C_7H_{14}	5

a. GC area percentages based on total peak area of heavy products.

Table 11
Representative Tentative Chemical Structures of the Heavy
Products Listed in Table 10

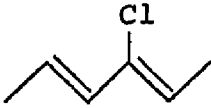
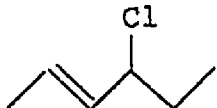
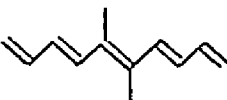
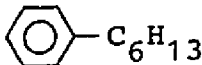
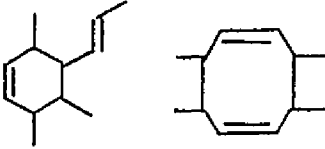
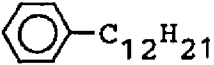
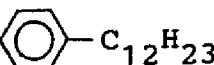
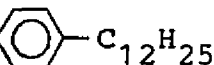
MW	Chemical Formula	Chemical Structure(s)
116	$C_6H_9^{35}Cl$ (Fig. 45)	
118	$C_6H_{11}^{35}Cl$ (Fig. 46)	
160	$C_{12}H_{16}$ (Fig. 47)	
162	$C_{12}H_{18}$ (Figs. 48-50)	
164	$C_{12}H_{20}$ (Figs. 51-53)	
242	$C_{18}H_{26}$ (Fig. 54)	
244	$C_{18}H_{28}$ (Fig. 55)	
246	$C_{18}H_{30}$ (Fig. 56)	

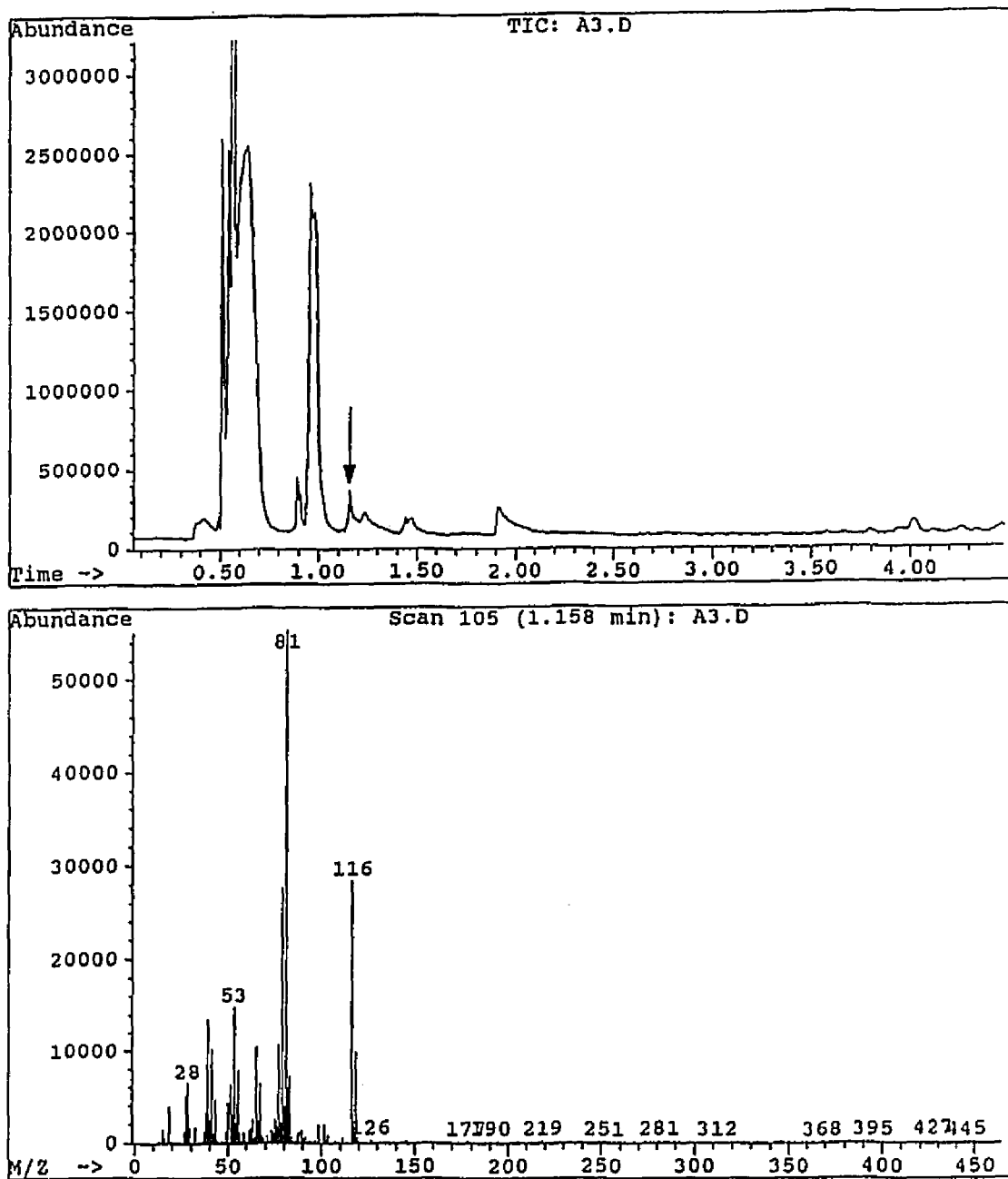
Figure 45. GC/MS data for C_6H_9Cl 

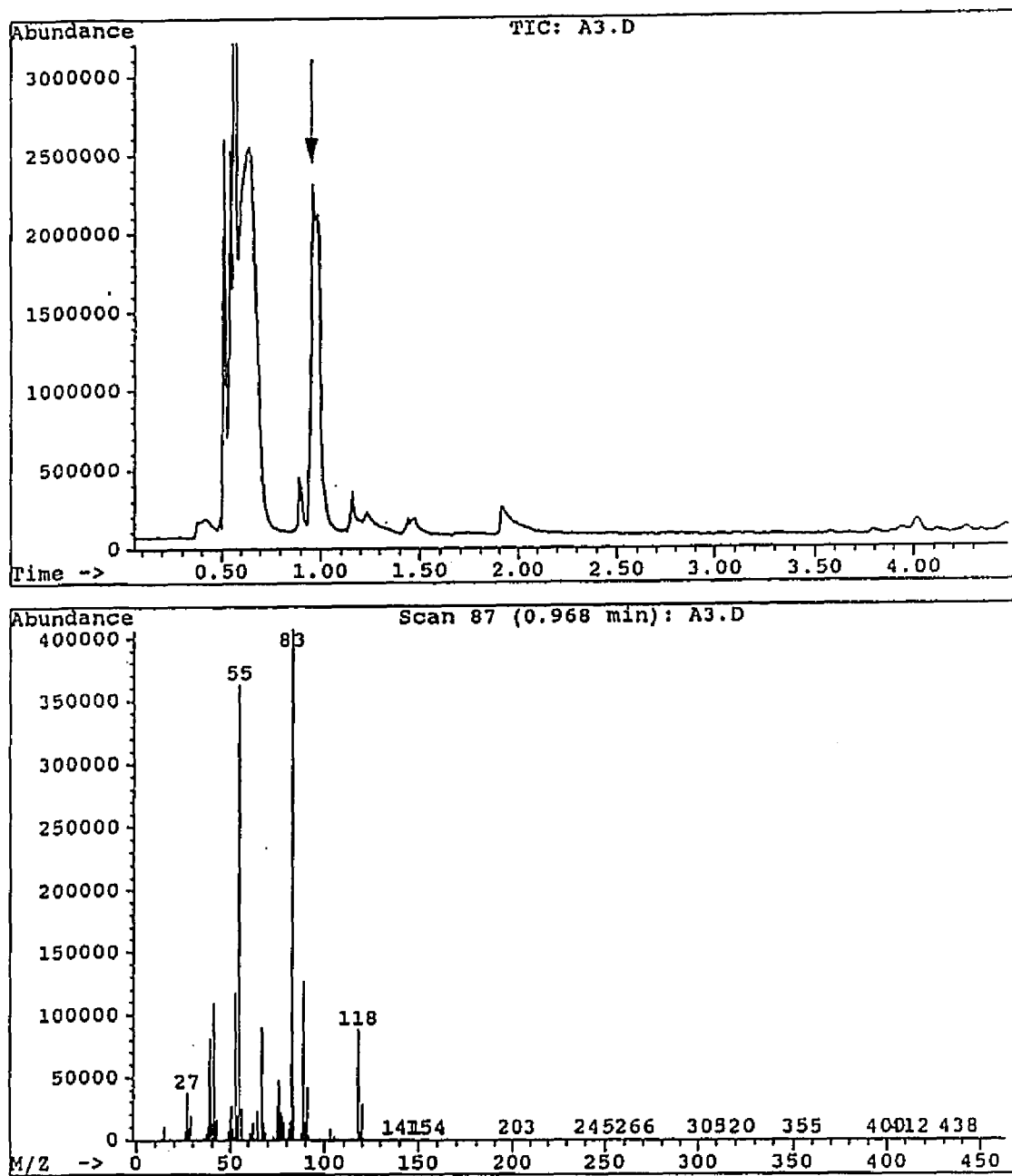
Figure 46. GC/MS data for $C_6H_{11}Cl$ 

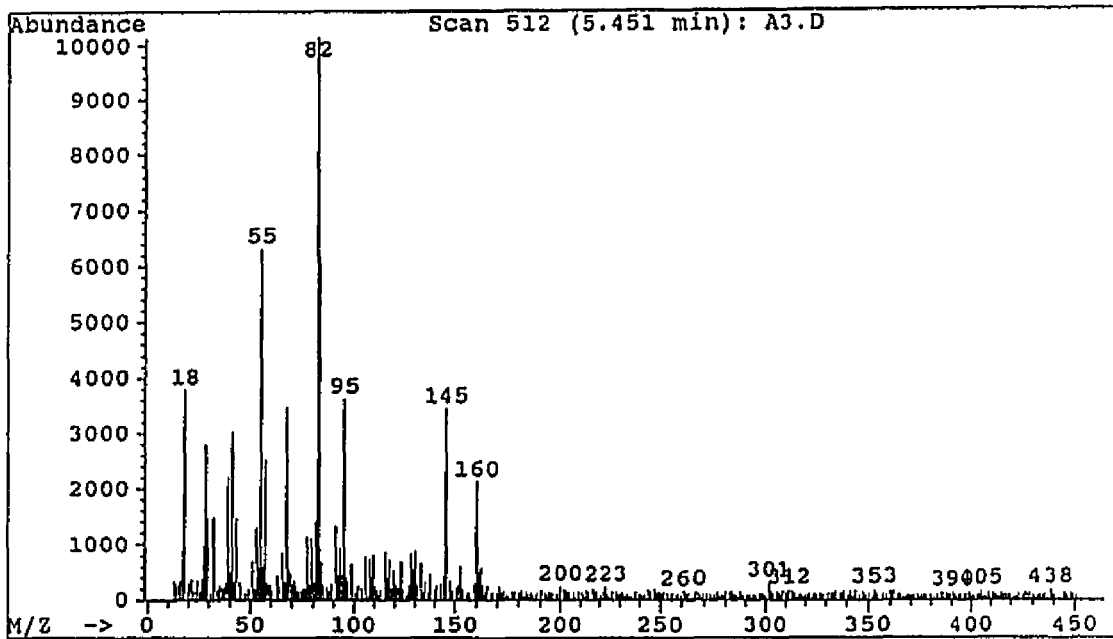
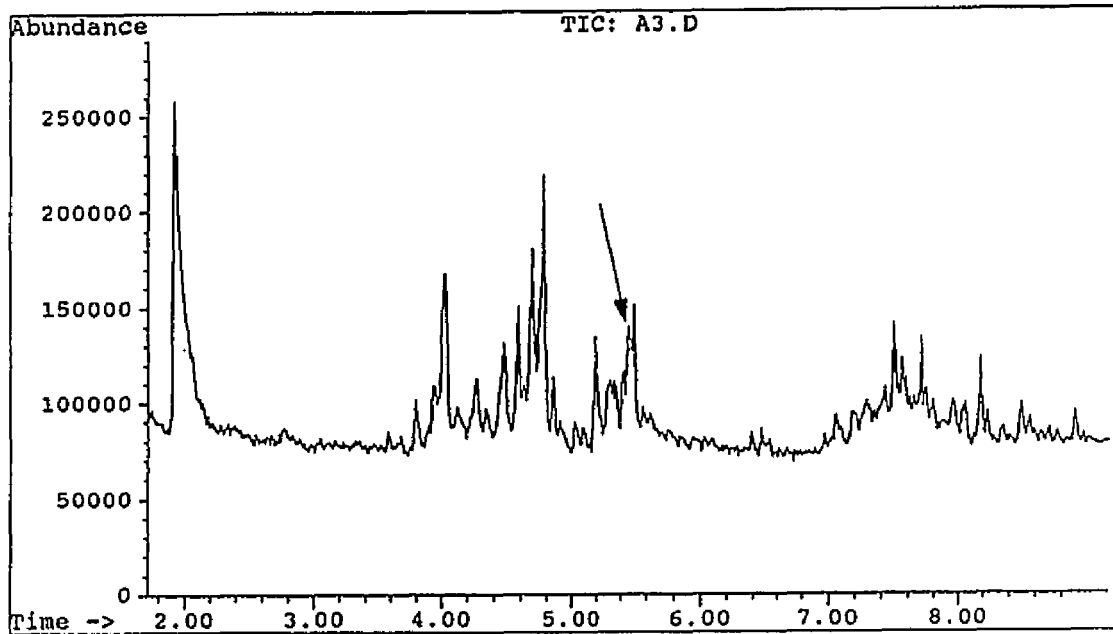
Figure 47. GC/MS data for $C_{12}H_{16}$ 

Figure 48. GC/MS data for $C_{12}H_{18}$

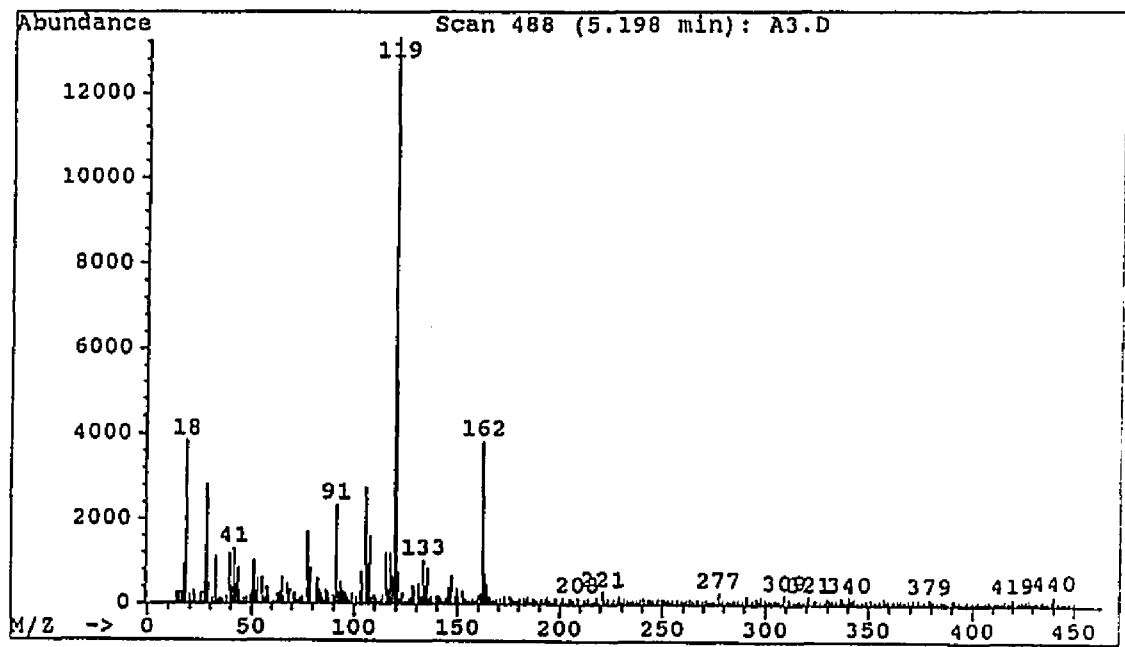
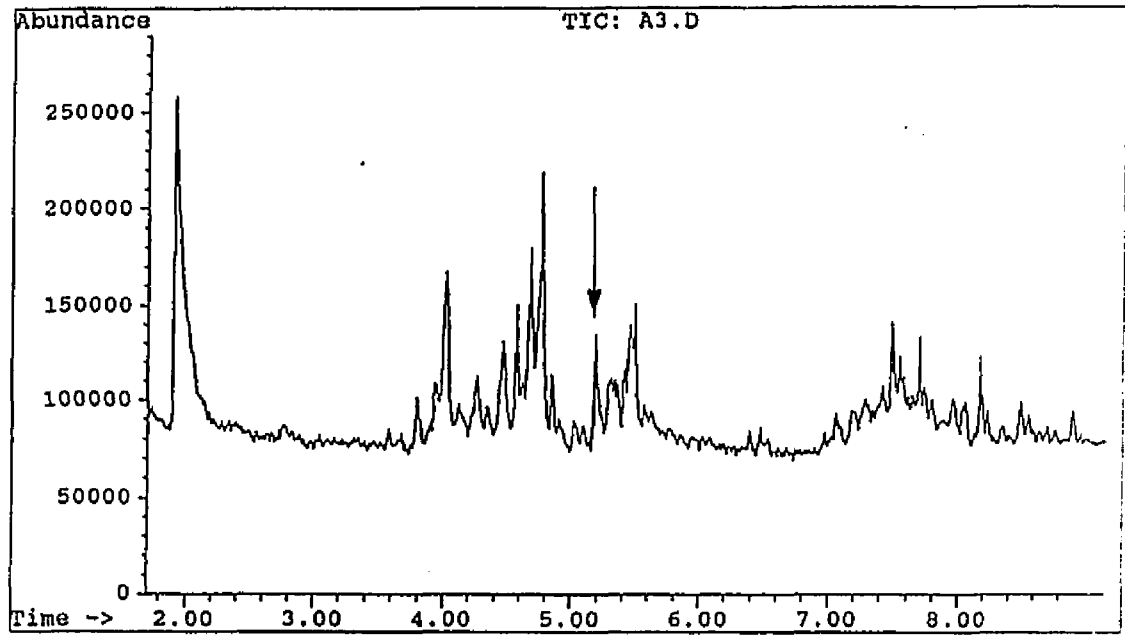


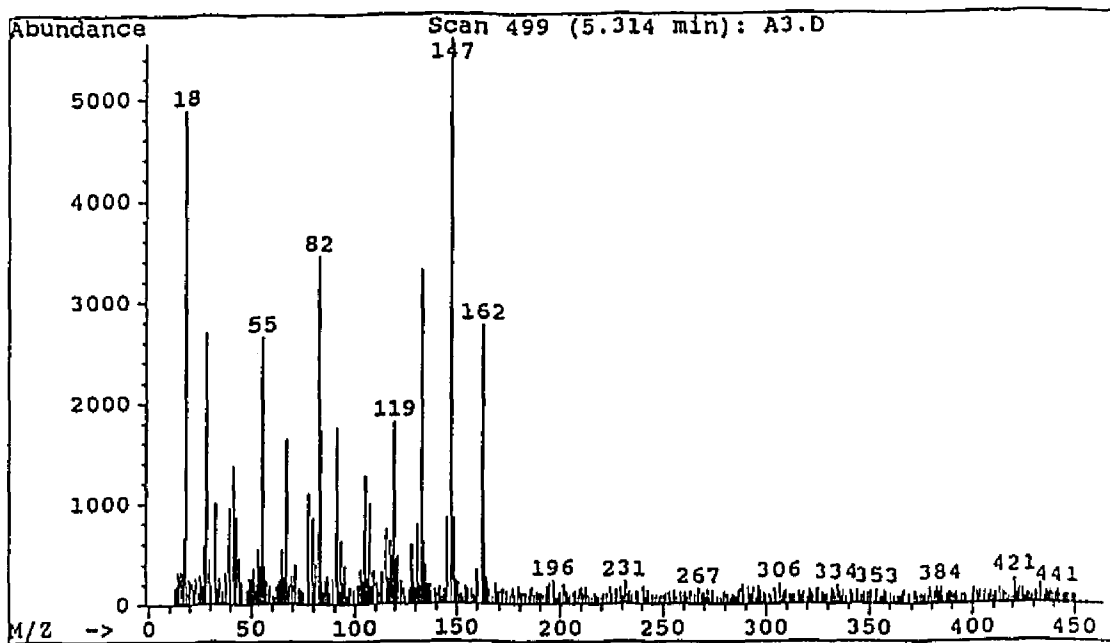
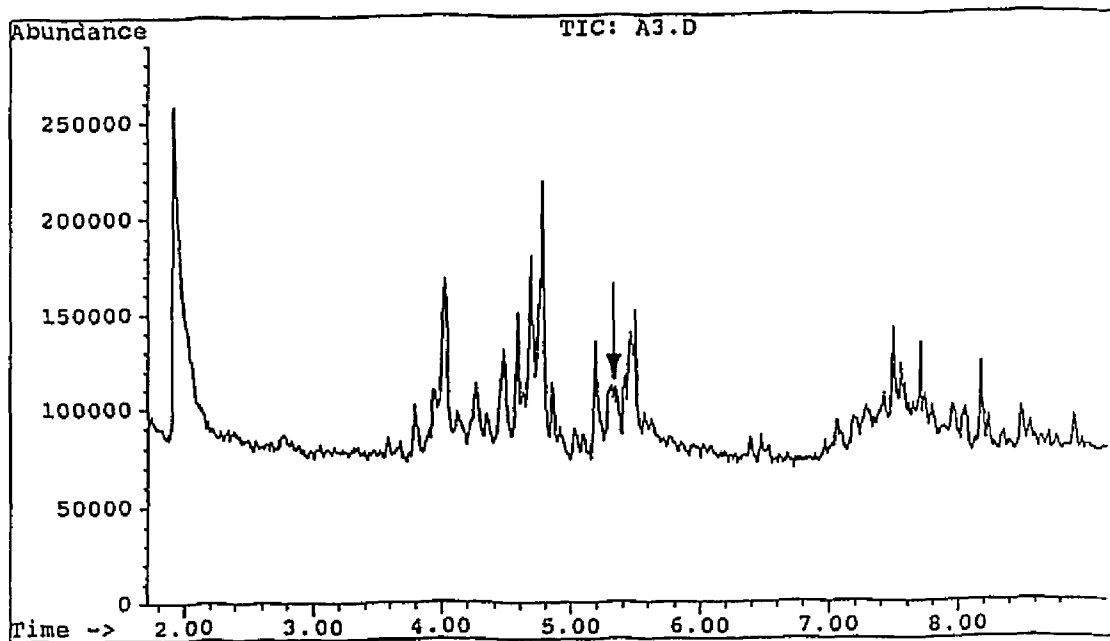
Figure 49. GC/MS data for $C_{12}H_{18}$ 

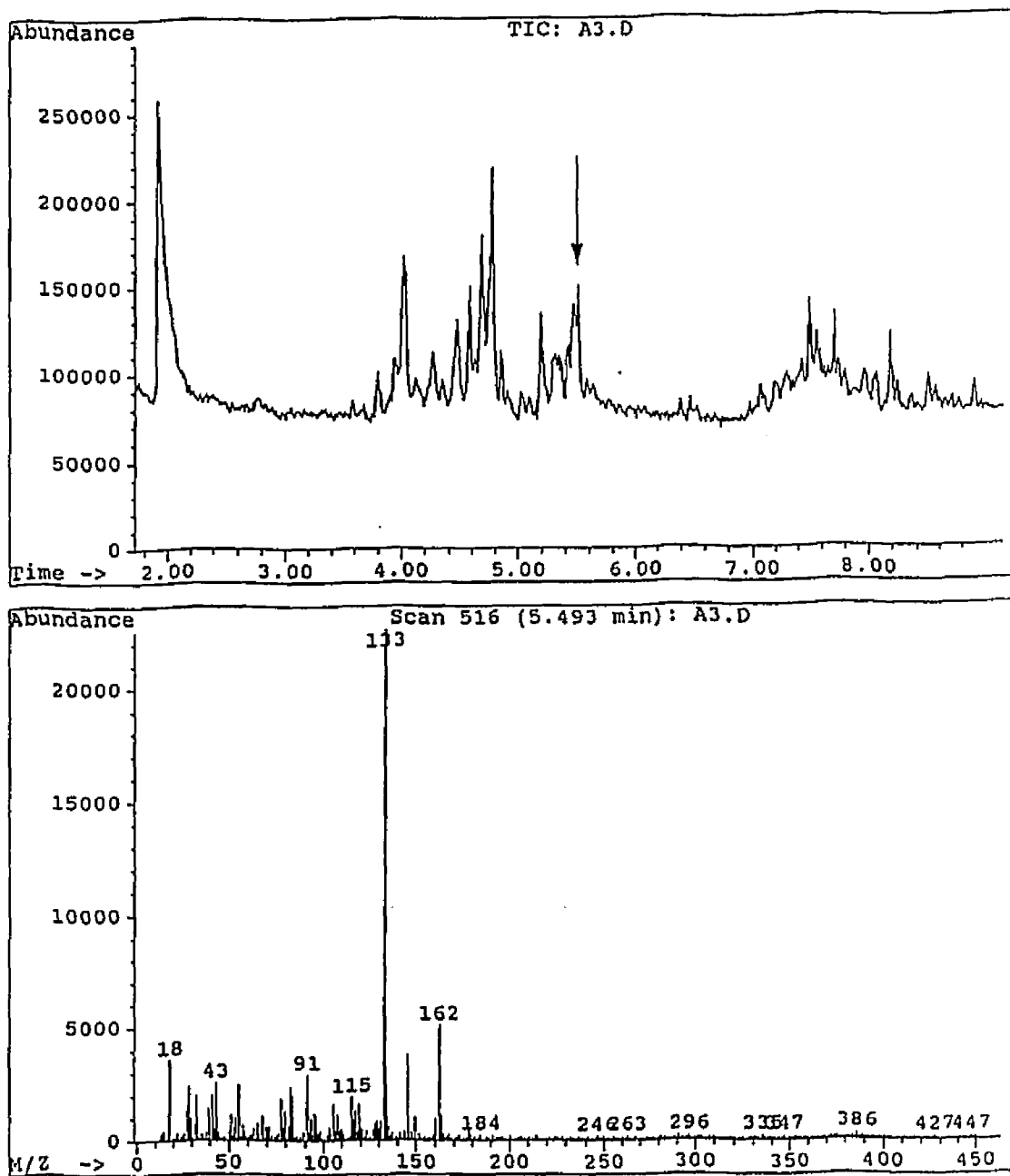
Figure 50. GC/MS data for $C_{12}H_{18}$ 

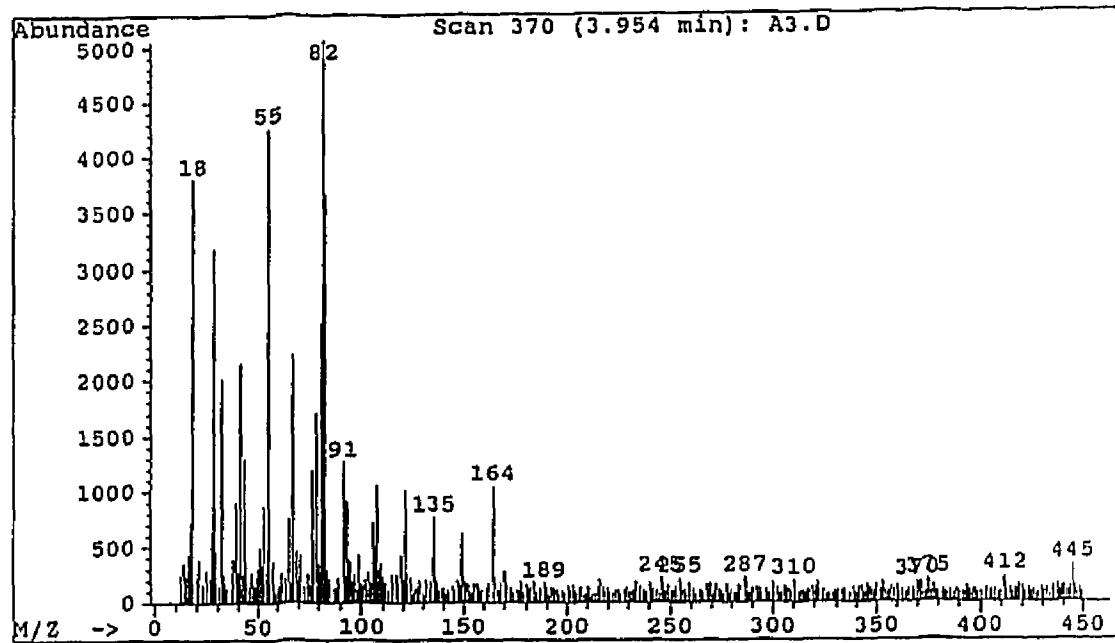
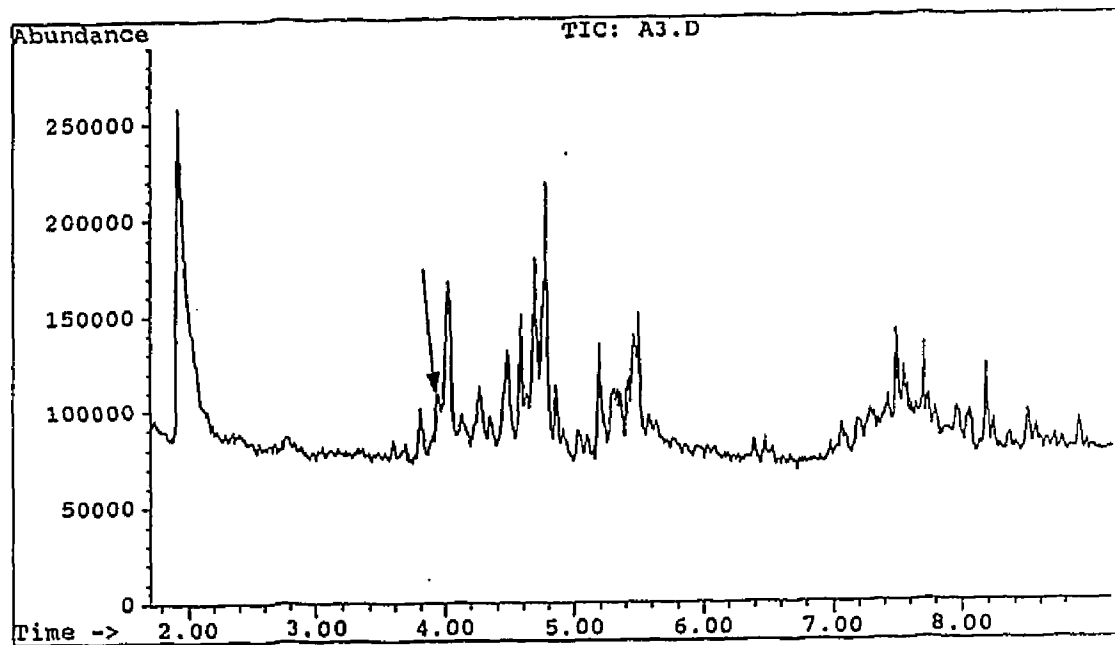
Figure 51. GC/MS data for $C_{12}H_{20}$ 

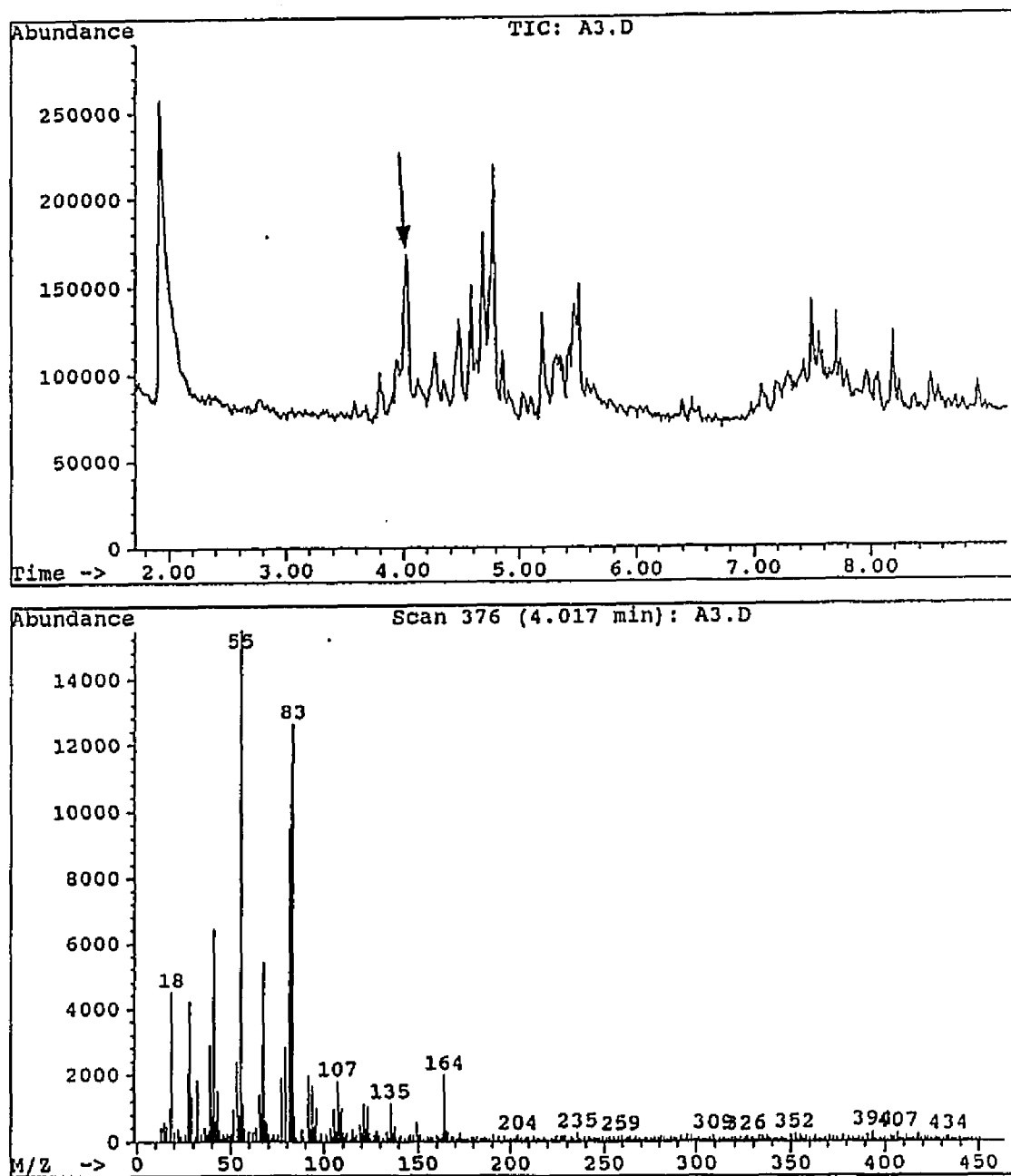
Figure 52. GC/MS data for $C_{12}H_{20}$ 

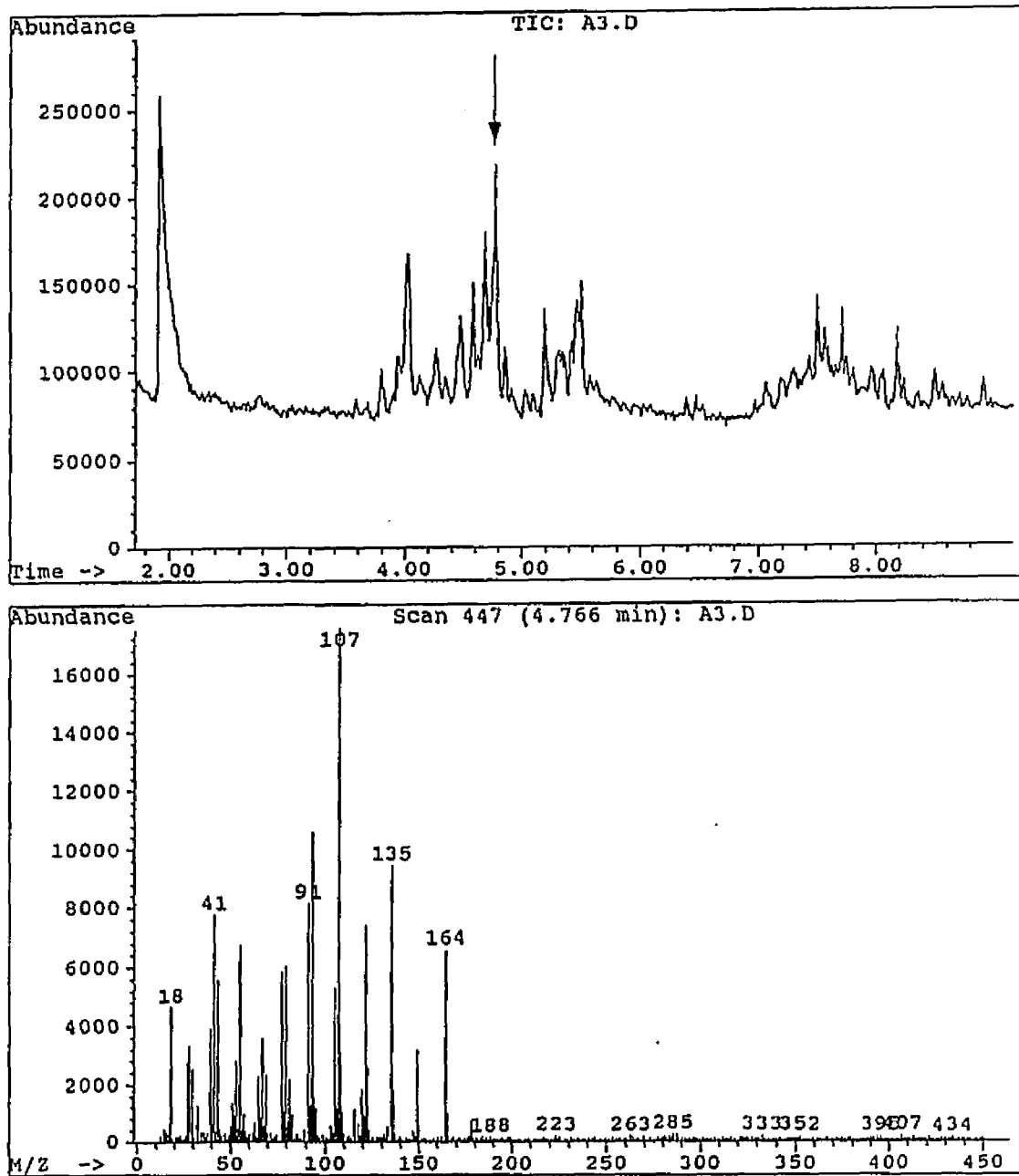
Figure 53. GC/MS data for $C_{12}H_{20}$ 

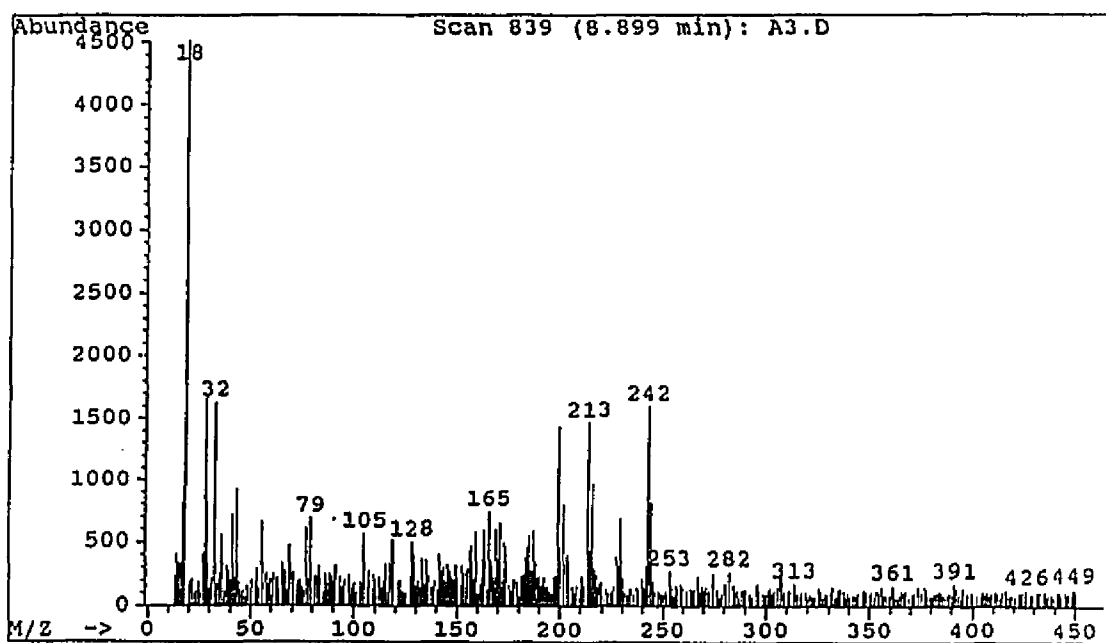
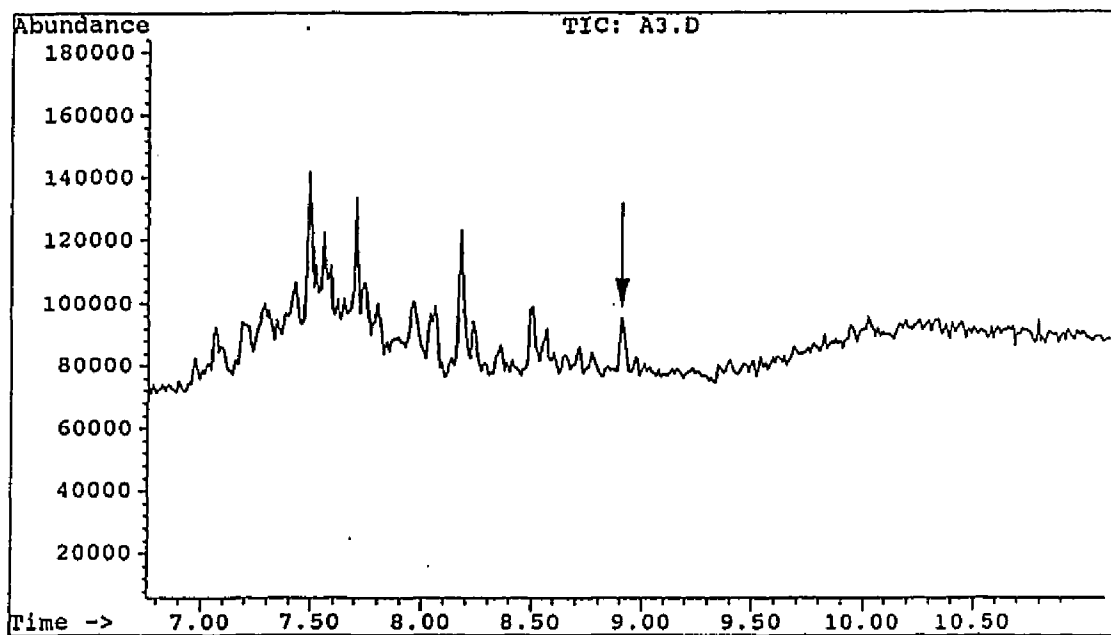
Figure 54. GC/MS data for $C_{18}H_{26}$ 

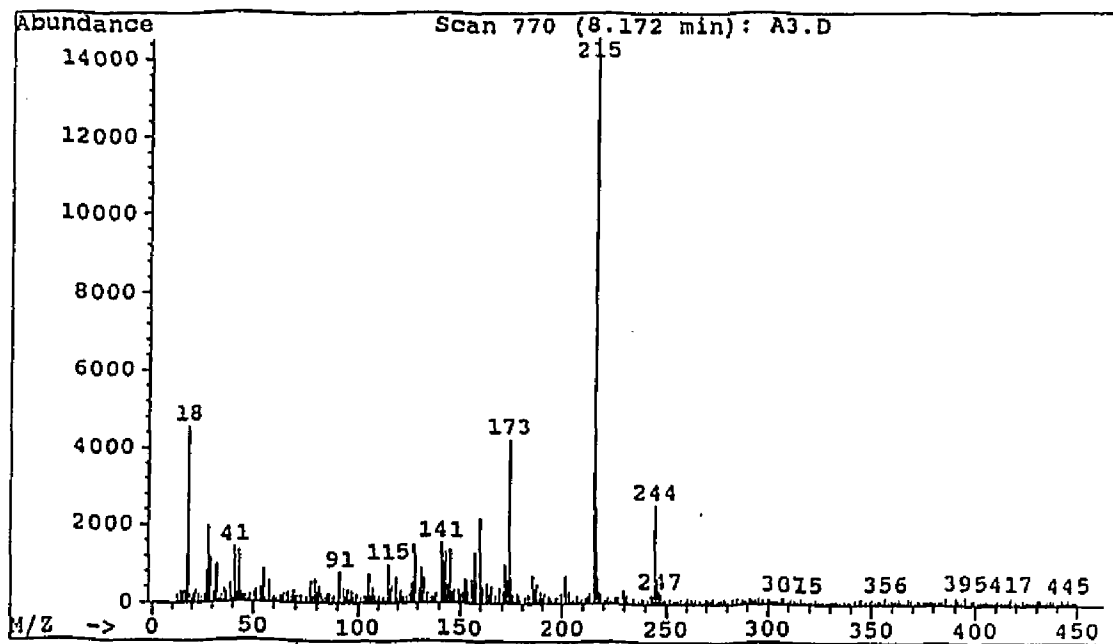
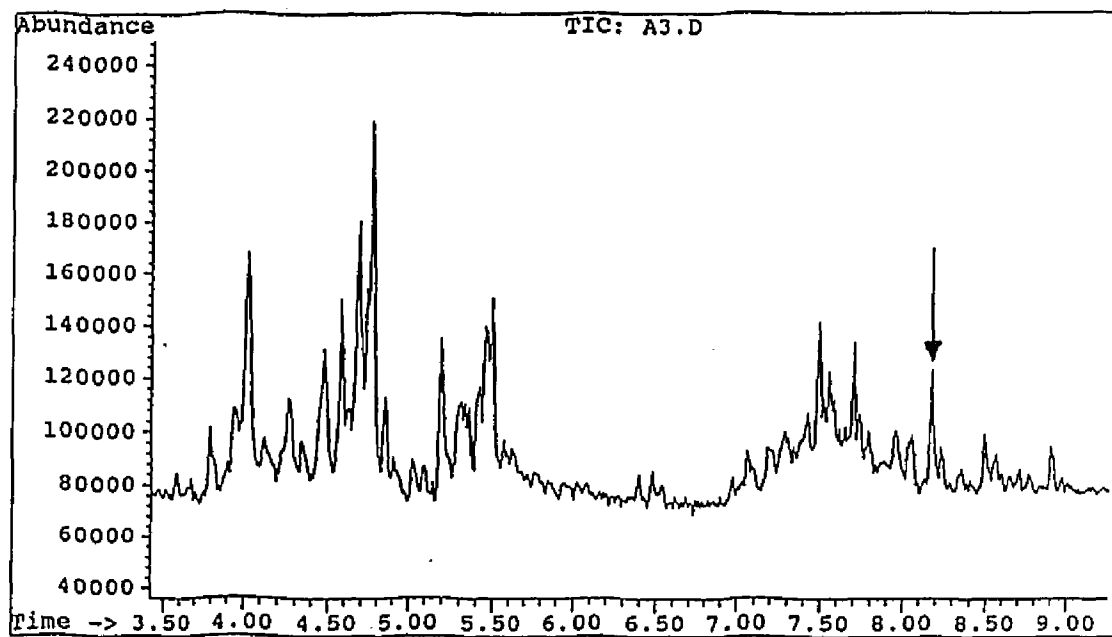
Figure 55. GC/MS data for $C_{18}H_{28}$ 

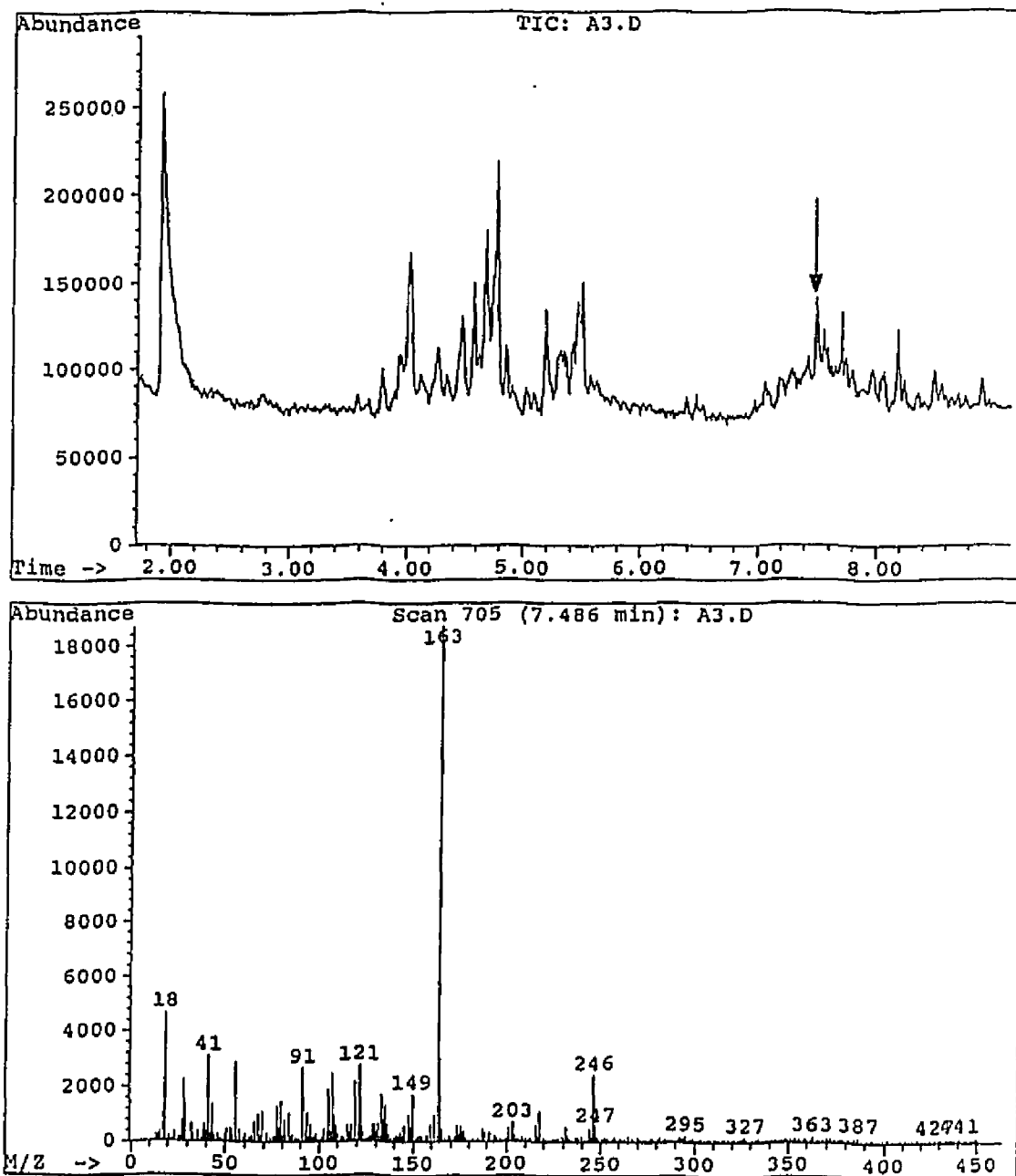
Figure 56. GC/MS data for $C_{18}H_{30}$ 

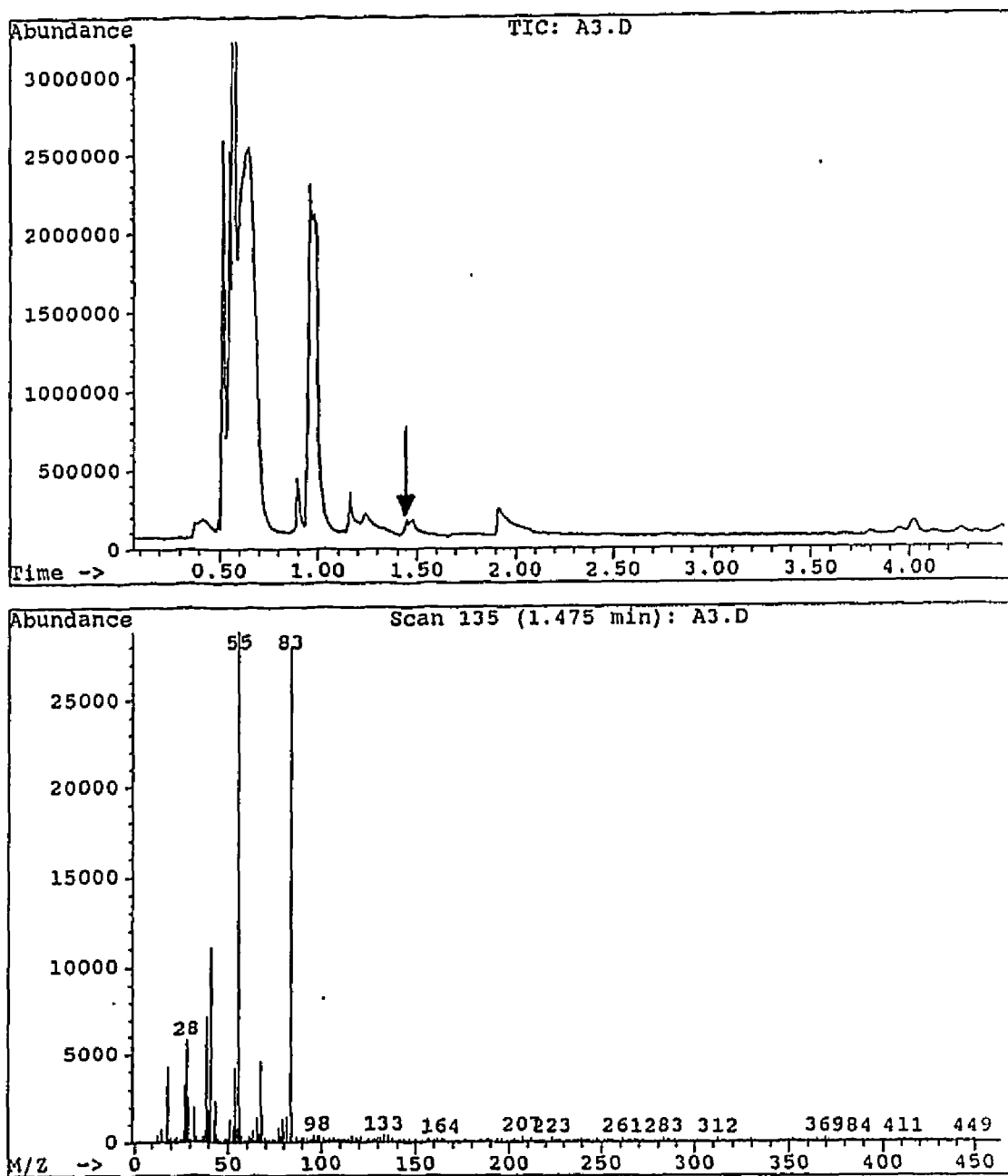
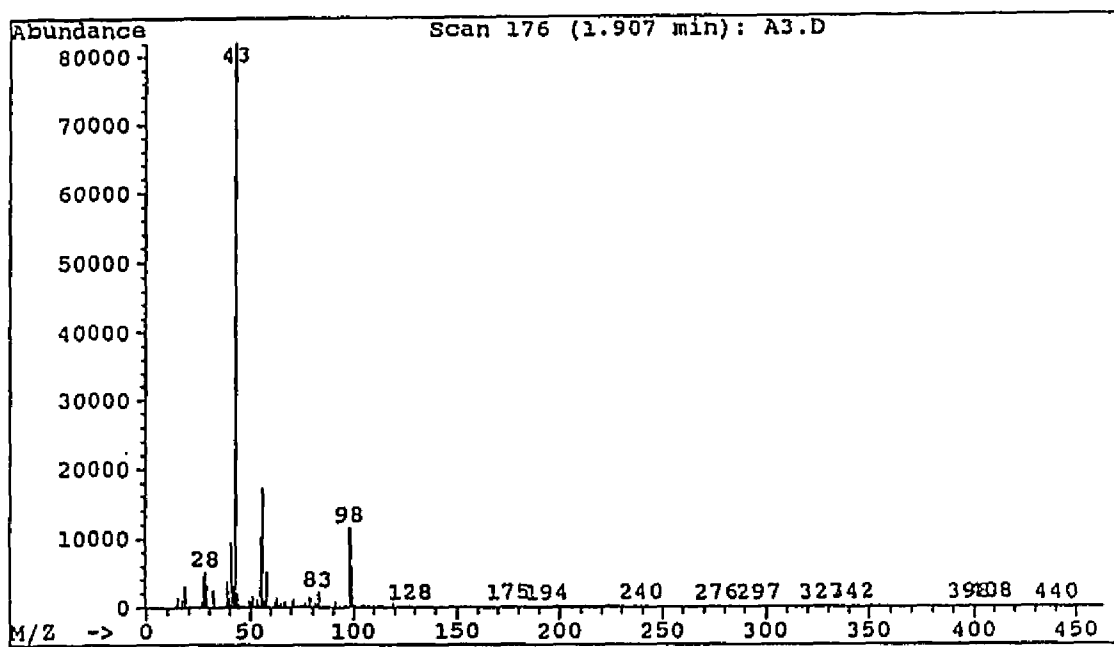
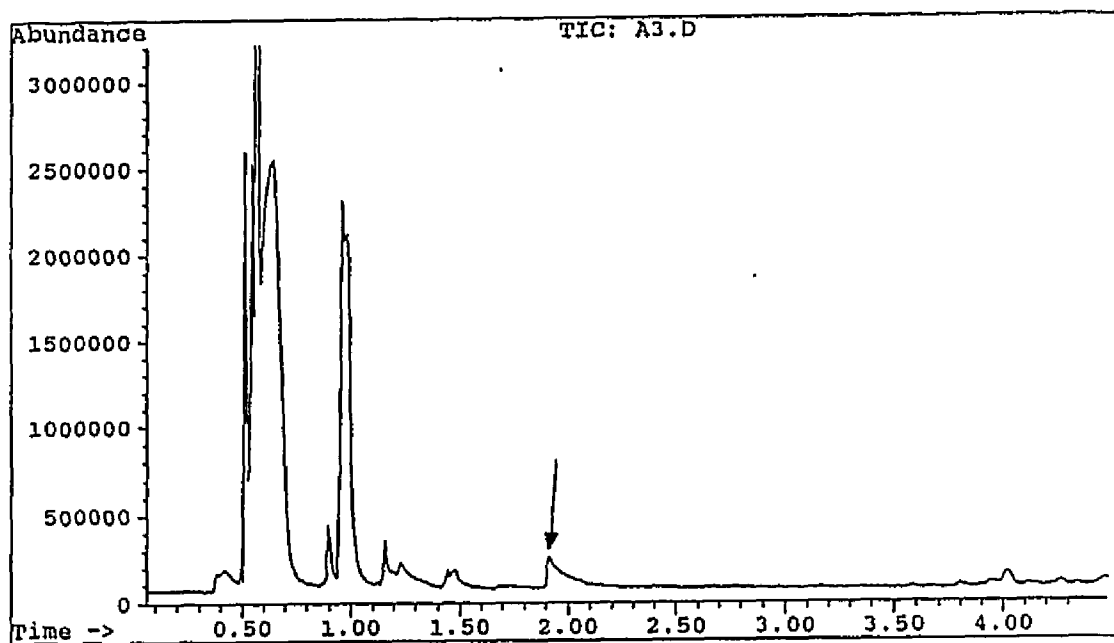
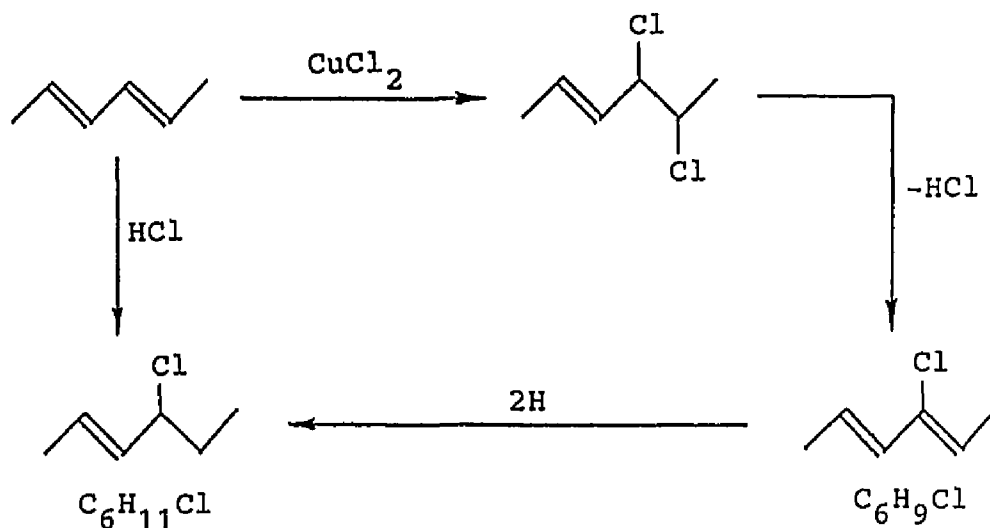
Figure 57. GC/MS data for C_6H_{11} 

Figure 58. GC/MS data for C_7H_{14} 

Scheme 26



occurring during the pyrolysis. These hydrogens may be added to an olefinic segment of the 3-chloro-2,4-hexadiene to form 4-chloro-2-hexene.

Some previous workers have observed alkene halogenation by CuCl_2 .^{39,110,111} Wescott and co-workers³⁹ conducted model-compound studies to compare the effects of MoO_3 and some copper-containing substances and showed that CuCl_2 can effect the slow addition of chlorine to an alkene linkage under conditions that are similar to those encountered in an early stage of the pyrolysis of PVC. In their rechlorination experiment,³⁹ CuCl_2 was allowed to react with cis-2-pentene under anaerobic conditions at 200 °C for 10 min to produce 2,3-dichloro-

pentane. Iida and Gotō¹¹¹ have suggested that the rechlorination can lead to alkyl chloride segments whose structures are not the same as those in the starting polymer, and which give relatively large amounts of volatile aliphatics upon pyrolysis. Since the combustion of aliphatic hydrocarbons generally produce only small amounts of smoke,⁴⁴ a change of the aliphatics/aromatics ratio in the volatiles can lead to smoke suppression.

In addition to the alkene monohalogenation products, C_6H_9Cl (MW 116) and $C_6H_{11}Cl$ (MW 118), moderate amounts of aliphatic dimers consisting of $C_{12}H_{16}$ (MW 160) and $C_{12}H_{20}$ (MW 164) also were detected by GC/MS. These materials constituted the second most abundant heavy product fraction. The $C_{12}H_{20}$ heavy products showed at least ten peaks in the chromatograms (Figures 51-53). Based on their fragmentation patterns in the mass spectra (Figures 51-53), the formation of these heavy products may have involved three types of reactions including the dimerization of olefins, Diels-Alder cyclization, and Lewis-acid-catalyzed dimerization.

Small amounts of aliphatic dimers, $C_{12}H_{16}$ (MW 160, Figure 47) also were found by GC/MS, and they may have been formed by the elimination of four hydrogen atoms from several isomeric $C_{12}H_{20}$ dimers (m/e 164).

Other important heavy products found in the reaction mixture apparently were aromatic oligomers. The two $C_{12}H_{18}$

(MW 162) isomers were assigned as (saturated alkyl)-substituted aromatic dimers (C_6 -benzenes, Figures 48-50). Although there was one GC peak, shown in Figure 49, indicating an aliphatic dimer structure, its intensity is small compared to that of the presumed alkyl-substituted aromatics. Aromatic trimers also were observed, and the GC/MS analysis showed that their three major components were $C_{18}H_{26}$ (MW 242), $C_{18}H_{28}$ (MW 244), and $C_{18}H_{30}$ (MW 246). The chromatogram of component $C_{18}H_{30}$ was very complex and consisted of many peaks (Figure 56). They were tentatively assigned as (saturated alkyl)-substituted C_{12} -benzenes. The less abundant components, $C_{18}H_{28}$ (Figure 55) and $C_{12}H_{26}$ (Figure 54), were assigned as (unsaturated alkyl)-substituted C_{12} -benzenes with one and two double bonds, respectively, in their side groups.

In contrast to the above results, Lattimer and Kroenke⁴⁹ found that large amounts of aromatic dimers (C_4 -benzene) were formed during the pyrolysis of 2,4-dichloropentane with Cu_2O at 350 °C. They claimed that 2,4-dichloropentane can "unzip" to generate a conjugated diene and then cyclize intramolecularly and intermolecularly to form aromatic rings.^{28,43} They⁴⁹ have also suggested that the reactions could be Lewis-acid catalyzed or Diels-Alder in nature since the Lewis-acid-catalyzed aliphatic dimers formed in the reaction mixture might lose two hydrogen atoms to produce aromatic isomers.

As for the C_6H_{11} (MW 83) aliphatic component, its odd molecular ion peak was an indication of a fragment ion, rather than a parent mass. It was temporarily assigned as an aliphatic oligomer with a 2-hexenyl portion. The C_7H_{14} (MW 98) aliphatic component, based on the analysis of its mass spectrum, was assigned as 4-methyl-2-hexene.

Analogous results were forthcoming from similar experiments performed with 1,3,5-hexatriene at 200 °C for 1 h. As before, of the five copper additives tested (Cu, Cu_2O , CuO, CuCl, and $CuCl_2$), only $CuCl_2$ induced the production of a significant amount of heavy products. In contrast to 2,4-hexadiene, a 1,3,5-hexatriene control run without any copper additives also produced many alkyl and aromatic oligomers due to Diels-Alder cyclization and olefin dimerization. However, when 1,3,5-hexatriene was treated with $CuCl_2$ at 200 °C for 1 h, more heavy products resulted. The chromatogram was less complicated than that of 2,4-hexadiene, presumably because the triene model compound itself produced some viscous gel (solid oligomers or polymers) at the initial stages of pyrolysis, and the heavy products detected by GC in the control run had several peaks which overlapped those obtained from the $CuCl_2$ experiment.

In comparison to the results of diene model-compound pyrolysis experiments, the most striking feature of the triene model-compound studies is that (unsaturated alkyl)-

substituted aromatic dimers, rather than aliphatic dimers, were the most abundant heavy products. In general, the formation of these heavy products, as before, apparently involved the following reactions: Diels-Alder cyclization, aromatization, Lewis-acid-catalyzed dimerization, and rechlorination (alkene monohalogenation). The representative GC/MS spectra of these heavy products are shown in Figures 59-68, and the relative abundances of the heavy products are summarized in Table 12.

A moderate amount of C_6H_9Cl (MW 116, Figure 59) was detected, and only one peak having this composition appeared in the chromatogram. Based on the mass spectrum, it was tentatively assigned as 3-chloro-1,5-hexadiene. It comprised 11% of the total amount of heavy products, and its formation suggests the occurrence of alkene halogenation by $CuCl_2$ as shown in scheme 27.

Scheme 27

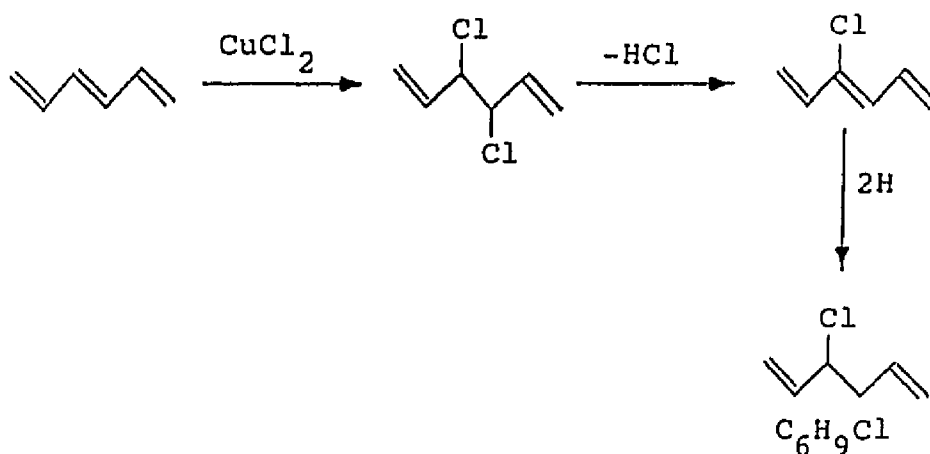


Table 12. Distribution of Degradation Products Obtained
from Reaction of 1,3,5-Hexatriene with CuCl_2
at 200 °C for 1 h

MW	Chemical Formula	Yield (%) ^a
116 (Fig. 59)	$\text{C}_6\text{H}_9^{35}\text{Cl}$	11
160 (Figs. 60-66)	$\text{C}_{12}\text{H}_{16}$	86
243 ^b (Fig. 67)	$\text{C}_{18}\text{H}_{27}$	2
248 (Fig. 68)	$\text{C}_{19}\text{H}_{20}$	1

a. GC area percentages based on total peak area of heavy products.

b. Fragment from heavy product.

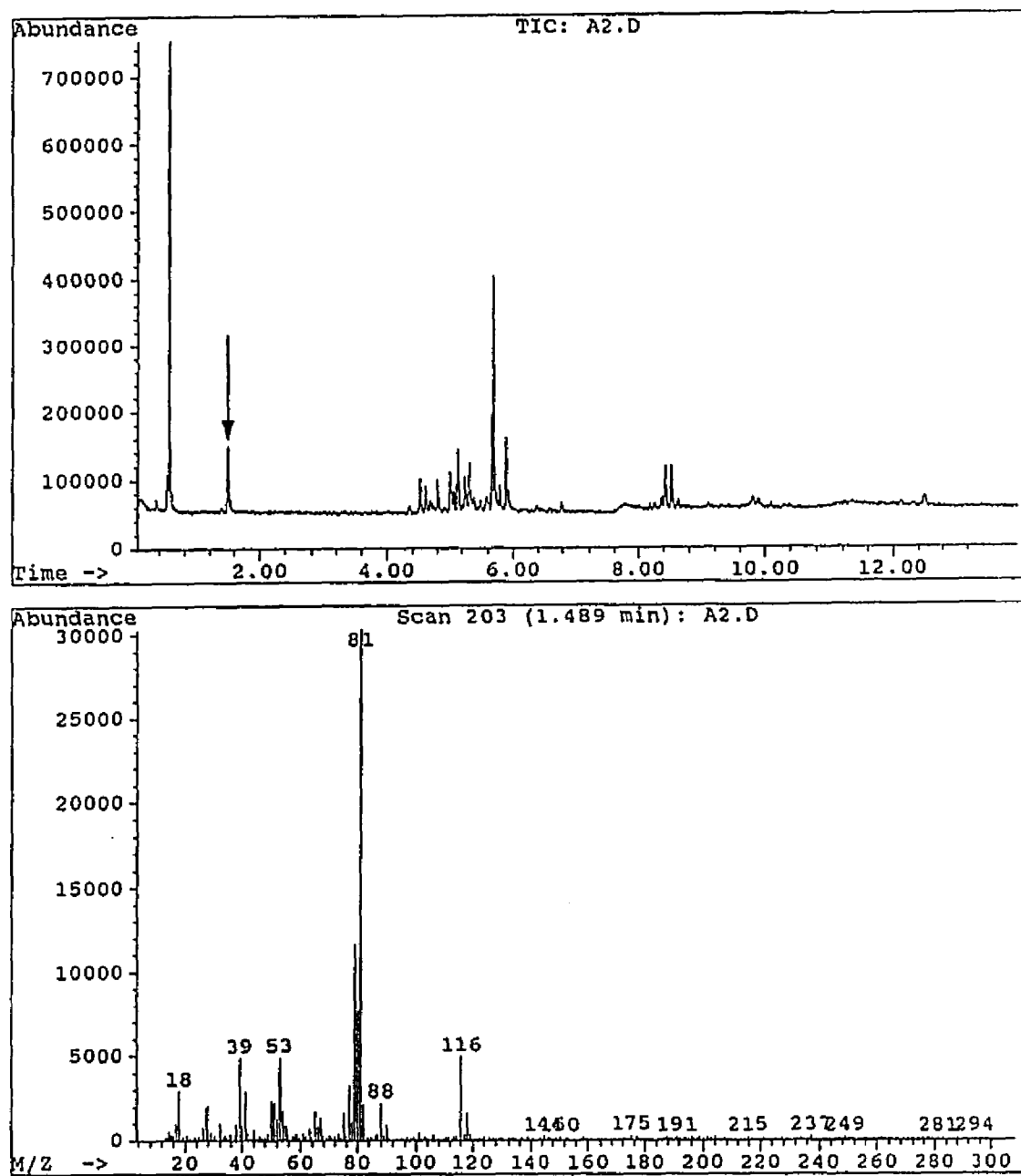
Figure 59. GC/MS data for C_6H_9Cl 

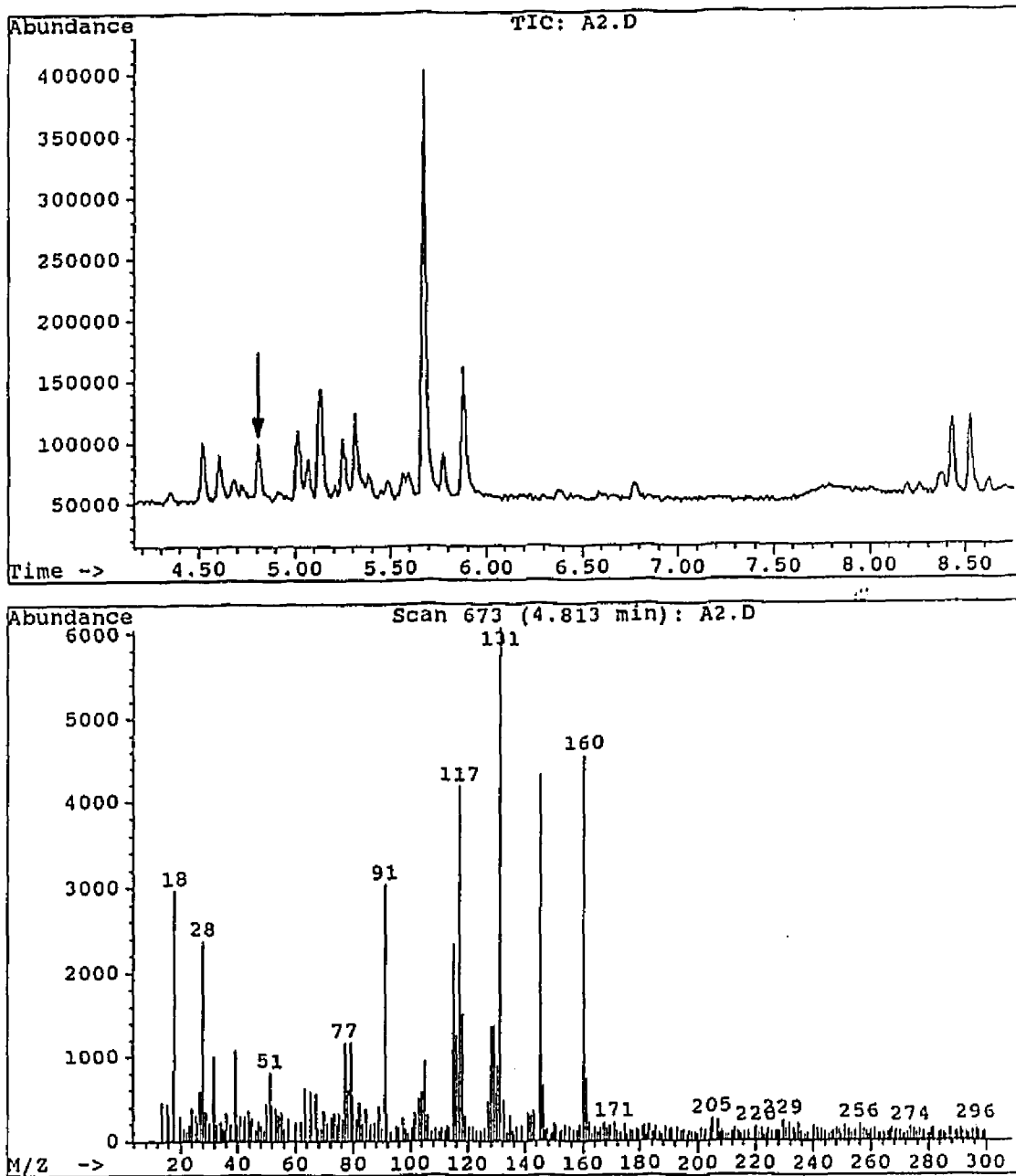
Figure 60. GC/MS data for $C_{12}H_{16}$ 

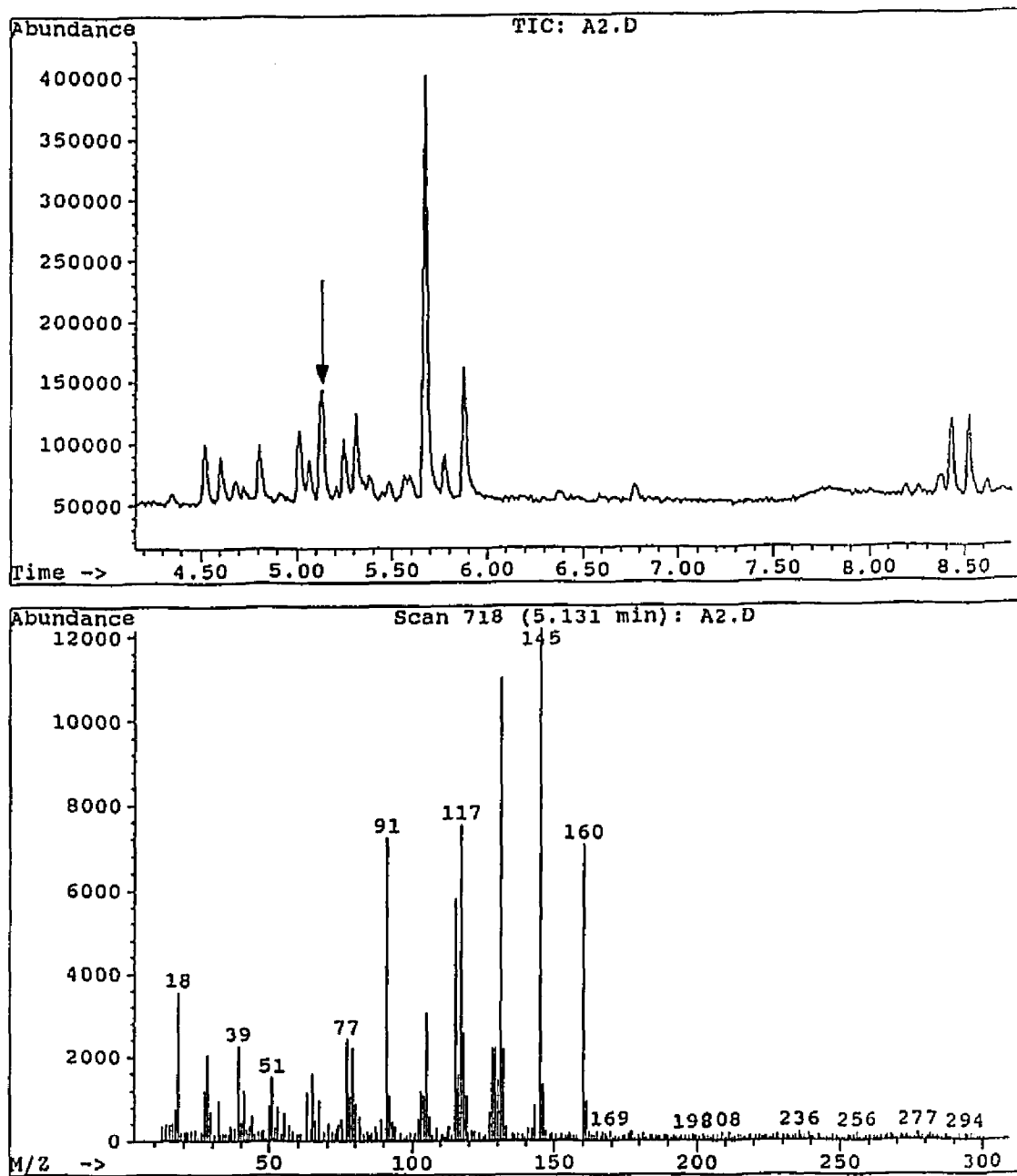
Figure 61. GC/MS data for $C_{12}H_{16}$ 

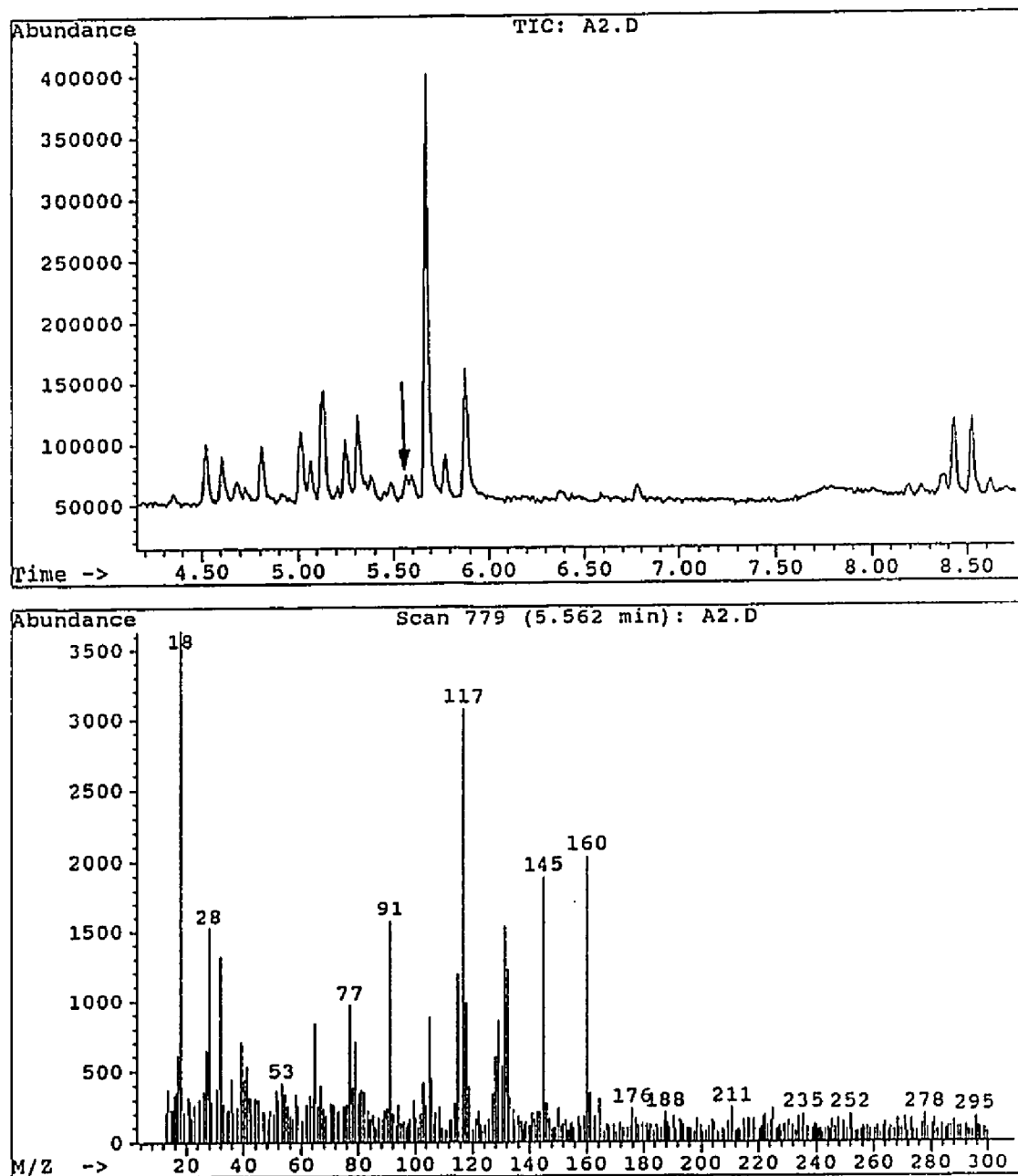
Figure 62. GC/MS data for $C_{12}H_{16}$ 

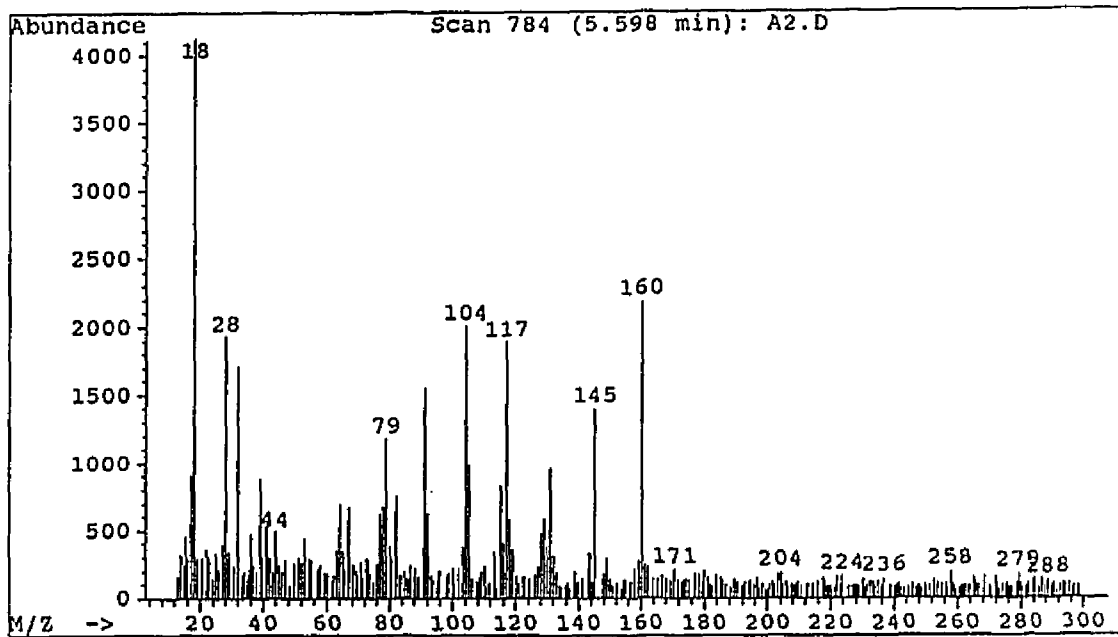
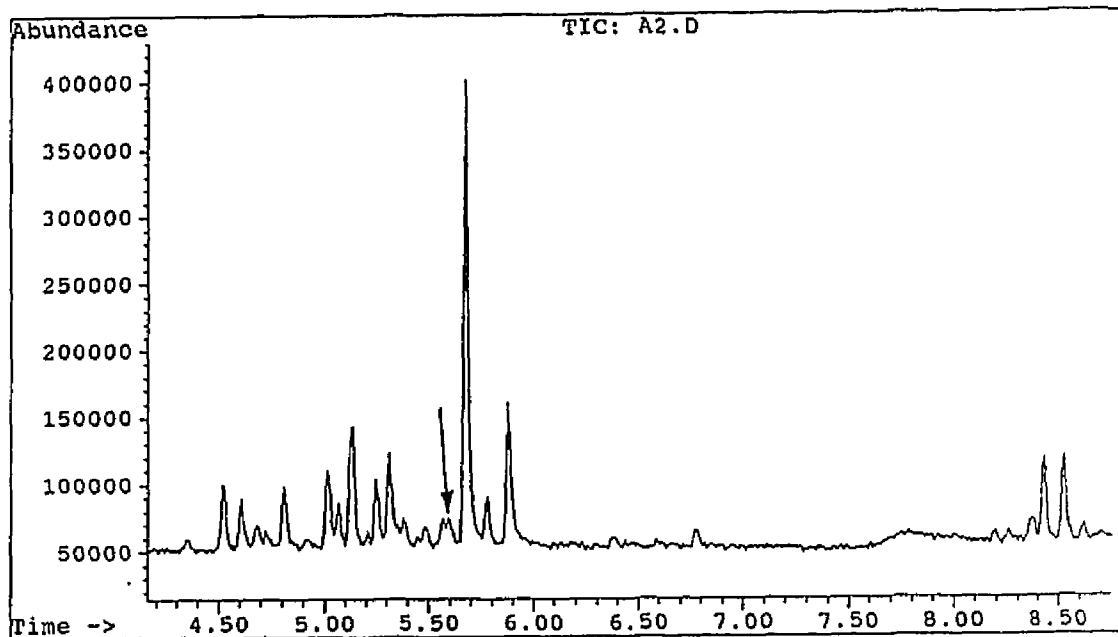
Figure 63. GC/MS data for $C_{12}H_{16}$ 

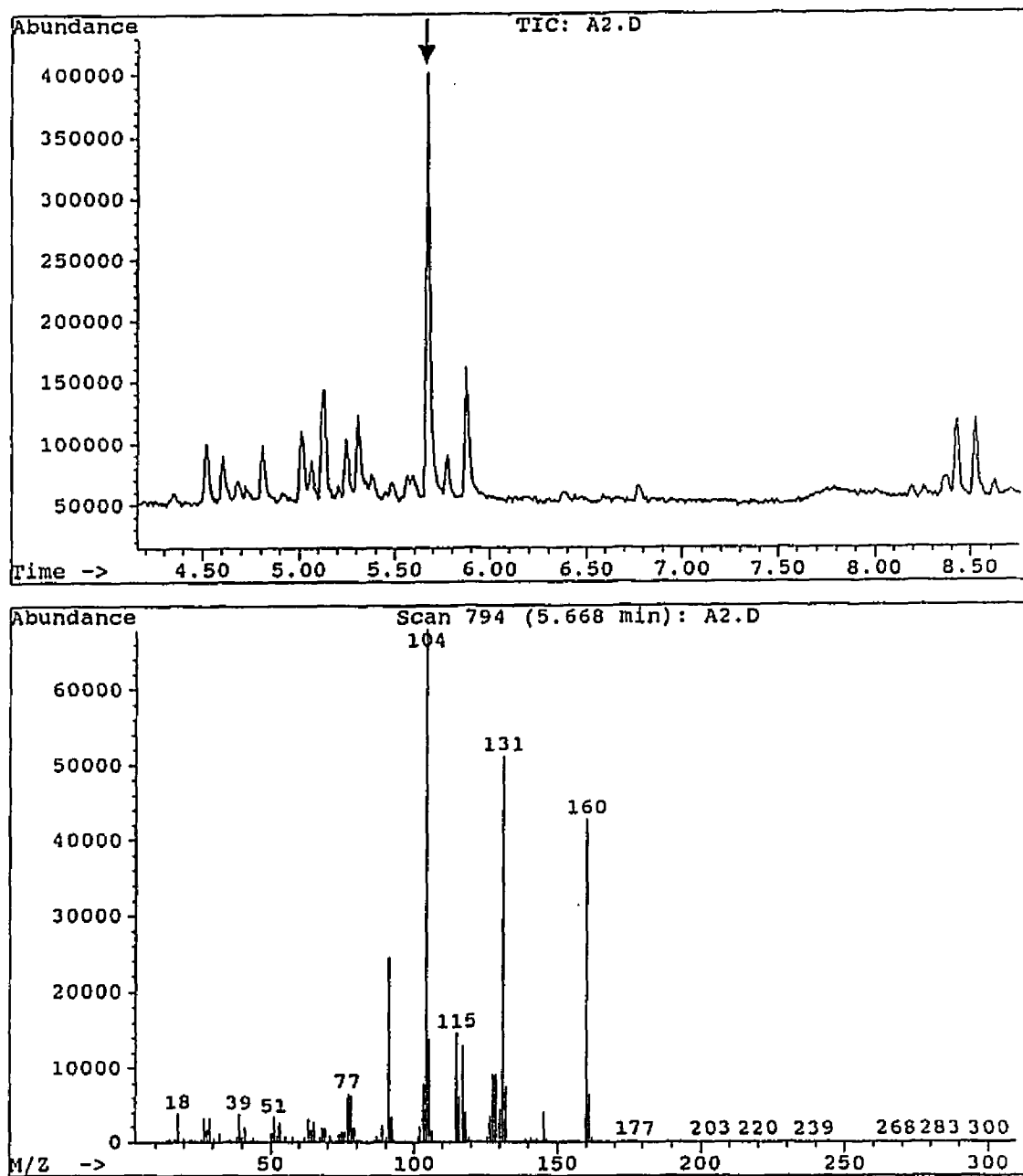
Figure 64. GC/MS data for $C_{12}H_{16}$ 

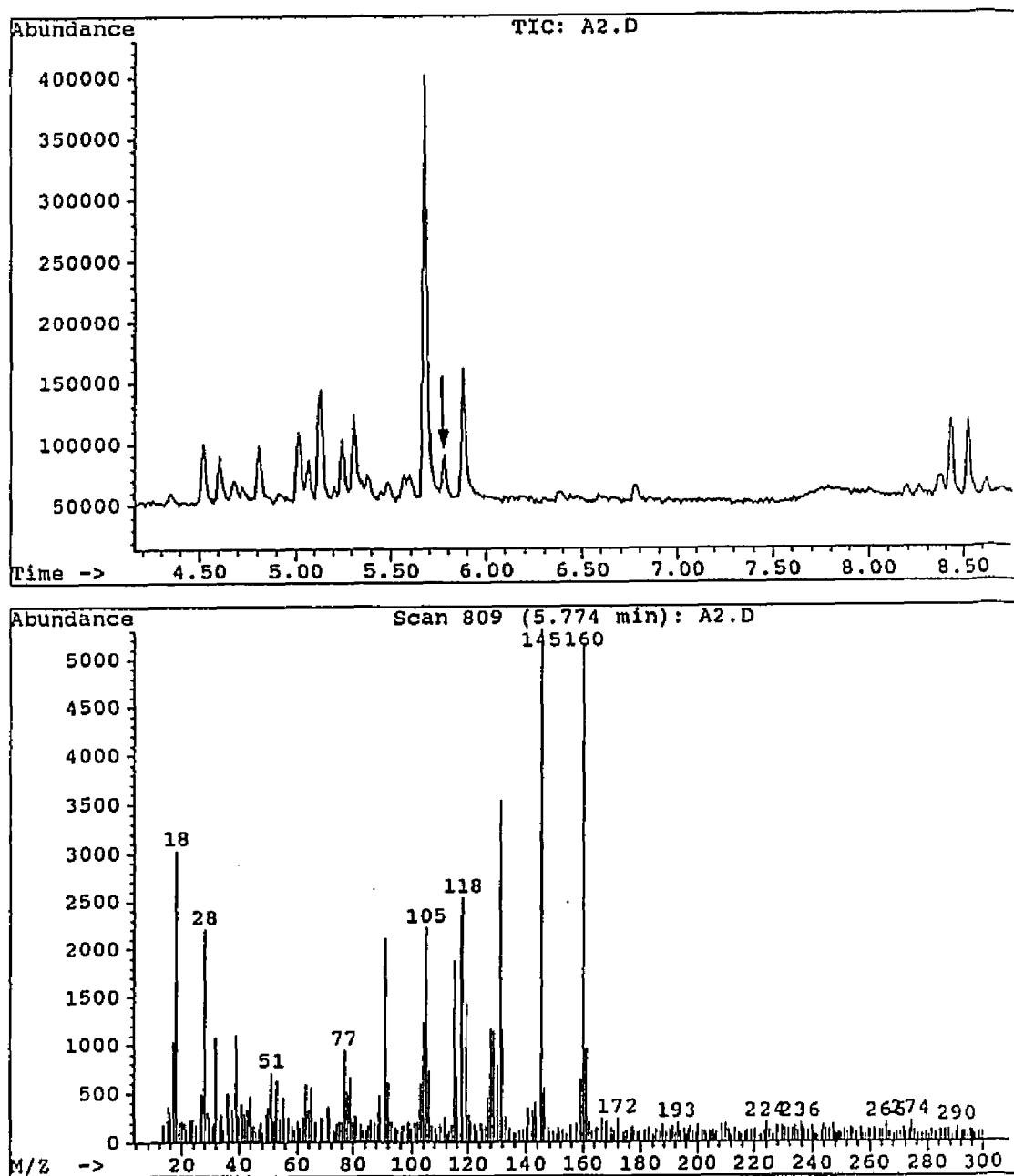
Figure 65. GC/MS data for $C_{12}H_{16}$ 

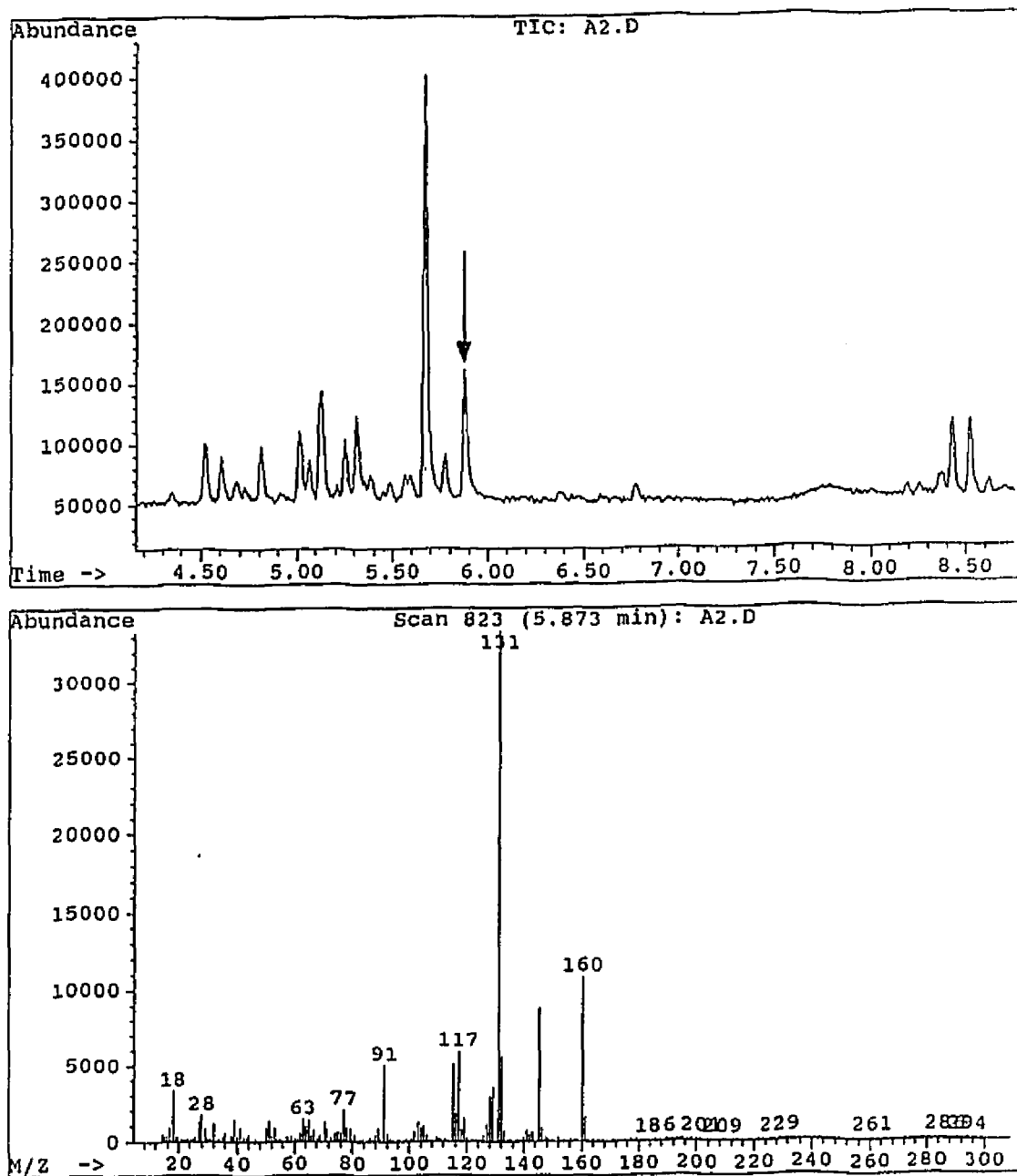
Figure 66. GC/MS data for $C_{12}H_{16}$ 

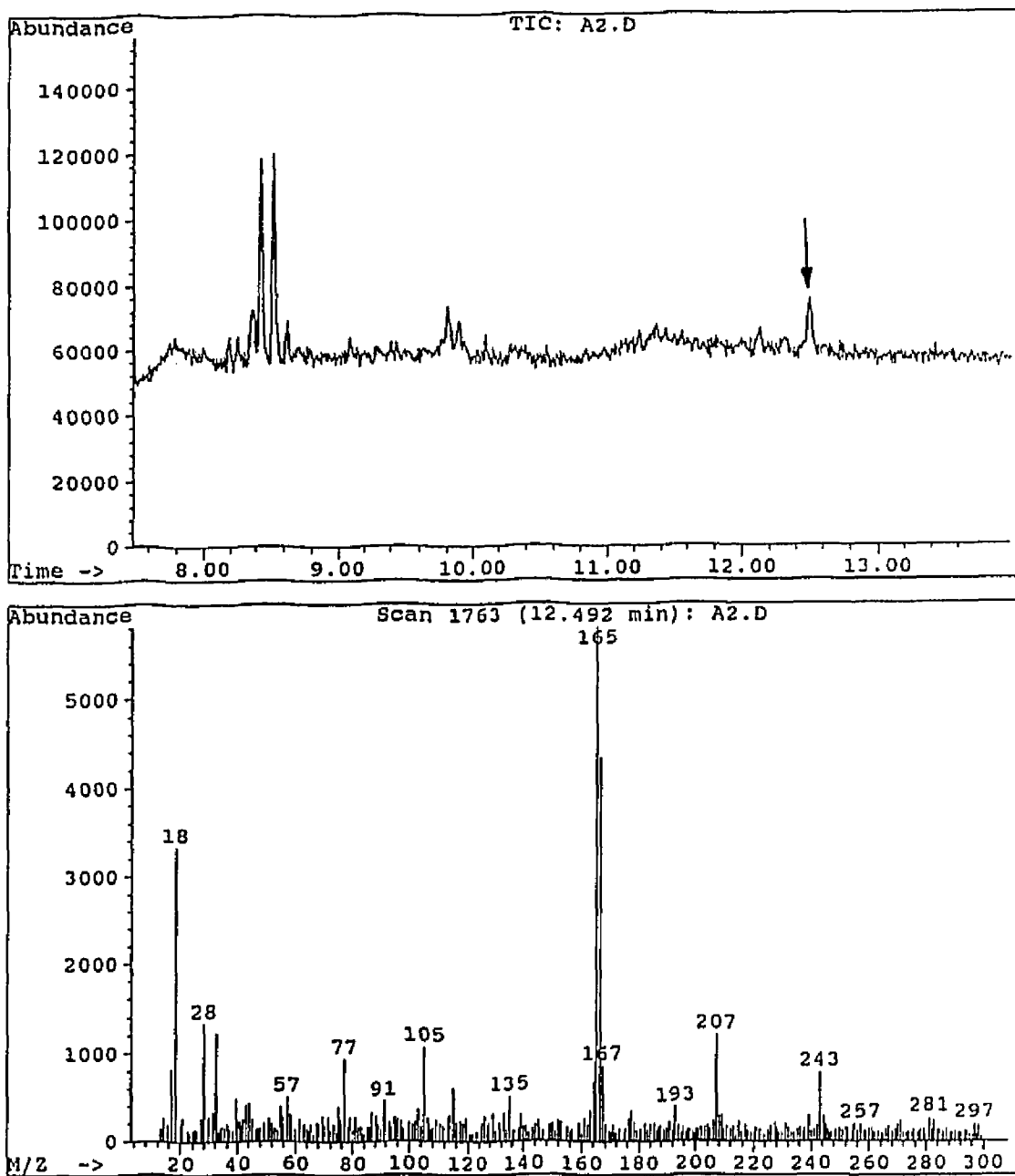
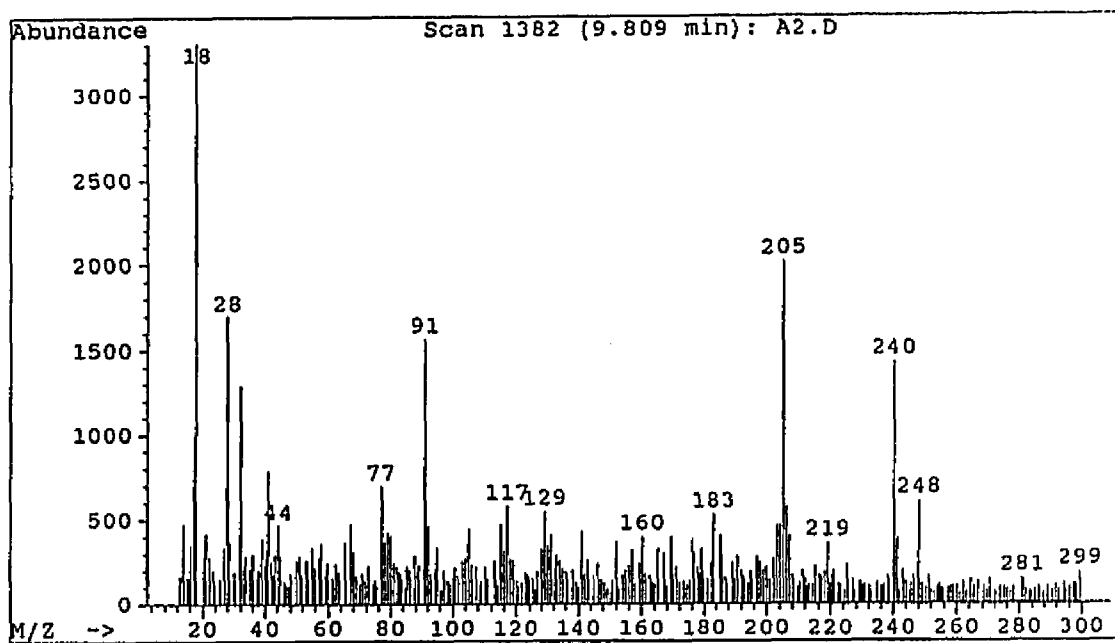
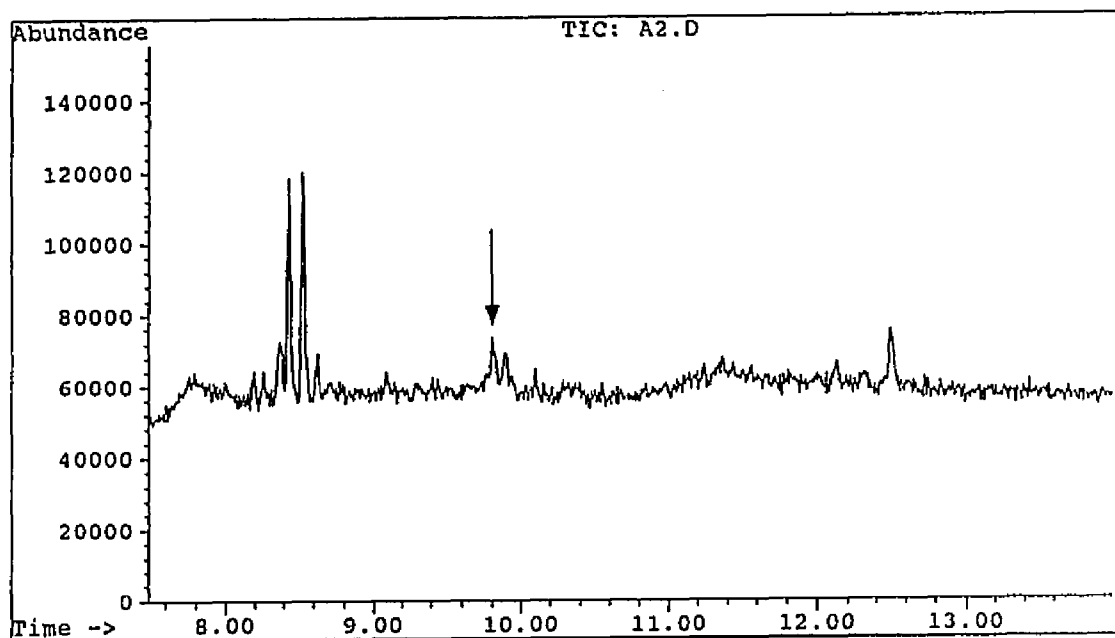
Figure 67. GC/MS data for $C_{18}H_{27}$ 

Figure 68. GC/MS data for $C_{19}H_{20}$ 

Wescott and co-workers³⁹ have conducted a similar test for rechlorination by allowing CuCl_2 (11%, w/v) to react with cis-2-pentene in an anaerobic atmosphere at 200 °C, and they have detected a small amount (3%, based on CuCl_2) of two isomeric $\text{C}_5\text{H}_{10}\text{Cl}_2$ compounds by GC/MS analysis. These products were conclusively shown to be the meso and racemic isomers of 2,3-dichloropentane. However, Wescott and co-workers³⁹ did not detect any of the subsequent dehydrochlorination products such as 2-chloro-2-pentene or 3-chloro-2-pentene, for example.

Numerous peaks for $\text{C}_{12}\text{H}_{16}$ (MW 160, Figures 60-66) products also were detected by GC/MS, and these products seemed to be mainly (unsaturated alkyl)-substituted aromatic dimers (C_6 -benzenes). They accounted for nearly 86% of the total amount of heavy products in the reaction mixture. Very little of the corresponding Lewis-acid-catalyzed aliphatic dimers (no m/e 77 peak detected, which corresponds to C_6H_5^+ fragment; see Figure 63) were detected by GC/MS.

Using a different model compound, 2,4,6-trichloroheptane, Lattimer and co-workers⁴⁹ have conducted similar pyrolysis experiments with different metal additives. It is interesting to compare our results with theirs since their model compound has the ability to form a conjugated triene structure under pyrolytic conditions. Lattimer and co-workers⁴⁹ found that when 2,4,6-trichloroheptane was pyrolyzed with Cu_2O at 350 °C for 10 min under anaerobic

conditions, only very low yields of aromatization products were formed. Instead, the most abundant heavy products were the Lewis-acid-catalyzed aliphatic dimers, $C_{14}H_{20}$. In comparison with our triene model compound, this result may have been caused by the generation of allylic chlorides such as 4-chloro-1,5-heptadiene and its isomers along with the triene species during the thermal degradation. Obviously these reactive allylic chlorides can compete with the triene species to form Lewis-acid-catalyzed oligomers instead of the aromatic heavy products. Lattimer and co-workers⁴⁹ also pyrolyzed 2,4,6-trichloroheptane in the presence of MoO_3 at 350 °C for 10 min and found that large amounts of aromatic oligomers were formed. They believe that 2,4,6-trichloroheptane can "unzip" during pyrolysis to form a polyene chain with three alternating double bonds, and that this chain can then cyclize both intramolecularly and intermolecularly to form aromatic structures. Although MoO_3 (or MoO_2Cl_2 formed in situ) is a much stronger Lewis acid than $CuCl_2$, we believe that $CuCl_2$ may promote the formation of heavy products by the same mechanism as in the case of MoO_3 ; and based on the current model-compound studies, it is clear that when the conjugated polyenes are exposed to $CuCl_2$, large amounts of aromatic heavy products can be formed.

As for the aromatic trimer fragment, $C_{18}H_{27}$ (MW 243, Figure 67), its precursor was tentatively assigned as an

(unsaturated alkyl)-substituted C_{12} -benzene which contained one double bond in the alkyl side group(s). The aromatic trimer, $C_{19}H_{20}$ (MW 248, Figure 68), was tentatively assigned as an (unsaturated alkyl)-substituted C_{13} -benzene which contained up to six double bonds in the alkyl side group(s). These aromatic heavy products all were very low in abundance and accounted for only 3% of the total heavy-product yield.

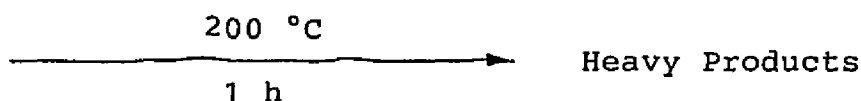
In summary, from the results of the conjugated diene and triene model-compound studies, we discovered that among the five copper additives tested (Cu, Cu_2O , CuO, $CuCl_2$, and CuCl), only $CuCl_2$ was capable of promoting the formation of an array of heavy products. In general, their formation can be explained in terms of Lewis-acid catalysis. Our results also showed that $CuCl_2$ behaved somewhat differently depending on the model compound chosen. In the case of 2,4-hexadiene, the most abundant heavy products were those generated by alkene monohalogenation (rechlorination); while in the case of 1,3,5-hexatriene, the most abundant heavy products were those generated by aromatization.

The nature of these experiments makes it difficult to accurately assess the significance of the results. It is particularly difficult to evaluate the relative significance of Lewis-acid chemistry and rechlorination reactions in the crosslinking of copper-containing PVC. There are many different types of chemical structures in thermally degraded PVC in addition to the conjugated

polyenes, and the relative abundances of the heavy products are determined by competitive chemical reaction pathways. Ideally, it would be necessary to have a model compound containing all of the different types of structures in order to assess the relative importance of these reactions. Nevertheless, in view of the results of the conjugated diene and triene model-compound studies, a more detailed Lewis-acid-catalyzed crosslinking chemistry is clearly revealed; and taken together with the results from the previous simple secondary chloride model-compound studies, it shows that polyene sequences can undergo several different types of crosslinking reactions under catalysis by copper additives.

2-4. Pyrolysis of a Mixture of a Secondary Allylic Chloride
and a Conjugated Diene in the Presence of Copper
Additives

(4-Chloro-2-Pentene + 2,4-Hexadiene) + Copper Additive



Since the thermal degradation of PVC was well-known to yield allylic chlorides and linear conjugated polyene segments,²⁸ the effects of copper additives on a model-compound mixture containing these two structures were studied.

When a mixture containing an equimolar amount of 4-chloro-2-pentene and 2,4-hexadiene was pyrolyzed in the presence of different copper additives (Cu, Cu₂O, CuO, CuCl, or CuCl₂) at 200 °C for 1 h, very complex mixtures resulted that were similar to these obtained in the corresponding experiments with single model compounds (see Sections 2-2 and 2-3). The starting materials were the largest components in the product mixtures, and the dehydrochlorination product (1,3-pentadiene) constituted only a small portion (less than 20%) in each case. Analyses by GC/MS showed the presence of considerable amounts of heavy products with molecular weights ranging from 118 to 286. The relative distributions of these heavy products

are summarized in Table 13, and representative GC/MS data and chemical structures for them are shown in Figures 69-84 and Table 14. The Cu and Cu₂O additives gave more complex mixtures than CuO, CuCl₂, and CuCl, and their total chromatograms are shown in Figures 85 and 86.

In striking contrast to the outcomes of the 4-chloro-2-pentene or 2,4-hexadiene single model-compound experiments with the same copper additives (Cu, Cu₂O, CuO, CuCl, and CuCl₂), the major Lewis-acid-catalyzed heavy products formed in all cases were those oligomers consisting of two different model-compound components. Of all the 15 (see Table 13) different types of heavy products, only those with molecular weights 136, 138, 164, 172, 204, and 240 were composed of the same model-compound units (see Tables 13 and 14). These findings indicated that the Lewis-acid-catalyzed oligomerization is a competitive process among all of the different types of structural units, and that in the case of secondary allylic chlorides and conjugated dienes, there is a strong tendency to form the "cross-oligomers" in addition to the "homo-oligomers". These results also suggest that the formation of the crosslinking network in PVC can be very extensive, since the intermolecular linkages can be formed not only among the same structural units, but also among those units having different structures, such as allylic chlorides and conjugated polyenes.

Table 13

Distributions^a of Heavy Products from Pyrolyses of a Mixture of
4-Chloro-2-pentene and 2,4-Hexadiene

MW	Formula	Control	Cu	Cu ₂ O	CuO	CuCl ₂	CuCl
118	C ₆ H ₁₁ ³⁵ Cl	0	36	2	51	64	71
136	C ₁₀ H ₁₆	trace	2	8	8	3	trace
137 ^b	C ₁₀ H ₁₇	trace	4	3	0	1	1
138	C ₁₀ H ₁₈	0	25	2	6	0	0
148	C ₁₁ H ₁₆	0	trace	2	5	1	2
150	C ₁₁ H ₁₈	0	4	32	11	trace	1
164	C ₁₂ H ₂₀	0	0	0	11	0	trace
172	C ₁₀ H ₁₇ ³⁵ Cl	0	14	19	0	11	9

a. GC area percentages based on total peak area of heavy products.

b. Fragment from heavy product.

Table 13. Continued

MW	Formula	Control	Cu	Cu ₂ O	CuO	CuCl ₂	CuCl
186	C ₁₁ H ₁₉ ³⁵ Cl	0	2	3	0	1	2
204	C ₁₅ H ₂₄	0	trace	trace	0	0	trace
218	C ₁₆ H ₂₆	0	9	20	3	6	5
232	C ₁₇ H ₂₈	0	0	2	5	0	trace
240	C ₁₅ H ₂₅ ³⁵ Cl	0	0	trace	0	5	0
254	C ₁₆ H ₂₇ ³⁵ Cl	0	4	2	trace	8	9
286	C ₂₁ H ₃₄	0	0	5	trace	0	0

Table 14
 Representative Tentative Chemical Structures
 of the Heavy Products from Pyrolyses of
 a Mixture of 4-Chloro-2-pentene and 2,4-Hexadiene

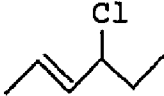
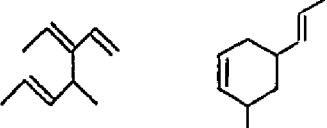
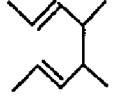
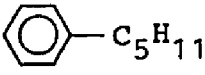
MW	Chemical Formula	Chemical Structure(s)
118	$C_6H_{11}Cl$ (Fig. 69)	
136	$C_{10}H_{16}$ (Figs. 70, 71)	
138	$C_{10}H_{18}$ (Fig. 72)	
148	$C_{11}H_{16}$ (Fig. 73)	
150	$C_{11}H_{18}$ (Figs. 74, 75)	

Table 14. Continued

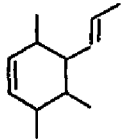
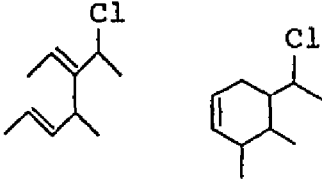
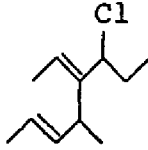
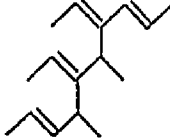
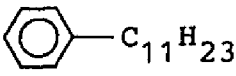
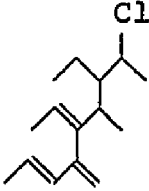
MW	Chemical Formula	Chemical Structure(s)
164	$C_{12}H_{20}$ (Fig. 76)	
172	$C_{10}H_{17}Cl$ (Figs. 77, 78)	
186	$C_{11}H_{19}Cl$ (Fig. 79)	
218	$C_{16}H_{26}$ (Fig. 80)	
232	$C_{17}H_{28}$ (Fig. 81)	
240	$C_{15}H_{25}Cl$ (Fig. 82)	

Table 14. Continued

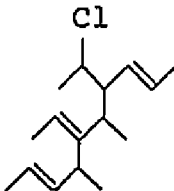
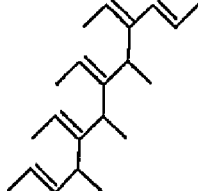
MW	Chemical Formula	Chemical Structure(s)
254	$C_{16}H_{27}Cl$ (Fig. 83)	
286	$C_{21}H_{34}$ (Fig. 84)	

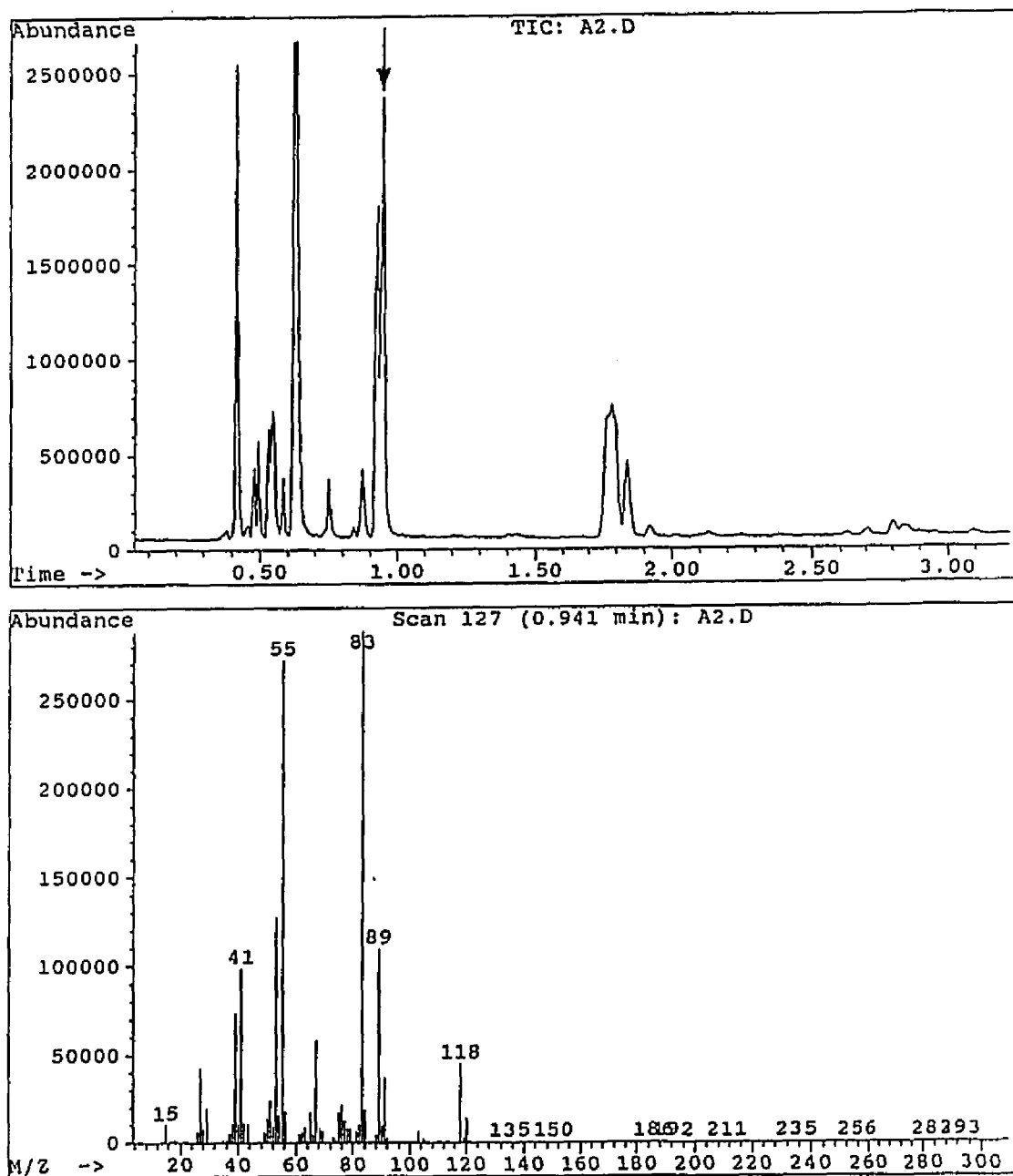
Figure 69. GC/MS data for $C_6H_{11}Cl$ 

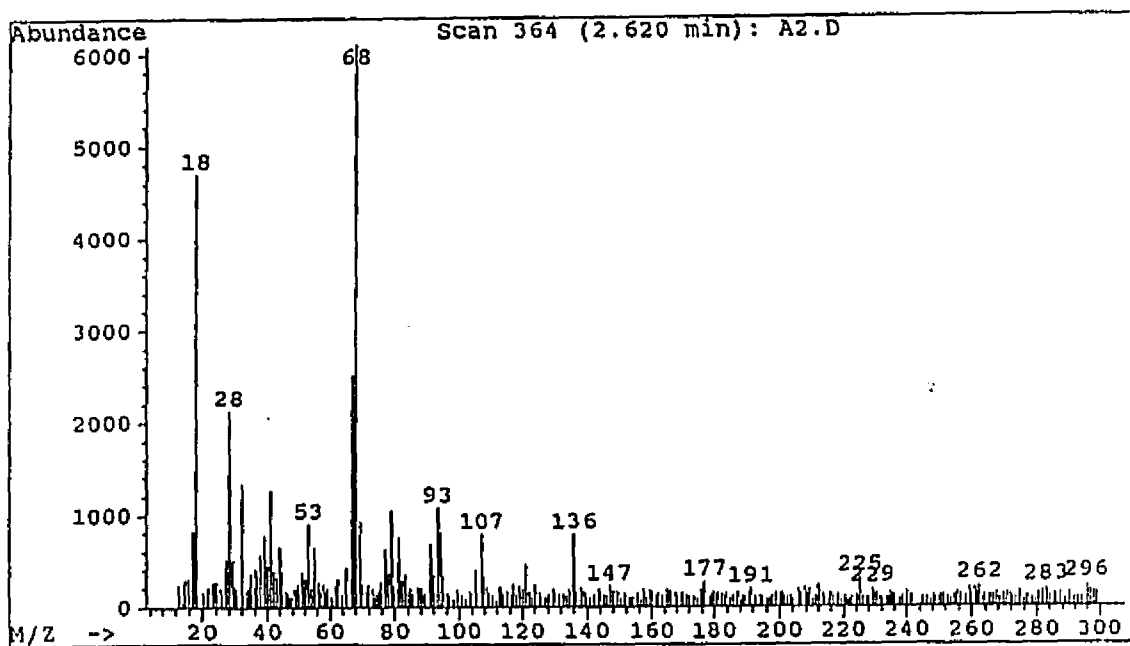
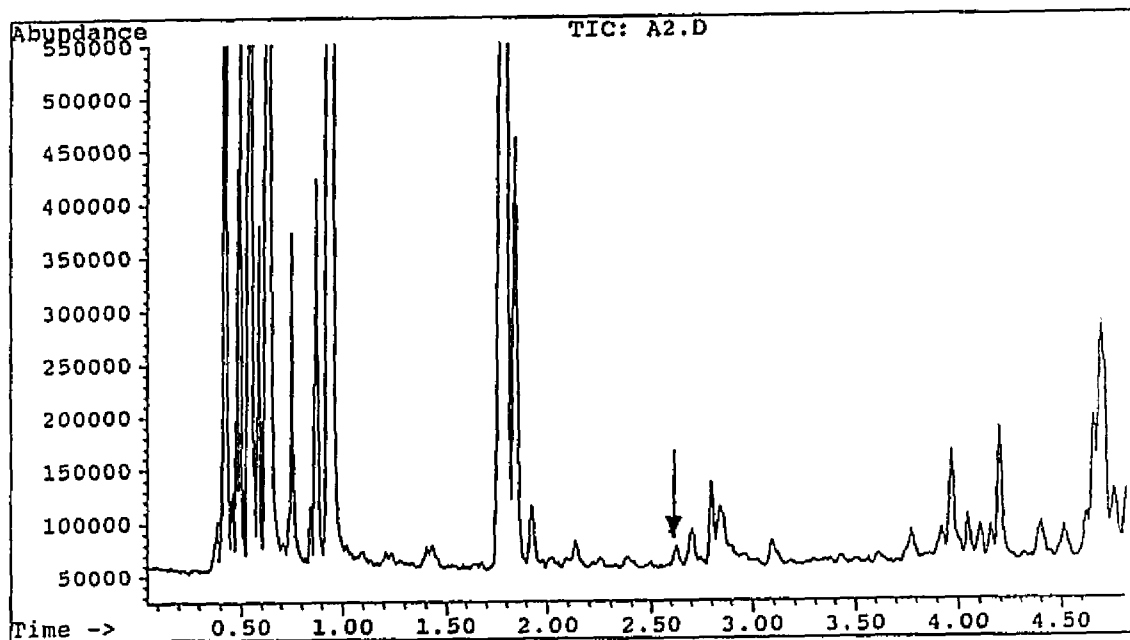
Figure 70. GC/MS data for $C_{10}H_{16}$ 

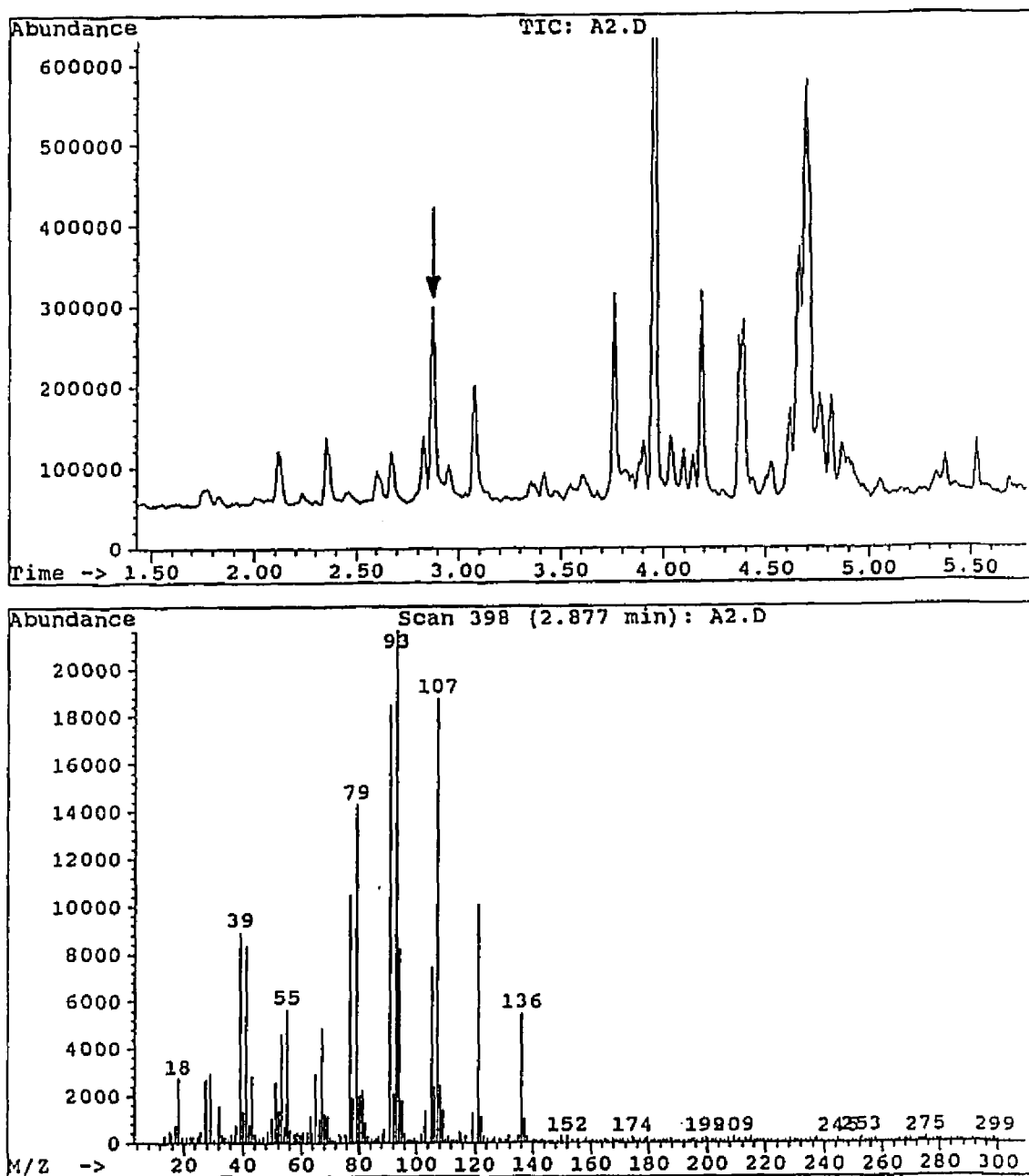
Figure 71. GC/MS data for $C_{10}H_{16}$ 

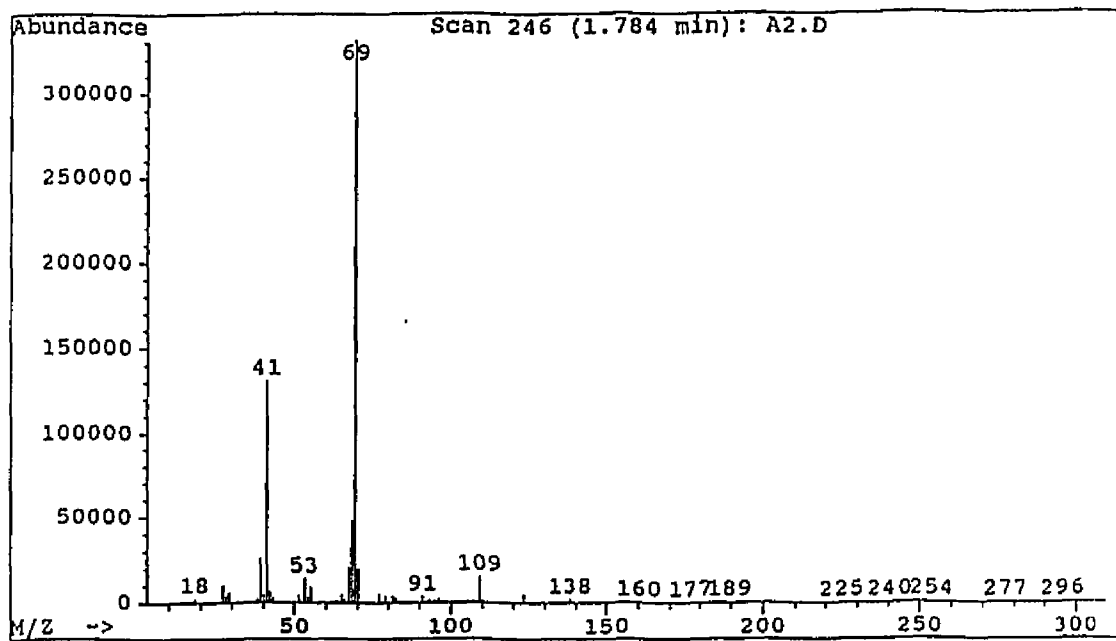
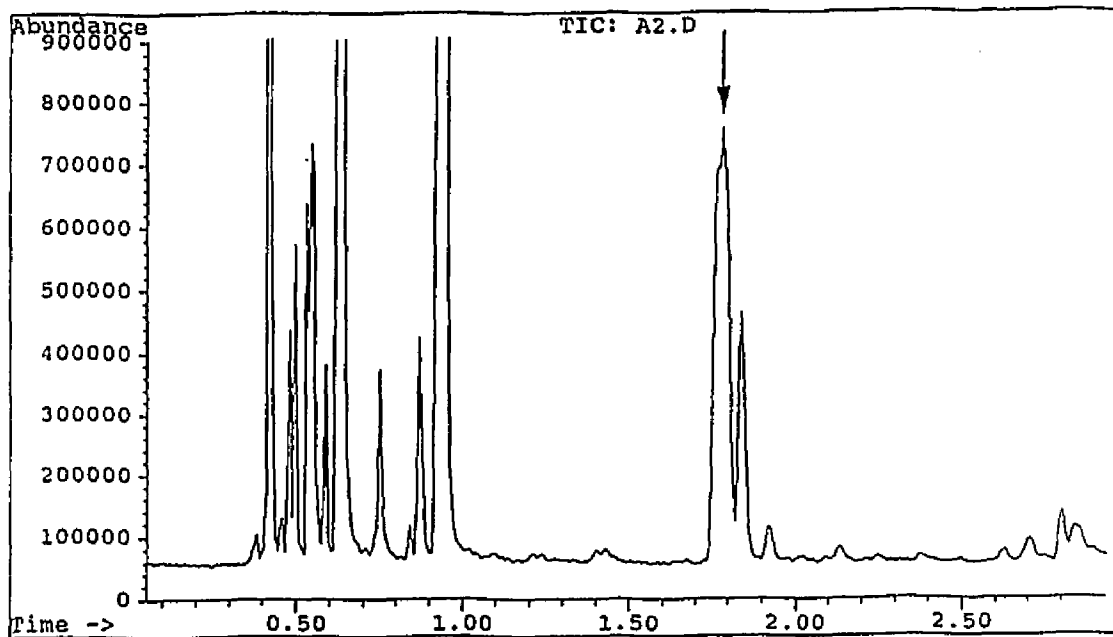
Figure 72. GC/MS data for $C_{10}H_{18}$ 

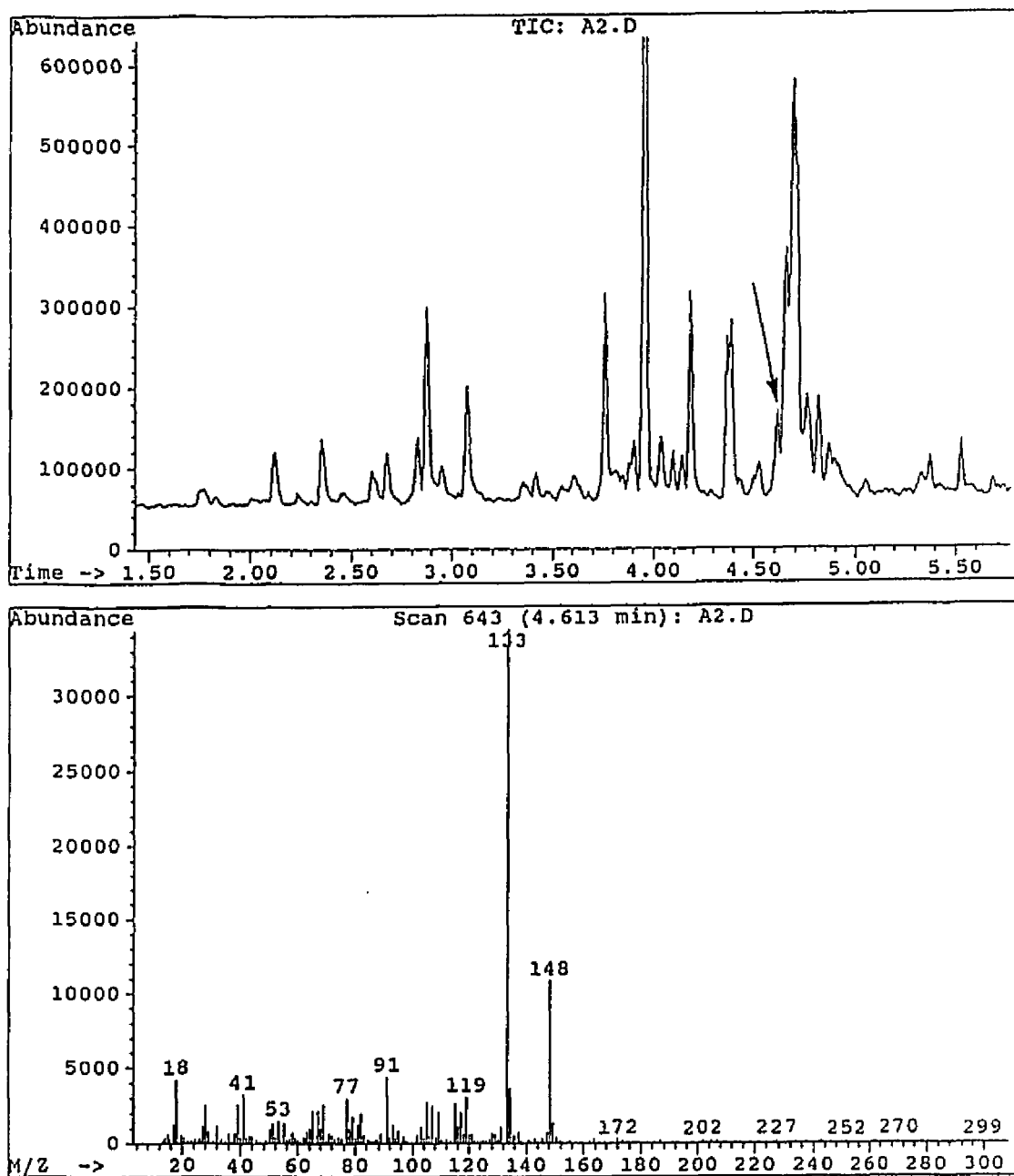
Figure 73. GC/MS data for $C_{11}H_{16}$ 

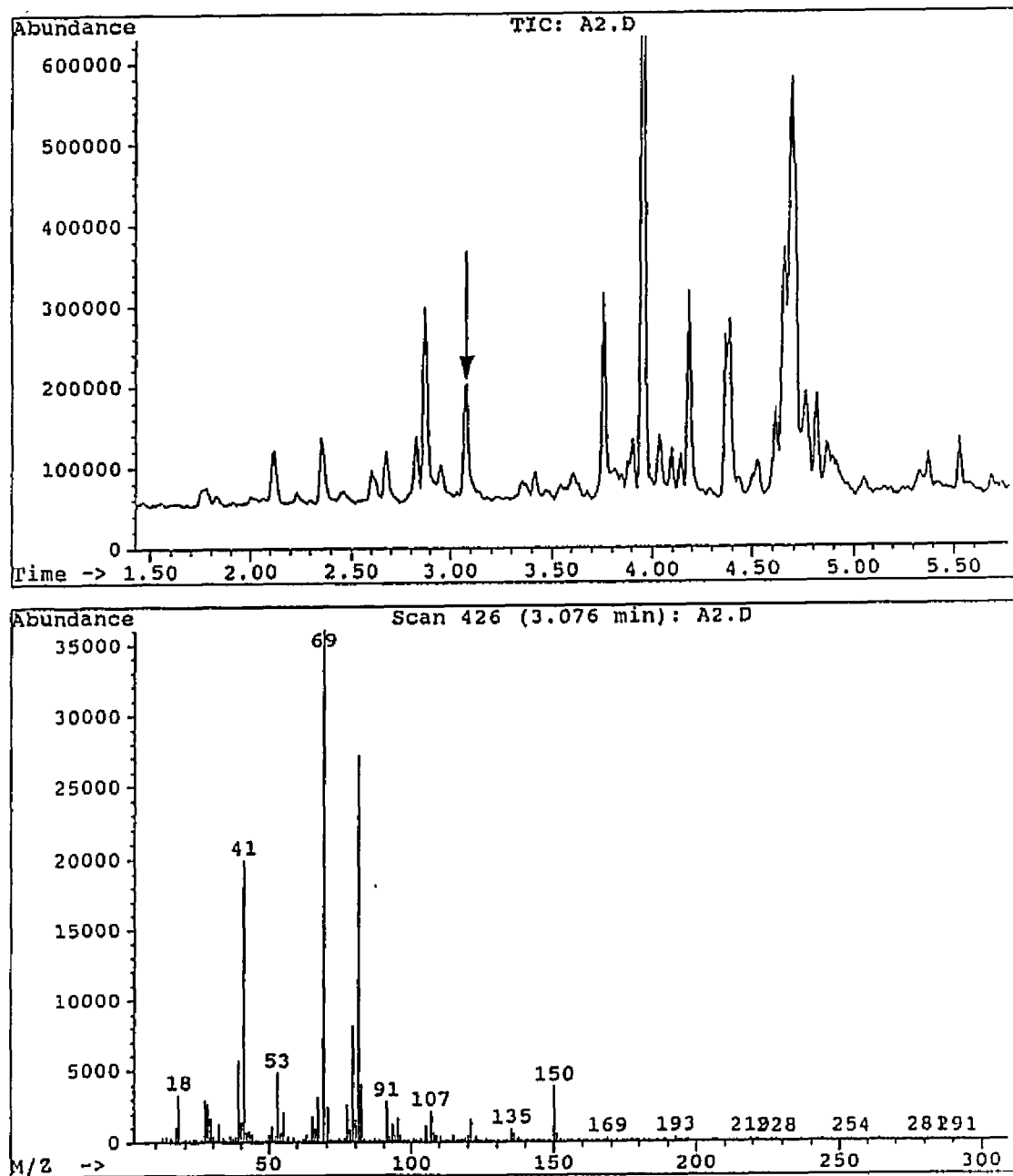
Figure 74. GC/MS data for $C_{11}H_{18}$ 

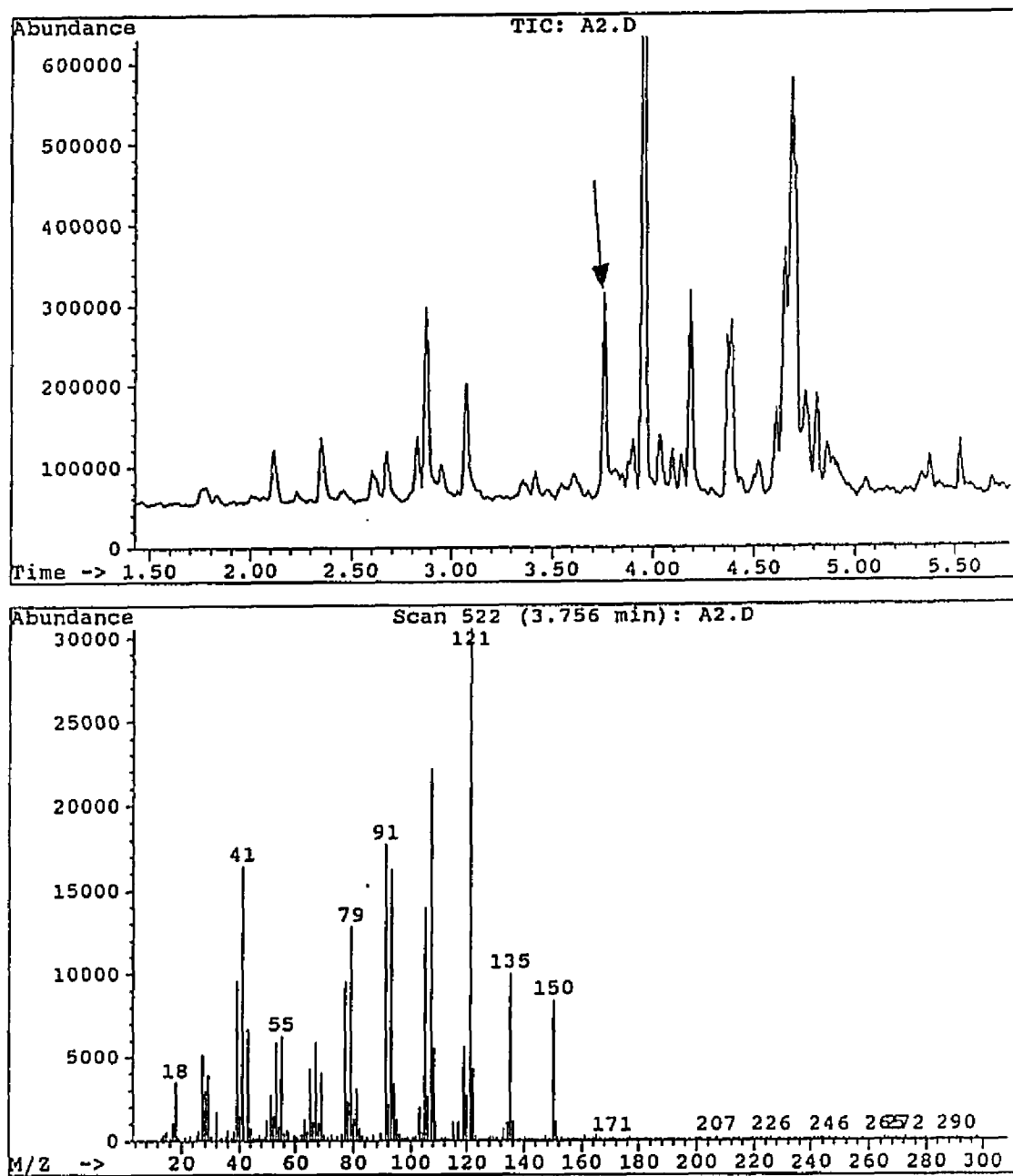
Figure 75. GC/MS data for $C_{11}H_{18}$ 

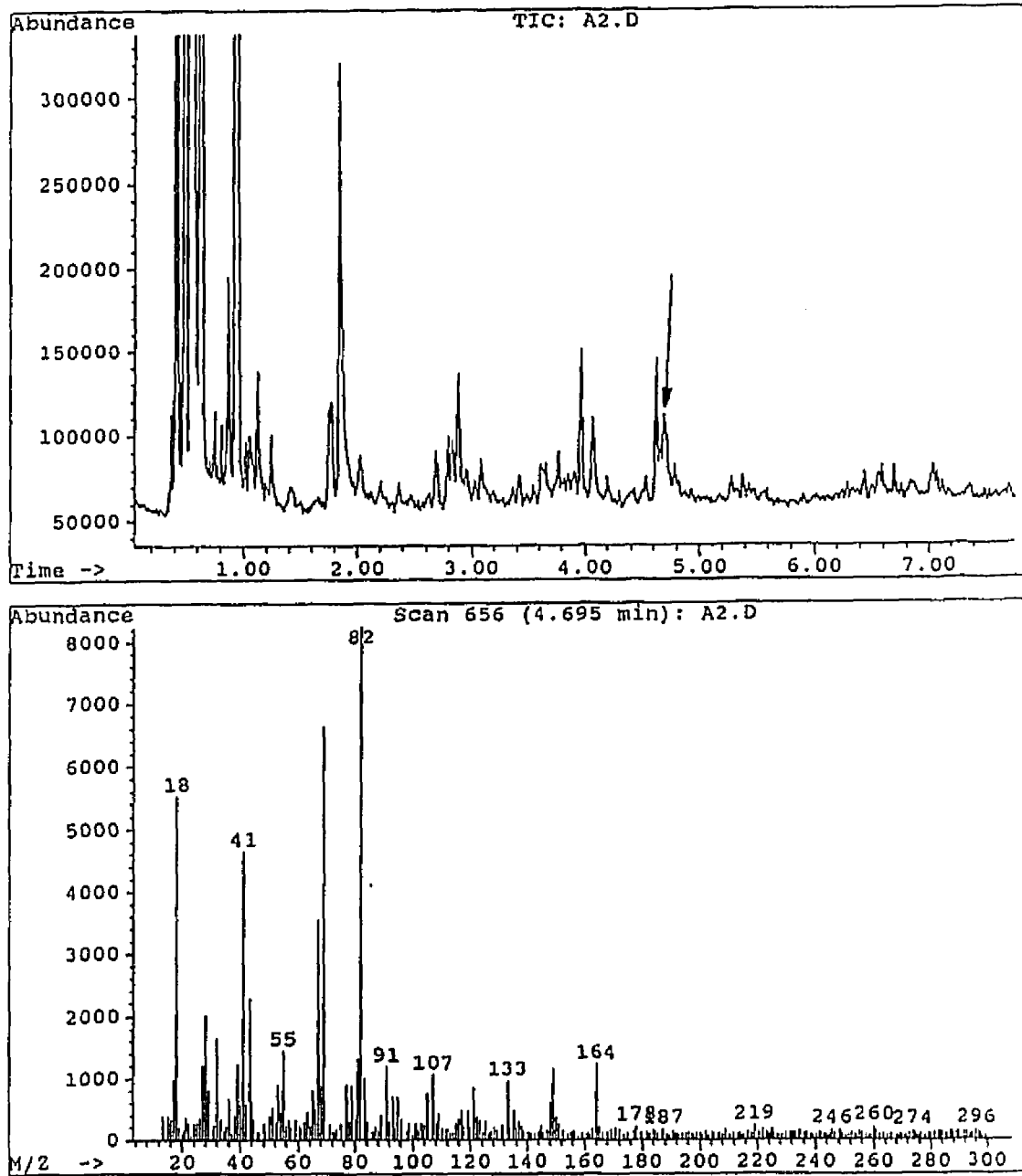
Figure 76. GC/MS data for $C_{12}H_{20}$ 

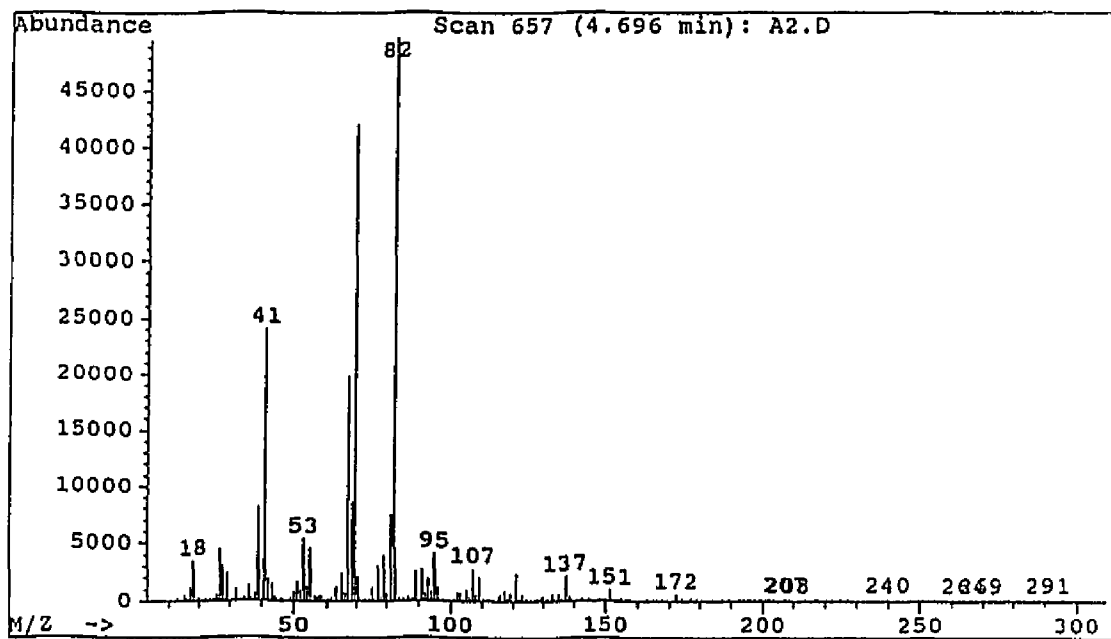
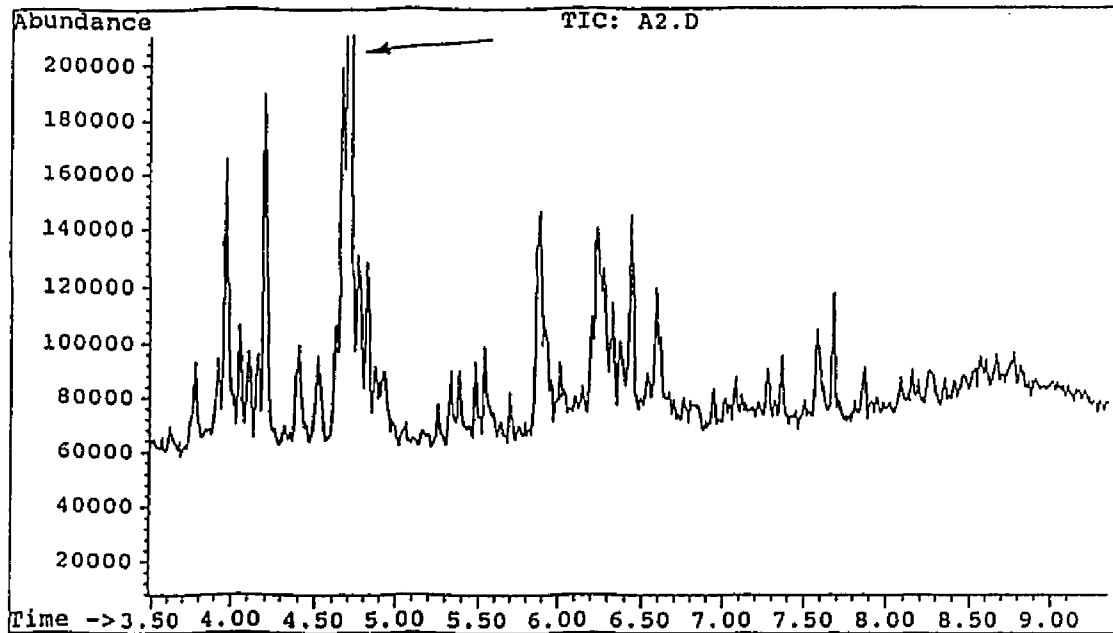
Figure 77. GC/MS data for $C_{10}H_{17}Cl$ 

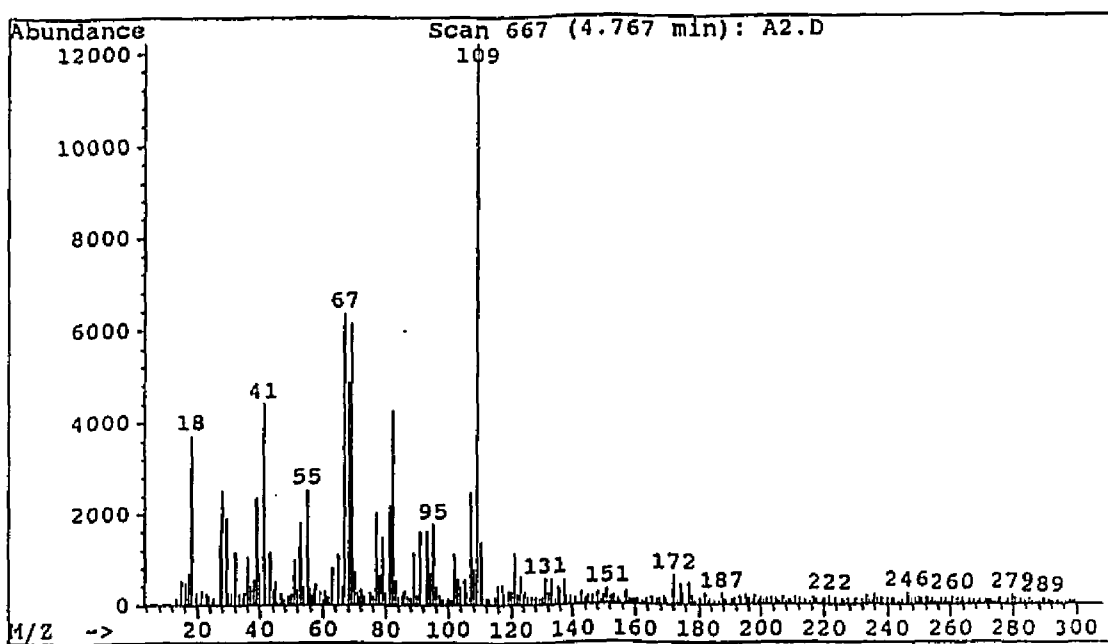
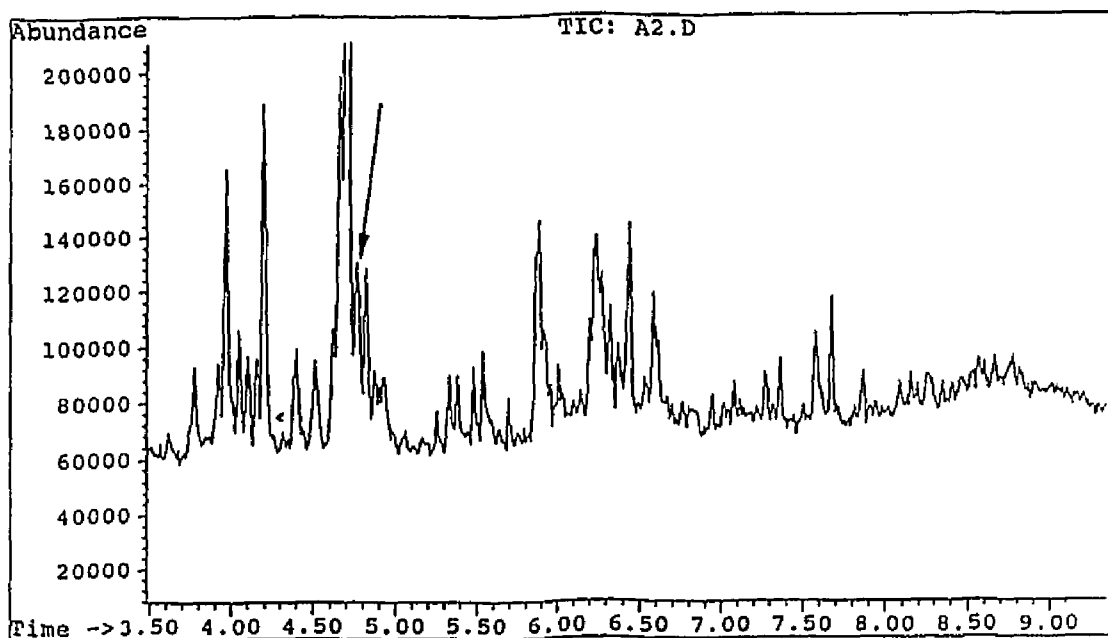
Figure 78. GC/MS data for $C_{10}H_{17}Cl$ 

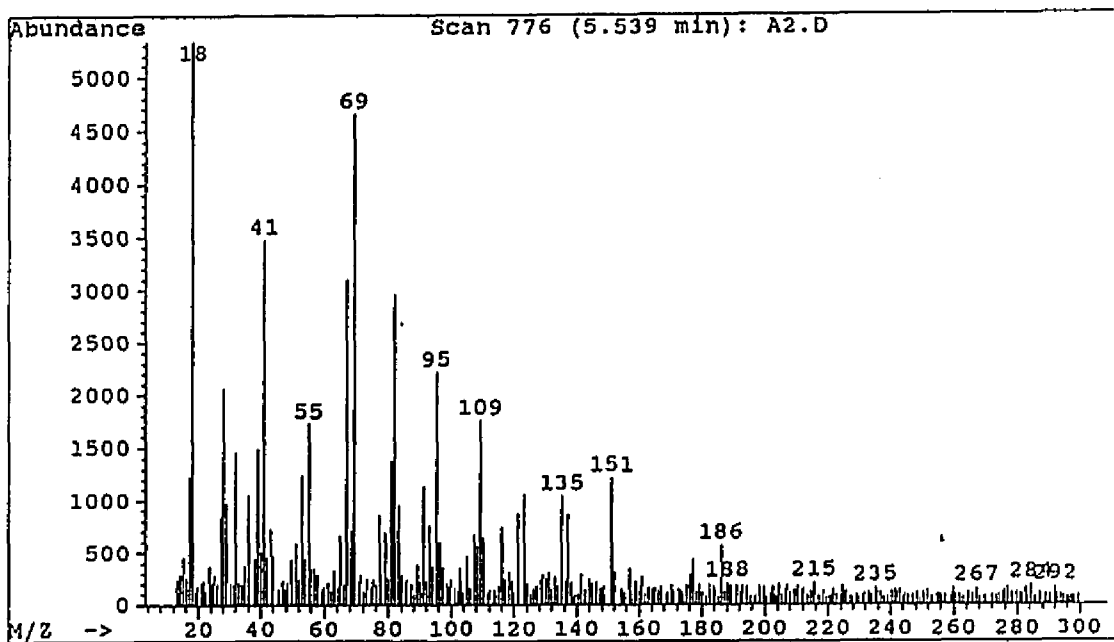
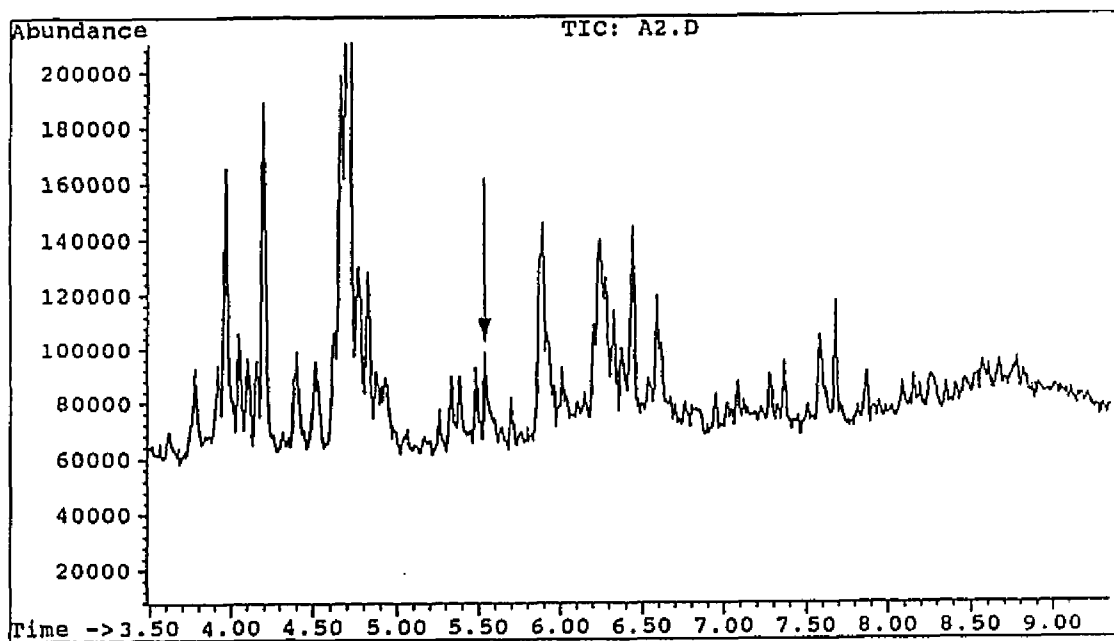
Figure 79. GC/MS data for $C_{11}H_{19}Cl$ 

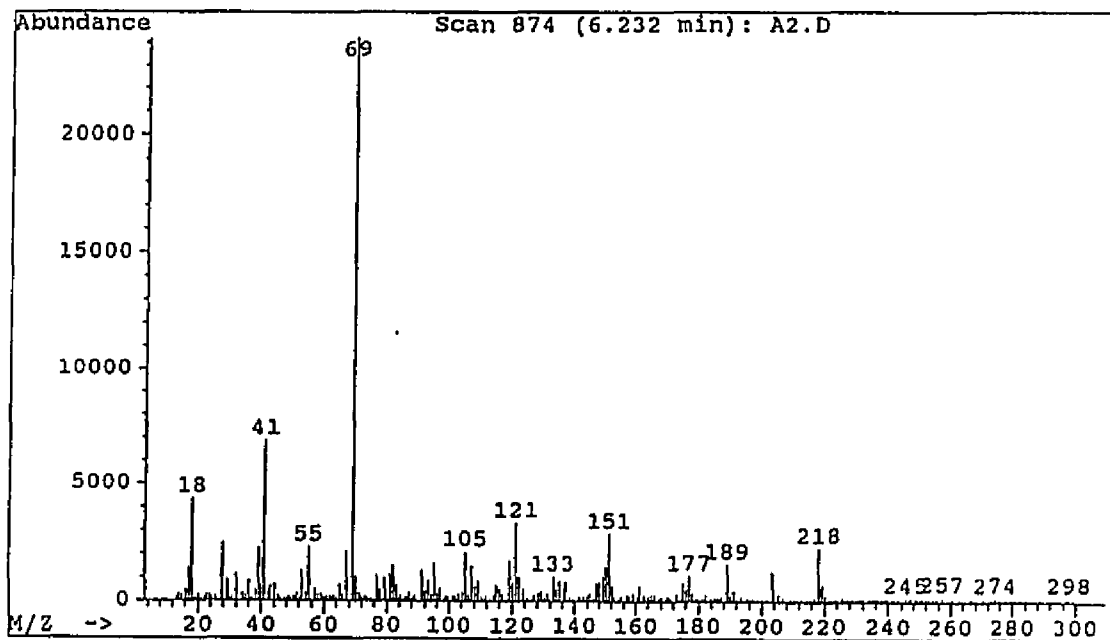
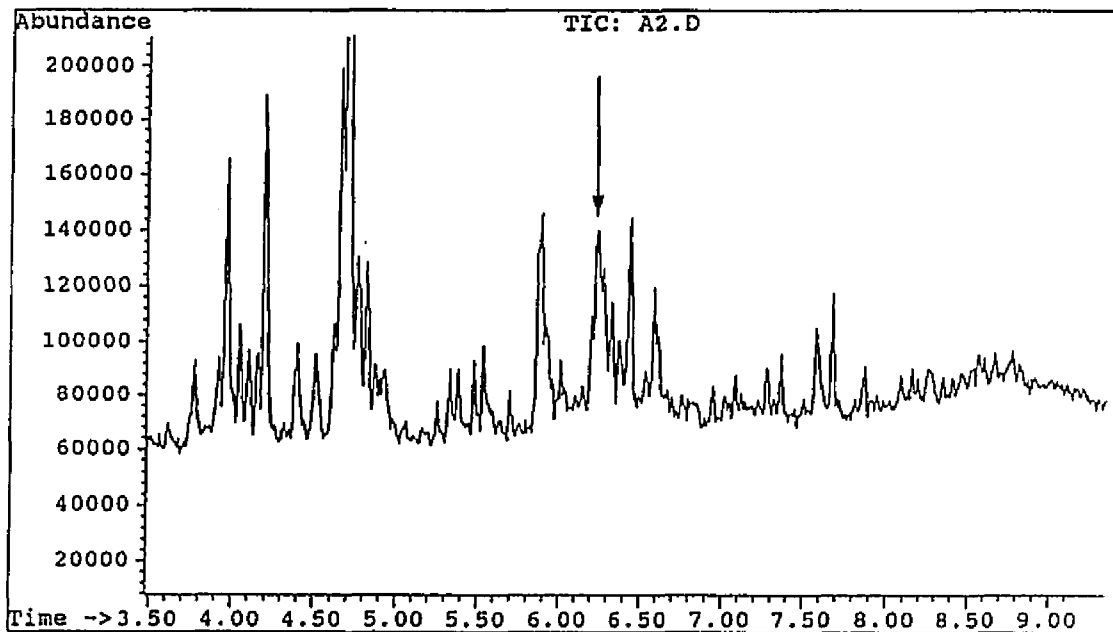
Figure 80. GC/MS data for $C_{16}H_{26}$ 

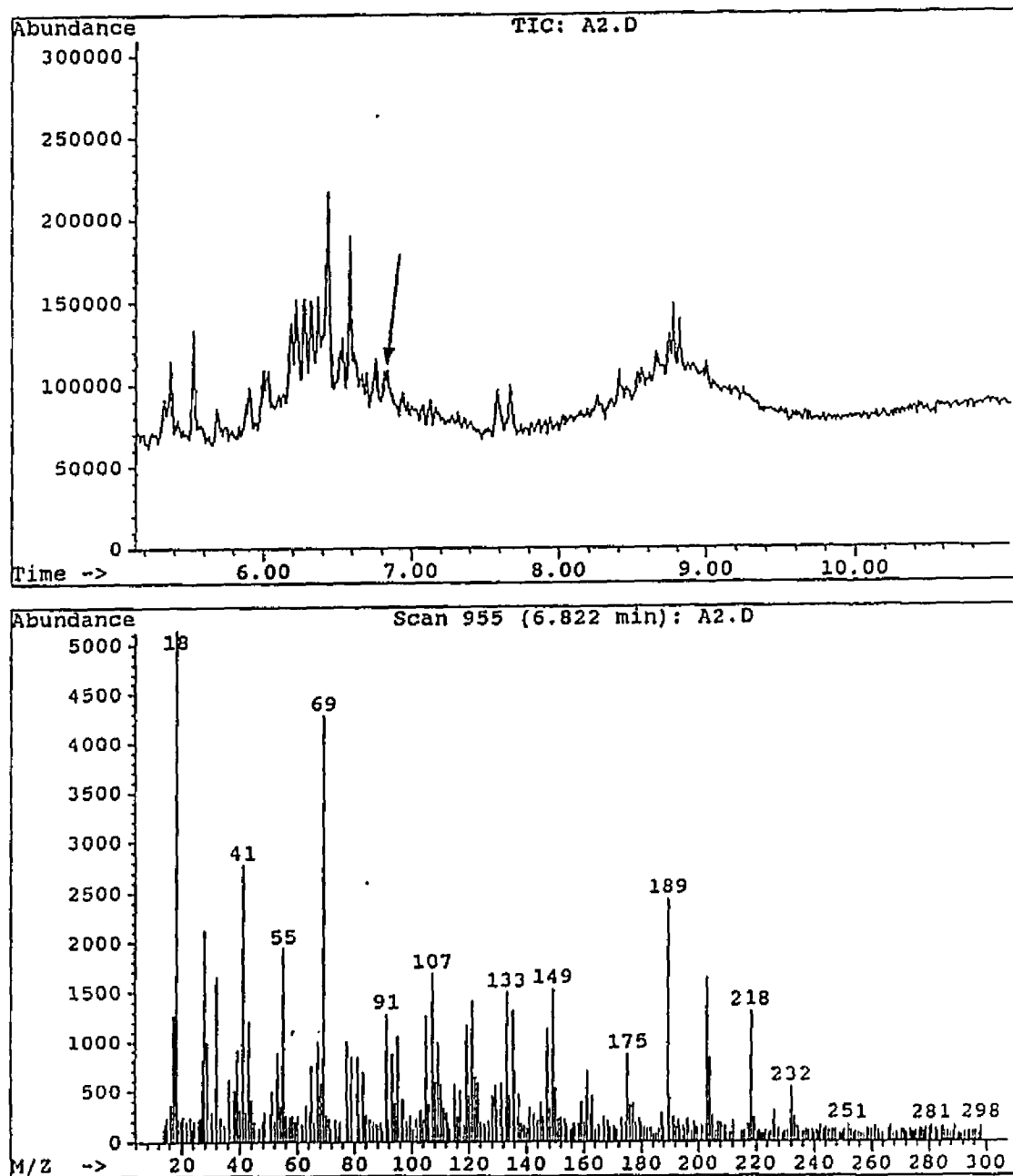
Figure 81. GC/MS data for $C_{17}H_{28}$ 

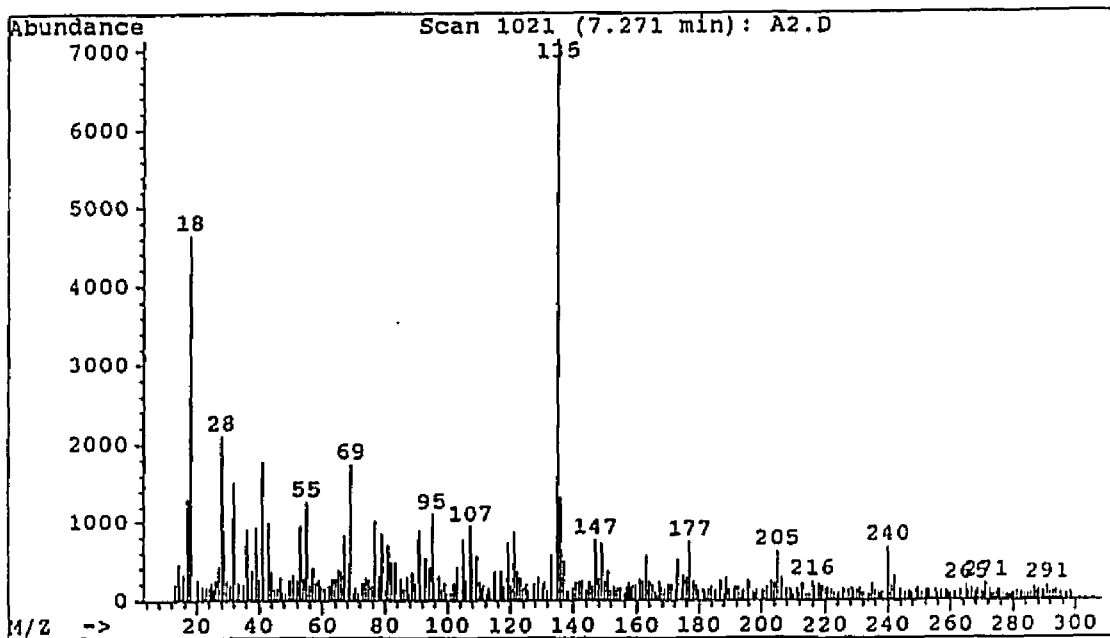
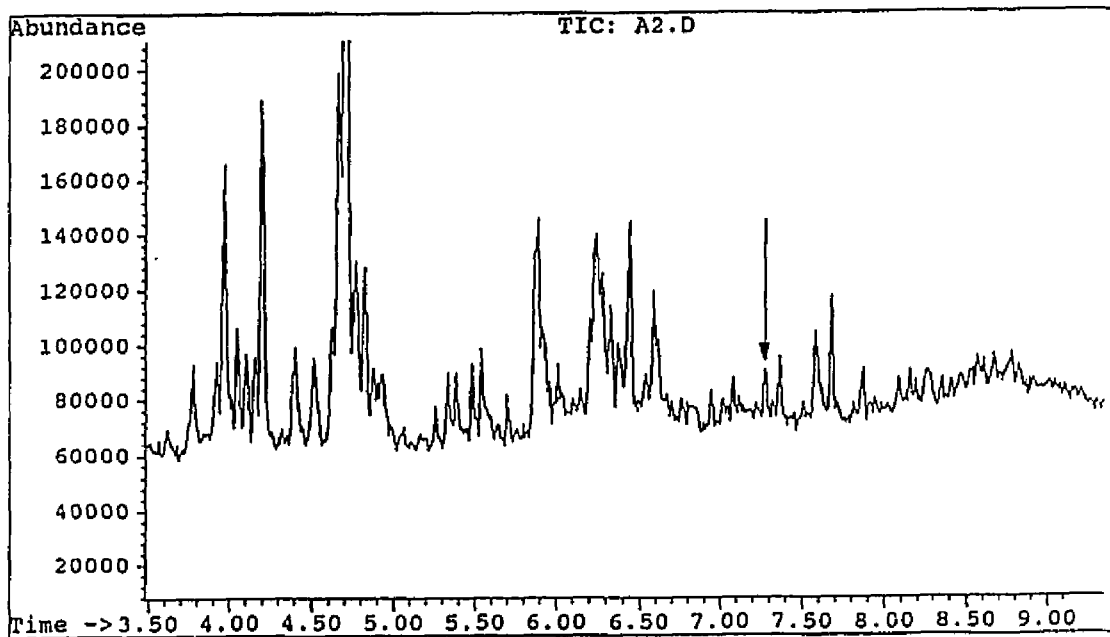
Figure 82. GC/MS data for $C_{15}H_{25}Cl$ 

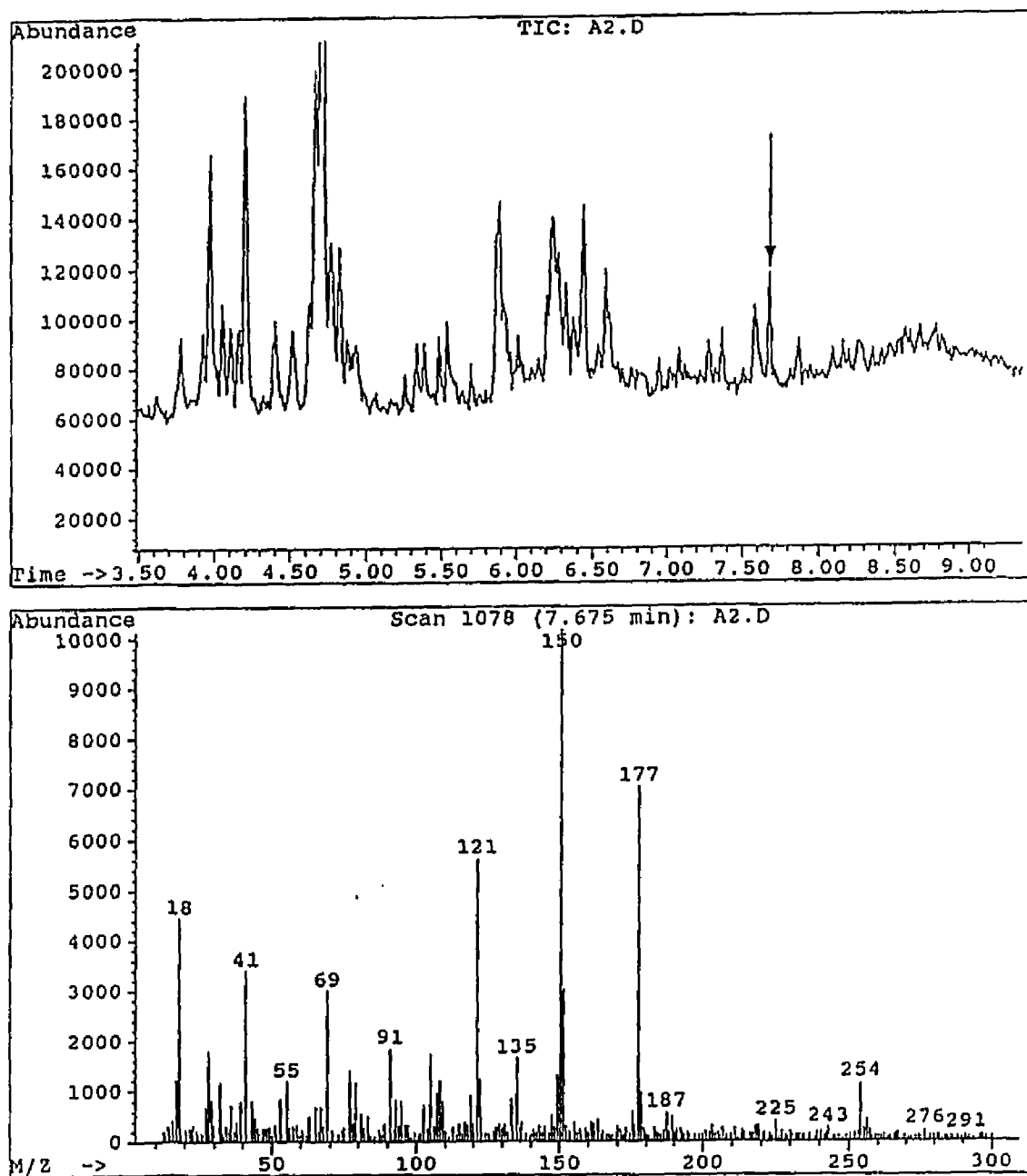
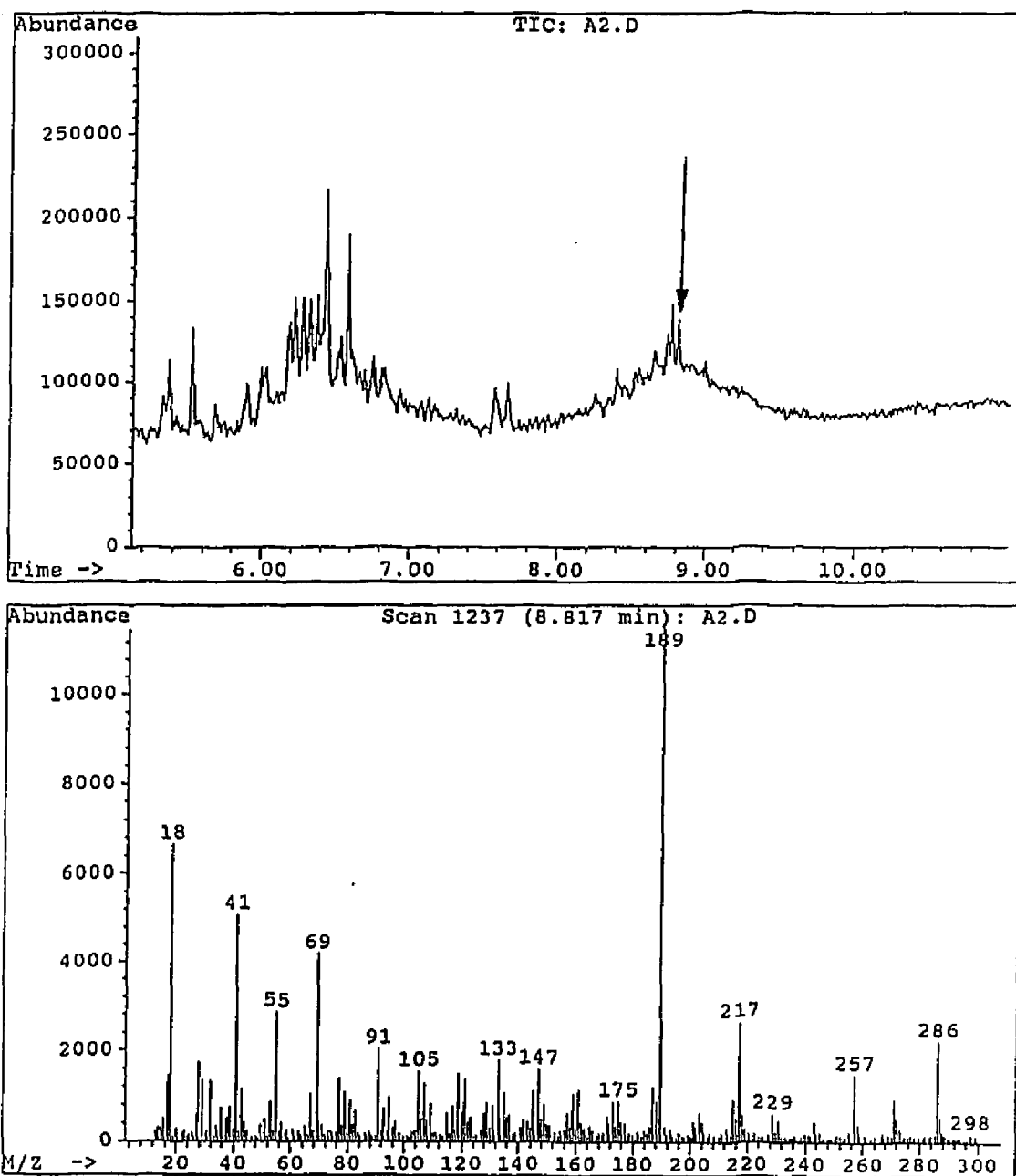
Figure 83. GC/MS data for $C_{16}H_{27}Cl$ 

Figure 84. GC/MS data for $C_{21}H_{34}$ 

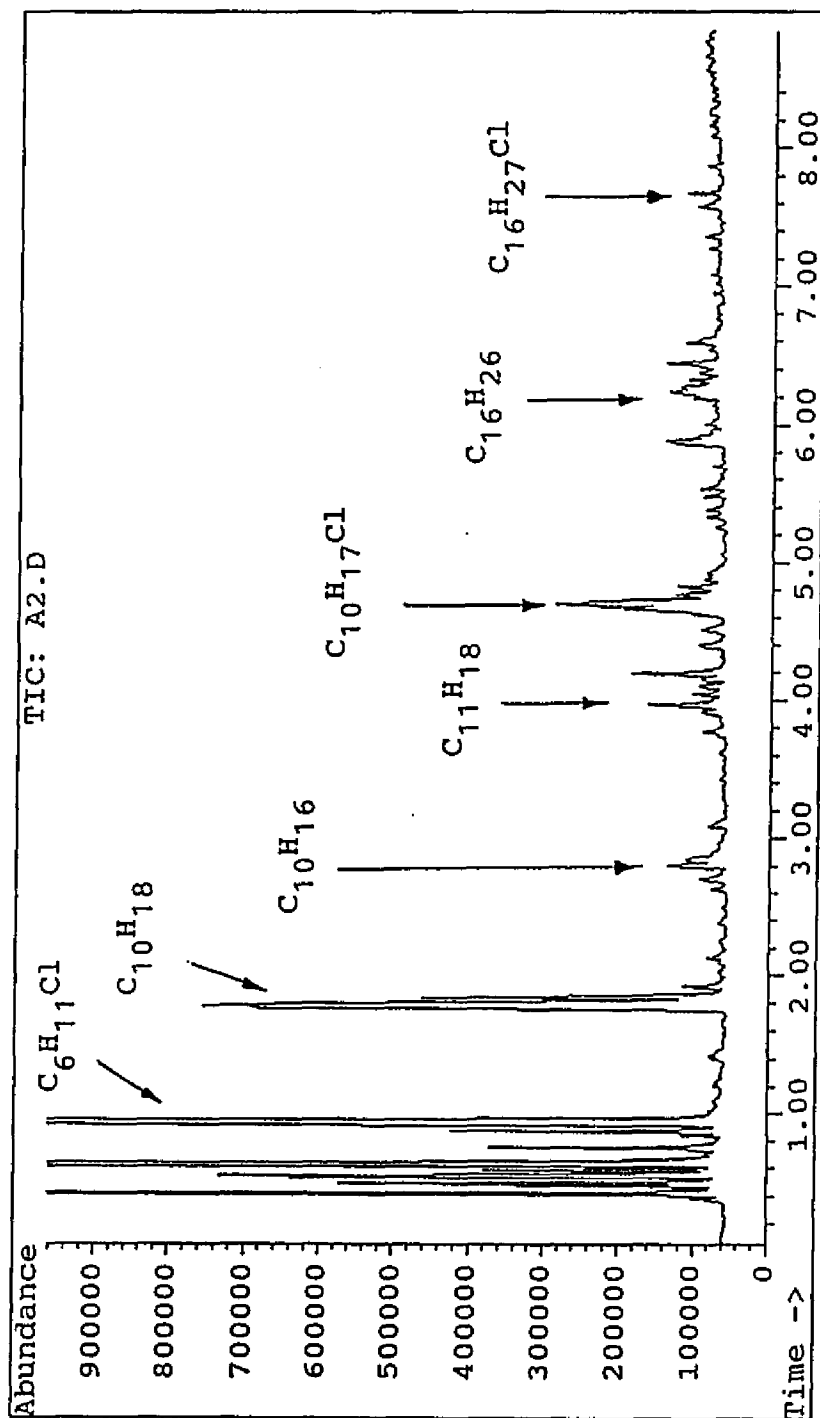


Figure 85. GC chromatogram of a mixture of 4-chloro-2-pentene and 2,4-hexadiene pyrolyzed in the presence of Cu at 200 °C for 1 h.

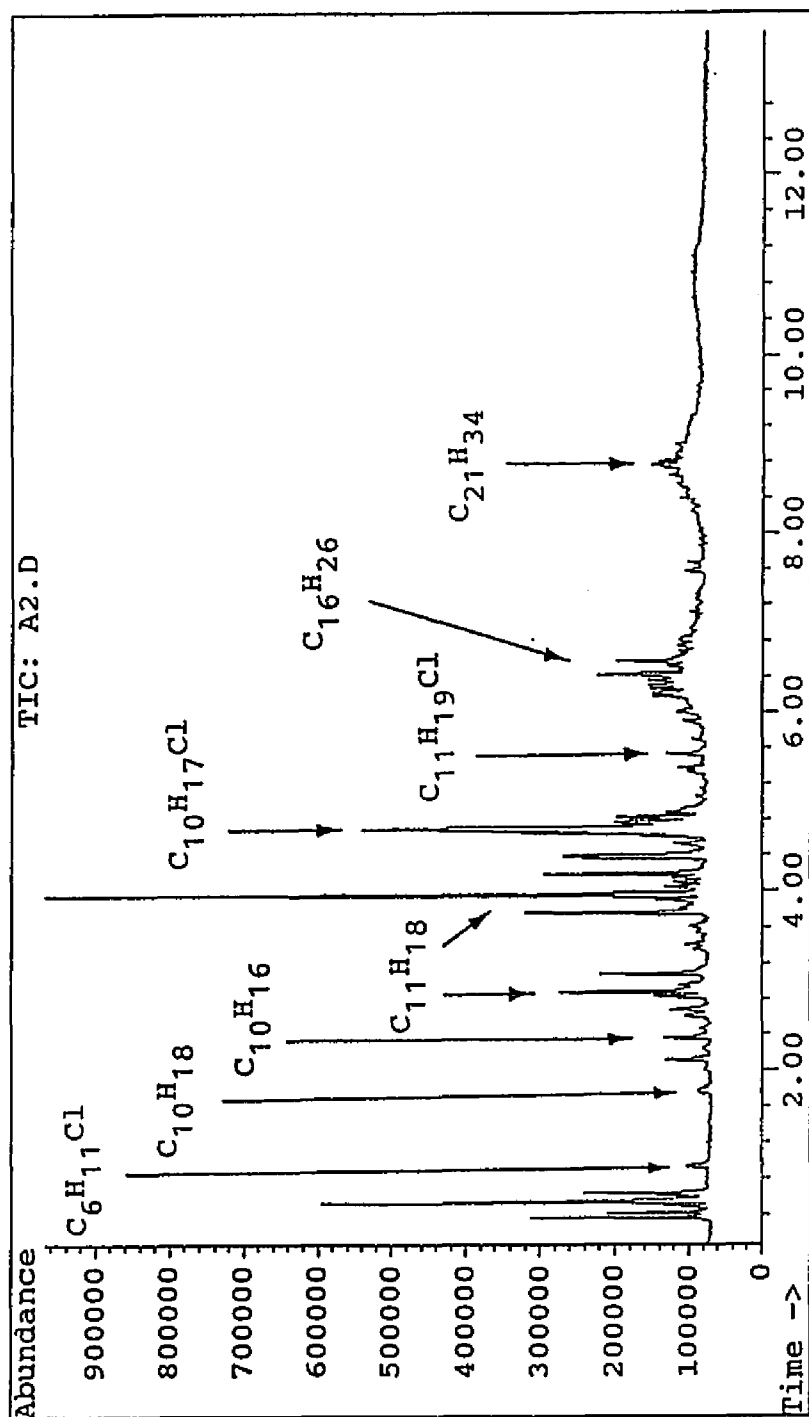


Figure 86. GC chromatogram of a mixture of 4-chloro-2-pentene and 2,4-hexadiene pyrolyzed in the presence of Cu_2O at 200 °C for 1 h.

In general, the chemical reactions responsible for the formation of these heavy products included those catalyzed by Lewis acids (olefin oligomerization, chloroalkylation, and aromatization), reductive-coupling dimerization, and alkene monochlorination. The relative significance of these reactions varied, depending upon the copper additive used.

For copper metal, the relative abundances of the heavy products resulting from these three types of reactions are nearly the same, in that the reductive-coupling dimers ($C_{10}H_{18}$, MW 138, Figure 72) account for 25% of the total heavy products, while the Lewis-acid-catalyzed oligomers (MW 148-286, Figures 73-84) and monochlorination products ($C_6H_{11}Cl$, MW 118, Figure 69; see Scheme 26) account for the rest (39% and 36%, respectively). It is worth noting that the percentage for the reductive-coupling dimer is much higher than in the case of the other copper additives used under the same conditions. These results once again confirm that under the catalytic effect of copper metal, the reductive coupling mechanism plays an important role in the formation of the heavy products.

For Cu_2O , the Lewis-acid-catalyzed heavy products (Figures 70, 71, and 73-84) are clearly the most abundant ones, accounting for 96% of the total. These results are in agreement with previous mechanistic studies conducted by many researchers,^{39,49,56,58} who performed sealed-tube

pyrolysis experiments and concluded that in the presence of Cu_2O , Lewis-acid catalyzed reactions are the major source of crosslinking structures in degraded PVC.

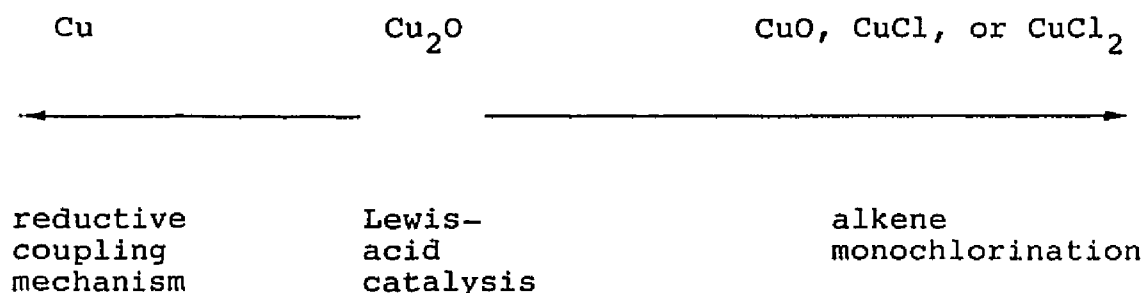
The monochlorination products, $\text{C}_6\text{H}_{11}\text{Cl}$, on the other hand, constitute only a small portion of the total heavy products in the presence of Cu_2O . This result is quite different from those obtained with the other copper additives, which gave the $\text{C}_6\text{H}_{11}\text{Cl}$ isomers in relatively high yields (36-71%; see Table 13). The reductive-coupling dimers also were detected in the reaction mixture but were low in abundance. Therefore, reductive coupling clearly does not play an important role in the case of Cu_2O . Lattimer and Kroenke,⁴⁹ in their 2,4-dichloropentane model-compound studies, obtained somewhat different results, in that dimers having three molecular formulas were observed: $\text{C}_{10}\text{H}_{14}$ (C_4 -benzenes), $\text{C}_{10}\text{H}_{16}$ (Lewis-acid dimers), and $\text{C}_{10}\text{H}_{18}$ (reductive-coupling dimers). All of these dimers were fairly abundant. On the other hand, Huang⁵⁸ and other workers,³⁹ in similar model-compound studies, found no trace of reductive-coupling products.

For CuO , CuCl , and CuCl_2 , the alkene monochlorination products were detected by GC/MS in large proportions, and for CuCl_2 , they constituted 71% of the total heavy products. The rechlorination of the polyene segments has been studied by several workers,^{39,110-112} and the present results suggest that this process may play an important smoke-

suppression role in the presence of CuCl_2 , CuCl , and CuO . However, in the model-compound studies (Part II, Section 2-3) involving the pyrolysis of 2,4-hexadiene with copper additives, we have shown that among the same five copper additives tested, only CuCl_2 can promote the formation of the same $\text{C}_6\text{H}_{11}\text{Cl}$ products. Hence, the results of the current studies suggest that in the case of CuCl and CuO the chlorine atom in the 4-chloro-2-pentene must have been added to the conjugated diene to produce the mono-chlorinated compounds. This process may first involve the dehydrochlorination of 4-chloro-2-pentene to produce HCl , followed by the addition of HCl to the olefinic segments (see Scheme 26). For CuCl_2 , the formation of $\text{C}_6\text{H}_{11}\text{Cl}$ may be due to the addition of extra two hydrogen atoms (available to the system due to aromatization occurring during the pyrolysis; see Scheme 26) to the $\text{C}_6\text{H}_9\text{Cl}$ olefinic segments. Rechlorination reactions involving alkenes and CuCl_2 have been pointed out and verified by several researchers.^{39,110-112}

Based on the results of the model-compound studies described above, it appears that in the presence of two different types of model compound, secondary allylic chloride and conjugated diene, three major chemical reactions are involved in the formation of heavy products: reactions catalyzed by Lewis acids, reductive-coupling dimerization, and monochlorination. Moreover, for different

copper additives (Cu, Cu₂O, CuO, CuCl, and CuCl₂), the formation of the major heavy products represents a balance among these three reaction pathways. For example, in the case of Cu₂O, Lewis-acid catalysis is clearly the major source of the heavy products, while in the case of Cu,



the importance of Lewis-acid catalysis decreases, and the reductive coupling mechanism takes over, in part. In the case of CuCl₂, the balance is clearly biased toward alkene monochlorination.

The results of the mixed model-compound pyrolysis experiments suggest that different copper additives can promote the crosslinking of PVC by different mechanisms. In addition to the Lewis-acid effects, other effects leading to reductive coupling and alkene monochlorination are operative.

2-5. Reaction of a Mixture of 4-Chloro-2-pentene and 1,3,5-Hexatriene with Copper Metal

Experiments performed with a mixture of 4-chloro-2-pentene and 1,3,5-hexatriene in the presence of Cu showed that the resultant heavy products consisted mainly of aromatic dimers, $C_{12}H_{16}$. In addition to the aromatic dimers, a moderate amount of rechlorination product, C_6H_9Cl , also was detected. The distribution of the heavy products is summarized in Table 15, and the relevant GC/MS data and representative structures are shown in Figures 87-93 and Table 16. The total chromatogram is shown in Figure 94.

Copper metal promoted numerous reactions: dehydrochlorination, aromatization, Lewis-acid catalyzed oligomerization and chloroalkylation, reductive-coupling dimerization, and alkene monochlorination. Almost all of the higher-mass products were aromatic hydrocarbons with unsaturated side groups. The most abundant aromatics, $C_{12}H_{16}$, were tentatively assigned as 3-hexenylbenzene and its isomers. In comparison to the results obtained with the mixture of 2,4-hexadiene and 4-chloro-2-pentene (see Section 2-4), the triene model compound demonstrated an ability to form an aromatic ring which was not found with the diene model compound. Lattimer and Kroenke⁴⁹ conducted similar model-compound studies and discovered that, in

Table 15

Distribution of the Heavy Products from Pyrolyses of
a Mixture of 4-Chloro-2-pentene and 1,3,5-Hexatriene

MW	Chemical Formula	Yield ^a (%)
116	C_6H_9Cl	16
136	$C_{10}H_{16}$	trace
138	$C_{10}H_{18}$	4
148	$C_{11}H_{16}$	8
160	$C_{12}H_{16}$	59
196	$C_{12}H_{17}Cl$	3
228	$C_{17}H_{24}$	10

a. GC area percentages based on total amount of the
heavy products.

Table 16
 Representative Tentative Chemical Structures of
 the Heavy Products from Pyrolyses of a Mixture
 of 4-Chloro-2-pentene and 1,3,5-Hexatriene

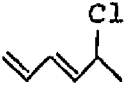
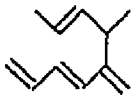
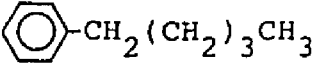
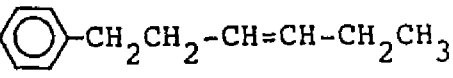
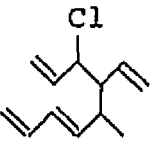
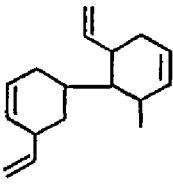
MW	Chemical Formula	Chemical Structure(s)
116	C_6H_9Cl (Fig. 87)	
138	$C_{10}H_{18}$ (Fig. 88)	
148	$C_{11}H_{16}$ (Figs. 89, 90)	 
160	$C_{12}H_{16}$ (Fig. 91)	
196	$C_{12}H_{17}Cl$ (Fig. 92)	
228	$C_{17}H_{24}$ (Fig. 93)	

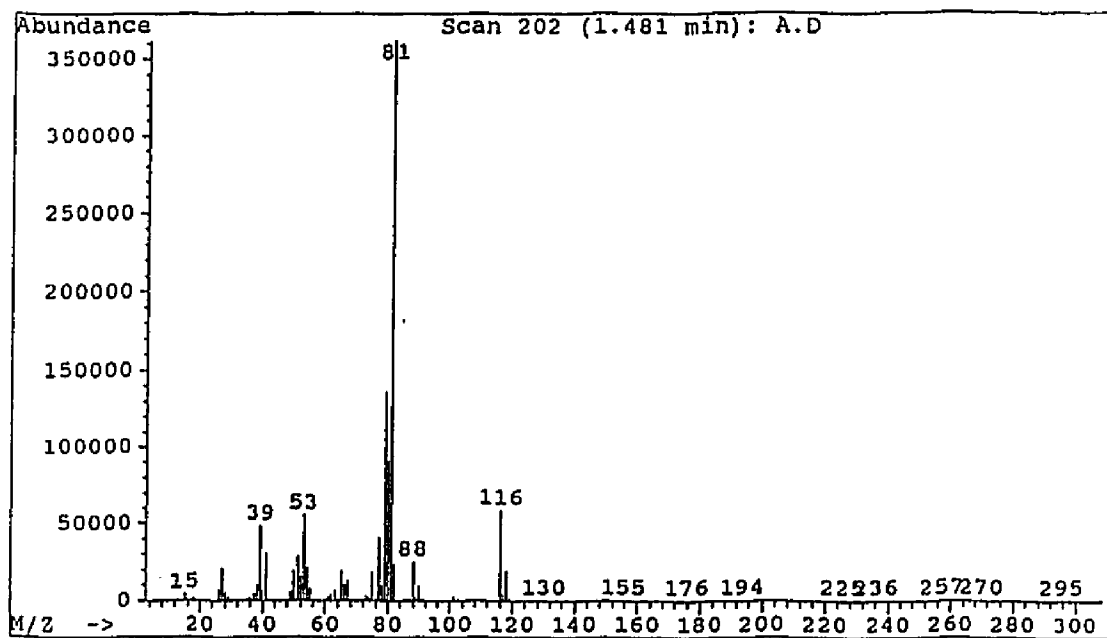
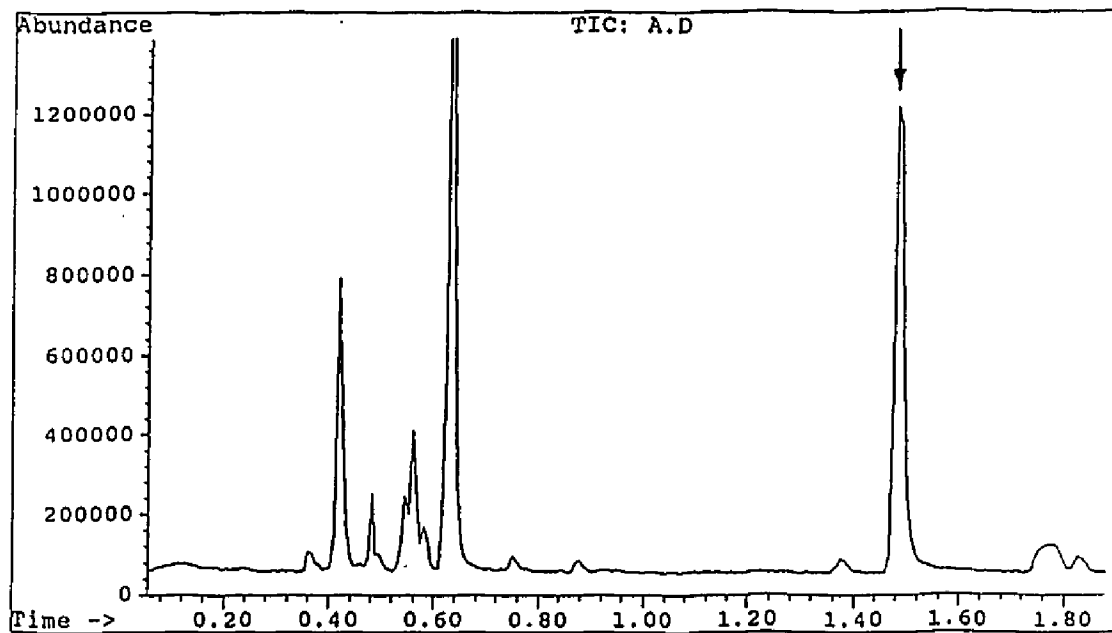
Figure 87. GC/MS data for C_6H_9Cl 

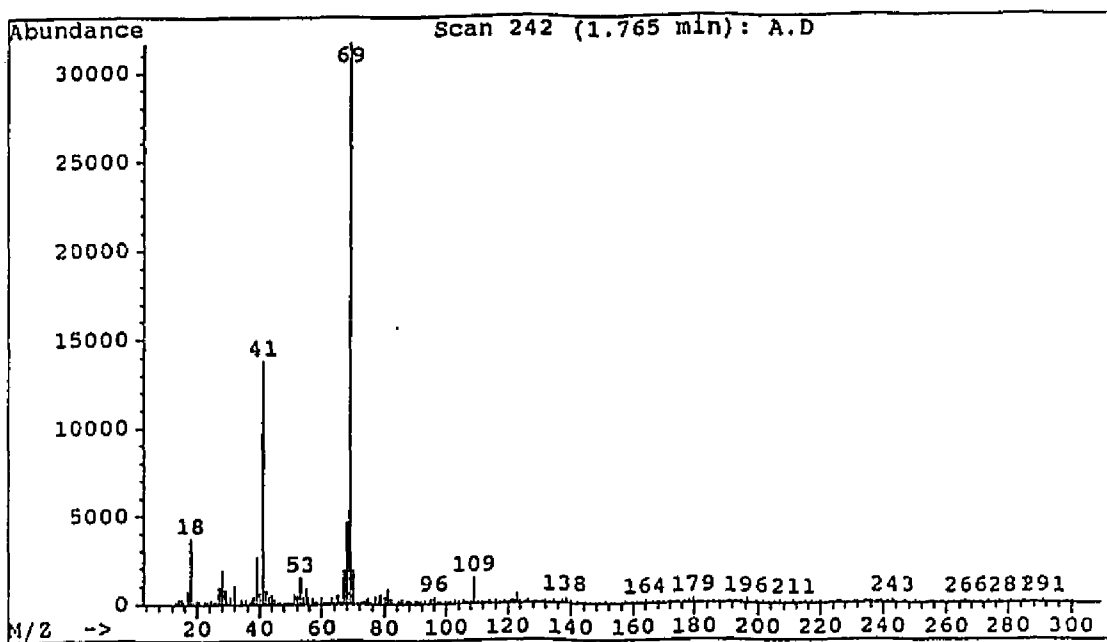
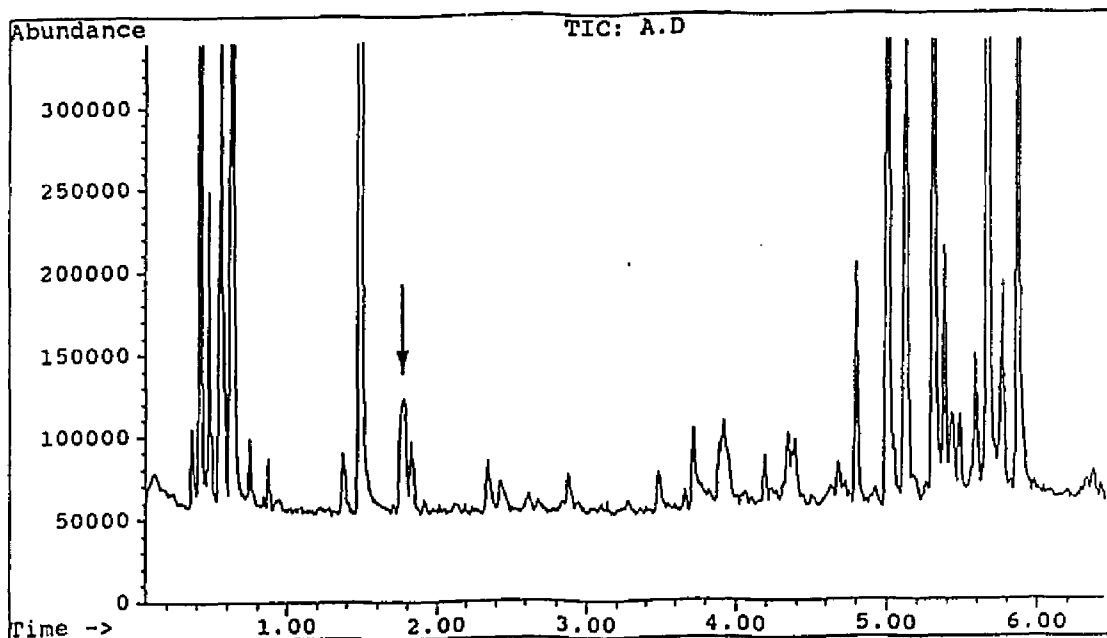
Figure 88. GC/MS data for $C_{10}H_{18}$ 

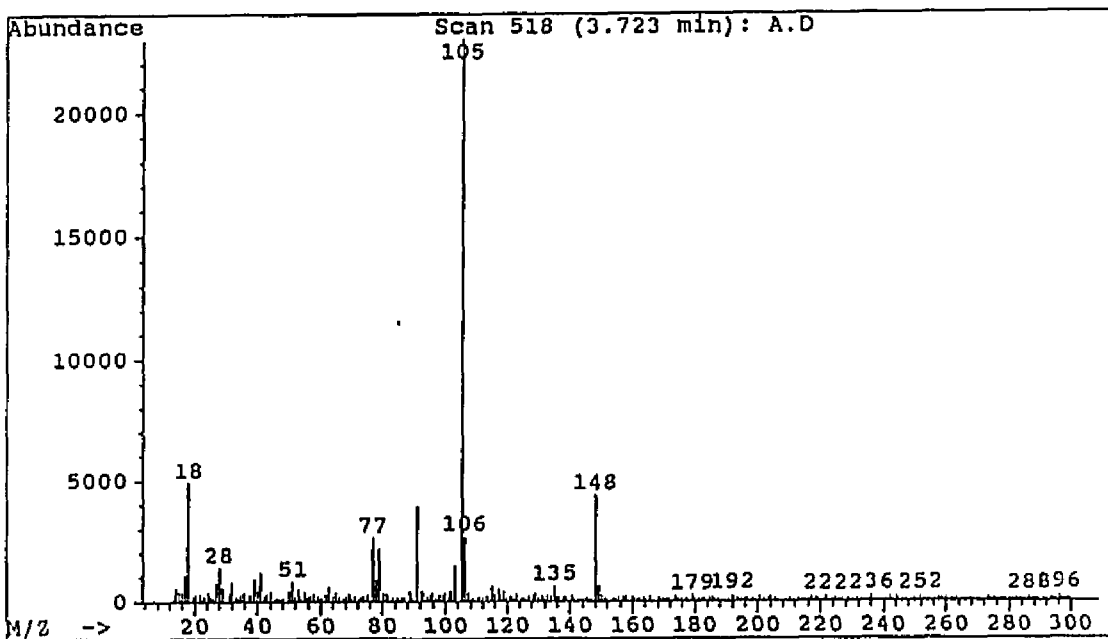
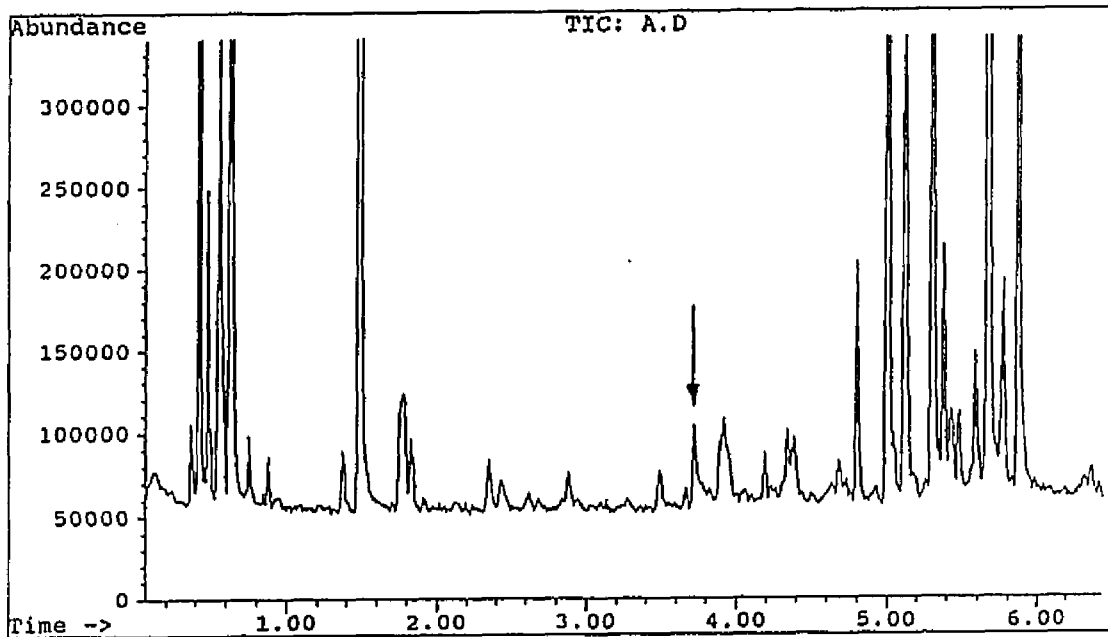
Figure 89. GC/MS data for $C_{11}H_{16}$ 

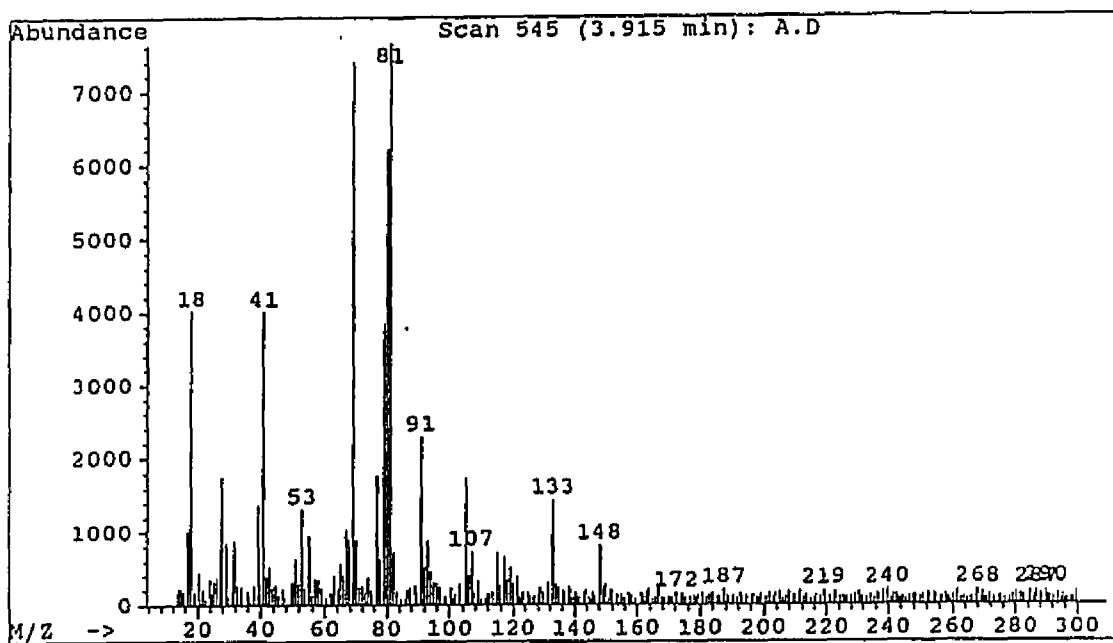
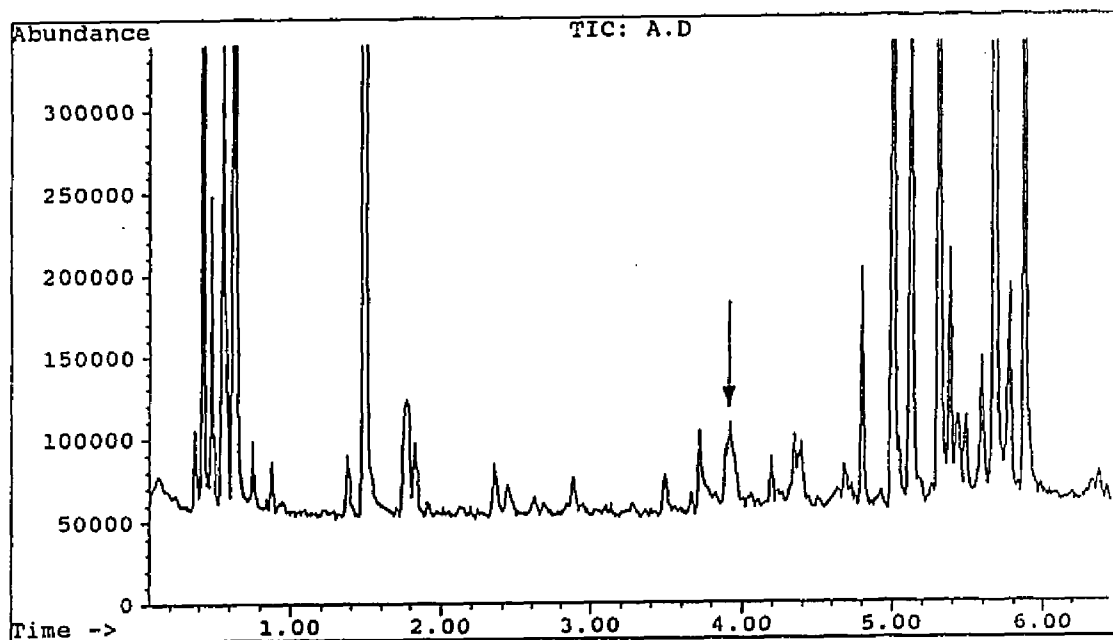
Figure 90. GC/MS data for $C_{11}H_{16}$ 

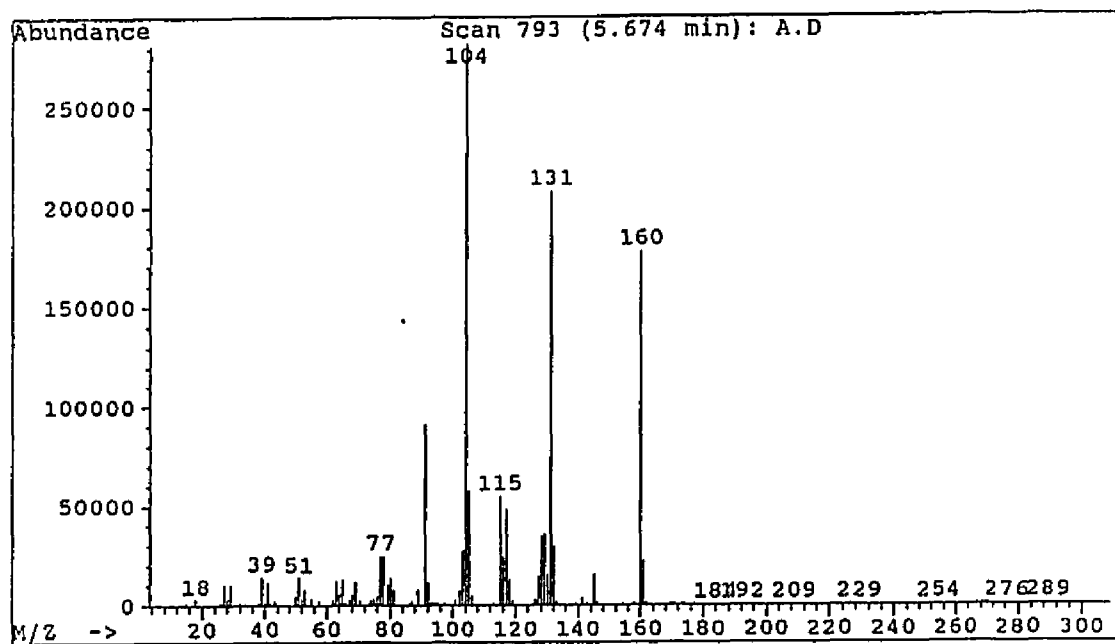
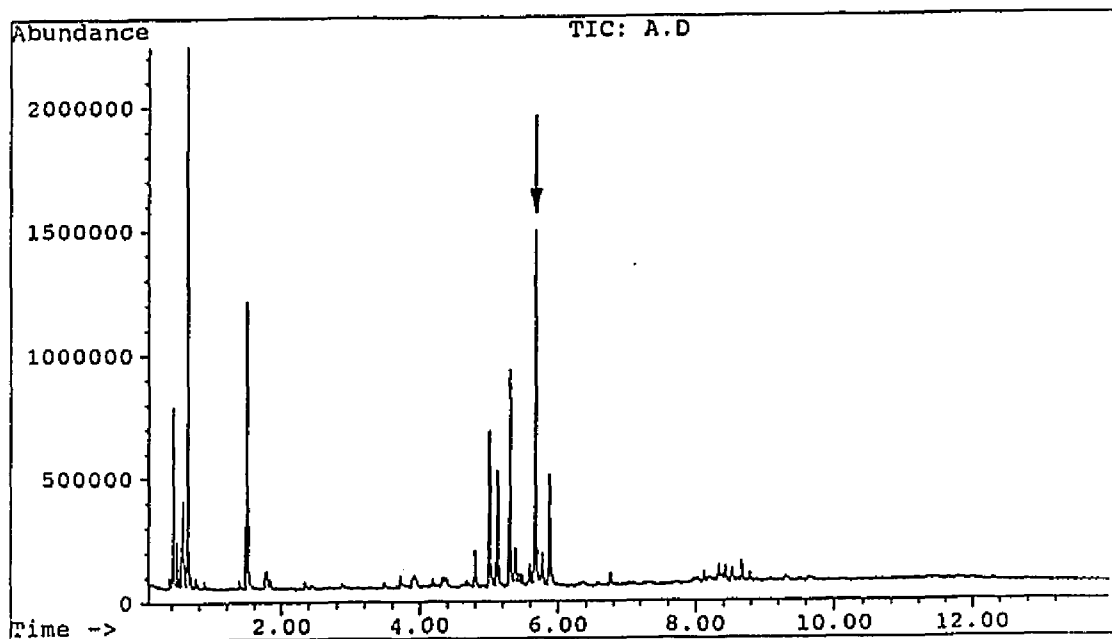
Figure 91. GC/MS data for $C_{12}H_{16}$ 

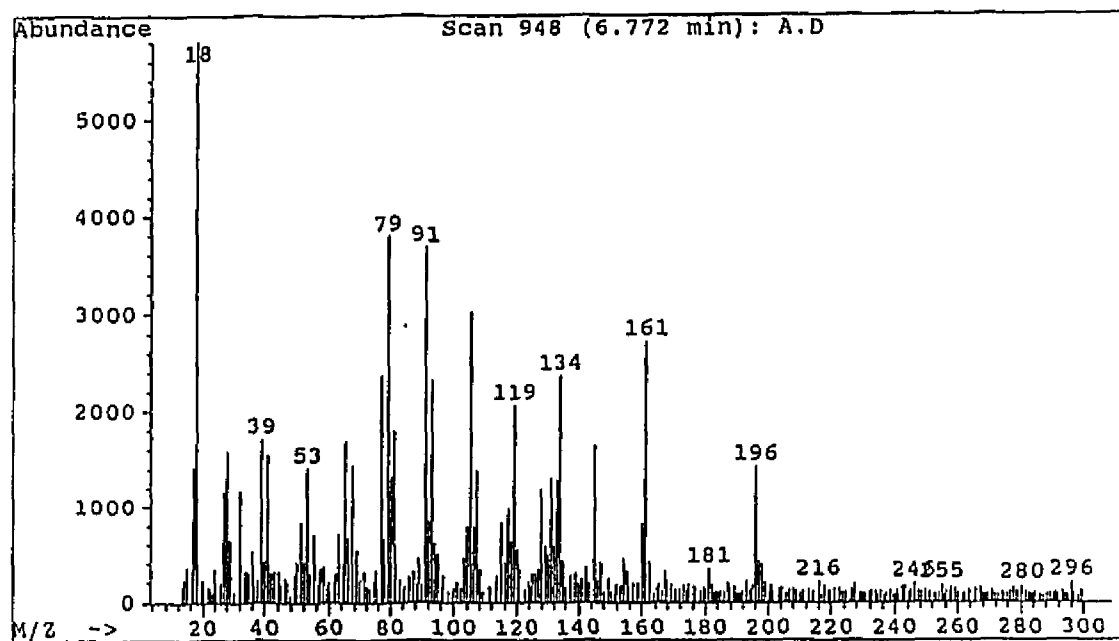
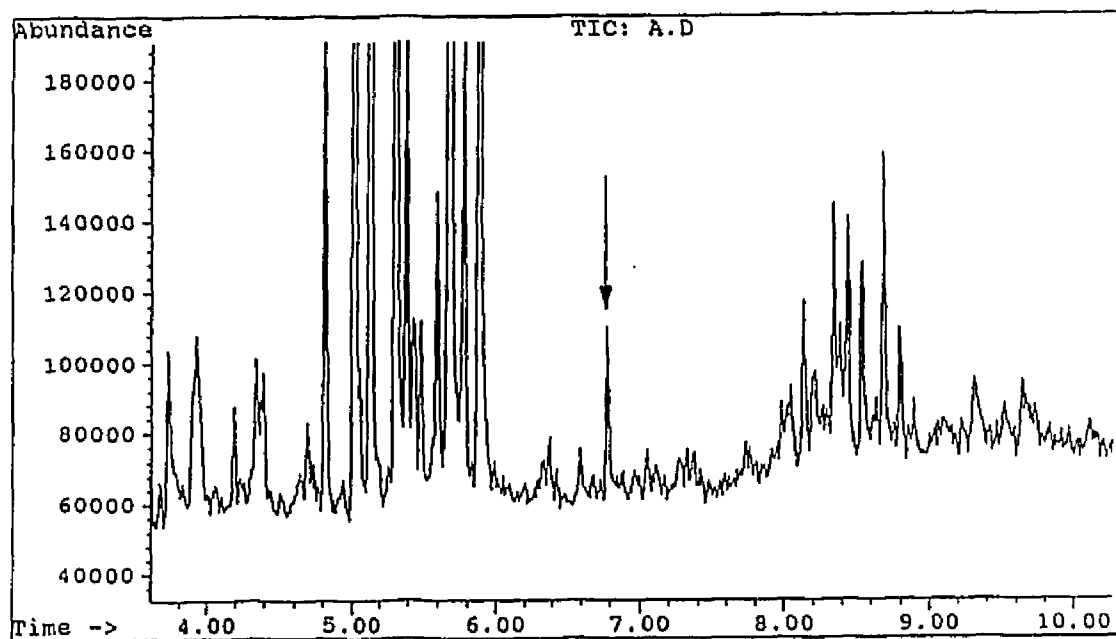
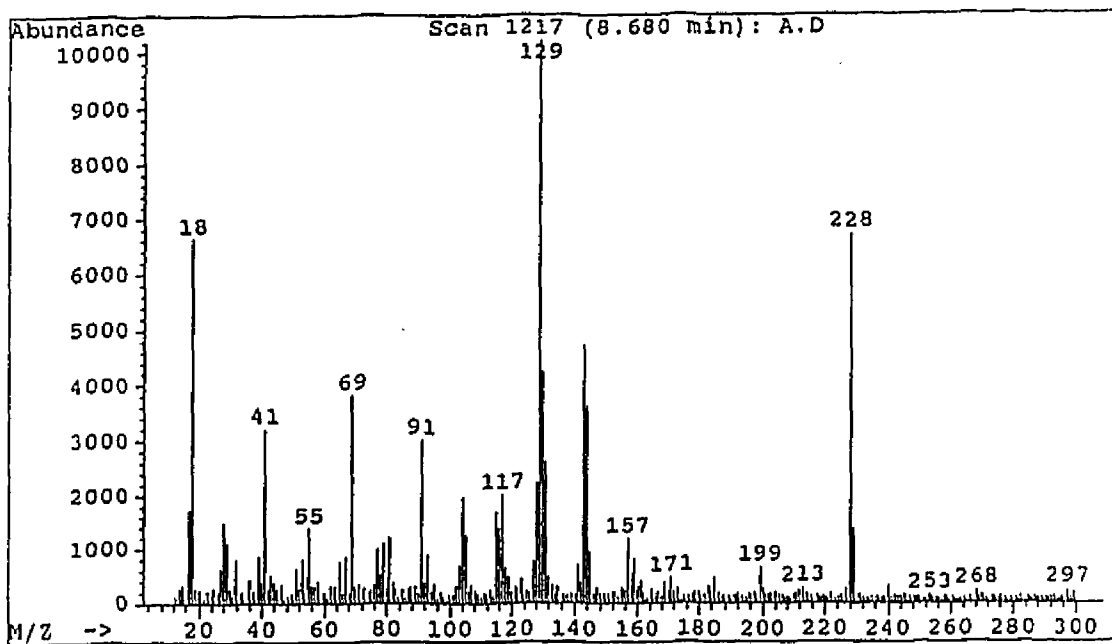
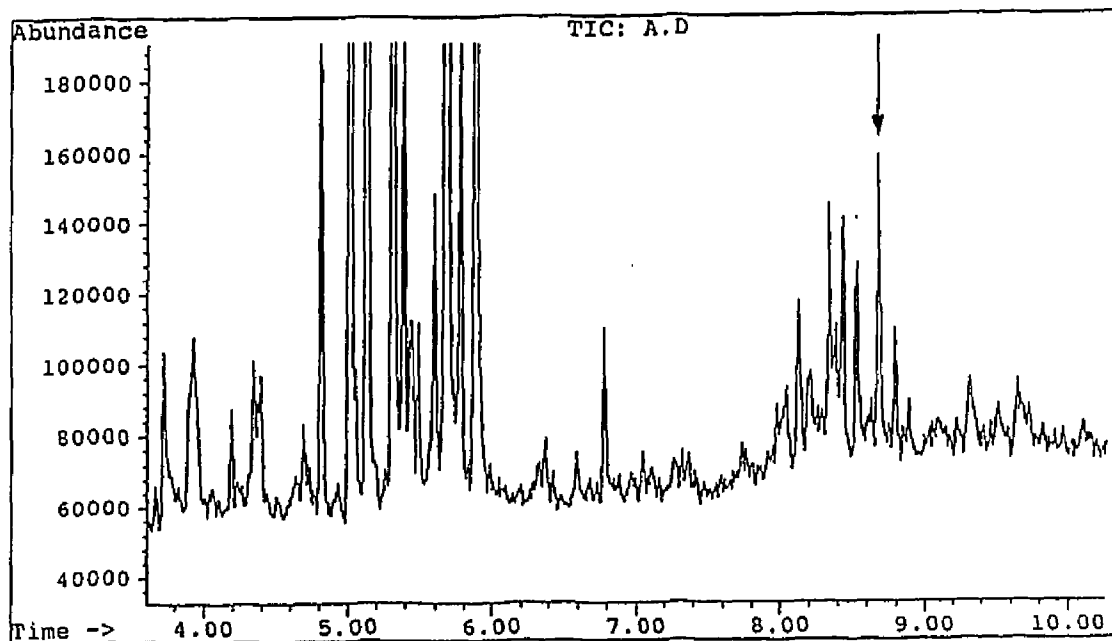
Figure 92. GC/MS data for $C_{12}H_{17}Cl$ 

Figure 93. GC/MS data for $C_{17}H_{24}$ 

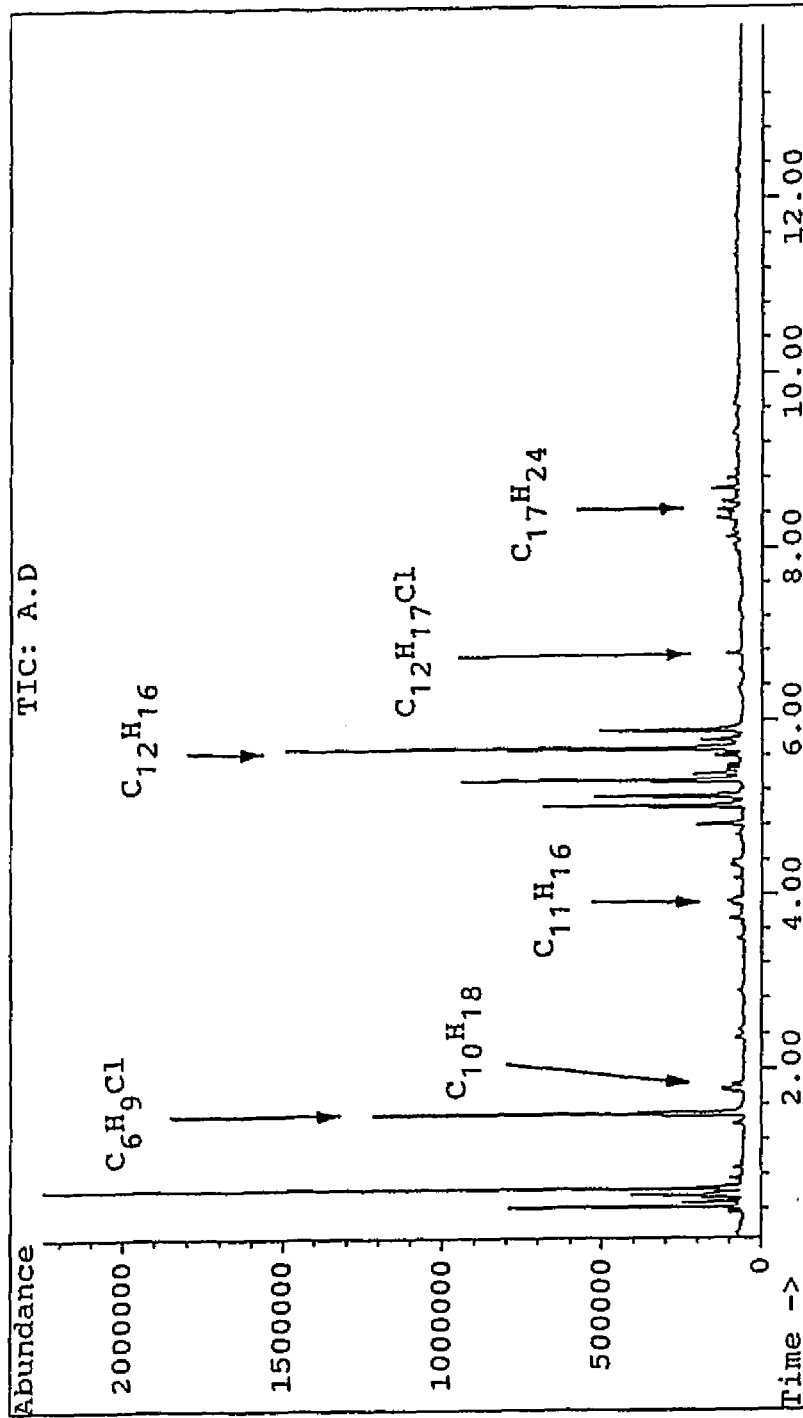


Figure 94. GC chromatogram of a mixture of 4-chloro-2-pentene and 1,3,5-hexatriene pyrolyzed in the presence of Cu at 200 °C for 1 h.

the case of 3-chloropentane, very low yields of aromatic products were produced in the presence of MoO_3 . However, in the case of 2,4-dichloropentane or 2,4,6-trichloroheptane, large amounts of aromatic heavy products were detected. Their results show that the lack of conjugated double bonds after dehydrochlorination precludes much of the interesting chemistry observed for the diene and triene model compounds.

Other aliphatic heavy products such as $\text{C}_{11}\text{H}_{16}$ and $\text{C}_{17}\text{H}_{24}$ were composed of two different model-compound components. This result suggests that linkages (cross-linking) among different structural segments in degraded PVC may be very extensive in the presence of Cu. Finally, the presence of dimers at the molecular weight expected for reductive-coupling products, $\text{C}_{10}\text{H}_{18}$, provides further supporting evidence for the ability of Cu to promote reductive-coupling dimerization.

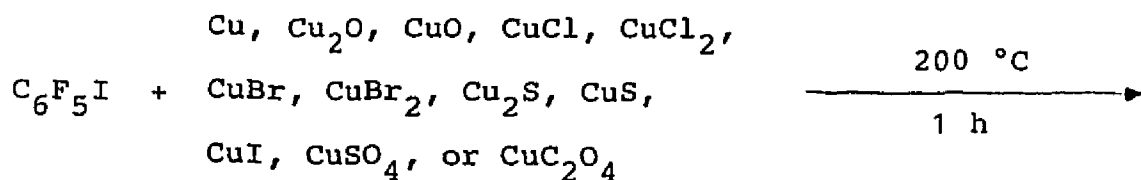
2-6. Pyrolysis of a Mixture of 3-Chloro-1-butene and 4-Chloro-2-pentene in the presence of Cu

The ability of the high-purity copper metal powder to promote cross-coupling between equimolar amounts of two secondary allylic chlorides (3-chloro-1-butene and 4-chloro-2-pentene) was examined by means of a sealed-tube pyrolysis experiment performed at 200 °C for 1 h. Analysis of the resultant reaction mixture by GC/MS showed that a cross-coupling reaction between the two allylic chlorides had occurred and that three isomeric C_9H_{16} aliphatic dimers had been formed in a way similar to that found in the case where the same model compounds had been treated with the activated copper slurry or film under argon at ambient temperature (see Section 1-1). The homo- and cross-coupling dimers were the most abundant heavy products and accounted for more than 40% of these materials. The starting materials were the largest components of the product mixture, and the dehydrochlorination products amounted to less than 10% of the total products. Other heavy products detected were those found in the corresponding reactions with single allylic chlorides, and they were all relatively low in abundance.

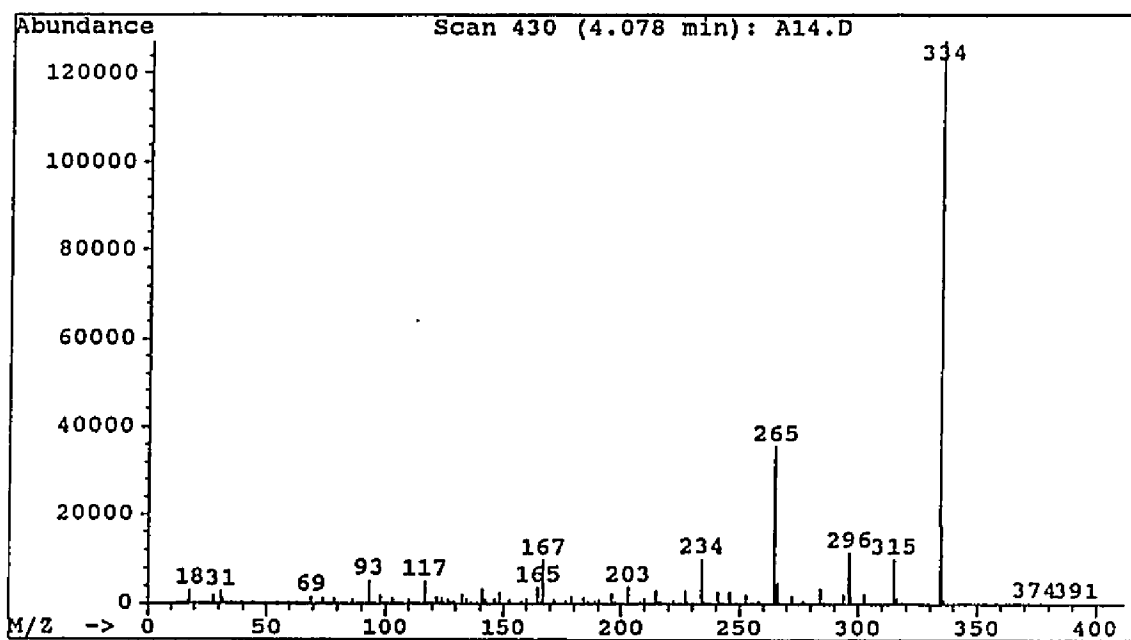
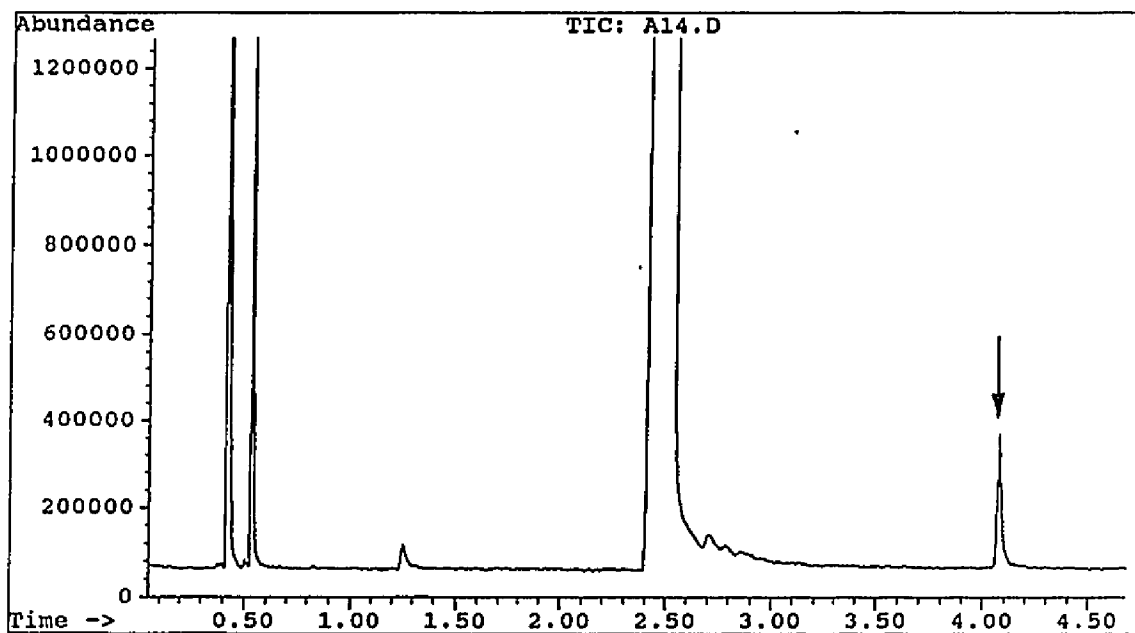
The results of the above experiment provide additional evidence to support the occurrence of reductive coupling among different allylic chloride segments in PVC under

the catalytic effect of copper, and they reaffirm the validity of the involvement of reductive coupling during the pyrolysis and combustion of the polymer.

2-7. Pyrolysis of Iodopentafluorobenzene in the Presence
of Various Copper Additives

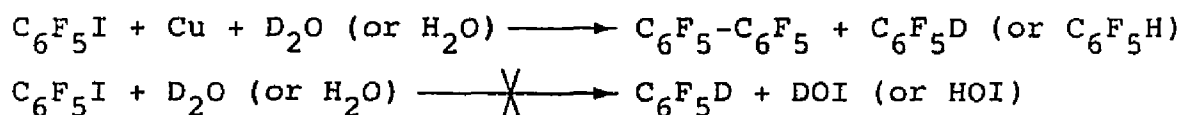


Reactions of $\text{C}_6\text{F}_5\text{I}$ (0.25 mL, 1.87 mmol) with twelve different copper additives (0.01 g in each case) were carried out at 200 °C for 1 h. Analyses of the resultant reaction mixtures by GC/MS showed that only high-purity copper metal (99.999%) and Cu_2O were able to promote reductive coupling of $\text{C}_6\text{F}_5\text{I}$ to form biaryl dimer $\text{C}_6\text{F}_5\text{-C}_6\text{F}_5$ (Figure 95). The GC yields of this dimer were 40 and 5%, respectively. A trace amount of biaryl dimer was also produced by CuO . The other copper additives tested all left $\text{C}_6\text{F}_5\text{I}$ unchanged. In comparison to the results of the similar secondary-allylic chloride pyrolysis experiments described in Section 2-2, the results of the experiments with $\text{C}_6\text{F}_5\text{I}$ reaffirm the conclusion that copper metal is capable of promoting the reductive coupling of certain organohalides. The results also suggest that to promote extensive crosslinking of PVC by reductive coupling, a highly reactive Cu^0 species must be generated during the pyrolysis and combustion process, since in the model-compound experiments where copper compounds such as copper

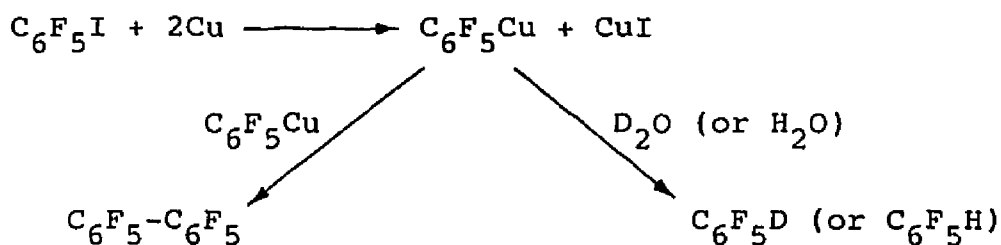
Figure 95. GC/MS data for $C_6F_5-C_6F_5$ 

oxides or chlorides were used, Lewis-acid effects clearly played a major role.

Additional experiments were performed with C_6F_5I , and D_2O (or H_2O) in the presence or absence of Cu at 200 °C for 1 h. The GC/MS analyses of the resultant mixtures showed that C_6F_5D (or C_6F_5H) was produced along with the $C_6F_5-C_6F_5$ dimers in the presence of Cu, as shown in Figures 96 and 97, respectively.



Possible mechanism:



These results suggest that perfluoroaryl halides are able to form stable organocopper intermediates during the pyrolytic process. In earlier studies, Rieke and Rhyne¹¹³ have, in fact, isolated and characterized the C_6F_5Cu produced from the reaction of C_6F_5I with activated copper. These data also imply that allylic alkyl halides may be able to generate alkylcopper intermediates when they are treated with activated copper or high purity copper metal

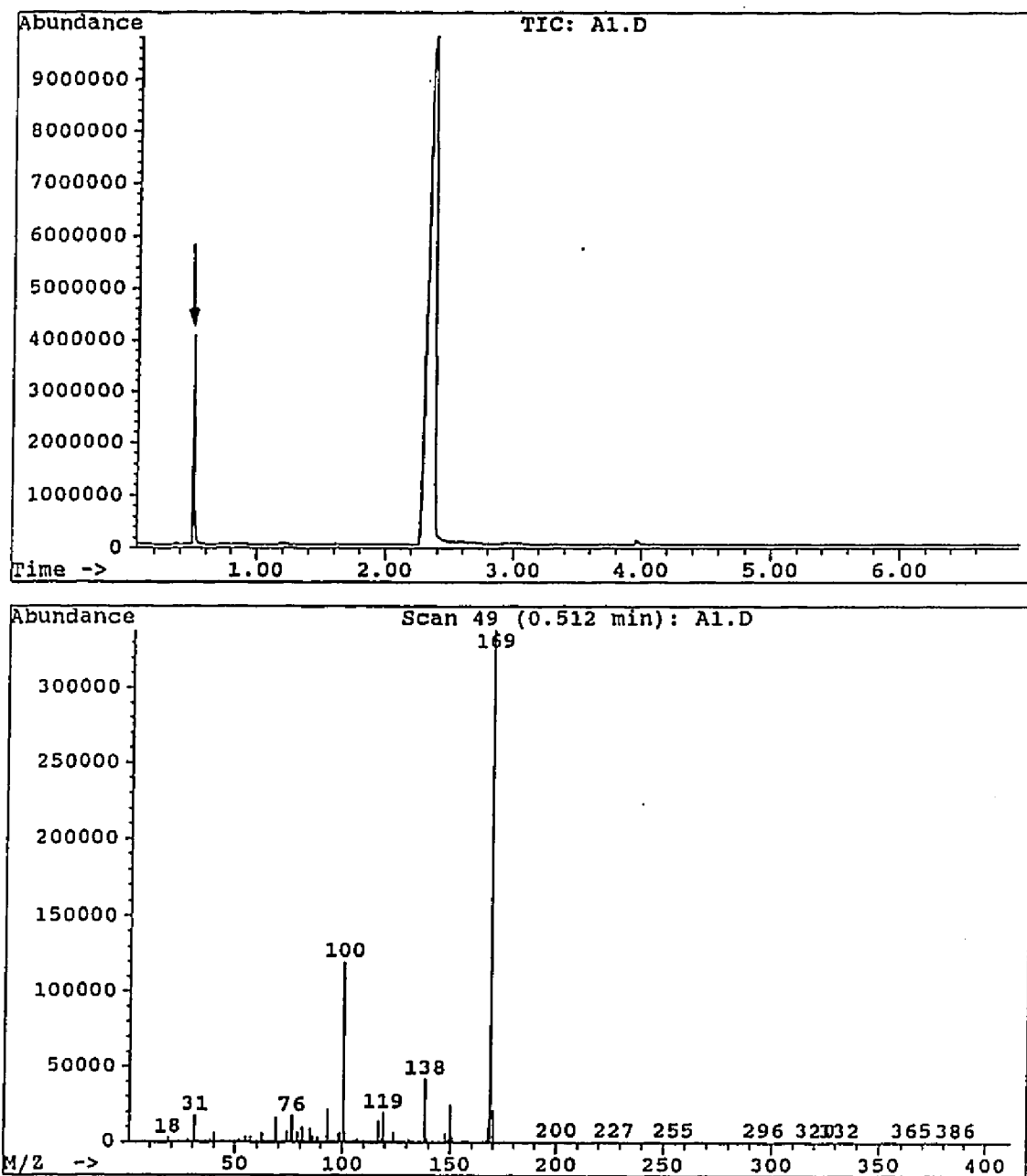
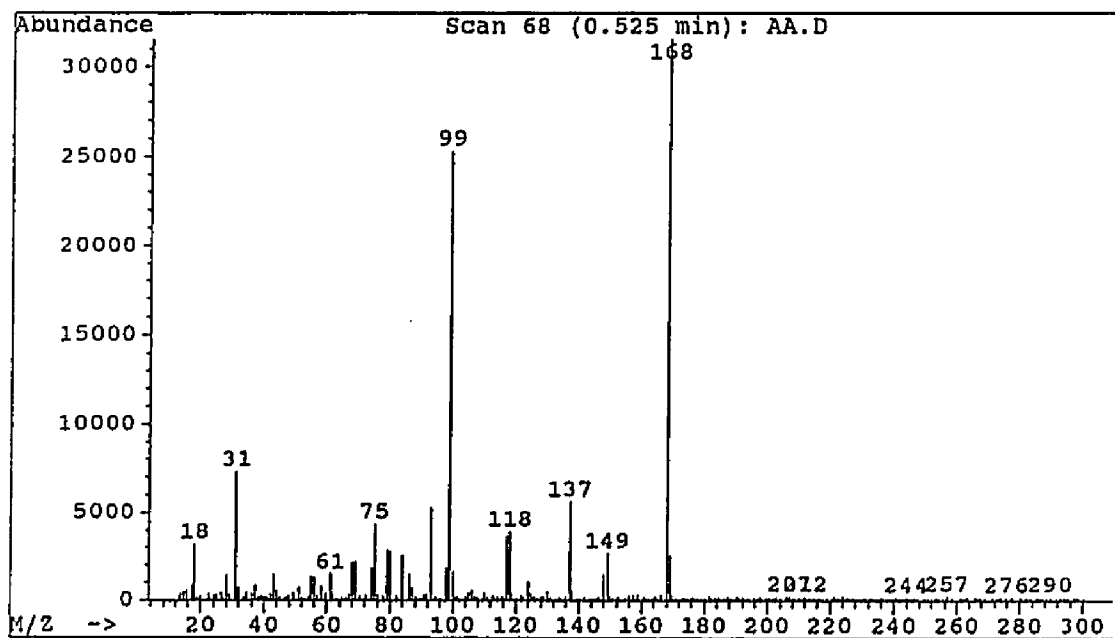
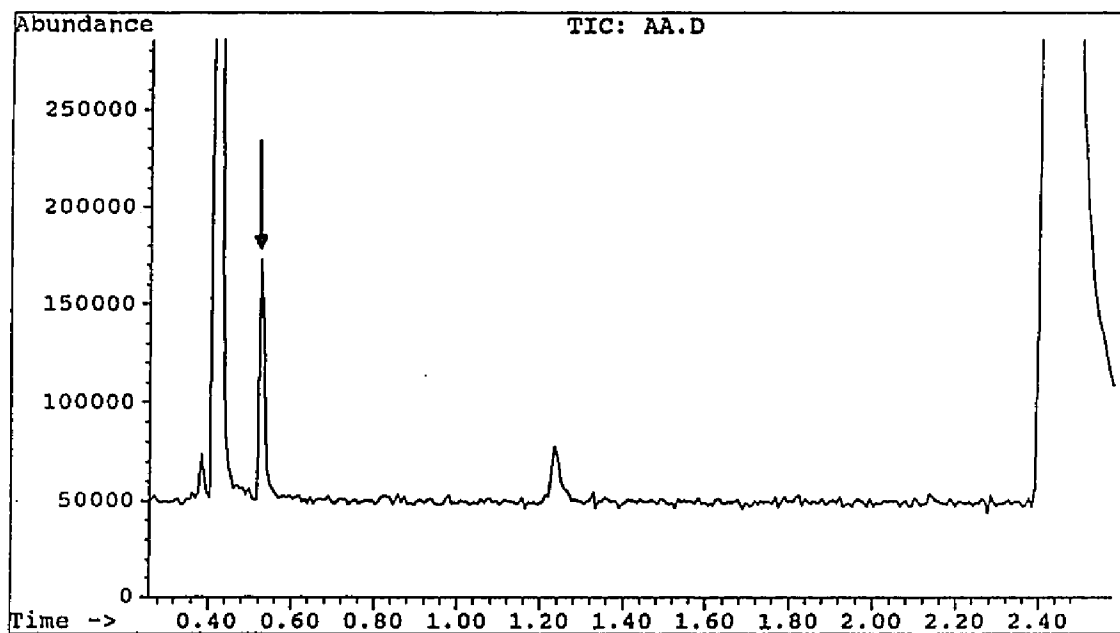
Figure 96. GC/MS data for C₆F₅D

Figure 97. GC/MS data for C_6F_5H 

during the pyrolysis and combustion of PVC. In an attempt to trap the intermediate, RCu , a similar sealed-tube experiment was carried out by pyrolyzing a mixture of D_2O , the high-purity copper metal, and 4-chloro-2-pentene at 200°C for 1 h. However, GC/MS analysis of the resultant mixture showed only that the reductive coupling dimers ($\text{C}_{10}\text{H}_{18}$) and other heavy products had been formed and that no trace of $\text{CH}_3\text{CHCHCHDCH}_3$ was present. Nevertheless, this finding does not necessarily prove that alkylcopper is not involved in the formation of coupling products, since alkylcopper species are much more thermally labile¹¹⁴ than the perfluoroaryl compounds and may readily decompose at high temperatures to form the coupling dimers, alkenes, and CuH , as suggested by Whitesides and co-workers¹¹⁵ in their study of the thermal decomposition of n-butylcopper.

Finally, for comparison purposes, two other metallic additives, Zn and MoO_3 , were treated with $\text{C}_6\text{F}_5\text{I}$ and found by GC/MS analysis to give no trace of $\text{C}_6\text{F}_5\text{-C}_6\text{F}_5$. Since $\text{C}_6\text{F}_5\text{I}$ is highly reactive toward coupling, the failure of Zn and MoO_3 to promote that process shows that copper metal possesses its own unique characteristics as a coupling agent when it is generated from its oxides or certain other copper compounds [such as copper(II) formate] during the pyrolysis process.

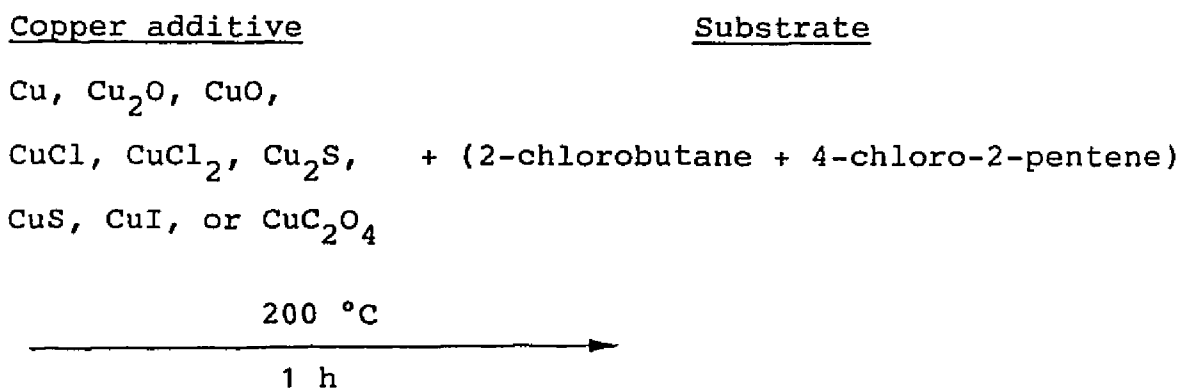
2-8. Reactions of a Simple Secondary Chloride or a Secondary Allylic Chloride with Benzene or Toluene

Since Friedel-Crafts reactions were well-known to be catalyzed by Lewis acids, five different copper additives (Cu, Cu₂O, CuO, CuCl, or CuCl₂, 0.01 g of each) were pyrolyzed at 200 °C for 1 h in the presence of 0.025 mL of benzene (0.280 mmol) (or toluene, 0.235 mmol) and 0.025 mL of 2-chlorobutane (0.237 mmol) (or 3-chloro-1-butene, 0.250 mmol), in order to study the effects of copper additives as Lewis-acid catalysts in thermally degrading PVC. Analyses by GC/MS of the resultant degradation mixtures showed that none of the copper additives was able to generate the corresponding alkylbenzene (or *p*-methyl-alkylbenzene). Only the dehydrochlorination and heavy products were found, as in the previous model-compound studies.

The results of the above experiments show that copper additives have insufficient Lewis acidity to promote Friedel-Crafts reactions even in the presence of a reactive aromatic compound such as toluene. Wescott and co-workers³⁹ have shown in similar experiments that 3-chloropentane alkylates benzene at 200 °C in the presence of MoO₃ to form the 2- and 3-isomers of pentylbenzene, while no alkylation is observed when the MoO₃ is replaced by CuCl₂. In similar studies Huang⁶² found that the weak Lewis acidities of

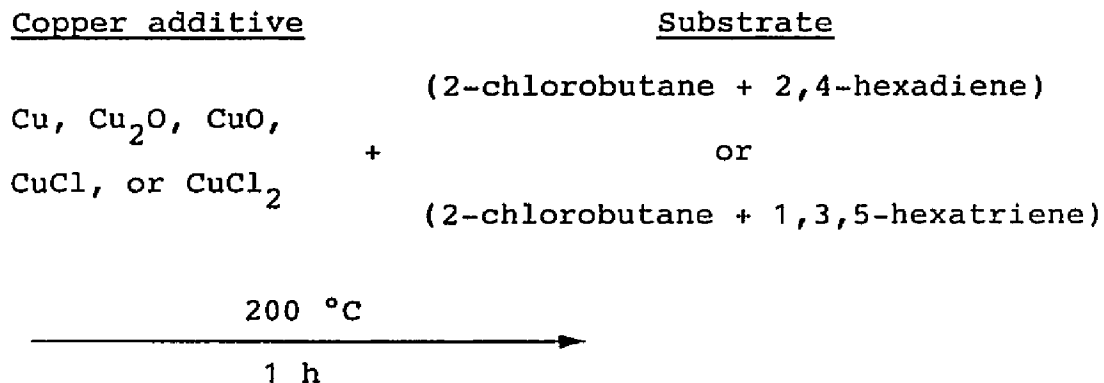
the copper species and the partial vaporization of the benzene and organic chloride model compounds all disfavored Friedel-Crafts substitutions. Whatever the correct explanation may be for copper metal, the present observations indicate that it does not serve mainly as a Lewis-acid catalyst to promote dehydrochlorination and oligomerization reactions, and that reductive coupling certainly is a possible result of the catalytic action of some copper metal additives in degrading PVC.

2-9. Reactions of a Mixture of a Simple Secondary Chloride
and a Secondary Allylic Chloride in the Presence of
Copper Additives



To learn whether copper additives would cause C-C bond formation between a model allylic chloride and a model simple secondary chloride, a mixture containing equal volumes (0.025 mL of each) of 2-chlorobutane (0.236 mmol) and 4-chloro-2-pentene (0.216 mmol) was pyrolyzed at 200 °C for 1 h in the presence of nine different copper additives. Analyses of the reaction mixtures by GC/MS showed that no reactions had led to the formation of C-C bonds between the two model compounds. This finding suggests that copper-catalyzed oligomerization (cross-linking) can occur only among allylic chloride segments in PVC, and that the dehydrochlorination of the simple secondary chlorides to form the allylic chlorides is vitally important to the final extensive crosslinking of the polymer.

2-10. Reactions of 2-Chlorobutane and a Conjugated Diene
or Triene in the Presence of Copper Additives



To examine the ability of copper additives to promote C-C bond formation between a simple secondary chloride and a conjugated diene or triene, five copper additives were used in pyrolysis experiments similar to those involving the mixture of 2-chlorobutane and 4-chloro-2-pentene. The pyrolysis experiments were carried out under the same experimental conditions as in Section 2-9, and the GC/MS results indicated that there was no formation of C-C bonds between 2-chlorobutane and the conjugated diene or triene. Taken together with the results given in Section 2-9, these results indicate that the oligomerization can occur only among the allylic chloride segments in PVC chains, and that simple secondary chlorides do not participate in the formation of crosslinking structures with themselves or with allylic segments in PVC.

CONCLUSIONS

Under very mild conditions, two different forms of activated copper metal have been shown to be able to promote the rapid reductive coupling of simple allylic chlorides that can be regarded as models for structural segments in PVC. The Cu^0 that functions in this way can be either (a) a slurry resulting from the reduction of $\text{CuI P}(\underline{n}\text{-Bu})_3$ with lithium naphthalenide or (b) a film created by the pyrolysis of copper(II) formate. Both the slurry and the Cu^0 film formed by pyrolysis were also shown to be able to promote the crosslinking of PVC itself. When solutions of the polymer in various solvents were exposed to the slurry, crosslinking that led to gelation occurred at temperatures that ranged from 66 to 259 °C. Accelerated crosslinking also was found with solid mixtures of PVC and copper(II) formate at 200 °C, a temperature where activated Cu^0 is generated rapidly from the additive. Moreover, the reductive coupling of model allylic chlorides and the crosslinking of solid PVC were promoted by a highly purified copper powder (nominal purity, 99.999%). The results obtained from these studies suggest that in PVC

polymer/copper additive binary mixtures, the in-situ formation of activated Cu^0 would lead to the reductive coupling of the polymer chains and ultimately to extensive crosslinking. Since the crosslinking of PVC is well-known to cause smoke suppression, the results of the present investigation also indicate that copper-promoted reductive coupling will tend to inhibit smoke formation when the polymer burns.

The sealed-tube model-compound pyrolysis experiments with a variety of copper additives show that the pyrolysis chemistry of PVC in the presence of such additives can be explained by three major types of reactions: those promoted by Lewis acids, reductive coupling, and monochlorination. The results of these pyrolysis studies also indicate that various copper additives can crosslink the decomposing PVC by different mechanisms, and that the formation of the crosslinking network represents a balance among them. In the case of Cu_2O , the Lewis-acid mechanism clearly is the major one involved in crosslinking, and monochlorination was shown to play an important role in the presence of CuCl_2 . Reductive coupling may make a significant contribution to crosslinking in certain cases. Based on the overall results, it can be concluded that copper additives function primarily by promoting early crosslinking of the thermally degrading PVC to yield char and thus interfere with the cyclization chemistry of the

conjugated polyene sequences that leads to smoke and flame during the combustion of the polymer.

REFERENCES

1. D. Braun and E. Bezdadea, Encyclopedia of PVC (L. I. Nass and C. A. Heiberger, Eds.; Marcel Dekker: New York, 1986). 2nd ed., Vol. 1, Chap. 8, and references cited therein.
2. Chem. Eng. News, 62(26), 15 (1984).
3. Chem. Eng. News, 72(22), 21 (1994).
4. Encyclopedia of Polymer Science and Engineering, 2nd ed., Suppl. Vol.; Wiley: New York, 1989.
5. D. H. Paul, J. Vinyl Technol., 153 (1993).
6. Chem. Eng. News, 51(14), 9 (1973).
7. N. Grassie, Polym. Deg. & Stab., 30, 3 (1990).
8. J. Kracklauer, Flame-Retardant Polymeric Materials, Plenum Press: New York, 2, 285 (1978).
9. Benjamin/Clarke Associates, Fire Deaths, Technomic: Lancaster, 1984.
10. H. L. Kaplan, A. F. Grand, and G. E. Hartzell, Combustion Technology, Technomic: Lancaster, 1983.
11. W. H. Starnes, Jr., Dev. Polym. Deg., 3, 135 (1981), and references cited therein.
12. B. Iván, T. Kelen, and F. Tüdös, Degradation and Stabilization of Polymers, Vol.2, H. H. Jellinek

- & H. Kachi, Eds., Elsevier: Amsterdam, 1989; pp. 570-3, and references cited therein.
13. T. Kelen, Polymer Degradation, Van Nostrand Reinhold: New York, 1983; pp. 77-96, and references cited therein.
 14. I. Mita, Aspects of Degradation and Stabilization of Polymers, H. H. Jellinek, Ed., Elsevier: Amsterdam, 1978; p. 24.
 15. C. David, Chemical Kinetics, C. H. Bamford and C. F. H. Tipper, Eds., Elsevier: New York, 1975; p. 1.
 16. M. M. O'Mara, J. Polym. Sci., Part A-1, 8, 1887 (1970), and references cited therein.
 17. M. M. O'Mara, Pure Appl. Chem., 49, 649 (1977), and references cited therein.
 18. P. Carty, E. Metcalfe, and S. White, Polymer, 33, 2704 (1992).
 19. W. H. Starnes, Jr., F. C. Schilling, I. M. Plitz, R. E. Cais, D. J. Freed, R. L. Hartless, and F. A. Bovey, Macromolecules, 16, 790 (1983), and references cited therein.
 20. T. Hjertberg and E. M. Sörvik, Polymer, 24, 685 (1983), and references cited therein.
 21. J. Wypych, Polyvinyl Chloride Degradation, A. D. Jenkins, Ed., Elsevier: New York, 1985; pp. 23-29.
 22. D. Braun and F. Weiss, Angew. Makromol. Chem., 13, 55 (1970).
 23. T. Suzuki and M. Nakamura, Jpn. Plast., 4, 16 (1970).

24. T. Hjertberg and E. M. Sörvik, Polymer, 24, 673 (1983).
25. T. Hjertberg, E. M. Sörvik, and A. Wendel, Makromol. Chem., Rapid Commun., 4, 175 (1983).
26. N. M. Boughdady, K. R. Chynoweth, and D. G. Hewitt, Aust. J. Chem., 44, 567 (1991).
27. G. Montaudo and C. Puglisi, Polym. Deg. & Stab., 33, 229 (1991).
28. W. H. Starnes, Jr. and D. Edelson, Macromolecules, 12, 797 (1979).
29. A. Ballistreri, S. Fotti, G. Montaudo, and E. Scamporrino, J. Polym. Sci., Polym. Chem. Ed., 18, 1147 (1980).
30. R. P. Lattimer and W. J. Kroenke, J. Appl. Polym. Sci., 26, 1191 (1981).
31. T. Iida, M. Nakanishi, and K. Gotō, J. Polym. Sci., Polym. Chem. Ed., 12, 737 (1974).
32. M. Bert, A. Michel, and A. Guyot, Fire Res., 1, 301 (1977-1978).
33. L. Lecomte, M. Bert, A. Michel, and A. Guyot, J. Macromol. Sci. (A)11(8), 1467 (1977).
34. P. Burille, M. Bert, A. Michel, and A. Guyot, J. Polym. Sci., Polym. Lett., 16, 181 (1978).
35. V. Bellenger, L. B. Carette, E. Fontaine, and J. Verdu, Eur. Polym. J., 18, 337 (1982).
36. R. M. Lum, J. Polym. Sci., Polym. Chem. Ed., 15, 489 (1977).

37. R. M. Lum, J. Appl. Polym. Sci., 23, 1247 (1979).
38. W. H. Starnes, Jr., L. D. Wescott, Jr., W. D. Reents, Jr., R. E. Cais, G. M. Villacorta, I. M. Plitz, and L. J. Anthony, Org. Coat. Plast. Chem., 46, 556 (1982), and references cited therein.
39. L. D. Wescott, W. H. Starnes, Jr., and A. M. Mujsce, J. Anal. Appl. Pyrolysis, 8, 163 (1985).
40. A. Ballistreri, S. Foti, P. Maravigna, G. Montaudo, and E. Scamporrino, Polymer, 22, 131 (1981).
41. G. Montaudo, C. Puglisi, E. Scamporrino, and D. Vitalini, J. Polym. Sci., Polym. Chem. Ed., 24, 301 (1986).
42. R. P. Lattimer and W. J. Kroenke, J. Appl. Polym. Sci., 25, 101 (1980).
43. R. P. Lattimer and W. J. Kroenke, J. Appl. Polym. Sci., 27, 1355 (1982).
44. D. H. Edelson, R. M. Lum, W. D. Reents, W. H. Starnes, Jr., and L. D. Wescott, Proceedings, Nineteenth Symposium (International) on Combustion; The Combustion Institute: Pittsburgh, August 1982; p. 807.
45. B. B. Troitskii, L. S. Troitskaya, V. N. Myakov, and A. F. Lepaev, J. Polym. Sci., Polym. Symp., 42, 1347 (1973).
46. M. V. Neiman, R. A. Papko, and V. S. Pudov, Polym. Sci. USSR (Engl. Transl.), 10, 975 (1968).

47. F. Tüdös, T. Kelen, T. T. Nagy, and B. Turcsányi, Pure Appl. Chem., **38**, 201 (1974).
48. T. Kelen, J. Macromol. Sci., Chem., **12**, 349 (1978).
49. R. P. Lattimer, W. J. Kroenke, and R. G. Getts, J. Appl. Polym. Sci., **29**, 3783 (1984).
50. W. J. Kroenke, J. Appl. Polym. Sci., **26**, 1167 (1981).
51. R. R. Hindersinn and G. Witschard, Flame Retardancy of Polymeric Materials, W. C. Kuryla and A. J. Papa, Eds., Marcel Dekker: New York, 1978; Vol. 4, Chap. 1.
52. J. J. Pitts, Flame Retardancy of Polymeric Materials, W. C. Kuryla and A. J. Papa, Eds., Marcel Dekker: New York, 1973; Vol. 1, Chap. 2.
53. R. P. Lattimer and W. J. Kroenke, Analytical Pyrolysis: Techniques and Applications, K. J. Voorhees, Ed.; Butterworths: Woburn, MA, 1984; p. 453.
54. D. Edelson, V. J. Kuck, R. M. Lum, E. Scalco, W. H. Starnes, Jr., and S. Kaufman, Combust. Flame, **38**, 271 (1980).
55. W. H. Starnes, Jr., L. D. Wescott, Jr., W. D. Reents, Jr., R. E. Cais, G. M. Villacorta, I. M. Plitz, and L. J. Anthony, Polymer Additives, J. E. Kresta, Ed., Plenum Publishing Corp.: New York, 1984; p. 237.
56. C.-H. O. Huang and W. H. Starnes, Jr., Proceedings, 2nd Beijing International Symposium on Flame Retardants, Geological Publishing House: Beijing, 1993; p. 168.

57. B. C. Gates, J. R. Katzer, and G. C. A. Schuit, Chemistry of Catalytic Processes, McGraw-Hill: New York, 1979; Chaps. 1 and 3.
58. W. H. Starnes, Jr. and C.-H. O. Huang, Polym. Prepr. (Am. Chem. Soc., Div. Polym. Chem.), 30(1), 527 (1989).
59. J. K. Kochi, Acc. Chem. Res., 7, 351 (1974).
60. T. Cohen and I. Cristea, J. Org. Chem., 40, 3649 (1975).
61. T. Kawaki and H. Hashimoto, Bull. Chem. Soc. Jpn., 45, 3130 (1972).
62. C.-H. O. Huang, Ph.D. dissertation, Polytechnic University, 1990.
63. W. H. Starnes, Jr., J. P. Jeng, S. A. Terranova, E. Bonaplata, K. Goldsmith, D. M. Williams, and B. J. Wojciechowski, Proceedings, 5th Annual BCC Conference on Flame Retardancy: "Recent Advances in Flame Retardancy of Polymeric Materials", Stamford, Connecticut, May, 1994.
64. G. W. Ebert and R. D. Rieke, J. Org. Chem., 53, 4482 (1988).
65. F. O. Ginah, T. A. Donovan, Jr., S. D. Suchan, D. R. Pfennig, and G. W. Ebert, J. Org. Chem., 55, 584 (1990).
66. F. Kőrösy, Nature, 160, 21 (1947).
67. H. R. Hudson and G. R. de Spinoza, J. Chem. Soc., Perkin Trans., 1, 104 (1976).
68. M. J. Spitulnik, Chem. Eng. News, 55(31), 31 (1977).

69. R. M. Magid, O. S. Fruchey, W. L. Johnson, and T. G. Allen, J. Org. Chem., **44**, 359 (1979).
70. R. M. Magid, O. S. Fruchey, and W. L. Johnson, Tetrahedron Lett., 2999 (1977).
71. G. Kauffman and L. Teter, Inorg. Synth., **7**, 9 (1963).
72. R. D. Rieke and P. M. Hudnall, J. Am. Chem. Soc., **94**, 7178 (1972).
73. D. Druesedow and C. F. Gibbs, Nat. Bur. Stand. Circular, **525**, 69 (1953).
74. C. B. Havens, Nat. Bur. Stand. Circular, **525**, 107 (1953).
75. M. Imoto and T. Otsu, J. Inst. Polytech., Osaka City Univ., Ser. C., **4**, 1 (1953).
76. A. Rieche, A. Grimm, and H. Mücke, Kunststoffe, **52**, 265 (1962).
77. W. I. Bengough and H. M. Sharpe, Makromol. Chem., **66**, 31 (1963).
78. R. Petiaud and Q.-T.-Pham, Makromol. Chem., **178**, 741 (1977).
79. U. Schwenk, I. Koenig, F. Cavanga, and B. Wrackmeyer, Angew. Makromol. Chem., **83**, 183 (1979).
80. A. Caraculacu and E. Bezdadea, J. Poly. Sci., Polym. Chem. Ed., **15**, 611 (1977).
81. T. Hjertberg and E. M. Sörvik, J. Macromol. Sci.-Chem., **A17**, 983 (1982).

82. A. W. Parkins and R. C. Poller, An Introduction to Organometallic Chemistry, Oxford University Press, Inc.: New York, 1986; pp. 12-19.
83. G. W. Ebert and R. D. Rieke, J. Org. Chem., 49, 5280 (1984).
84. P. L. Timms, Angew. Chem., 87, 213 (1975).
85. M. J. Drews, C. W. Jarvis, and G. C. Lickfield, Fire and Polymers, (M. J. Comstock, Ed.), ACS Symposium Series 425, American Chemical Society: Washington, D.C., 1990; p. 109.
86. M. Tamura and J. K. Kochi, J. Organomet. Chem., 42, 205 (1972).
87. G. M. Whitesides, W. F. Fischer, Jr., J. San Fillippo, Jr., R. W. Bashe, and H. O. House, J. Am. Chem. Soc., 91, 4871 (1969).
88. Y. Uegaki and T. Nakagawa, J. Appl. Polym. Sci., 21, 965 (1977).
89. S. Van der Ven and W. F. de Wit, Angew. Makromol. Chem., 8, 143 (1969).
90. K. Thinius, W. Reicherdt, and H. Krause, Plaste Kaut., 17(10), 739 (1970).
91. A. Rieche and A. Grimm, Kunststoffe, 52, 398 (1962).
92. B. A. Howell and C. V. Rajaram, J. Vinyl Technol., 15, 202 (1993).
93. S. K. Brauman, J. Appl. Polym. Sci., 26, 353 (1981).

94. Z. Mayer, J. Macromol. Sci., Rev. Macromol. Chem., C10, 263 (1974).
95. D. Braun, Degradation Stab. Polym., Proc. Plenary Main Lect. Int. Symp., G. Geuskens, Ed., Wiley: New York, 1975; p. 23.
96. W. H. Starnes, Jr., Polym. Prepr. (Am. Chem. Soc., Div. Polym. Chem.), 18(1), 493 (1977).
97. W. H. Starnes, Jr., Adv. Chem. Ser., 169, 309 (1978).
98. I. A. Abu-Isa, J. Polym. Sci., Part A-1, 10, 881 (1972).
99. K. J. Klabunde and J. S. Roberts, J. Organomet. Chem., 137, 113 (1977).
100. K. S. Minsker, D. V. Kazachenko, D. V. Abdullina, R. G. Kouler, and A. A. Berlin, Polym. Sci. USSR (Engl. Transl.), 15, 974 (1973).
101. H. Kuzmany, E. A. Imhoff, D. B. Fitchen, and A. Sarhangi, Mol. Cryst. Liq. Cryst., 77, 197 (1981).
102. J. Světlý, R. Lukáš, J. Michalcová, and M. Kolinský, Makromol. Chem., Rapid Commun., 1, 247 (1980).
103. P. Yates and P. Eaton, J. Am. Chem. Soc., 82, 4436 (1960).
104. G. I. Fray and R. Robinson, J. Am. Chem. Soc., 83, 249 (1961).
105. T. Inukai and T. Kojima, J. Org. Chem., 32, 869 (1967).
106. T. Cohen, A. H. Lewin, M. J. Zovko, and W. H. Rosewater, Chem. Commun., 80 (1967).

107. R. G. R. Bacon, S. G. Seeterram, and O. J. Stewart, Tetrahedron Lett., 21, 2003 (1967).
108. R. M. Silverstein, G. C. Bassler, and T. C. Morrill, Spectrometric Identification of Organic Compounds, Wiley: New York, 1981; p. 15.
109. F. W. McLafferty, Interpretation of Mass Spectra, University Science Books: Mill Valley, CA, 1980; pp. 60-63.
110. S. Uemura and M. Okano, Bull. Inst. Chem. Res., Kyoto Univ., 50, 423 (1972).
111. T. Iida and K. Gotō, J. Polym. Sci., Polym. Chem. Ed., 15, 2427 (1977).
112. T. Iida and K. Gotō, J. Polym. Sci., Polym. Chem. Ed., 15, 2435 (1977).
113. R. D. Rieke and L. D. Rhyne, J. Org. Chem., 44, 3445 (1979).
114. H. Gilman, R. G. Jones, and L. A. Woods, J. Org. Chem., 17, 1630 (1952).
115. G. M. Whitesides, E. R. Stedronsky, C. P. Casey, and J. San Fillippo, Jr., J. Am. Chem. Soc., 92, 1426 (1970).

VITA

Jong Paul Jeng

Born in Tainan, Taiwan, Republic of China, October 27, 1957, he received his degree of Bachelor of Science in Chemistry from Chung-Yuang Christian University located in Chung-Li, Taiwan in 1980. Then he took two years of military service in the Navy before joining the United Microelectronics Corporation as a process engineer in Hsin-Chu, Taiwan in 1983. He came to the College of William and Mary in Virginia from the Polytechnic University in New York in the fall of 1989 to perform his doctoral research in the field of polymer science with Dr. William H. Starnes, Jr., who also moved from Polytechnic to William and Mary at that time. A major part of his research was sponsored by the International Copper Association.